SUMOYLATION OF NEMO AND NF-κB ACTIVATION BY A RNA HELICASE, DP103 DEFINES THE METASTATIC POTENTIAL OF HUMAN BREAST CANCERS

HAY HUI SIN

A THESIS SUBMITTED FOR THE DEGREE OF

DOCTOR OF PHILOSOPHY

DEPARTMENT OF PHARMACOLOGY

NATIONAL UNIVERSITY OF SINGAPORE

2012

ACKNOWLEDGEMENTS

I would like to express my most heartfelt appreciations to the following people who have had helped me in one way or another in the course of my Ph.D. years. Firstly, many thanks to my supervisor, Dr Alan Prem Kumar, who has been so supportive and encouraging. He had given me so many opportunities and directions not only in my project but also in my life. I would also like to thank my co-supervisors, Dr Vinay Tergaonkar and Dr Celestial Yap who have also gave many valuable opinions and advices for my project.

Next, I would like to thank Dr Martin Lee, who was my supervisor for my honors project. He was the one who introduced DP103 to me which is such an amazing protein!

I would also like to extend my gratitude to Professor Shigeki Miyamoto, Professor Lim Chwee Teck, Professor Manuel Salto-Tellez and A/Professor Goh Boon Cher for collaborating with my project.

I would also like to take the opportunity to thank my parents, siblings and friends whom gave me lots of support throughout these years. Last but not least, I would like to thank Dr Shin Eun Myoung for her great assistance, Ms Jenny Goh, Ms Lucy Chen, Ms Sayo Loo, Ms Angele Koh, Mr Rohit Surana, Mr Ben Chua and everyone in APK and VT lab for the encouragement, friendship, support and for making the lab a fabulous place to work at!

TABLE OF CONTENTS

SUMMARY

Mortality from breast cancer is almost entirely the result of invasion and metastasis of neoplastic cells; therefore, understanding gene products involved in breast cancer metastasis is an important research goal. I discovered DP103, a RNA helicase, to be correlated with the level of maglinancies and its suppression led to the decrease in the ability of highly invasive breast cancer cells to migrate and invade. MMP9 is found to be a major matrix metalloproteinase involved in the degradation of the cell's extracellular membrane to facilitate metastasis.

A panel of breast cancer cell lines was screened for MMP9 expression. Interestingly, this screen shows cell lines that are highly metastatic such as MDA-MB-231 and BT549 display high expression levels of MMP9 and they are highly correlated to DP103 levels. When grouping patients with positive DP103 expression to positive and negative MMP9 expression, Kaplan-Meier correlation analysis show patients with positive DP103 and MMP9 expression have poorer survival outcomes ($p=0.029$).

Next, using EMSA and luciferase reporter assay, it is shown that this decrease in MMP9 levels is regulated by NF-κB and not AP-1. Additionally, under the stimulation of known NF-κB genotoxic agents, NF-κB activity was also decreased when DP103 was knockdown. I also discovered that DP103 coimmunoprecipitated with NEMO, an essential NF-κB modulator, and that it is required for the SUMOylation of NEMO upon genotoxic stress. Downregulation of DP103 abrogated this modification to occur. Additionally, it was observed that DP103 enhances the interaction of NEMO and PIASy,

an E3 SUMO ligase, while decreasing that of NEMO and the specific desumoylating enzyme, SENP2.

Using a clinically approved drug, a reduction of DP103 and cell invasion after statins treatment was observed. Importantly, forced expression of DP103 is able to rescue this inhibition of metastasis. The *in vivo* model using nude mice with MDA-MB-231 cells injected showed a reduction in metastases formed and DP103 expression when they are fed with simvastatin.

Together, my study identifies DP103 as the "missing" key regulator of NF-κB activation under genotoxic stress. Importantly, DP103 is a novel prognostic marker that identifies patients who are at risk for developing metastases, thus enabling oncologists to begin tailoring treatment strategies to individual patients.

LIST OF TABLES

LIST OF FIGURES

LIST OF ABBREVIATIONS

APS	Ammonium persulfate
AR	Androgen receptor
ATM	Ataxia Telangiectasia Mutated
CPT	Camptothecin
DMEM	Dulbecco's modified eagle's medium
DMSO	Dimethyl Sulfoxide
DOX	Doxorubicin
DNA	Deoxyribonucleic Acid
ECM	Extracellular Cellular Matrix
ER	Estrogen Receptor
EMSA	Electrophoretic mobility shift assay
FBS	Fetal Bovine Serum
GAPDH	Glyceraldehyde-3-phosphate dehydrogenase
H&E	Hematoxylin and eosin
HER2	Human Epidermal Factor 2
HPRT	hypoxanthine-guanine-phosphoribosyltransferase
IDC	Invasive ductal carcinoma
IHC	Immunohistochemistry
kDa	Kilo Dalton
L	Litre
M	Molar
MEGM	Mammary Epithelial Growth Medium

mg	milligram
ml	milli litre
MTT	3-(4,5-Dimethylthiazol-2-yl)-2,5-diphenyltetrazolium-bromide
MMP	Matrix metalloproteinase
NEMO	NF-κB essential modulator
nM	nano molar
PBS	Phosphate buffered saline
PIAS	Protein inhibitor of activator STAT
PR	Progesterone Receptor
RNA	Ribonucleic Acid
RPMI	Roswell Park Memorial Institute
RT-PCR	Reverse Transcription-Polymerase Chain Reaction
SDS-PAGE	Sodium Dodecyl Sulphate - Polyacrylamide Gel Electrophoresis
SENP	Sentrin-specific protease
SF-1	Steroidogenic factor 1
siRNA	Small Interfering RNA
SUMO	Small ubiquitin-related modifier
TMA	Tissue Microarray
TNFα	Tumour Necrosis Factor α
µg	micro gram
µl	micro litre
V	Volt
VP16	Etoposide

PATENT FILED

We have recently filed a provisional patent with the US Patent & Trade Marks Office on 22 December 2011, under the title 'DEAD-box Helicase DP103 (DDX20, Gemin3), a Novel Prognostic Marker and Therapeutic Target in Metastatic Breast Cancer' (US Provisional Application No.: 61/579,042).

The principal inventor for this patent is my main supervisor, Dr Alan Prem Kumar while Dr Vinay Tergaonkar, Dr Martin Lee Beng Huat, Dr Gautam Sethi and myself are the co-inventors.

CHAPTER 1 INTRODUCTION

1.1 Breast Cancer

1.1.1 Worldwide, Asia and ethnicity trends

Breast cancer is one of the most common malignancies among women around the world. It is a complex disease that results from a multi-stage process involving the deregulation of a number of different signaling cascades. It is also the most frequent non-skin cancer to affect women worldwide, and remains one of the top public health burdens. Breast cancer accounts for nearly 1 in 3 cancers diagnosed among women in the United States. According to the American Cancer Society, approximately 230 480 new cases of invasive breast cancer and 39 520 cancer deaths are expected to occur among women in United States in 2011. Changes in reproductive patterns such as delayed childbearing and having fewer children are recognized as risk factors for breast cancer (Desantis et al., 2011).

The risk of getting cancer varies geographically. Despite having a lower breast cancer incidence rate compared to Western countries, the breast cancer risk has been increasing in most Asia countries. The age-standardized incidence rates of breast cancer increased from 32.5 per 100 000 women in 1983 to 35.0 per 100 000 in 2004 and a further increase to 45.9 per 100 000 in 2008 for Asia women (Kwong et al., 2011).

Amongst the highest in Asia, breast cancer is the leading cause of cancer death in Singaporean women for the past 30 years, with relatively large yearly variations

attributable to the relatively small female population (Shin et al., 2010). Currently, it accounts for 29.7% of all female cancers. About 1100 new cases are diagnosed annually and approximately 270 women die in Singapore each year from breast cancer, translating to breast cancer diagnoses in about three women daily, with approximately three cancer deaths every four days. The rate of increase in incidence in Singapore is also one of the highest in the world at 5.7% per year in premenopausal women and 3.9% per year in postmenopausal women, in contrast to only 1.5% per year in the United States (Jara-Lazaro et al., 2010). The risk of breast cancers across different ethnic groups differs in Singapore, with Singapore Indian women having the highest risk of 37.9 per 100 000 per year. Singapore Chinese and Malay women had a slightly lower risk of 28.3 and 34.3 per 100 000 per year (Singapore Cancer Registry, 21 June 2011).

1.1.2 Classifications of breast cancers

Breast cancer, instead of constituting a monolithic entity, comprises of heterogeneous tumors with different clinical characteristics, disease courses, and responses to specific treatments. As such, breast cancers can be classified by difference schemata, as discussed below:

Histopathology

Histopathologic classification is based upon characteristics seen upon light microscopy of biopsy specimens. The majority of breast cancers are derived from the epithelium lining the ducts or lobules and are classified as mammary ductal carcinoma. Carcinoma *in situ* refers to the proliferation of cancer cells within the

epithelial tissue without invasion of the surrounding tissue. In contrast, invasive carcinoma invades the surrounding tissue. Invasive ductal carcinoma (IDC) is the most common type observed, representing 75% of all types of breast cancer, while invasive lobular carcinoma represents the next most frequent histologic type of breast tumor. Together, these two make up about 90% of breast cancers, while the remainder are categorized as medullary, neuroendocrine, tubular, apocrine, metaplastic, mucinous, inflammatory, comedo, adenoid cystic and micropapillary types (Li, 2005; Weigelt et al., 2010).

Grading

Grading focuses on the appearance of the breast cancer cells with reference to that of normal breast tissue. Well differentiated tissues are graded as low grade of a score of 1, moderately differentiated as intermediate grade with a score of 2 and poorly differentiated as high grade with a score of 3 or 4, as the cells progressively lose the features seen in normal breast cells. The Nottingham modification of the Scarff-Bloom-Richardson grading system is a commonly used scale, which grades breast carcinomas by adding up scores for tubule formation, nuclear pleomorphism and mitotic count, each of which is given 1 to 3 points. The scores for each of these three criteria are then added together to give an overall final score and corresponding grade (Bloom and Richardson, 1957; Genestie et al., 1998).

Staging

Breast cancers can also be classified according to the size of the cancers in the primary and secondary sites. The TNM classification for staging breast is developed and maintained by the International Union Against Cancer (UICC) to achieve

consensus on a globally recognized standard for classifying the extent of cancer spread. It also includes characteristics like nodal spread and metastasis. Stage 0 is a pre-cancerous condition, while stage 1 to 3 tumors are within the breast or regional lymph nodes and stage 4 is a metastatic cancer with less favorable prognosis (http://www.cancer.gov/cancertopics/factsheet/detection/staging).

Receptor Status

Under this classification, breast cancers are categorized according to the status of three receptors, namely estrogen receptor (ER), progesterone receptor (PR) and human epidermal growth factor receptor 2 (HER2) receptor. Tumors with the absence of these three receptors are referred to triple-negative breast cancers (Bauer et al., 2007).

Intrinsic subtypes model

Advances in gene expression analyses enabled a new classification of breast cancers by their molecular profiles into six intrinsic subtypes: luminal A, luminal B, HER2-enriched, basal-like, normal breast-like and claudin-low (Eroles et al., 2012; Sorlie, 2004). This new classification is based on a large scale analysis, using biological characteristics to group breast cancer tumors. The distinctive features of each subtype are summarized as below:

Subtype	Freq	ER/PR/HER2	Histologic grade	Prognosis
Basal-like	10-20%	ER-, PR-, HER2-	High	Bad
HER2-enriched	10-15%	ER-, PR-, HER2+	High	Bad
Normal breast-like	5-10%	ER-/+ , HER2-	Low	Intermediate
Luminal A	50-60%	ER+, PR+, HER2-	Low	Excellent
Luminal B	10-20%	ER+/-, PR+/-, HER2-/+	High	Intermediate/bad
Claudin-low	12-14%	ER-, PR-, Her2-	High	Bad

Table 1: Features of intrinsic subtypes of breast cancer

Treatments for Luminal A and B include aromatase inhibitors, selective estrogen receptor modulators and pure selective regulators of ER, though luminal B tumors respond better to neoadjuvant chemotherapy. Comparatively, HER2-enriched tumors have high chemosensitivity with higher response rate than luminal A and B tumors. Basal-like breast tumors posses worse prognosis than luminal subtypes and have higher relapse rate despite its high response to chemotherapy. The high incidence of p53 and BRCA1 mutations also led to genetic instability. Normal breast subtype, on the other hand, is considered rare and there are doubts about the real existence as it is thought to be a technical artifact from high contamination with normal tissue during microarrays. Claudin-low subtype is the last subtype to be identified and it is characterized by a low expression of genes involved in intercellular adhesion while generally been associated with the acquisition of cancer stem cell phenotype (Prat et al., 2010).

1.1.3 Therapies for hormone-positive breast cancers

Current therapies for the treatment of breast cancers revolve around the presence (or absence) of specific markers, namely ER, PR and HER2. Expressions of the first two receptors are determined by immunohistochemistry (IHC) from breast tissues, while

HER2 expressions are determined by both IHC and fluorescence in situ hybridization (FISH). ER status is used to segregate the hormone-positive breast cancer patients for treatment using anti-estrogen (endocrine) therapy.

Estrogen is a hormone known to regulate menstruation in females. However, dysregulation of estrogen causes cancer by turning on hormone-responsive genes that promote DNA synthesis and cell proliferation. Endocrine therapy works to reduce the effect of estrogen on the body so that it can no longer turn on the growth of hormone-receptor-positive breast cancer cells. Different treatments either block hormone receptors, eliminate hormone receptors or lower estrogen levels in the body. Tamoxifen, the ER modulator, improves survival among women with early and advanced breast cancer and further improvements are provided by aromatase inhibitors and the ER-degrading agent, fulvestrant (2005; Gibson et al., 2009; Gradishar, 2010; Robertson et al., 2009). Their long-term efficacy, however, is limited by relapse of disease and development of resistance. Despite continuous expression of ER at relapse in either locally recurrent or secondary metastatic tumors, up to 50% of patients with hormone-positive primary breast cancer who develop metastatic disease do not respond to first-line endocrine treatment, and the remainder will eventually relapse despite an initial response (Ring and Dowsett, 2004).

The HER family of proteins are activated by numerous extracellular ligands, which dimerize upon binding, become phosphorylated, and transduce intracellular signals that regulate a variety of cellular processes. Patients who are HER2 positive are treated with targeted therapies like the monoclonal antibodies trastuzumab and lapatinib, which bind to HER2 and disrupt HER2-dependent signaling and trigger

antibody-dependent cytotoxicity (Kim et al., 2009; Valabrega et al., 2007). HER2 overexpression confers intrinsic resistance to endocrine therapy, hence in tumors that are both HER2 and ER positive, they responded poorly to endocrine therapies (De Laurentiis et al., 2005; Lipton et al., 2002). Such resistance can be partially overcome by combining anti-estrogen and anti-HER2 therapies. In a randomized Phase III study, the addition of trastuzumab with an aromatase inhibitor improved outcomes for patients with metastatic breast tumors that expressed both ER and HER2 (Kaufman et al., 2009).

In addition to approved agents, there are a number of novel strategies against HER2 that have shown activity in tumors that have progressed during treatment. Trastuzumab-DM1 is an anti-HER2 antibody-drug conjugate that specifically recognizes HER2-positive tumor cells, thereby targeting them for degradation (Lewis Phillips et al., 2008). In a study of trastuzumab-DM1 versus trastuzumab plus docetaxel, trastuzumab showed similar efficacy to the combination with almost non-existent side effects (Mathew and Perez, 2011).

Resistance to anti-HER2 therapies can be due to cross-talk between the ER and HER themselves or between signaling pathways downstream of these receptors such as PI3K, Akt or mTOR (Prat and Baselga, 2008). A recent Phase Ib study therefore combined everolimus, a mTOR inhibitor, with paclitaxel and trastuzumab in patients with HER2-overxpressing metastatic breast cancer who were pretreated with trastuzumab (Andre et al., 2010). The overall response rate in 27 patients was 44%, and the overall disease was controlled for at least six months in 74% of those treated.

1.1.4 Therapies for hormone-negative / triple-negative breast cancers

Tumors with the absence of ER, PR or HER2 are known as triple-negative breast cancers and are predominantly of high histological grade and affect patients less than 50 years old more frequently (Haffty et al., 2006; Thike et al., 2010). Triple-negative breast cancers are more prevalent in African-American women (Bauer et al., 2007), often present as interval cancers and are significantly more aggressive than tumors of other molecular subtypes (Dent et al., 2007; Rakha et al., 2007). This aggressiveness is best exemplified by the fact that the peak risk of recurrence is between the first and third years and the majority of deaths occur in the first 5 years following therapy. In contrast, the recurrence risk of non-triple negative group remained constant overtime. However, a substantial number of triple-negative cancer patients appear to be cured if they remain recurrence free for the first several years after diagnosis (Anderson et al., 2006; Dent et al., 2007; Tischkowitz et al., 2007). Some key additional histological features of triple-negative tumors include increased mitotic activity and atypical mitotic figures, high Ki67 index, high nuclear-cytoplasmic ratio, pushing margins of invasion and stromal lymphocytic infiltration (Fulford et al., 2006; Livasy et al., 2006; Rakha et al., 2006). The metastatic spread of triple-negative tumors are reported to show specific patterns with a higher propensity for incidence of metastases to the brain and lungs and a lower incidence to the liver, bone and axillary lymph nodes (Fulford et al., 2007; Smid et al., 2008; Tsuda et al., 2000).

While effective endocrine therapies exist for women with hormone receptor positive or HER2 positive breast cancers, chemotherapy is the only systemic therapy available for women with triple-negative disease besides surgery and radiation therapy. Anthracycline, an inhibitor of topoisomerase II and thereby causes DNA strand break,

is commonly used as a neo-adjuvant therapy for treatment of triple-negative breast cancers. In a study involving 255 patients with triple-negative breast cancer receiving anthracycline or anthracycline and taxane-based regimens, the pathological response rate of triple-negative tumor was 22% compared to that for non-triple negative cancers at 11% (Liedtke et al., 2008). In other studies, 17% of triple-negative cancers have been shown to have a pathological complete response after neo-adjuvant platinum-based chemotherapy (Sirohi et al., 2008).

Germline *BRCA1* mutations has been reported in a subset of triple-negative breast cancers (Collins et al., 2009; Turner et al., 2007; Young et al., 2009). Tumors with this mutations have defects in the DNA repair machinery and are highly sensitive to platinum-based drugs. For example, a neo-adjuvant trial of women with BRCA1 mutations and triple-negative cancer showed a 90% complete pathological responses to a single agent cisplatin (Byrski et al., 2008). Another type of treatment involves the use of PARP inhibitors which prevent the repair of DNA single strand break upon damage. These inhibitors were initially developed to enhance the cytotoxicity of radiation and certain DNA-damaging agents (Farmer et al., 2005; Halmosi et al., 2001). In recent years, they have been shown to have single-agent activity in some tumors. Inhibition of PARP in a DNA repair-deficient tumor can lead to gross genomic instability and cell death by exploiting the paradigm of synthetic lethality. Several studies have evaluated the role of PARP inhibitors for treatment of breast cancer, in the context of BRCA-mutated tumors and had shown effective results. In a study, olaparib (AstraZeneca), a PARP inhibitor was given to 54 patients with *BRCA1* or *BRCA2* mutations and advanced breast cancers. The overall response rate was 41% among the 27 patients assigned to the drug without significant toxicity. These findings

were complemented by the impressive clinical benefit from 34% to 56% and the rate of overall response from 32% to 52% when iniparib (Sanofi), another PARP inhibitor was combined with carboplatin and gemcitabine in a randomized Phase II trial evaluating iniparib in patients with metastatic triple-negative breast cancers (O'Shaughnessy et al., 2011). The addition of iniparib also prolonged the median progression-free survival from 3.6 months to 5.9 months and the median overall survival from 7.7 months to 12.3 months. On the basis of these results, a Phase III trial is currently ongoing (http://clinicaltrials.gov/ct2/show/NCT00938652?term=NCT00938652&rank=1). A neo-adjuvant trial of women with BRCA1 mutations and triple-negative cancer showed a 90% complete pathological responses to a single agent cisplatin (Byrski et al., 2008). However, other studies showed that triple-negative tumors did not show increased sensitivity to taxanes or platinum-based drugs (Chabalier et al., 2006; Rottenberg et al., 2007), indicating that these targeted therapies are still limited by the heterogeneity of breast cancers.

There are a number of challenges that still need to be addressed in the treatment of triple-negative breast cancers. Besides the nature of such tumors, the identification of biomarkers of response and early markers of clinical benefits are necessary. The study of mechanisms of resistance to different therapies is also critically important. A frequent mechanism of resistance in breast cancers is the constitutive activation of NF-κB (Nakshatri et al., 1997; Wu and Kral, 2005). Therefore, knowledge of the mechanism of such resistance will benefit the search for candidate genes for targeted therapies. Ongoing research are focused on developing standardized and validated biomarkers that are able to indicate an early response (or lack thereof) to targeted agents in a variety of tumor types. These developments would have to be tested in

clinical patient samples before moving into clinical trials. All these efforts will help to define new prognostic and predictive markers to identify patients with triple-negative breast cancers that is most likely to benefit from treatment.

1.2 Metastasis

Cancer metastasis is the multi-stage process by which cancer spreads from the place at which it first arose as a primary tumor to distant locations in the body. This process consists of sequential steps which are interconnected through a series of adhesive interactions and invasive processes. Due to its heterogeneity nature, mechanisms involving metastasis remain poorly understood.

The steps involved in the metastatic cascade are shown in Figure 1. Firstly, development of a new blood supply to the growing tumor or angiogenesis occurs. This is then followed by the disaggregation of tumor cells from the primary tumor mass which then invade and migrate through the cell's basement membrane, as well as the extracellular matrix (ECM) surrounding the tumor epithelium and the blood vessels. The tumor cells then move into the blood vessel and travel to their secondary site. These circulating tumor cells subsequently adhere themselves to the endothelial cell lining at their target organ sites, invade through the ECM and surrounding basement membrane to the target organ tissue. After colonization, these tumor cells start to grow and develop their own blood vessels to support their growth (Steeg, 2003).

The principle sites of metastasis in breast cancers are the bone, lungs, liver and brain . The incidence of metastases to the brain and lungs is higher compared to the liver and bone for triple-negative breast cancers. This indicates a site specific preference which is controlled by the presence or the absence of hormones.

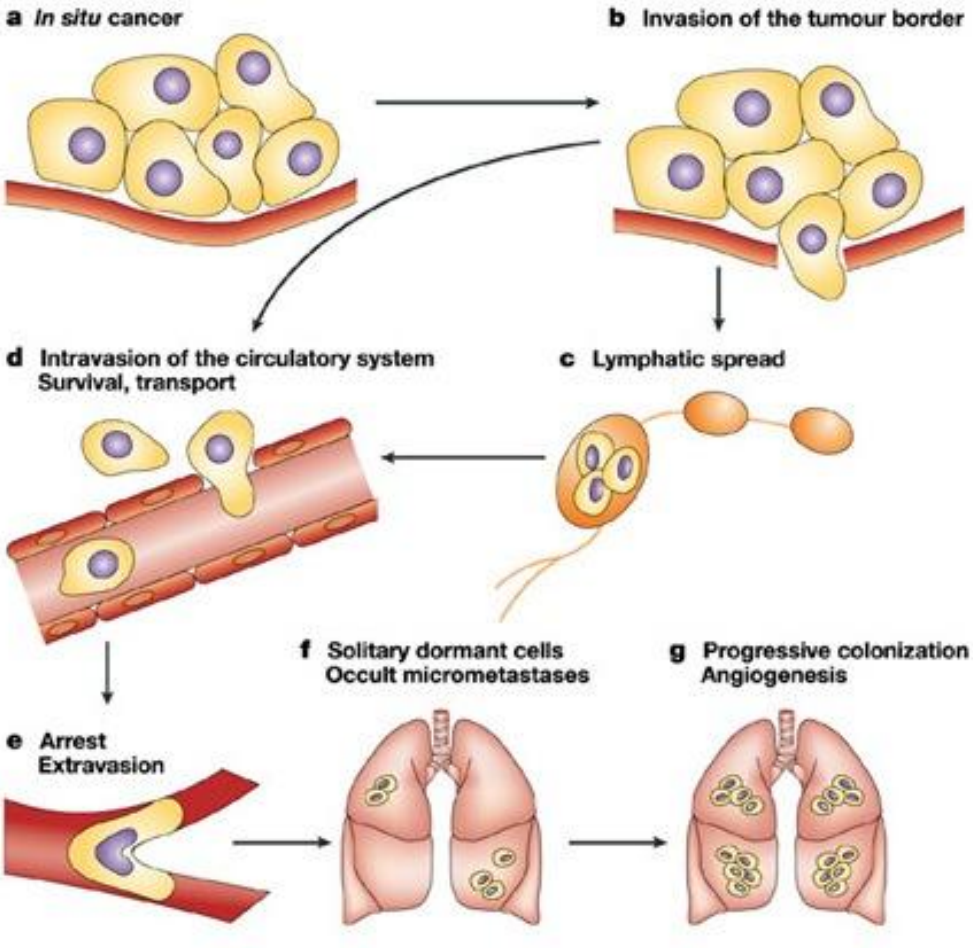

Figure 1. The metastasis cascade (Adapted from Steeg, 2003).

1.2.1 Tumor Angiogenesis

Angiogenesis is the formation of new blood vessels from pre-existing vasculature. It can occur under normal physiological conditions to aid wound healing or during pregnancy to provide the blood circulation between the mother and her fetus. The establishment of angiogenesis ensures that cell proliferation, migration and differentiation will occur subsequently. These require a balance of both pro-angiogenic and anti-angiogenic factors. Angiogenin (Fett et al., 1985), fibroblast growth factor (Gospodarowicz, 1976), interleukin-8 (Smith et al., 1994), placental growth factor (Takahashi et al., 1994), platelet-derived growth factor (Ishikawa et al., 1989), transforming growth factor α and β (Falcone et al., 1993) and vascular endothelial growth factor (Takahashi et al., 1994) are some examples of genes that promote angiogenesis. On the other hand, anti-angiogenic factors include endostatin, human chorionic gonadotrophin, interferon α, β and γ, thrombospondin-1, tissue inhibitors of matrix metalloproteinases and vasostatin (Bridges and Harris, 2011; Sharma et al., 2011; Zogakis and Libutti, 2001). Deregulation of these genes will disrupt the balance and favor persistent angiogenesis to occur, resulting in diseases like diabetic retinopathy (Murata et al., 1995), rheumatoid arthritis (Folkman, 1995), age-related macular degeneration (Lip et al., 2001) and cancers (Folkman, 1995).

1.2.2 Disaggregation of cells from primary tumor

Loss of cell-cell adhesion within the primary tumor mass permits the disaggregation of tumor cells and hence aids initial dissemination. Compared with normal epithelial cells, cancer cells show diminished cell-cell adhesiveness (Cavallaro and Christofori, 2004). Cadherins are a large family of adhesion molecules that interact with the actin

component of the cytoskeleton and are involved in maintaining the tight intercelluar adhesion interactions (Angst et al., 2001). Abrogation of E-Cadherin had been shown to be associated with the metastatic phenotype in cancers (Christofori and Semb, 1999; Perl et al., 1998). The down-regulation of E-Cadherin has also been reported *in vivo* in breast cancers (Meyer and Hart, 1998; Perl et al., 1998). Additionally, catenin was shown to be required for cell-cell adhesion as the lack of it resulted in weak adhesion (Watabe et al., 1994).

1.2.3 Invasion and ECM degradation

Invasion is the active translocation of neoplastic cells across tissue boundaries and through host cellular and ECM barriers. It is dependent on the concerted efforts of several proteins from within the cell to cell surfaces as well as the external microenvironment. The family of cell-cell adhesion receptors (CAMs) has been widely studied for their role in cancer invasion. For example, intercellular adhesion molecules (ICAMs), L-, E- and P-selectins, vascular cell adhesion molecules (VCAMs) and neural cell adhesion molecules (NCAMs) have all been reported to be overexpressed in metastatic cancers (Buitrago et al., 2011; Johnson, 1999; Yamaoka et al., 2011).

Under normal physiological conditions, proteolysis of ECM is seen during wound healing, tissue remodelling, embryo morphogenesis and trophoblast implantation (Curran and Murray, 2000). Degradation of the ECM by matrix metalloproteinases (MMPs) is essential for almost every step in metastasis, for example in aiding cells crossing the ECM barriers and the epithelial membrane as well as facilitating

intravasation, extravasation and colonization at distant sites (Egeblad and Werb, 2002). A tilt in the delicate balance in the regulation of proteases and protease inhibitors can cause uncontrollable invasion to occur.

The family of MMPs is one of the major enzymes that degrade the ECM. So far, there are at least 24 different MMPs known to exist in the mammalian systems (Curran and Murray, 2000; Klein and Bischoff, 2011). All the MMPs possess specific domains that are conserved between different members. The presence of zinc ions at the catalytic active site determine the enzyme's activity (Klein and Bischoff, 2011). Most MMPs are synthesized and secreted in a zymogen form (pro-enzyme) and activation of the enzyme is necessary to cleave off a 10kDa amino-terminal domain (Baramova et al., 1994). Based on their domain organisation and substrate specificity, the members of this family are divided into 4 subgroups, namely (i) interstitial collagenases; (ii) gelatinases; (iii) stromelysins and (iv) membrane-type MMPs. The collagenases subgroup consist of MMP1, MMP8 and MMP13. These MMPs catalyse the degradation of fibrillar forms of collagen.

1.2.4 Gelatinases or Type IV collagenases

The gelatinases, also known as type IV collagenases, degrade gelatin and types IV, V, VII, IX and X collagen, of which type IV collagen being the most abundant in the basement membranes. MMP2 (gelatinase A) and MMP9 (gelatinase B) are the two members in this subgroup (Deryugina and Quigley, 2006). They are thought to have similar substrate specificity with respect to ECM substrates, but different towards growth factor receptors (Levi et al., 1996). Besides degradation of the ECM and

basement membrane, MMPs also aid in the release of growth factors, for instance VEGF and fibroblast growth factor (FGF), which then stimulate angiogenesis (Curran and Murray, 2000). However, how MMPs can mediate these regulations remain unknown.

There have been many evidence over the decades documenting the association of MMPs in the process of tumorigenesis and metastasis. For instance, back in the 1990s, it was already shown that MMP2 and MMP9 are highly expressed in invasive colon, gastric, ovarian and thyroid adenocarcinomas compared to normal colorectal, gastric mucosa and benign ovarian cysts (Levy et al., 1991; Liu et al., 2010; Monteagudo et al., 1990). In a recent study, the immunohistochemical expression of MMP2 and MMP9 and the correlation between their expression levels and prognostic clinicopathological parameters were investigated in 140 patients with IDC (Sullu et al., 2011). Their study showed that MMP9 staining was the strongest in high grade, triple-negative and ER-negative tumors and tumors with distant metastases. At the same time, it was known that high MMP9 expression was associated with a shorter disease-free survival and overall survival times, hence indicating high MMP9 expression is related to poor prognostic clinicopathological factors in IDC. On the other hand, MMP2 expression did not show consistent nor significant findings. In another study, high serum levels of MMP9 are linked to rapid progression, poor overall survival and secondary metastasis in cancer patients with melanoma (Nikkola et al., 2005).

1.2.5 TIMPs

Proteolytic activity of MMPs are inhibited by tissue inhibitors of metalloproteinases (TIMPs). They perform their function by forming high-affinity 1:1 stoichiometric, non-covalent complexes with the active MMPs (Baramova et al., 1994; Deryugina and Quigley, 2006). There are four members in the TIMP family, namely TIMP1, 2, 3 and 4. Each of their N- and C-terminal domains contains six conserved cysteine residues that form three disulfide loops (Stetler-Stevenson, 2008). The N-terminal region binds to the MMPs' catalytic domain and inhibits MMP activity, whereas the C-terminal region interacts with the pro-forms of MMP2 and MMP9 C-terminal hemopexin domain to stabilize the proenzyme inhibitor complex. TIMPs are able to inhibit all active MMPs, but not with the same efficacy. TIMP1 preferentially inhibits MMP1, MMP3, MMP7 and MMP9 while TIMP2 is more effective in inhibiting MMP2. TIMP3 can inhibit MMP2 and MMP9, while TIMP4 inhibits MMP2 catalytic activity (Bourboulia and Stetler-Stevenson, 2010).

Besides being the inhibitors of MMPs, TIMPs are also revealed to be involved in several biological activities including cell differentiation, angiogenesis and apoptosis (Brew and Nagase, 2010; Stetler-Stevenson, 2008). TIMP2 inhibits the endothelial cell growth *in vitro* and angiogenesis *in vivo* upon stimulation with endothelial growth factors, VEGF-A or FGF-2. The identified mechanism is independent of TIMP2-mediated MMP inhibition (Stetler-Stevenson, 2008).

1.2.6 MMPs as targets in anti-metastatic therapies

Due to the strong and direct association of MMPs in breast cancers, an inhibition of the enzyme's activity and function will help to inhibit tumor metastasis. However, due to their multiplicity and widespread effects of their actions, TIMPs cannot be used as an anti-cancer target. Hence, most research has focused on synthetic inhibitors. Different types of synthetic MMPs inhibitors like peptidomimetics, non-peptidomimetics inhibitors, tetracycline derivatives target MMPs in the extracellular space (Brown, 2000; Overall and Lopez-Otin, 2002). Some used antisense and small interfering RNA (siRNA) to selectively decrease the level of mRNA of a specific MMP. However, targeted delivery of these oligonucleotides to the tumor site poses a huge problem (Brown, 2000). Systemic use of siRNA for therapies is still controversial due to the limitations of siRNA such as low enzymatic tolerability, cellular internalization and body distribution after systemic administration (Guo et al., 2010; Pirollo and Chang, 2008; Tamura and Nagasaki, 2010).

Marimastat, a broad spectrum peptidomimetic MMPs inhibitor, mimics the peptide structure of natural MMP substrates and binds to MMPs, thereby preventing the degradation of the basement membrane by these proteases. It was found to show significant increase in survival in patients with early stage, metastasis-free disease (Bramhall et al., 2001). However, this drug has side effects like musculoskeletal syndrome which requires attention for patients on this treatment. Non-peptidomimetic MMPs inhibitors like BAY12-9566, prinomastat and BMS-275291 are synthesized based on the crystal structure of the active site of MMPs to improve specificity and oral bioavailability compared to peptidomimetic inhibitors (Price et al., 1999; Tonn et al., 1999). However, they also met with limited efficacy and side effects in several

clinical trials. The trial involving the use of BAY12-9566 in patients with small cell lung cancer showed a significant increase in both disease progression and mortality in the treated group when compared with placebo (Brown, 2000). The side effects of marimastat are characterised as a musculoskeletal syndrome which persists if patients continue to take the drug in the face of symptoms (Moore et al., 2003).

Another generation of MMPs inhibitors, tetracycline derivatives, inhibit the enzymatic activity of MMPs as well as blocking the transcription of MMPs. Metastat (COL-3), minocycline and doxycycline are some members in this family of inhibitors. Their toxicity level are lower and doxycycline is currently the only Food and Drug Administration (FDA) approved MMPs inhibitor for the prevention of periodontitis (Sapadin and Fleischmajer, 2006). However, its effect on the treatment of metastatic breast cancer remains unknown.

A major limitation in using MMP inhibitors in cancer therapy is the method of evaluation of their efficacy in clinical trials. Traditional readouts such as tumor size, proliferation and apoptosis markers are not likely to be affected by anti-invasive strategies. Metastatic progression of a cancer is also a very indirect readout of cell invasion and cannot be easily assessed in phase I and II trials with patients who are already in their advanced stage of cancer (Overall and Lopez-Otin, 2002). The multi-level complexities of the process of metastasis from the first step of angiogenesis to the last step of development of the secondary tumor makes it difficult to determine accurately the stages of cancer and or predict treatment response.

A shift in the mindset to profile a tumor could be important. Besides evaluating a tumor histopathologicaly and genetically, the susceptibility of a tumor towards metastasis could serve as a prognostic framework for targeted treatments. Hence, the desire to identify good prognostic and predictive markers for metastatic breast cancers remains strong and urgent.

1.3 DEAD/DExD Box Family

RNA and DNA helicases are enzymes that catalyze the separation of double-stranded nucleic acids in an energy-dependent manner. They utilise the free energy change of binding and hydrolyse a nucleotide triphosphate to dissociate duplexes or displace bound proteins. Helicases are classified into three superfamilies and two families by the occurrence and characteristics of conserved motifs in the primary sequence.

DEAD-box and the related DEAH, DExH and DExD families belong to the superfamily 2 of the RNA helicases. They share eight conserved motifs (Tanner and Linder, 2001), but can be differentiated by variations within them. The DEAD-box family is the largest of the superfamily and is characterised by the presence of nine conserved motifs. Over 40 members of the DEAD-box family have been isolated from a variety of organisms including bacteria, yeast, insects, amphibians, mammals, and plants (Jankowsky and Jankowsky, 2000; Linder and Slonimski, 1989). The conserved motifs in DExD/H helicases are clustered in a 'central' core region that is about 350 to 400 amino acids long, while DEAD box helicase members have a characteristic amino acid sequence Asp-Glu-Ala-Asp (D-E-A-D) in the Walker B motif, hence their name is dervied. Motif A (AXXGXGKS/T) has an ATPase activity. These two motifs, as known as Motifs I and II, are responsible for the binding of the nucleotide triphosphate-Mg^{2+} complex (Wittinghofer and Pai, 1991). Motif III is defined as having a helicase function and Motif VI has been thought to bind nuclei acids (Korolev et al., 1998).

DEAD-box proteins commonly display ATP-dependent RNA helicase activity (Crawford et al., 1997) and have been shown to have important roles in cell

development, differentiation and proliferation. Although some DEAD-box proteins play general roles in cellular processes such as translation initiation (eukaryotic initiation factor 4A (Rozen et al., 1990)), RNA splicing (PRP5, PRP28, and SPP81 in yeast (Dalbadie-McFarland and Abelson, 1990; Jamieson et al., 1991; Strauss and Guthrie, 1994)), and ribosomal assembly (SrmB in *Escherichia coli* (Nishi et al., 1988)), the function of most DEAD-box proteins remains unknown.

1.3.1 Roles of DEAD-box proteins

DEAD-box proteins are involved in the regulation of many processes involving RNA, from transcription level to degradation as shown in Figure 2.

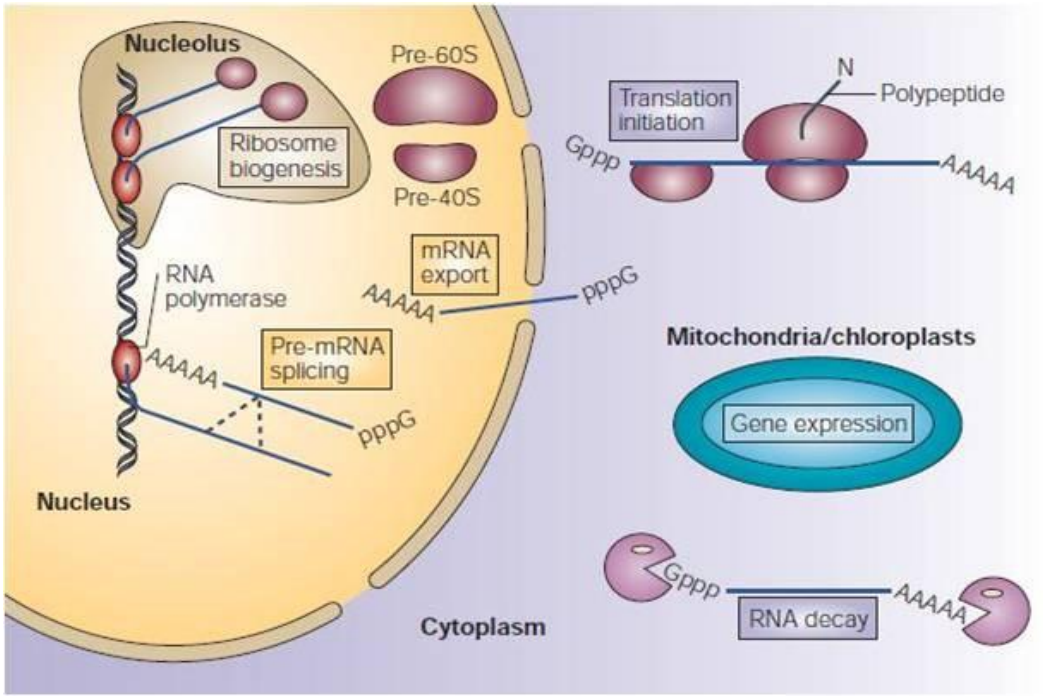

Figure 2. Functions of DEAD box proteins (Adapted from Rocak and Linder, 2004).

Firstly, some DEAD-box proteins are found to be associated with gene transcription. For instance, DP103 is found to be a co-repressor in transcription of several genes, which will be discussed extensively in chapter 1.4. Other DEAD-box members p68 and p72 which are highly related to each other but also having distinct non-overlapping functions, were found to be coactivators and corepressors of transcription. p68/p72 both act as a coactivator for ERα (Endoh et al., 1999; Watanabe et al., 2001; Wilson et al., 2004). Later, it was discovered that p68/p72 interacts with the histone acetyltransferases CREB binding site (CBP)/p300, indicating p68 and p72 to be important components in the transcription machinery (Fujita et al., 2003). They also function as corepressors during their interaction with HDAC1 (Wilson et al., 2004). Interestingly, p68 acts as a coactivator of the transcriptional function of p53 in response to DNA damage (Bates et al., 2005), but represses p53-dependent expression of Δ133 p53 isoform (Moore et al., 2010).

Another function of DEAD-box proteins involves splicing of pre-mRNA. Prp5 is found to be required in the early stages of pre-spliceosome assembly (Xu et al., 2004) while p68, Sub2/UAP56, Ded1 and Prp28 are involved in the progression towards the active spliceosome (Rocak and Linder, 2004).

Ribosome biogenesis marks another function of DEAD-box proteins and a large number of them are associated with rRNA maturation in eukaryotes and prokaryotes (de la Cruz et al., 1999). However, their precise role during ribosome biogenesis is not known though some suggest that they have an RNA-RNA rearrangement activity *in vivo*, on top of their bona fide ATPases and helicases activity (Nicol and Fuller-Pace, 1995; Rocak et al., 2005).

Several DEAD-box proteins are associated with the export of mRNA through the nuclear pore. One of them is Dbp5, which binds RNA cotranscriptionaly. It interacts with the nuclear pore complex and shuttles between the nucleus and cytoplasm (Weirich et al., 2004; Zhao et al., 2002). On the other hand, eIF4A and Ded1 from *S. cerevisiae* are found to be essential for translation initiation (Linder, 2003).

1.3.2 DEAD-box proteins in cancers

There has not been many reports on the relevance of members of the DEAD-box family on cancers. Of those that were reported, most of the DEAD-box proteins are upregulated in different cancers. However, the mechanisms behind this upregulation are not elucidated.

Both p68 and p72 are found to be overexpressed in colon adenomas and carcinomas, with p68 being ubiquitinated in these tumors (Causevic et al., 2001; Shin et al., 2007). Furthermore, proliferation and the ability to form tumors *in vivo* were greatly decreased when both p68 and p72 were suppressed (Shin et al., 2007). p68 is also overexpressed in prostate cancer and is associated with higher tumor grades and poor prognosis in patients (Clark et al., 2008). p68 is involved in aberrant post-translational modification, whereby its phosphorylation is associated with cancer development, but this is not seen in p72 (Yang et al., 2007). More studies will need to be carried out to elucidate the mechanisms as to how these DEAD-box proteins play their role in cancer development.

Ddx3, on the other hand, is involved in the transformation of epithelial to mesenchymal transition. It was also shown to promote cell motility and invasion, as well as the ability to form colonies in soft agar, via the downregulation of the expression of the cell adhesion molecule E-cadherin (Botlagunta et al., 2008). $p21^{waf1/cip1}$ was subsequently identified to be a target gene of Ddx3, and the up-regulation of $p21^{waf1/cip1}$ expression accounted for the colony-suppressing activity of Ddx3, all of which are independent of its helicase activity. Furthermore, a declined expression of Ddx3 mRNA and protein was found in a significant number of hepatoma specimens, leading to the reduction of $p21^{waf1/cip1}$ expression, independently of p53 status. All these suggest that Ddx3 might be a candidate tumor suppressor gene (Chao et al., 2006).

In hereditary, non-hereditary retinoblastoma (RB) and neuroblastoma, both copies of the RB1 gene were shown to be mutated (Bookstein et al., 1988). MYCN oncogene amplification is also required for the formation of these malignant tumors (Schwab, 1991). Ddx1 is often found to be co-amplified with MYCN in both of these childhood tumors (Godbout et al., 1998). A tissue microarray from 176 primary breast cancer samples found Ddx1 to be overexpressed and half of the patient cohort had experienced early relapse despite standard adjuvant therapy. They observed cytoplasmic staining of Ddx1 which was thought to be a nuclear enzyme, hence associating this with the early recurrence in patients with breast cancer (Germain et al., 2011). However, the authors failed to provide validation for their microarray data by alternative technology such as qPCR. Instead they provided data through their use of matched tissue microarrays from a subset of the initial cohort. Despite this, the

authors did not show any correlative data between Ddx1 mRNA expression and Ddx1 cytoplasmic staining (Balko and Arteaga, 2011).

Another DEAD box member, Ddx48 was identified as a novel autoantigen in 2005 (Xia et al., 2005). ELISA results using patients sera showed that humoral response directed against Ddx48 occurred in 33.33% of pancreatic cancer patients, 10% in colorectal cancer patients, 6.67% in gastric cancer patients and 6.67% in hepatocellular cancer patients. None of the sera from patients with chronic pancreatitis, lung cancer and normal individuals exhibited reactivity against it.

1.4 DP103 / Ddx20 / Gemin 3

DP103 (also termed Gemin3 and DDX20) is a member of the DEAD-box family of helicases. It is a protein of 824 amino acids that contains the DEAD-box motif at its N terminus (Figure 3) and had been cloned by several groups (Campbell et al., 2000; Charroux et al., 1999; Grundhoff et al., 1999; Ou et al., 2001).

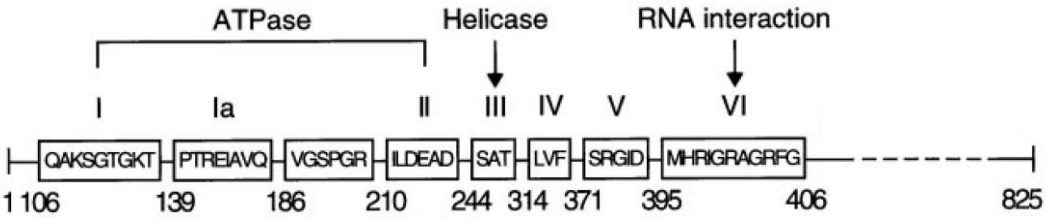

Figure 3. Pictorial representation of DP103 showing different motifs (Adapted from Ou et al., 2001).

DP103 was first characterised by Grundhoff and group in 1999 and they showed DP103 interacts directly with Epstein-Barr virus nuclear antigens EBNA2 and EBNA3C which regulates transcription of both latent viral and cellular genes. This 103kDa protein was observed in EBV-positive and EBV-negative B cell lines as well as in the T-cell line Jurkat, in SK-NS-H neuroblastoma cells and HeLa cells. The N-terminal and C-terminal of DP103 do not show any significant homology to other proteins within or outside the DEAD box family, hence suggesting a possible specialised role of these regions of DP103. The C-terminal region was shown to interact with EBNA2 and EBNA3C, another indication that the C-terminal region may be important in mediating its interaction with other cellular proteins, for example cofactors. DP103 was almost exclusively found in the soluble nuclear fractions in these cell lines. Additionally, in a panel of human tissues, *DP103* gene expression was

found to be low in colon, skeletal muscle, liver, kidney and lung, but very strong expression in primary malignant melanoma tumor samples, an indication that DP103 may be highly expressed in proliferating cells (Grundhoff et al., 1999).

DP103 was then found to interact with the spinal muscular atrophy protein, SMN to modulate gene expression. SMN is part of a multiprotein complex and together with SIP1 (SMN interacting protein 1), they are concentrated in gems bodies. SMN and SIP1 are important for the assembly of small nuclear ribonucleoproteins (snRNPs) (Liu et al., 1997), where Sm proteins combine with snRNAs that are exported from the nucleus. Once properly assembled and modified, the snRNPs recruit the necessary nuclear import receptors and translocate into the nucleus where they function in pre-mRNA splicing (Zieve and Sauterer, 1990). Importantly, DP103 was found to co-localise with SMN in gems, with its C-terminal mediating the interaction (Charroux et al., 1999).

More information about the function of DP103 was unveiled in 2001 when Ou et al discovered DP103 to be a regulator of steroidogenic factor-1 (SF-1) which is essential for development of the gonads, adrenal gland and the ventromedial hypothalamic nucleus. SF-1 plays a pivotal role in regulating the expressions of steroidogenic enzymes and proteins in the endocrine and reproductive system. The loss of this protein results in abnormal gonadotrope differentiation, phenotypic male-to-female sex reversal, low serum levels of corticosteroids and early neonatal death (Luo et al., 1994; Shinoda et al., 1995). In this aspect, DP103 acts to repress the transcriptional activity of SF-1, thereby down-regulating SF-1 target genes during development and function of reproductive and steroid-producing tissues. At the same time, they

deduced that it is the C-terminal region of DP103 that is capable of repressing the transcriptional activity. Additionally, the RNA helicase activity of DP103 is dispensable for the repression influence. Post-translational modifications were then found to be able to modulate the receptor activity. Phosphorylation of SF-1 is thought to increase the receptor activity while SUMOylation will result in transcriptional repression (The mechanism of SUMOylation will be covered in chapter 1.5). Interestingly, DP103 was found to promote PIAS-mediated SUMOylation of SF-1 (Lee et al., 2005b), bringing to light for the first time a functional mechanism for the repressive ability of DP103. The importance of DP103 was amplified when Mouillet and group showed that homozygous DP103-null mice die early in embryonic development, before a four-cell stage. At the same time, although heterozygous mice are healthy and fertile, the females have larger ovaries, altered estrous cycle and reduced basal secretion of adrenocorticotopic hormone (ACTH) (Mouillet et al., 2008).

DP103 acting as a co-repressor was again demonstrated in macrophages. Induction of Ets repressor METS during macrophage differentiation contributes to terminal cell cycle arrest by repressing the transcription of cell cycle control genes like *c-Myc*, *c-Myb* and *Cdc2*. METS selectively repress Ets target genes involved in Ras-dependent proliferation, but does not repress genes that are targets of Ras-dependent differentiation. DP103 was found to be co-immunoprecipitated with METS, and subsequently elucidated that the C-terminal domain of DP103 interacts with METS directly and is important for the anti-proliferative effects (Klappacher et al., 2002). However, the mechanisms responsible for this repression remained uncovered. DP103 was also found to interact with and repress the Early Growth Response 2 (Egr2/Krox-

20) transcription factor, which is important for myelination of the peripheral nervous system and for establishing segmentation in the developing vertebrate hindbrain (Gillian and Svaren, 2004). The transcriptional repression by DP103 was postulated to act through the recruitment of histone deacetylases (HDAC) as DP103 was shown to co-immunoprecipitate with HDAC2 and HDAC5 (Klappacher et al., 2002). DP103 therefore demonstrates intrinsic transcriptional repression activity through direct interaction with various proteins. Its role as a transcriptional coactivator, on the other hand, remain elusive.

Despite the above studies on the functions of DP103, its connection to cancer was unknown, until a study done in 2005. A protein microarray was done on mantle-cell lymphoma patients and showed an increase in DP103 expression in these patients (Ghobrial et al., 2005). Furthermore, in another microarray data done on colorectal cancer (CRC) patients' tissues, when comparing gene expression profile in primary tumors with and without distant metastases, DP103 expression is found to be upregulated in CRC patients that developed distant metastases ($n=100$; $p<1 \times 10^{-10}$, http://www.ebi.ac.uk/arrayexpress [Array express ID: E-GEOD-18105]). These point to a high possibility of the association of DP103 not only to cancer, but also possible anew marker for metastasis.

The link between DP103 to metastasis was further strengthened in a recent United States Patent Application by Chan et al. published in 2010 on the use of compounds that block cancer metastasis showed DP103 as the only DEAD-box helicase member to be a potential target listed in the patent from their microarray data (Publication

Number: US 2010/0004190 A1). These suggest a possible role of DP103 in tumorigenesis and in particular, cancer metastasis.

1.5 SUMOylation

1.5.1 The SUMO family

SUMO (Small ubiquitin-related modifier) was discovered to be a reversible post-translational protein modifier in the late 1990s. SUMO proteins are ubiquitously expressed in eukaryotes. In yeast, the SUMO homologue is called SMT3 (suppressor of mitf two 3). Other organisms, like plants and vertebrates, have several SUMO genes.

In humans, there are 4 distinct members, namely SUMO1, SUMO2, SUMO3 and SUMO4. These proteins are about 12kDa in size and resemble the three-dimensional structure of ubiquitin (Bayer et al., 1998). Though so, there is less than 20% similarities in the amino acid sequences with ubiquitin and are different in their overall surface-charge distribution. On top of that, SUMO proteins have an unstructured stretch of 10-25 amino acids at their N-terminal that is not found in any other ubiquitin-related proteins. So far, the only function for this N-terminal tail is the formation of the SUMO chains. SUMO1, SUMO2 and SUMO3 are ubiquitously expressed throughout the organism, whereas SUMO4 seems to be expressed mainly in the kidney, spleen and lymph node (Guo et al., 2004).

SUMO proteins are expressed in an immature form, where they have a C-terminal stretch of amino acids of varying lengths after the Gly-Gly motif. SUMO-specific proteases like sentrin-specific proteases (SENPs) cleave away this extension for conjugation of SUMO to its targets to occur. The mature forms of SUMO2 and SUMO3 are 97% identical, but only share 50% sequence homology with SUMO1.

And thus, SUMO1 and SUMO2/3 are described to serve distinct functions with conjugation to different target proteins (Rosas-Acosta et al., 2005; Saitoh and Hinchey, 2000). SUMO4, on the other hand, is not widely studied and is unclear whether it can be cleaved into the mature form *in vivo* and if it is functional (Guo et al., 2004; Owerbach et al., 2005).

SUMOylation is an essential process in most organisms. For example, disruption of SUMO1 in mice led to embryonic lethality and SUMO1 haploinsufficiency resulted in split lip and palate in mice, an indication of possible developemental defects (Alkuraya et al., 2006).

1.5.2 The SUMOylation pathway

SUMOylation is directed by an enzymatic cascade analogous to that in ubiquitination. The SUMOylated pathway is outlined in Figure 4. The first step of SUMOylation is the activation of a mature SUMO protein, as mentioned earlier, by the SUMO-specific E1 activating enzyme heterodimeric AOS1-UBA2 (Desterro et al., 1999; Okuma et al., 1999). The C-terminal of this mature form has a diglycine motif that is required for the effective adenylation by the SUMO E1 enzyme. Once formed, the SUMO adenylate is attacked by a conserved Cys on the E1 enzyme to form an E1-SUMO thioester, which is then transferred to a conserved Cys on a SUMO E2 enzyme, thereby generating an E2-SUMO thioester. The E2 conjugating enzyme for SUMOylation is Ubc9, which is the one and only E2 enzyme known thus far. Many SUMO-modified proteins contain an acceptor Lys within a ψKX(D/E) consensus motif, where ψ is a large hydrophobic residue (Rodriguez et al., 2001). These residues

directly interacts with Ubc9 and have a critical role in regulating the stability of interactions between the E2 enzyme and the substrate (Sampson et al., 2001). Finally, Ubc9 transfers SUMO to the substrate, an isopeptide bond is formed between the C-terminal Gly residue of SUMO and a Lys side chain of the target, catalysed by the SUMO E3 ligases .

SUMO E3 ligases are characterised by the presence of the SP-RING motif. SP-RING ligases bind their targets and Ubc9 directly and bind SUMO non-covalently via a SUMO-interacting motif (SIM). One of the subgroups of SP-RING ligases is the family of PIAS (protein inhibitor of activated STAT) proteins. In humans, the members include PIAS1, PIAS3, PIASxα, PIASxβ and PIASy. Other subgroups of SP-RING ligases include MMS21 or NSE2 which is part of an octameric SMC5-SMC6 complex essential for DNA repair and vegetative growth and also telomerase-independent mechanisms of telomere lengthening in alternative lengthening of telomeres (ALT) cells (Potts and Yu, 2007). The third class of SUMO E3 ligases is the human Polycomb group member Pc2. Polycomb group proteins (PcG) form PcG bodies which are involved in gene silencing.

PIAS family members are the best known E3 ligases for the process of SUMOylation and were initially identified in studies for understanding the JAK/STAT pathway (Chung et al., 1997; Liu et al., 1998). PIAS1, PIAS3 and PIASx were shown to interact with STAT1, STAT3 and STAT4 respectively (Arora et al., 2003; Chung et al., 1997; Liu et al., 1998), resulting in the inhibition of STAT-mediated gene activation. Subsequently, studies showed that this inhibition is brought about by the SUMOylation of STAT1, strongly enhanced by PIAS proteins (Rogers et al., 2003).

This post-translational modification is critical in the STAT pathway for the proper regulation of cytokine signaling pathways (Shuai, 2006).

PIAS proteins have also been revealed to be required in the regulation of NF-κB pathway. Both PIAS1 and PIAS3 had been observed to interact with p65, thereby repressing its transcriptional activity (Jang et al., 2004; Liu et al., 2005). In addition, PIASy was shown to interact with NEMO to enhance its SUMOylation under genotoxic stress (Mabb et al., 2006).

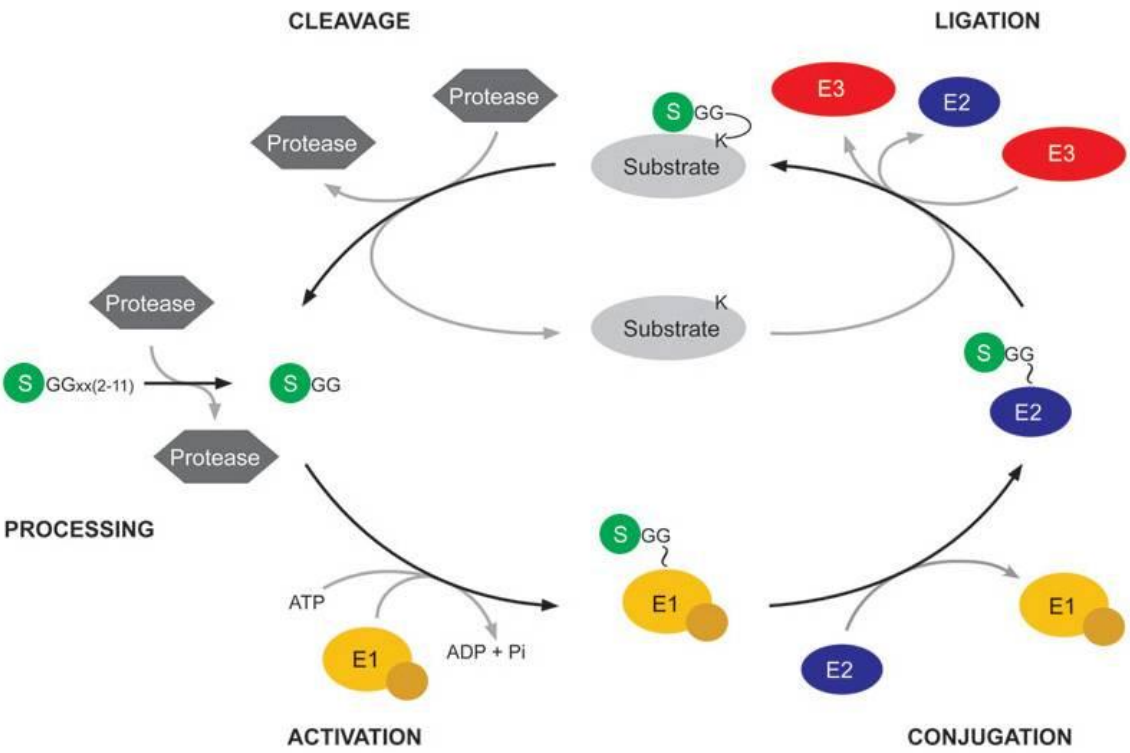

Figure 4. The mechanism of SUMOylation. (Adapted from Katharina Maderböck and Andrea Pichler, Conjugation and Deconjugation of Ubiquitin Family Modifiers (book chapter)).

Usually, SUMOylation results in the addition of a single SUMO protein to individual acceptor Lys residues. However, the formation of polySUMO chains has been observed both *in vivo* and *in vitro*. For example, in mammalian, SAE1/SAE2 and Ubc9 catalyze the formation of polymeric chains of SUMO2 and SUMO3 on protein substrates *in vitro* and SUMO2 chains are detected *in vivo* (Tatham et al., 2001). However, this ability is not shared by SUMO1, reiterating that modifications by SUMO1 and SUMO2/3 may have distinct functional consequences.

Proteases are required for the deSUMOylation of substrates from the SUMO groups. So far, a single gene family that encodes SUMO-specific Cys proteases has been identified. In yeasts, they are Ulp1 and Ulp2 (Li and Hochstrasser, 1999; Li and Hochstrasser, 2000) and in humans, the homologues are sentrin-specific proteases, SENPs. There are six members in this family, namely SENP1, SENP2, SENP3, SENP5, SENP6 and SENP7 (There is no SENP4). SENP proteins are also required for the maturation of newly synthesized SUMO proteins. Members in this family differ in their activity in maturation, isopeptide cleavage and also their activity towards different SUMO proteins. SENP3 and SENP5 prefer to deSUMOylate SUMO2/3 from substrates (Di Bacco et al., 2006). In terms of localisation, SENP2 complexes with nuclear pore proteins (Zhang et al., 2002) while SENP5 is enriched in the nucleolus. SENP1, on the other hand, shuttles between cytoplasm and the nucleus (Bailey and O'Hare, 2004).

1.5.3 The SUMOylation consequences

In contrast to ubiquitin, SUMO is not used to tag proteins for degradation. SUMOylation can promote or inhibit the formation of specific protein complexes, affect subnuclear localization of proteins and regulate transcription positively and/or negatively (Hay, 2005).

Generally, there are three consequences for a modified protein. Firstly, SUMOylation can interfere with the interaction between the target and its partner. For instance, SUMOylated p300 interacts with HDAC6, resulting in transcriptional repression (Girdwood et al., 2003). SUMOylation of p68, on the other hand, was enhanced by the presence of PIAS1, which in turn can act as a transcriptional co-activator or a co-repressor (Bates et al., 2005; Caretti et al., 2006).

Secondly, SUMOylation provides a binding site for an interacting partner, typically via a non-covalent SUMO-interaction/binding motif (SIM/SBM). Daxx is one of the very few proteins to possess a SIM/SBM motif and findings showed that Daxx requires this non-covalent SUMO interaction for repression (Kuo et al., 2005).

Lastly, SUMOylation can result in a conformational change of the modified target. A known example is the SUMOylation of DNA-repair enzyme thymine DNA glycosylase (TDG). TDG recognizes and binds to a mismatch on DNA and excises the corrupted base. However, TDG binds tightly to the reaction product, with which SUMOylation of TDG helps to reduce the DNA affinity via a conformational change. This then allows release of the enzyme into the nucleoplasm (Hardeland et al., 2002).

1.5.4 SUMOylation, cancer progression and metastasis

The SUMOylation process is involved in several aspects of cancer including the onset of tumor formation to metastasis. Here, I shall discuss some SUMO target genes that are involved in tumorigenesis.

Androgen receptor (AR) is a critical transcription factor for prostate cancer development and progression (Balk and Knudsen, 2008) and has been identified as a SUMO target in which SUMOylation reduces hormone-induced transcriptional activity of AR (Poukka et al., 2000). DeSUMOylation of HDAC1 by SENP1 was found to enhance AR-dependent transcription via reduction of deacetylase activity in the transcription complex (Cheng et al., 2004). In accordance with this report, SENP1 is overexpressed in human prostate cancers specimens (Cheng et al., 2006).

The transcriptional activity of ER and PR has been shown to be regulated by SUMOylation. SUMOylation on ERα within the hinge region is critical for ERα-dependent transcriptional activation (Sentis et al., 2005). On the contrary, PR SUMOylation represses its transcriptional activity (Daniel et al., 2007). The examples of AR, ER and PR suggest that in such nuclear hormone-receptor associated transcription machinery, post translational modifications may hold significant roles to the tight regulation of the activity of these receptor. Errors in this regulation may result in the induction of hyperproliferation of cells and thus contribute to cancer development and progression.

SUMOylation is also involved in p53-mediated cellular processes such as senescence and DNA repair. The ectopic expression of PIASy induces premature senescence in

human primary fibroblasts, and its deficiency results in the delayed onset of Ras-induced senescence in murine embryonic fibroblasts (Bischof and Dejean, 2007; Bischof et al., 2006). p53, itself, can be SUMOylated and studies had shown that it leads to its reduced activation (Gostissa et al., 1999; Muller et al., 2000).

The final stage of cancer progression is metastasis, and although the role of SUMOylation in this process has not been widely studied, recent reports indicate strongly that SUMOylation plays critical roles in the expression of metastatic suppressor gene *KAI1/CD82* and also in the regulation of TGF-β signaling (Kang et al., 2008; Kim et al., 2005).

KAI1 is a member of tetraspanin family that suppresses tumor metastasis by inhibiting cancer cell mortality and invasiveness (Dong et al., 1995; Liu and Zhang, 2006). While overexpression of *KAI1* gene represses tumor metastasis in mouse models (Dong et al., 1996; Kim et al., 2005), its expression is significantly downregulated in a variety of clinically adanced cancers of the prostate, bladder, esophagus squamous cells and also the breast (Dong et al., 1996; Uchida et al., 1999; Yang et al., 2000; Yu et al., 1997). Studies revealed the role of Tip60, a transcriptional coactivator, who contribtes to KAI1 expression. In these studies, Tip60 acts as an antagonist for β-catenin and in metastatic cancer cells, the β-catenin/reptin corepressor complex replaces Tip60 (Kim et al., 2005). SUMOylation of reptin then potentiates the association between reptin and HDAC1 and enhances the repressive function (Kim et al., 2006b). At the same time, SENP1 had been shown to modulate the deSUMOylation of reptin to release the repressive ability (Kim et al., 2006b).

Tumor-derived TGF-β promotes tumor cell metastasis by inducing epithelial-mesenchymal transition and angiogenesis (Leivonen and Kahari, 2007). TGF-β signals through serine/threonine kinase receptor complexes which includes type I (TβRI) and type II (TβRII) receptors. Kang and group identified TβR1 to be a SUMO target in 2008 (Kang et al., 2008). SUMOylation of TβRI requires the kinase activation of both TβRI and TβRII, and it enhances the affinity of TβRI kinase to Smad proteins, which are the cytoplasmic mediators in the TGF-β pathway. This resulted in a more efficient phosphorylation and activation of Smad2/3 in response to TGF-β (Kang et al., 2008).

Collectively, SUMOylation appears to be able to enhance the metastatic potentials of malignant cells through the regulation of transcription in different pathways. Thus, it can be speculated that in the event of excessive SUMOylation, cells are more prone to gain metastatic ability to become malignant. Furthermore, given that there are increasing number of oncogenes and tumor suppressor genes that are elucidated to be able to undergo SUMOylation, uncovering biological importance of SUMO modification in different proteins will provide tremendous information to understanding and developing therapeutic agents for treatment of malignant cancers.

1.6 The NF-κB pathway

1.6.1 Canonical and Non-canonical NF-κB pathways

NF-κB (Nuclear factor of κB) is a sequence-specific transcription factor that is known to be involved in the inflammatory and innate immune responses. The name was given because it was found in the nucleus bound to an enhancer element of the immunoglobulin kappa light chain gene in B cells. Initially thought to be a B-cell specific transcription factor, it was later shown to be present in every cell type and holds multiple important functions in living organisms (Hayden and Ghosh, 2004; Hoffmann and Baltimore, 2006).

There are several pathways leading to the activation of NF-κB (Figure 5), of which the most well known and categorized is the canonical pathway, triggered by a wide array of stimuli including inflammatory cytokines, bacterial and viral products. The NF-κB dimer, consisting of p65 and p50, is kept inactivated in the cytoplasm by inhibitor of κB (IκB) proteins. Upon stimulation by microbial or viral infections, or exposure to pro-inflammatory cytokines, IκB kinase (IKK) complex is activated, phosphorylating the NF-κB-bound IκB. This action causes IκB to be targeted for ubiquitination and subsequent degrading, in the process liberating the NF-κB dimers. These free dimers then translocate into the nucleus and turn on transcription of NF-κB targeted genes. The canonical pathway plays a pivotal role in innate and adaptive immune responses and stress responses, and also embryonic development (Hayden and Ghosh, 2004; Hoffmann and Baltimore, 2006; Pahl, 1999).

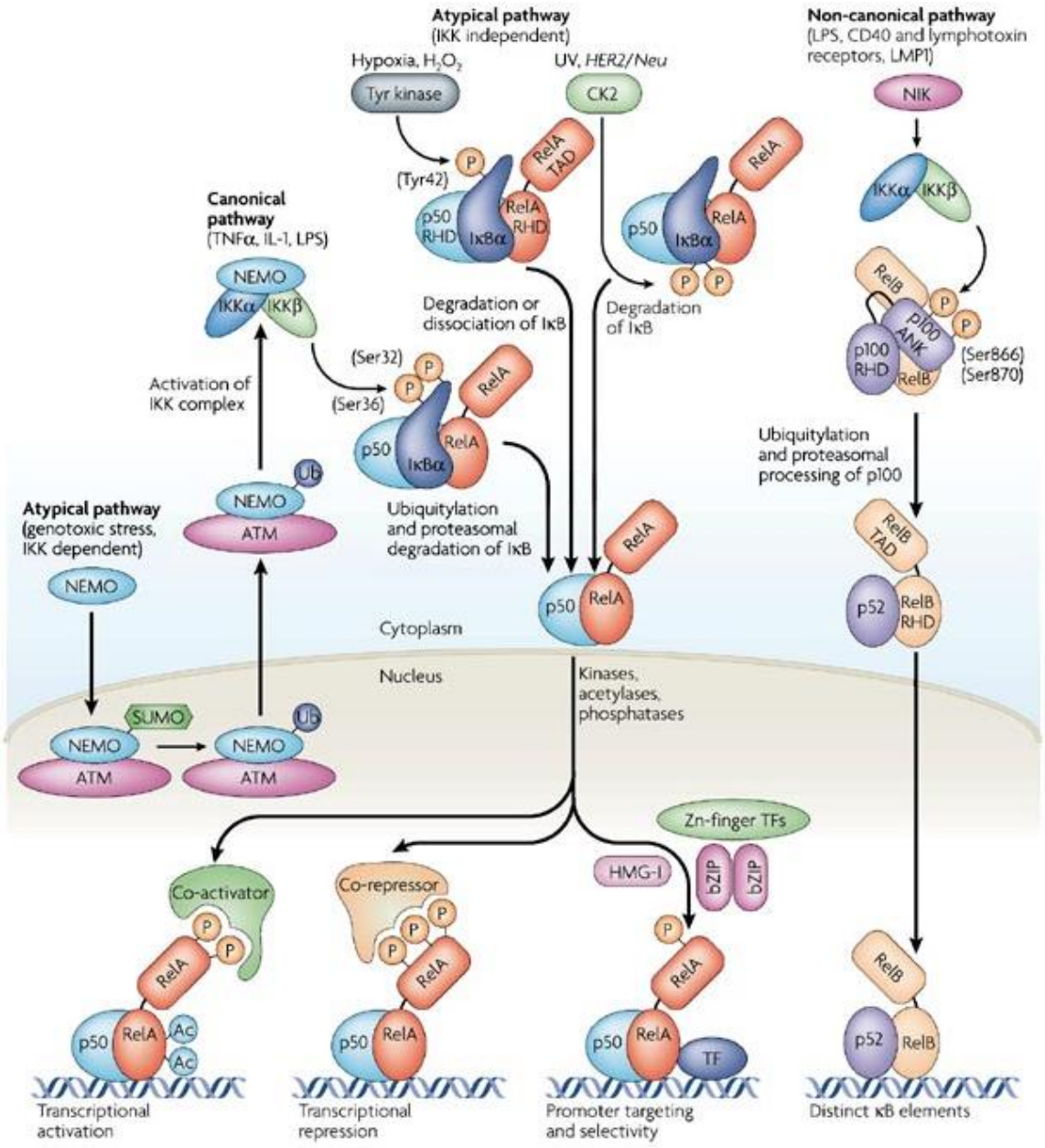

Figure 5. Different NF-κB pathways (Adapted from Perkins, 2007).

The non-canonical pathway, on the other hand, is inducible by LPS, CD40 and lymphotoxin receptors, LMP1, which selectively activates the NF-κB-inducing kinase (NIK) and Ikk1, leading to the phosphorylation of p100. This results in ubiquitination and partial proteolytic processing of the 26S proteosome to give p52. p52 then dimerises with Rel-B to translocate into the nucleus for transcriptional activation of targeted genes. The non-canonical pathway plays an important role in B-cell maturation and the formation of secondary lymphoid tissues (Hoffmann and Baltimore, 2006; Weih and Caamano, 2003)

1.6.2 Atypical NF-κB pathway by genotoxic stress

In recent years, another NF-κB pathway, termed as the atypical pathway, was discovered. Activation of this pathway requires a stimulus such as genotoxic stress causing DNA damage in the nucleus. Upon DNA double-strand break formation, ataxia telangiectasia mutated (ATM) is rapidly phosphorylated and kicks start a cascade of phosphorylations of several key targets implicated in cell cycle control, DNA repair or stress responses (Li et al., 2001).

NF-κB essential modulator (NEMO) or IKKγ usually exists in the cytoplasm in a complex with IKKα and IKKβ. All signals that are transduced, regardless via which pathway, have to go through NEMO. Hence, NEMO is known to be a 'master' regulatory protein, and that the loss of it will cause inability for NF-κB activation. Mutations in NEMO gene results in immunodeficiencies like incontinentia pigmenti and hypohidrotic ectodermal dysplasia (Hayden and Ghosh, 2004). Under genotoxic stress, free NEMO in the cytoplasm translocates into the nucleus, and undergoes a

series of post-translational modifications. Firstly, NEMO is SUMOylated specifically by SUMO1 but not SUMO2/3 at lysine residues 277 and 309 (Huang et al., 2003). This process is also independent of ATM (Huang et al., 2003) and requires PIASy as the major E3 ligase (Mabb et al., 2006). Though only a small fraction of the total NEMO pool undergoes this modification, mutations in the acceptor sites for these modifications completely block NF-κB activation by multiple genotoxic agents (Wu and Miyamoto, 2008). In contrast, these mutations of NEMO do not significantly perturb activation under the canonical pathway, suggesting the critical need for NEMO SUMOylation for NF-κB activation under genotoxic stress.

After NEMO is SUMOylated, it is targeted for phosphorylation by ATM at serine 85 and then subsequently targeted for monoubiquitination at the same lysine residues where SUMOylation occurs (Huang et al., 2003; Wu et al., 2006). Monoubiquitination of NEMO sets the trigger for its export out of the nucleus, back to the cytoplasm, where NEMO then reunites with IKKα and IKKβ to form the IKK complex, entering the canonical pathway to activate NF-κB. DeSUMOylation of NEMO occurs rapidly since SUMOylation is a reversible process and SENP2 has been recently identified to be the major deSUMOylating enzyme to do so (Lee et al., 2011). Despite these, the functional significance of SUMOylation of NEMO in cancer metastasis has not been studied.

1.6.3 NF-κB and Cancers

Even though there are abundant findings over the years, the molecular mechanisms involved in the initiation and progression into metastasis of cancer are still largely unknown. It is due to the fact that cancers are commonly heterogeneous and are presented very differently clinically. As such, therapeutic strategies for treatment of cancers do not yield optimistic results.

NF-κB activation participates in many levels of different pathways and its inhibition may lead to the suppression of cancer development. Constitutive or deregulated activation of NF-κB is found in many malignancies, including that of breast (Ghosh and Karin, 2002).

p65 was found to be activated in the majority of human breast cancer cell lines and correlated with the conversion of breast cancer cells to hormone-independent growth (Nakshatri et al., 1997). Another study reported that antagonist to NF-κB blocked epidermal growth factor-induced NF-κB activation and caused apoptotic death in ER negative breast cancer cells (Biswas et al., 2000). On the other hand, it was demonstrated, in rats, that NF-κB activation is an early event, occurring before malignant transformation of the mammary tumors (Kim et al., 2000). This is a strong indication that the activation of NF-κB plays an early and critical role in the malignant transformation of mammary glands. The expression of p65 in human breast cancer was also examined. Several groups saw increased NF-κB activity in *in vitro* human cell lines, *in vivo* rat breast cancer and clinical biopsies, with significantly increased staining of p65 in the nuclear region. Additionally, several mRNA of NF-κB regulated

genes were also found to be elevated in breast tumors compared to their adjacent normal tissues (Cogswell et al., 2000; Sovak et al., 1997).

Though the precise mechanisms of NF-κB activation in cancer progression are not known, it has been generally linked to be modulating the expression of many important genes involved in mammary carcinogenesis. NF-κB directly induces the expression of MMP9, chemokine receptor CXCR4 and urokinase-type plasminogen activator (uPA), thereby promoting extracellular matrix degradation and cancer cell migration (Helbig et al., 2003; Sliva et al., 2002). Therefore, constitutive activation of NF-κB in cancers would indicate that these genes are also upregulated. The NF-κB signaling system will therefore represent a critical intra-cellular pathway for breast cancer development and any drugs which are able to target this pathway should yield positive results.

Having said that, thus far, many therapeutic strategies aiming to suppress the NF-κB activation are faced with a brick wall. Many tumors are found to be chemo-resistant to such drugs, very possibly due to the fact that increased NF-κB would also cause cells to be resistant to apoptosis, and thereby resisting chemotherapeutic drugs (Karin, 2006; Pahl, 1999). However, inhibition of NF-κB will enhance the sensitivity of tumor cells to apoptosis induced by chemo-therapeutic agents. Some groups had demonstrated that the use of parthenolide, an NF-κB inhibitor, was able to increase the sensitivity of breast cancer cell to taxol treatment (Patel et al., 2000). Another group showed that using BAY11-7082, a pharmacological IκB inhibitor, had also increased sensitivity of breast cancer cells to doxorubicin and taxol (Weldon et al., 2001).

There have been extensive reports of clinically available drugs that interfere with NF-κB activity, either directly or indirectly. Statins, used clinically for the treatment of hypercholesterolemia, inhibit the rate-limiting enzyme of the mevalonate pathway 3-hydroxy-3-methylglutaryl-CoA reductase which plays a central role in the production of cholesterol in the liver (Figure 6). Extensive studies over the years had demonstrated that statins exert pleiotropic effects like, pro-apoptotic, growth inhibitory and prodifferentiation responses on neoplastic cells of diverse origins (Denoyelle et al., 2001; Kang et al., 2009; Li and Brown, 2009; Menge et al., 2005).

Furthermore, some had reported that statins are able to inhibit metastasis in cancers by interfering with NF-κB activation and downregulating NF-κB-regulated metastatic genes like MMP9 and CXCR4 (Aberg et al., 2008; Ghosh-Choudhury et al., 2010; Mannello and Tonti, 2009). Additionally, malignant cells appear to be highly dependent on the sustained availability of the end products of the mevalonate pathway and deregulated or elevated activity of HMG-CoA reductase had been shown in different tumors (Wong et al., 2002). Others reported high mRNA levels of HMG-CoA reductase to be correlated with poor prognosis and that inhibitors of HMG-CoA reductase are able to reduce cancer incidence by 28-33% (Clendening et al., 2010). Despite so, the use of statins alone for anti-cancer therapy may require deeper analysis due to conflicting reports showing increased incidence of cancers (Gazzerro et al., 2012; Sacks et al., 1996).

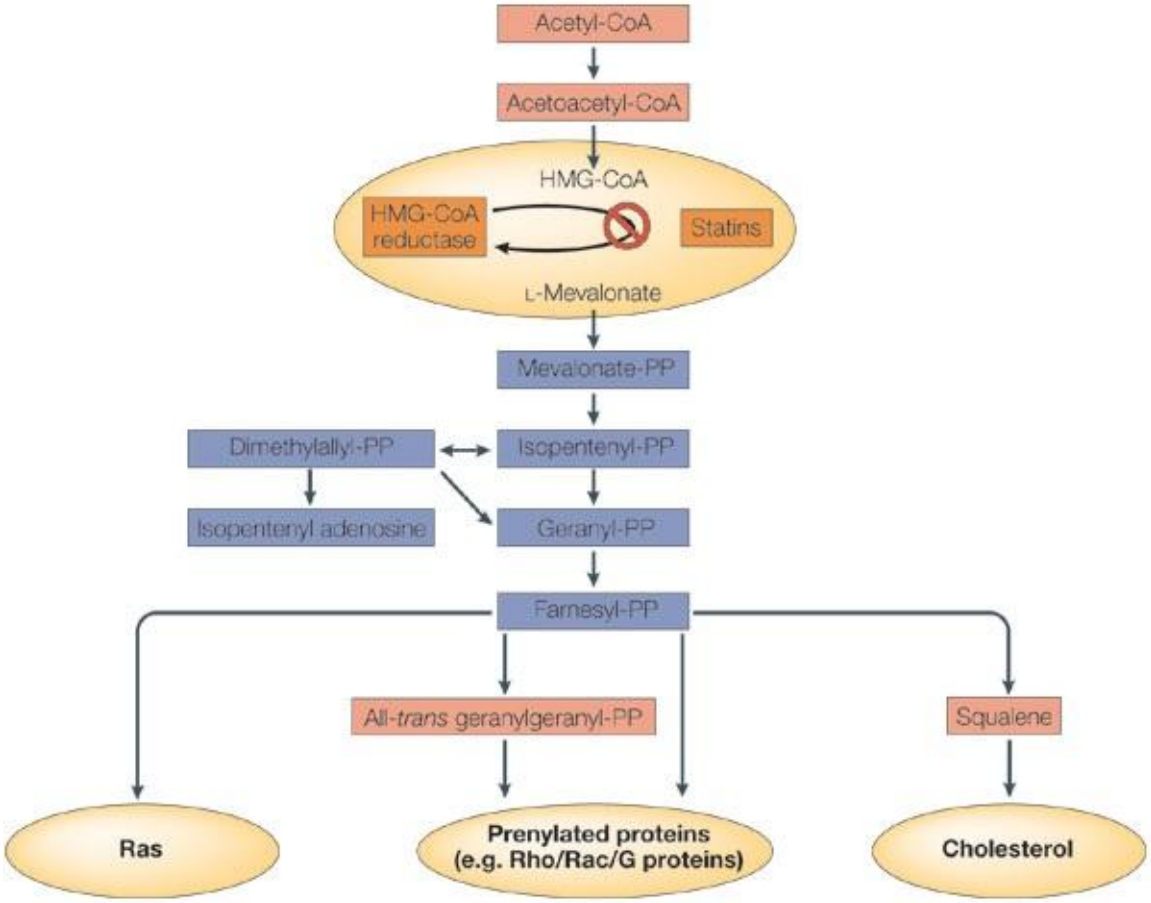

Figure 6. Mevalonate pathway and site of Statins inhibition (Adapted from Menge et al., 2005).

Taken together, adjuvant therapies using inhibitors of NF-κB pathway and chemotherapeutic drugs seem to be a very promising treatment for cancers. However, there remain concerns about the specificity of the NF-κB inhibitors as the activation of NF-κB also plays critical roles in several physiological processes. The inhibitors must be able to selectively target the diseased tissues or cells and keep toxicity to its minimum. Hence, more studies are required to elucidate the precise mechanism of action of different members in the NF-κB pathways and elucidate a therapeutic candidate for the treatment of cancers.

1.7 Scope of study

Mortality from breast cancer is almost entirely the result of invasion and metastasis of neoplastic cells from the primary tumors to distant organ sites. Therefore, understanding the genes and gene products involved in breast cancer metastasis is an important research goal. As it is not possible to accurately predict the risk of metastasis development in individual patients, nowadays, more than 80% of patients receive adjuvant chemotherapy, but approximately 40% of them relapse and ultimately die of metastatic breast cancer.

Therefore, new prognostic markers are urgently needed to identify patients who are at the highest risk for developing metastases. Furthermore, improving our understanding of the molecular mechanisms of the metastatic process might also improve clinical management of the disease.

As discussed previously in Chapter 1.4, it suggests a possible association of DP103 to cancer metastasis. Hence, my project aims to first confirm and deduce the role of DP103 to breast cancer and cancer metastasis. We will also analyze the strength of DP103 as a prognostic marker for breast cancer metastasis. Upon establishing this potential association, we will then look further into the mechanism of how DP103 is able to promote tumorigenesis, with a focus on SUMOylation as well as in the NF-κB pathway.

CHAPTER 2 MATERIALS AND METHODS

2.1 General buffer preparation

- **Phosphate buffered saline (PBS).** 137mM NaCl, 2.7mM KCl, 4.3mM Na_2HPO_4, 1.4mM KH_2PO_4, pH 7.4
- **TE Buffer.** 10mM Tris-HCl, 1mM EDTA, pH 8.0

- **Bacteria Transformation**
  - **LB broth.** 1% (w/v) Bacto-tryptone, 0.5% (w/v) Bacto-yeast extract, 0.5% (w/v) NaCl, pH 7.0
  - **LB agar.** 1% (w/v) Bacto-tryptone, 0.5% (w/v) Bacto-yeast extract, 0.5% (w/v) NaCl, 2% (w/v) Bacto-agar

- **Agarose Gel Electrophoresis**
  - **10X TBE.** 0.89M Tris, 0.89M Boric Acid, 0.02M EDTA
  - **6X Sample Loading Buffer.** 0.25% (w/v) Bromophenol blue, 0.25% (w/v) Xylene cyanol, 30% (v/v) glycerol

- **SDS-PAGE and Western Blotting**
  - **Tris, pH 8.8.** 1.5M Tris base, 0.4% (w/v) SDS, pH adjusted to 8.8 with concentrated HCl
  - **Tris, pH 6.8.** 0.5M Tris base, 0.4% (w/v) SDS, pH adjusted to 6.8 with concentrated HCl
  - **10X SDS-PAGE Running buffer.** 0.25M Tris base, 1.92M Glycine, 1% (w/v) SDS

- **1X Transfer buffer.** 0.025M Tris base, 0.192M Glycine, 20% Methanol
- **Blocking buffer.** 5% skim milk powder in 1X TBS-T
- **1X TBS-T.** 50 mM Tris.HCl, pH 7.4 and 150 mM NaCl, 0.1% Tween-20
- **5X Loading Dye.** 0.25M, pH 6.8 Tris-HCl, 0.5M DTT, 0.25% Bromophenol blue, 50% glycerol, 10% SDS

- **SDS-PAGE gel**
  - **10% Resolving gel**
    - 30% Acrylamide 3.3ml
    - 1.5M Tris (pH 8.8) 2.5ml
    - 10% SDS 0.1ml
    - 10% APS 0.1ml
    - TEMED 0.004ml
    - dH_2O 4.0ml
  - **5% Stacking gel**
    - 30% Acrylamide 0.5ml
    - 1.0M Tris (pH 6.8) 0.38ml
    - 10% SDS 0.03ml
    - 10% APS 0.03ml
    - TEMED 0.003ml
    - dH_2O 2.1ml

- **Protein extraction**
    - **1X RIPA buffer.** 50mM Tris at pH 7.5, 150mM NaCl, 1% v/v NP-40, 1% v/v deoxycholic acid, 0.1% v/v SDS and 1mM EDTA. 1mM PMSF, leupeptin, pepstatin A, aprotinin and Na_3VO_4 were added freshly before use

- **Measurement of Cell Viability**
    - **Crystal Violet Solution.** 0.75% crystal violet, 50% ethanol, 1.75% formaldehyde, 0.25% NaCl
    - **MTT Solution.** 5mg/ml MTT dissolved in 1X PBS and filtered

2.2 Cell lines and cell culture

MCF-7, MDA-MB-231, HS578t and BT549 human breast cancer cells were grown in Roswell Park Memorial Institute (RPMI) 1640 medium supplemented with 10% fetal bovine serum (FBS), 2mM L-glutamine and 0.05mg/ml gentamicin (BioWhittaker). BT474 cells were grown in Dulbecco's Modified Eagle's Medium/F12 (DMEM/F12) medium with the same supplements as above. SKBr3 cells were grown in McCoy's 5A media with the same supplements as above. MCF10A and 184A1 cells were grown in Mammary Epithelial Growth Medium (MEGM, Clonetics, La Jolla, CA) supplemented with 10% FBS, 2mM L-glutamine, bovine pituitary extract and 0.05mg/ml gentamicin. Xenograft-derived breast cancer cell lines (MCF10A1, MCF10AT1KCl.2, MCF10CA1h, and MCF10CA1aCl.1) were maintained in DMEM/F12 with 5% horse serum, 100U/ml Pen/Strep, 10µg/ml Insulin, 20ng/ml EGF (Millipore, Bedford, MA), 0.5µg/ml Hydrocortisone and 100ng/ml cholera toxin. All cell lines except xenograft-dervied were purchased from American Type

Culture Collection (ATCC, Manassas, VA), media and supplements from Hyclone (Logan, UT) unless otherwise indicated. Doxorubicin, VP16 (Etoposide) and Camptothecin were purchased from Calbiochem (La Jolla, CA). All other chemicals and reagents are from Sigma (St Louis, MO) unless otherwise indicated. Glutamine decomposes in culture medium in a time and temperature dependent manner. At 37°C, glutamine's half-life is eight days; at 4°C, its half-life is 40 days. Ammonia is the product of decomposition and it is potentially toxic. Hence, culture media need to be supplemented with glutamine. Gentamicin is an aminoglycoside antibiotic to control low levels of possible contamination. The cell lines were subcultured in 75cm^2 flasks (NUNC, NY, USA) every three days with a ratio of 1:3. For experiments, cells were resuspended from culture flasks using trypsin. Cells were then pelleted by centrifugation at 1300rpm and the supernatant removed. Cells were resuspended in media and counted using a haemocytometer before being seeded into six-well plates or 100mm tissue culture dish (Falcon, NJ, USA). The cells were then incubated for 48h to allow for attachment before performing any transfection or drug treatment.

2.3 Small-interferring RNA (siRNA)

Two unique siRNAs targeting non-conserved coding regions of DP103 were purchased from Invitrogen (Stealth RNAi™, Life Technologies, Grand Island, NY):

#1: 5'- CCA GUG AUC CAA GUC UCA UAG CUU U-3';

#2: 5'- GCU GCC GCU UCU CAU UCA UAU UAU U-3'.

They were tested for knockdown for DP103 and a combination of both siRNAs were used for all experiments subsequently as the reduction of DP103 was most significant (See Chapter 3.2). 5'-AGC UUC AUA AGG CGC AUG CTT (luciferase gene sequence inverted) was used as control siRNA (Qiagen, Valencia, CA).

2.4 Plasmid Constructs

Full length-hFLAG-DP103 pcDNA3 was cloned from full length 2FLAG-hDP103, a kind gift from Dr Christopher Glass from Univeristy of California, San Diego and are used in Klappacher et al., 2002. Helicase-dead mutant 2FLAG-hDP103-GNT pcDNA was derived from 2FLAG-hDP103 pcDNA by PCR-mutagenesis (Stratagene, La Jolla, CA) using sense primer 5'-TCTGGTACCGGGAATACCTGTGTGTTC-3' and antisense primer 5'-GAACACACAGGTATTCCCGGTACCAGA-3. The critical lysine residue needed to bind ATP (GKT) was mutated to an asparagines residue (GNT). Changing the conserved GKT to GNT has been shown to reduce ATP binding in RNA helicases by 98% (Richter et al., 1996). Flag-SENP2, HA-PIASy and Myc-NEMO are kind gifts from Professor Shigeki Miyamoto from University of Wisconsin-Madison and are used in Mabb et al., 2006 and Huang et al., 2003.

For retroviral DP103 plasmid construction, a forward primer containing AgeI site and a reverse primer containing XhoI site was used to amplify the DP103 cDNA from Full length-hFLAG-DP103 pcDNA3. The amplified fragment was cloned into AgeI-XhoI cut pBobi plasmid, which contains a lentiviral backbone with the restriction sites placed immediately downstream of the Flag tag which is preceded by a CMV promoter. The primer sequences are: sense primer 5'-ATT AACCGGTATGGACTACAAGGAC-3' and antisense primer 5'-ATTACTCGAGTCACTGGTTACTATGCATC-3'.

2.5 Virus preparation and infection

pBobi-Flag-DP103 was co-transfected with pREV, pMDL and pVSVG plasmids into HEK293T cells at a ratio of 10:2.5:6.5:3.6 (in μg) per 10 cm dish. Virus containing media was collected at 48hrs and 72 hrs from a set of 4 transfected plates. The media

was then filtered and centrifuged at 23 000 rpm for 1.5 hrs. The virus pellet was resuspended in 800uL media and 50uL of concentrated virus used to infect cells in a 6-well plate followed by expansion for experiments.

2.6 Transfections

For transient transfections, cells were plated at 2 x 10^5 cells per 6-well plate or 3 x 10^6 per 100mm dish 48h prior to transfection. Transfections were carried out using Lipofectamine™ RNAiMAX (Invitrogen, Life Technologies, Grand Island, NY) for siRNA according to the manufacturers' instructions. The media was changed to DMEM supplemented with 10% FBS without any antibiotics 1h prior to transfection. Lipofectamine™ RNAiMAX and siRNAs (25nM of each oligomer, #1 and #2 were used to get a final concentration of 50nM) were separately diluted in Opti-MEM Reduced Serum Media (Invitrogen, Life Technologies, Grand Island, NY) for 5min before mixing together for another 20min of incubation at room temperature. The mixture was then added dropwise to the cells and returned to the 5% CO_2 incubator for overnight transfection. After 18h, the media was removed, cells washed with 1X PBS and then supplemented with fresh complete media till day of harvest or drug treatment. For plasmid transfection, jetPRIME™ (Polyplus-transfection, Illkirch, France) was used. DNA was diluted in jetPRIME™ buffer first and jetPRIME™ reagent was then added. The mixture was vortexed briefly, incubated at room temperature for 10min before adding dropwise to the cells. They were returned to the 5% CO_2 incubator for overnight transfection. After 18h, the media was removed, cells washed with 1X PBS and then supplemented with fresh complete media till day of harvest or drug treatment.

2.7 Protein isolation and concentration determination

At time of harvest, cells were washed with ice-cold 1X PBS and harvested into a 1.5ml eppendoff tube using a rubber policeman. Cells were then centrifuged to collect cell pellets. 1X RIPA lysis buffer, which is supplemented with Phenylmethylsulfonyl fluoride (PMSF, serine protease inhibitor), leupeptin (*N*-acetyl-L-leucyl-L-leucyl-L-argininal, naturally occurring protease inhibitor for cysteine, serine and threonine peptidases), pepstatin A (aspartic proteases inhibitor) and aprotinin (serine protease inhibitor) were added to the pellets. 1mM of sodium orthovanadate (Na_3VO_4) acts as tyrosine phosphatase inhibitors. NP-40 serves as detergent used to solubilize the lipid in the cell membrane and other lipoproteins in the tissue. Deoxycholic acid also serves as detergent to solubilise fats. Sodium dodecyl sulphate (SDS) imposes a negative charge on solubilised proteins, thus aiding in protein migration during electrophoresis. Protein concentration determination of cell lysates was carried out using the Coomassie Dye (PIERCE, IL, USA) in a 96-well format. One microlitre of cell lysate was added to 200µl of Coomassie Dye and its absorbance at 595nm was read using a Spectrofluoro Plus spectrophotometer (TECAN, GmbH, Grödig, Austria). The Coomassie Plus Protein Assay is based on an absorbance shift from 465nm to 595nm that occurs when the reagent binds to proteins in an acidic solution. The mechanism of the reaction is the anionic form of the dye complexes with proteins, resulting in a colour change from brown to blue. The dye interacts chiefly with arginine residues and weakly with histidine, lysine, tyrosine, tryptophan and phenylalanine residues. The reaction reaches a stable endpoint so the absorbance reading does not shift over time. Protein standards were prepared using bovine serum albumin (PIERCE, IL, USA).

2.8 SDS-PAGE and western blot analysis

For detection of protein expressions, 30μg of total protein per sample was incubated at 95°C for 10min before being subjected to SDS-PAGE (Polyacrylamide Gel Electrophoresis) at 80V for 20min followed by 125V for 1h using the BioRad Mini-PROTEAN 3 Cell (CA, USA). Kaleidoscope prestained standards (BioRad, CA, USA) were also subjected to SDS-PAGE to facilitate the estimation of molecular sizes of the protein bands obtained. The resolved proteins were then transferred onto nitrocellulose transfer membrane by wet transfer method at 380mA for 1h 15min using the BioRad Mini Trans-Blot Electrophoretic Transfer Cell (CA, USA). After the transfer, the membrane was then blocked with 5% (w/v) fat-free milk in Tris-buffered saline/0.1% (v/v) Tween-20 (TBS-T) for 1h. Tween-20 is a mild detergent that reduces non-specific binding of antibody to lipid and protein. After three washes with TBS-T to remove excess milk, the membrane was incubated with the respective primary antibodies diluted in 5% BSA in TBS-T at 4°C overnight. The following day, the membrane was washed with TBS-T to remove unbound primary antibody, and then exposed to 1:10000 dilution of IgG-HRP-conjugated secondary antibodies in 5% (w/v) fat-free milk in TBS-T for one hour at room temperature. After three washes with TBS-T to remove unbound secondary antibodies, the probed proteins were then detected with Kodak Biomax MR X-ray film by enhanced chemiluminescent using SuperSignal Chemiluminescent Substrate (PIERCE, IL, USA). Human anti-mouse DP103 (1:1000 dilution) was purchased from BD Transduction Laboratories (San Diego, CA), human anti-rabbit MMP9 (1:1000 dilution), human anti-rabbit ICAM (1:1000 dilution), goat anti-mouse and goat anti-rabbit from Cell Signaling (Danvers, MA), human anti-rabbit NEMO (1:500 dilution), human anti-rabbit IKK2 (1:500 dilution), human anti-mouse p65 (1:1000 dilution) from Santa Cruz (CA, USA) and

human anti-mouse SUMO-1 (1:2000 dilution) from Zymed (South San Francisco, CA).

2.9 RNA isolation

Total RNA was extracted using TRIzol® reagent according to the manufacturer's instructions (Invitrogen, Life Technologies, Grand Island, NY). Cells were scrapped in TRIzol® and transferred to 1.7ml eppendoff tubes. The homogenates were then stored for 5min at room temperature to permit complete dissociation of nucleoprotein complexes. They were then supplemented with chloroform, vortexed and centrifuged at 13 000rpm for 15min. Following centrifugation, the mixture separates into a lower red phenol-chloroform phase, interphase and an upper colourless aqueous phase. RNA remains exclusively in the aqueous layer whereas DNA and proteins are in the interphase and organic bottom phase respectively. The top colourless layer was then transferred into a fresh tube and equal volume of isoamyl alcohol/Chloroform (24:1) was added to reduce foaming and ensure deactivation of RNase. After centrifugation for another 15min, the top colourless layer was transferred to a new tube and equal volume of isopropanol was added and freezed in -80°C for at least half an hour. The samples were then thawed and spun down for 45min to precipitate the RNA. Precipitated RNA will form gel-like/white pellet at the side and bottom of the tube. The supernatant was then discarded and the pellet was washed with 75% ethanol. The samples were then centrifuged at 13000rpm for another 15min. Supernatant was then removed and RNA pellet was air-dried. The RNA was dissolved in ultra-pure water and concentration measured using NanoDrop® ND-1000 spectrophotometer (NanoDrop Technologies, Wilmington, DE).

2.10 Reverse Transcription-Polymerase Chain Reaction (RT-PCR) and Quantitative Realtime-PCR

Each RT reaction contains 1µg of total RNA, 1X RT buffer, 5mM $MgCl_2$, 425µM of each dNTPs, 2µM random hexamers, 0.35U/µl RNase inhibitor, 1.1U/µl MultiScribe™ reverse transcriptase and made up to 10µl with sterile water. RT reaction was carried out in PCR thermal cycle (Mastercycler gradient, Eppendorf, Hamburg) using the following steps. The reaction mix is heated at 25°C for 10min, followed by 37°C for 1h and finally at 95°C for 5min to terminate the reaction. A negative control for RT in which sterile water replaced the RNA template was included.

Five microlitres of the 10µl cDNA reaction volume was used in quantitative Realtime-PCR using ABI PRISM 7500 (Applied Biosystems, Foster City, CA, USA) with 18S as an internal control (Applied Biosystems, Hs99999901_s1). Fluorescence was measured with the Sequence Detection Systems 2.0 software. Quantitative Realtime PCR was performed in multiplex (both target and endogenous control co-amplified in the same reaction) with distinct fluorescent dyes. Primers and probes for various genes were purchased as kits from Applied Biosystems with their catalog numbers as follows: DP103: Hs 00200516_m1, CXCR4: Hs 00607978_s1.

2.11 Immunoprecipitation

For detection of endogenous protein interactions, whole cell lysate was prepared. A total of 3×10^6 cells were treated as indicated and cell pellets lysed in lysis buffer. 1mg of proteins were pre-cleared with magnetic G beads (Millipore, Bedford, MA) for 1h before rotating with 1µg of indicated antibody or normal mouse or rabbit IgG overnight at 4°C to preserve the proteins. Magnetic G beads were added the next day.

After 1½h of rotating, magnetic-enriched IP samples were washed four times in cold wash buffer (200mM Tris [pH 8.0], 100mM NaCl, 0.5% NP-40, 2mM DTT, 0.5mM PMSF, 1mM sodium orthovanadate, 1μg/ml leupeptin, 1μg/ml aprotinin). The samples were boiled in 5x SDS loading buffer, and proteins were separated by SDS-PAGE. Proteins were then transferred to PVDF membranes and subjected to western blotting with the indicated antibodies.

2.12 Wound healing assay

MDA-MB-231 and BT549 cells were treated according to experimental design. Before plating the cells, two parallel lines were drawn at the underside of the well. These lines served as fiducial marks for the wound areas to be analysed. In preparation for marking the wound, the cells should be fully confluent. The growth medium was aspirated and replaced by calcium-free PBS to prevent killing of cells at the edge of the wound by exposure to high calcium concentrations. Two parallel scratch wounds were made perpendicular to the marker lines with a 1000μl blue tip. The medium was then changed to complete media. After incubation for 48h, the wounds are observed using bright field microscopy and multiple images were taken at areas flanking the intersections of the wound and the marker lines at the start and end of the experiment. Three measurements of the gap distance between the wound were taken at the start and end of the experiment from the images, and their averages are converted to percentages to depict percentage change with the control setup taken to be at 100%.

2.13 2D migrational assay

Glass cylinders (Bioptechs, Butler, PA) of 6 mm inner diameter were placed vertically on tissue culture dish. About 20 000 cells were seeded inside the glass cylinders and incubated at 37°C in a humidified atmosphere at 5% CO_2 for 24 hours. The cylinders were then carefully lifted from the dish to reveal an undisturbed circular monolayer patch of cells, which were then washed thrice with 1X PBS to remove dead cell debris and refilled with 2ml of complete medium. Live video monitoring assays of the migrating cells at the edge of the monolayer were performed using phase contrast microscopy (Biostation IM, Nikon). Rectangular fields of view with pixel resolution 1280 x 960 (microscope objective of 10x magnification) were chosen from the monolayer edge using the proprietary software and videos were recorded for 24h with 10min intervals in between the frames (total 145 frames). Fifty cells from 6-8 rows of the leading edge of the monolayer were manually tracked using the open source software Image J. Monolayer edge distances (MED) were measured as the average of the displacements (n=5 per field of view measured for 4-5 videos per experiment) between the initial and final positions of the monolayer edge. 2D track plots and plot related measurements were performed using the Chemotaxis tool plugin (Integrated BioDiagnostics) for Image J. The following are the definitions used to estimate the cell migration parameters:

- Accumulated Distance (AD) – The total distance traversed by individual cells as estimated by measuring the length of the cell tracks.
- Euclidean Distance (ED) – The displacement between the initial and the final positions of individual cells as estimated by the distance between the starting and ending position of the cell tracks.

- Mean Cell Speed – The average speed of migration of all the tracked cells during the 24 hour duration. The speed of individual cells is measured as the ratio of the accumulated distance to the total time period of observation.
- Confinement Ratio – A ratio between the Euclidean distance and the Accumulated distance that is used as an indicator of the straightness of the cell migration tracks. A value of 1 indicates an absolutely straight path while values towards 0 indicate tortuous paths.
- Center of mass (CM): Center of mass of the coordinates of all endpoints (final positions) of the cell tracks.

  $x = {}^{1}/_{n} \cdot \sum \text{Endpoint x value}$

  $y = {}^{1}/_{n} \cdot \sum \text{Endpoint y value}$

  where x and y represent the coordinates of the endpoints of a particular cell track.

- $\text{CM Length} = \sqrt{x^2+y^2}$

  where CM Length represents the distance from the origin to the center of mass.

2.14 *In vitro* and 3D invasion assay

In vitro invasion assay was performed using BD Bio-Coat Matrigel invasion assay system (BD Biosciences, San Jose, CA) according to the manufacturer's instructions. Briefly, cells were trypsinized 48h post-transfection, 2 x 10^5 cells suspended in serum-free medium and seeded into the Matrigel transwell chambers consisting of polycarbonate membranes with 8-µm pores. Regular medium containing 10% FBS was added to the bottom chamber to act as chemoattractant. After incubation for 24h, the media in the transwell chamber was removed, and upper surface of the chambers

was wiped off with a cotton swab. The invading cells were fixed and stained with crystal violet solution. The invading cell numbers were counted in five randomly selected microscope fields (×200) and their averages were converted to percentage with the control setup taken to be at 100%.

For 3D invasion assay, Nutragen^{TM} collagen solution (Inamed Biomaterials, Fremont, CA, US) was mixed with NaOH, 10X PBS, and MDA-MB-231-GFP cells suspended in serum-free DMEM on ice. The final solution contained 4mg/ml of collagen-I and 200 000/ml cells. After 30 to 60min of incubation under 37°C humidified chamber, self-assembly of a piece of semi-spherical cell-seeded collagen gel in the central well of a glass-bottomed dish was formed. Complete cell culture media were immediately supplied to the gel to support cell growth. After 40h, these GFP-expressing cells were imaged in 3D collagen hydrogel using confocal fluorescence microscopy (Nikon TE2000-EZ C1 system). Ten hours of time-lapsed confocal imaging was then carried out in an environment chamber maintaining 37°C and 5% CO_2 atmosphere, which was completed within 70 hours post siRNA transfection. Quantitative image analysis was achieved using 3D reconstruction and cell tracking function provided by Imaris (Bitplane, Zurich, Switzerland).

2.15 Electrophoretic mobility shift assay

The EMSA technique is based on the observation that protein:DNA complexes migrate more slowly than free DNA molecules when subjected to non-denaturing polyacrylamide or agarose gel electrophoresis. Cell pellets were lysed in lysis buffer (50mM KCl, 0.5% IGEPAL CA-630, 25mM HEPES pH 7.8, 10μg/ml leupeptin, 20μg/ml Aprotinin, 125mM DTT, 1mM PMSF) and kept on ice to break the cell membrane. They were then spun down and supernatant was removed as cytoplasmic

extract. The nuclear pellet was washed with washing buffer (50mM KCl, 25mM HEPES pH 7.8, 10μg/ml leupeptin, 20μg/ml Aprotinin, 125mM DTT, 1mM PMSF) before resuspending it in extraction buffer (50mM KCl, 25mM HEPES pH 7.8, 10% glycerol, 10μg/ml leupeptin, 20μg/ml Aprotinin, 125mM DTT, 1mM PMSF). The pellet was then freezed at -70°C for at least half an hour, before thawing and centrifugation. The supernatant collected was the nuclear extract. The same sample was divided into 2 separate samples for analysis with double-stranded NF-κB, AP-1 and Oct-1 [γ-^{32}P] radiolabeled probes.

NF- κB: 5'-TCA ACA GAG GGG ACT TTC CGA GAG GCC-3' (designed by us)

AP-1: 5′- CGC TTG ATG ACT CAG CGG GAA-3′ (Lukiw et al., 1998)

Oct-1: 5'- TGT CGA ATG CAA ATC ACT AGA A-3' (Feng and Williams, 2003)

The DNA probe was labeled radiolabeled by incubation at 37°C for 30min with the following: 5x forwarding buffer, ^{32}P-γ-ATP and T4 kinase (10 unit/μl). The labeled probe was then spun at 3000 rpm for 1 min to get rid of the buffer, followed by loading into the G50 micro column (Pharmacia Biotech, UK) and spun for 2 min for purification. EMSA was performed in a reaction mixture containing 2x reaction buffer (50% glycerol, 1M Hepes pH 7.9, 1M Tris-HCl pH 8.0, 0.5M EDTA pH 8.0, 100mM DTT), 0.5μg/μl poly (dI-dC), protein samples and 1μg/μl BSA and kept on ice for 10min before adding DNA probes. The mixture was then kept at room temperature for another 20min before loading into a non-denaturing polyacrylamide gel and run for 1h. The gel was then dried and analyzed with a PharosFX Plus system (BioRad, Hercules, CA). The Oct-1 probe was served as an EMSA control for equal protein loading.

2.16 Gel zymography

Gelatinolytic enzymes secreted by cultured cells were identified and quantified by electrophoresis of serum-free conditioned medium in gelatin-embedded polyacrylamide gel. Cells were treated according to experimental setup and finally cultured in serum-free media for 24h. At time of harvest, the medium was collected and the non-concentrated supernatants were concentrated using Vivaspin® concentrators (Vivascience, Stonehouse, UK). The concentrates were then mixed with SDS sample buffer without DTT (reducing agent). Electrophoresis was carried out on 10% denaturing polyacrylamide gels containing 10% gelatin. Following electrophoresis, the gels were rinsed twice with 50mM Tris-HCl buffer (pH 7.5) containing 2.5% Triton X-100 for 15min each time, and incubated at 37°C for 16h in a buffer composed of 0.15M NaCl, 10mM $CaCl_2$ and 50mM Tris-HCl (pH 7.5). The gels were stained with 0.05% Coomassie blue in 10% ethanol and 10% acetic acid, and destained with 10% ethanol and 10% acetic acid. Media collected from MCF10A cells treated with various concentrations of TNF-α were used as a reference as MMP9 activity increases upon such stimulation (Stuelten et al., 2005).

2.17 Luciferase assay

MDA-MB-231 and BT549 (1.25×10^5 cells/well) were plated in 12-well plates. Experiments were set up as described. Cells were seeded for 48h prior to transfection. Cells were transfected with siRNA against DP103 described above. After 24h, the cells were then transfected with luciferase reporter plasmid containing 3x NF-κB or AP-1 binding sites together with *Renilla* plasmid (Clonetech, Palo Alto, CA). Renilla transfection was used to check for transfection efficiency. At time of harvest, the promoter activity was assessed with a dual-luciferase assay kit (Promega, Madison,

WI). Feeding medium was removed from the wells, washed once with 1x PBS, and lysed with ice-cold 100µl of reporter lysis buffer. Ten microlitres of cell lysate was then added to 50µl of luciferase substrate solution, following which 50µl of stop & glow buffer was added for Renilla reading. Bioluminescence generated was measured using a Sirius luminometer (Berthold Technologies, Herefordshire, UK). The luminescence readings obtained were normalized to the protein concentration of the corresponding cell lysate and presented as fold difference with reference to the control setup.

2.18 Measurement of cell viability via crystal violet and 3-(4, 5-Dimethylthiazol-2-yl)-2, 5-diphenyltetrazolium bromide (MTT) assay

Cell growth/cytotoxicity was assessed by determining the number of intact cells over time using the crystal violet uptake assay. At the end of drug treatment or transfection, medium was removed from the wells. The cells were then washed once with 1X PBS. This was followed by incubation with 0.5ml of crystal violet solution for ten minutes. Excess crystal violet solution was carefully washed away with distilled water for several times and the wells were left to air-dry. The remaining crystals were dissolved in a 1% SDS in 1X PBS solution and its absorbance read at 595nm using the Spectrofluoro Plus spectrophotometer (TECAN, GmbH, Grödig, Austria). The amount of dye released reflects the quantity of intact cells present in each well.

Another assay that was used to assess cell viability is MTT. Similar to crystal violet assay, MTT is also a functional assay. Similar experimental set up was performed. MTT assay is based on the ability of mitochondrial dehydrogenase enzyme from viable cells to cleave the tetrazolium rings of the pale yellow MTT and form dark blue formazan crystals which is largely impermeable to cell membranes, thus resulting in

its accumulation within healthy cells. Three hours before the end of treatment, MTT solution was added into each well containing cells at 1:10 dilution. The cells were then incubated at 37°C with 5% CO_2. Three hours after the incubation, the medium was removed carefully with a pipette tip and DMSO was added to each well to solubilise the crystals. The number of surviving cells is directly proportional to the level of formazan product formed. The quantity of formazan present was determined by measuring its absorbance at 550nm using the Spectrofluoro Plus spectrophotometer (TECAN, GmbH, Grödig, Austria).

2.19 Clinicopathological data

The study cohort consisted of 98 breast cancer cases (invasive ductal carcinomas representing all grades and stages) treated by surgical resection at the National University Hospital of Singapore. The median age of patients was 52 years (range 29–86). The distribution of patients according to the three most common ethnic groups in Singapore showed that they were of Chinese (81%), Malay (15%) or Indian (4%) descent. Histopathological staging was based on the TNM staging system and grading of tumors. This work was approved by the ethics committee of the National University of Singapore (DSRB Domain B/09/284).

Another cohort of a total of 48 primary breast cancer and 15 benign breast tissue samples derived from 63 patients who underwent surgery at the First Affiliated Hospital of Anhui Medical University (Hefei, Anhui, People's Republic of China) between 2009 and 2010 was obtained. All tissue samples were hematoxylin and eosin stained and had been reviewed by two independent pathologists in Anhui Medical University. Total RNA from these breast tumor tissue samples was extracted by TRIzol® (Invitrogen, Life Technologies, Grand Island, NY), reversely transcribed

into cDNA by using RevertAid First Strand cDNA Synthesis Kit (K1622, Fermentas, Germany) and Real-time PCR was carried out by using SYBR Premix Ex Taq (DRR041A, TaKaRa, Shiga, Japan) in a Stratagene MX3000P detection system (Stratagene, La Jolla, CA, USA). Primer sequences used for qPCR expression in patient tissues from First Affiliated Hospital of Anhui Medical University are DP103-F: 5'-TGCCAGTAAACAGATGC-3', DP103-R: 5'-GTGCCAAAGGGTATGA-3'; MMP9-F: 5'-CGAACTTTGACAGCGACAAGA-3', MMP9-R: 5'-AGGGCGAGGACCATAGAGG-3'; GAPDH-F: 5'-TGCACCACCAACTGCTTAGC-3', GAPDH-R: 5'-GGCATGGACTGTGGTCATGAG-3'.

2.20 Immunohistochemistry

Formalin-fixed, paraffin-embedded tissue was cut into 5 μm section, de-paraffinized in xylene, rehydrated through graded ethanol, quenched for endogenous peroxidase activity in 3% (v/v) hydrogen peroxide, and processed for antigen retrieval by heating in 10 mM citrate buffer (pH 6.0) at 90-100°C. Sections were incubated at 4°C overnight with DP103 antibody from Santa Cruz (CA, USA) and MMP9 antibody from Cell Signaling (Danvers, MA) in 1:100 dilution.

2.21 Tissue microarray construction

Tissue microarray (TMA) blocks containing cores from 98 breast cancer patients were constructed as described previously (Das *et al.*, 2008; Salto-Tellez *et al.*, 2007). Briefly, a needle with 0.6 mm diameter was used to punch a donor core from morphologically representative areas of a donor tissue block. The core was subsequently inserted into a recipient paraffin block using an ATA-100 tissue arrayer

(Chemicon, USA). Three cores were taken from the center of tumor tissue and a single core was taken from histologically-normal colon epithelium of matched cases. Consecutive tissue microarray sections of 4μm thickness were cut and placed on slides for immunohistochemical analyses by pathologists A/Prof Manuel Salto-Tellez (CSI, NUH) and Dr Thomas Choudary Putti (Pathology, NUH). The expression status of MMP9 and DP103 is scored by immunohistochemistry following standard 4-tiered scoring practice, ranging from 0 to +3. For statistical analyses (by biostatistican Mr Ong Chee Wee, CSI), negative (0) and weak expression (+1) were grouped together and termed as 'negative expression' of the proteins. Moderate (+2) and strong (+3) expression was termed as 'positive expression'. McNemar's test was used for the analysis of scorings. Survival duration was measured from date of diagnosis till date of cancer-specific death, and censored for surviving cases. Survival curves were plotted using the Kaplan-Meier method and compared using the log-rank test. Student's t tests were performed using the software Origin Pro and results are represented as mean ± standard deviation.

2.22 Treatment of cells with Drugs

Simvastatin and Lovastatin were purchased from Merck (San Diego, CA, USA) in sodium salt form. A stock solution of 60mM was prepared by diluting the powder in calculated amount of DMSO, depending on the molecular weight of the compound and then stored in -20°C freezer. Various concentrations of the statins were then prepared by diluting the stock solution with complete medium to attain the indicated final concentrations.

Specific MMP9 Inhibitor I, Broad spectrum MMP inhibitor (GM6001) and specific MMP2/9 inhibitor (SB-3CT) were purchased from Calbiochem (La Jolla, CA). They

were dissolved in DMSO and stored at -80°C freezer. Various concentrations of the statins were then prepared by diluting the stock solution with complete medium to attain the indicated final concentrations.

2.23 Metastatic qPCR Array and microarray

Total RNA was extracted and reverse transcription was carried out as described above. The relative expressions of various genes were then analyzed using quantitative RT-PCR (ABI PRISM 7900, Applied Biosystems, Foster City, CA, USA). Multiple gene markers distributed around the genome and three housekeeping genes were used for real-time PCR analysis using the SYBR GreenER qPCR SuperMix for ABI PRISM (Invitrogen, Life Technologies, Grand Island, NY). Triplicate reactions were performed for each marker in a 384-well plate using a two-step amplification program of initial denaturation at 95°C for 10 min, followed by 40 cycles of 95°C for 20 sec and 60°C for 30 sec. A melting curve analysis step was carried out at the end of the amplification, consisting of denaturation at 95°C for 1 min and reannealing at 55°C for 1 min. Sequences of primers used are as described previously (Pandey et al., 2010; Qian et al., 2011) and can be found in Appendix 1.

DP103 expression levels were analyzed in breast tumors using a multi-institutional "microarray meta-cohort" totaling 759 primary breast cancer cases. The normalized microarray data set and associated clinical annotations are described in Miller et al., 2011 and can be downloaded at https://sites.google.com/site/millerirgs/ as supplemental data files 1 and 2 (Miller et al., 2011). Briefly, all tumor samples were analyzed from frozen tissue collected at surgery and profiled on an Affymetrix U133 series microarray according to standard Affymetrix protocols. Raw data (ie, CEL files) were normalized by Robust Multichip Average (RMA) using the Bioconductor

"Affy Package (R)" as previously described (Irizarry et al., 2003). Batch effects between cohorts were corrected using the Partek Genomics Suite Batch Remover program. Differential expression of DP103 between breast cancer subgroups was assessed by Mann–Whitney U test and Student's t-test.

2.24 *In vitro* SUMOylation assay

SENP2 and PIASy were prepared by IP with anti-HA antibody from HEK293 cells transfected with HA-tagged SENP2 or PIASy constructs. His-DP103 was bacterial recombinant protein purified from pSY5-His-DP103. NEMO protein was produced using wheat germ lysates by *in vitro* TNT reaction with TNT® Quick Coupled Transcription/Translation System kit (Promega, Madison, WI). *In vitro* SUMOylation was performed by preparing a reaction mix containing 1mg/ml recombinant SUMO-1, 1unit/µl SUMO E1 and 0.4mg/ml Ubc9 proteins, and incubating at 37°C for 2h as in Mabb et al., 2006. After 2h, the mixture was incubated for 3min at 95°C before being resolved using 12% polyacrylamide gels and immunoblotted with different antibodies.

2.25 *In vivo* mouse model

The sodium salt of Simvastatin was used for this study. Simvastatin was sonicated into suspension in saline for animal experiments. To ensure that toxicity would not be a factor, we conducted a preliminary dosage-tolerance study for the proposed 0 (saline), 25 and 50mg/kg dosages of Simvastatin using 4 mice for each dose, similar to our previous studies (Shibata et al., 2004). The animals were injected intra-peritoneal (i.p.) with the appropriate dose 3 times a week for 9 consecutive weeks. No deaths occurred in any of the groups and only the 50mg/kg group showed a 10% weight loss at week 9 compared with controls, indicating that no dose adjustments

were necessary. To avoid any confounders in our setup, we chose the feeding dose of Simvastatin to be 25mg/kg.

MDA-MB-231 cells (1 x 10^6 cells suspended in 200µl PBS) were inoculated i.p. into the tail vein of sixteen female nude mice. Two weeks later, when tumors had developed to about 0.2cm in diameter, groups of eight mice each were injected i.p. with either vehicle alone or with 25mg/kg Simvastatin three times a week for six weeks. At the end of the six weeks, the mice were killed with diethyl ether and exsanguinated.

At necropsy tumors and lymph nodes, routinely those from the axillary and femoral regions as well as those appearing abnormal, were removed, fixed in 4% formaldehyde solution in phosphate buffer and processed through to paraffin embedding. Lungs were inflated with the formaldehyde solution prior to excision and immersion in fixative. The individual lobes were subsequently removed from the bronchial tree, trimmed into seven pieces and examined for metastatic foci before being similarly processed to paraffin embedding. All paraffin-embedded tissues were cut at 4 µm, with sequential sections stained with hematoxylin and eosin (H&E) for histopathological examination and reserved unstained for immunohistochemistry.

2.26 Statistical Analysis

Statistical analyses for other experiments not mentioned previously were performed using the SPSS package (version 15.0 for Windows, SPSS Inc., USA). The Student's t-test analysis was performed with significance set at the 5% level.

CHAPTER 3 RESULTS

3.1 DP103 expression in breast tissues: Is there any correlation between DP103 levels and the state of malignancy?

3.1.1 Expression of DP103 in different breast tissue malignancies

Before the work done for this thesis, the expression of DP103 in breast malignancies was unreported. We retrieved a total of 194 breast tissue samples (97 breast cancers and 97 paired normal breast tissue) from the archives of the Department of Pathology, National University Hospital, Singapore and constructed a tissue microarray. Out of the 194 tissue samples, only 43 pairs of breast cancer and its paired normal breast tissue were successfully stained to make comparison. Staining was defined as immunostaining of cytoplasm above background level and scored as follows: (1+) representing weak expression; (2+) representing moderate expression; and (3+) representing strong expression. The absence of cytoplasmic staining was reported as negative (0). Table 2 shows the numbers of patients in each individual score. We used the cut-off value for negative or positive expression of DP103 to be 0 and 1+ versus 2+ and 3+ respectively and pooled the scores in Figure 7. A significant number of patients had high expression of DP103 in their tumor and low expression of DP103 in their matched normal tissue as compared to other combinations ($p<0.001$). Two pictures representing the immunohistochemical staining of high DP103 in invasive breast tissues compared to that in matched normal breast tissues are shown in Figure 8.

		DP103 Expression (Tumor)				Total
		0	**1+**	**2+**	**3+**	
DP103 Expression (Normal)	**0**	1	2	3	4	10 (23%)
	1+	1	3	7	11	22 (51%)
	2+	0	1	0	7	8 (19%)
	3+	0	0	0	3	3 (7%)
Total		2 (5%)	6 (14%)	10 (23%)	25 (58%)	43

McNemar P<0.001

Table 2. Number of cases screened for DP103 protein expression in human patient breast tumor and paired normal tissues, sorted according to individual scores (n=43).

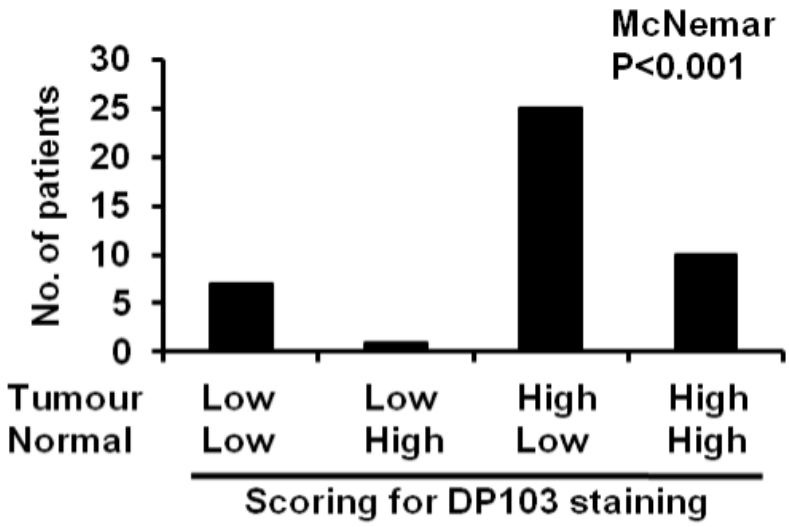

Figure 7. Graph showing number of cases screened for DP103 protein expression in human patient breast tumor and paired normal breast tissues, sorted according to negative (low) or positive (high) score groupings (n=43).

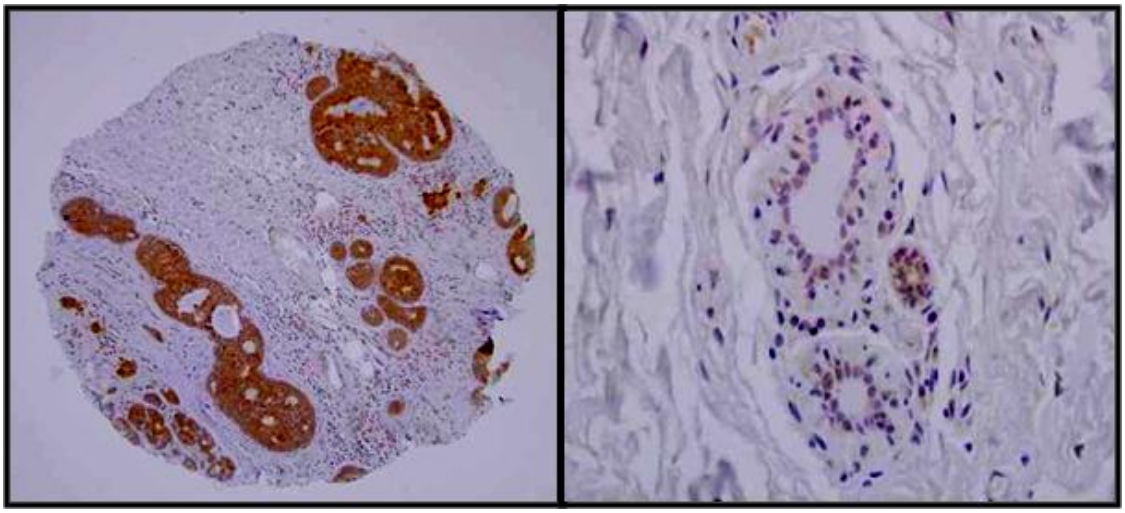

Figure 8. Two representatives of tissue microarray showing higher DP103 staining in invasive breast ductal carcinoma (left) and low staining in matched normal breast tissue (right).

3.1.2 Expression of DP103 in breast cell lines

To confirm the observation that DP103 is highly expressed in invasive breast cells and low in normal breast cells, a panel of breast cell lines, comprising of human normal breast epithelial, poorly invasive breast adenocarcinomas and highly invasive breast adenocarcinoma (Table 3) was analyzed for basal mRNA and protein levels of DP103. Figure 9 shows that both the mRNA and protein expression of DP103 are the highest in MDA-MB-231 and BT549, both which are highly invasive in nature, relatively lower levels in poorly invasive MCF7 and BT474, and having the lowest expressions in human breast normal epithelial MCF10A, 184A1 and poorly invasive adenocarcinoma SKBr3 cell lines.

Cell lines	Tumor Type	Tumorigenicity
MCF7	Poorly invasive adenocarcinoma	Yes
BT474	Poorly invasive adenocarcinoma	Yes
MCF10A	Normal non-tumor epithelial	No
MDA-MB-231	Highly invasive adenocarcinoma	Yes
BT549	Highly invasive adenocarcinoma	Yes
SKBr3	Poorly invasive adenocarcinoma	Yes
184A1	Normal non-tumor epithelial	No

Table 3. Characteristics of the panel of breast cell lines.

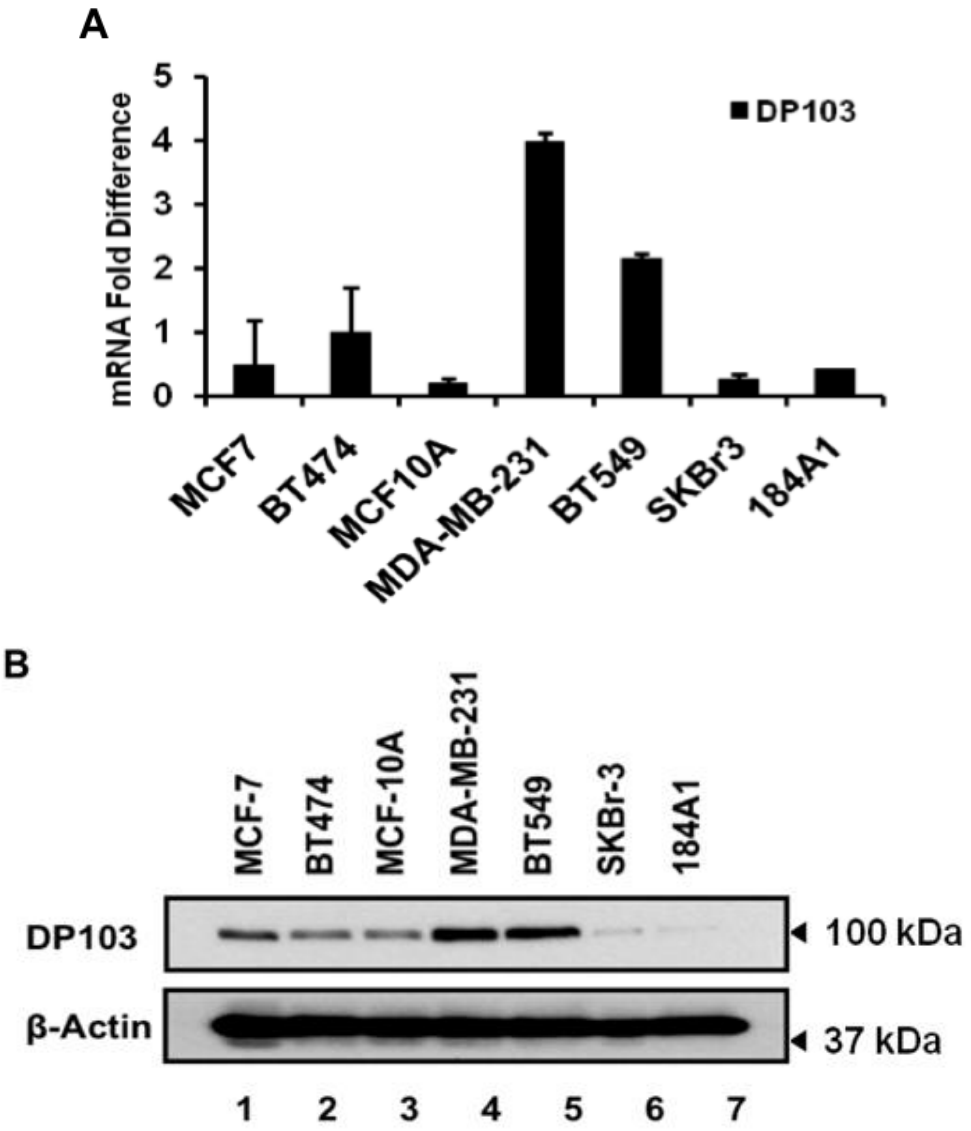

Figure 9. DP103 expression in a panel of breast cell lines. RNA of different breast cell lines were extracted and qPCR were performed with DP103 primer, normalized with 18S and represented as fold difference (A). Cells of different breast cell lines were harvested, lysed for protein and western blotting was performed using DP103 antibody (B).

3.1.3 Expression of DP103 in isogenic xenograft-derived MCF10AT series cell lines

Since the cell lines used in Figure 9 are all derived from different sources, the relationship between the increased expressions of DP103 with the degree of invasiveness cannot be established. Hence, we determined basal DP103 expression in an isogenic xenograft-derived MCF10 breast cancer progression model system. The MCF10 breast cancer progression model system was originally derived from Fred Miller's laboratory (Choong et al., 2010; Choong et al., 2011; Dawson et al., 1996). Immortalized breast epithelial cell line MCF10A (10A1) was transfected with T24 c-Ras oncogene and injected into nude mice. By reestablishing cells in tissue culture from one of the carcinomas, a cell line designated MCF10AT1 was derived that forms simple ducts when transplanted in Matrigel into immunodeficient mice. With time *in vivo*, the epithelium becomes proliferative and a cribriform pattern develops within the xenografts. A significant number progress to lesions resembling atypical hyperplasia and carcinoma *in situ* in women, and some progress to invasive carcinomas. Pre-malignant MCF10AT (AT1k), low grade MCF10CA1h (CA1h), and high grade MCF10CA1a (CA1a) cell lines were generated by reestablishing cells in tissue culture from these lesions representing successive transplant generations (Figure 10). With each generation, cells are somewhat more likely to progress to high risk lesions resembling the human proliferative breast disease.

High grade CA1a cells were previously characterized to metastasize following orthotopic mammary fat pad and intravenous tail vein injections while 10A1 and AT1k cells failed to form tumors (Hurst et al., 2009; Santner et al., 2001; Worsham et al., 2006). As shown in Figure 11, basal levels of DP103, both at mRNA and protein

levels directly correlated with increasing invasive potential of these cell lines, with the lowest level of DP103 being observed in the normal 10A1 cells and highest expression being observed in the highly metastatic CA1a cells. The importance of this finding is that DP103 expression increases with the progression of breast cancer, strongly indicating a role of DP103 in promoting tumorigenesis.

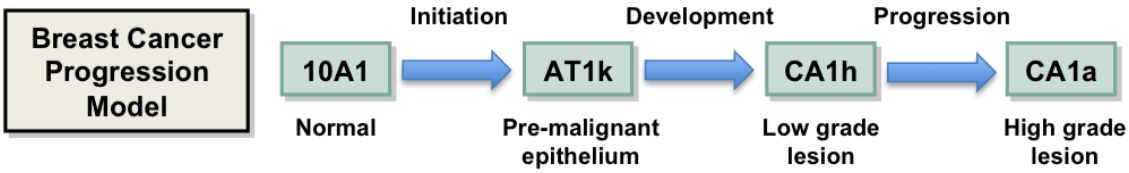

Figure 10. Overview of MCF10AT series cell lines (Adapted from Choong et al., 2010).

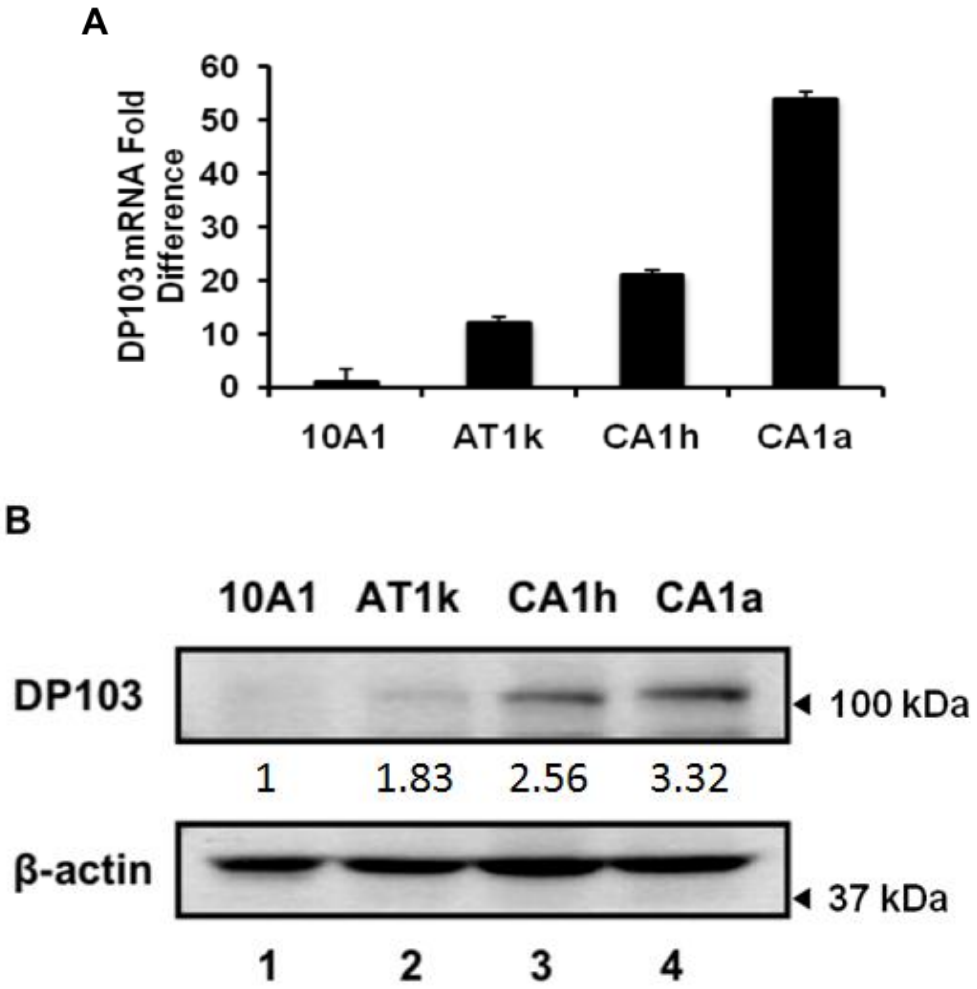

Figure 11. RNA and protein expression of DP103 from four isogenic cell lines. RNA were extracted and qPCR were performed with DP103 primer, normalized with 18S and represented as fold difference (A). Total cell lysates were harvested, lysed for protein and western blotting was performed using DP103 antibody. The densitometry values (indicated below the blot) were normalized with respect to the β-actin control (B).

3.1.4 Expression of DP103 in human cancer patients

To determine if the same trend is also observed clinically, we obtained a total of 48 primary breast cancer and 15 benign breast tissue samples derived from patients who underwent surgery from our collaborator Dr Zhu Tao from Hefei National Laboratory for Physical Sciences at Microscale and School of Life Sciences, University of Science and Technology of China, Hefei, Anhui, P.R. China.

RNA was extracted from each of these patient samples and DP103 expression was examined. Patients whose breast cancer had metastasized showed upregulated expression of DP103 in the primary tumor when compared to breast cancer patients who did not show tumor metastasis. The tissues of patients with benign breast diseases were used to act as a control and DP103 expression was observed to be the lowest (Figure 12).

Together with the results from the xenograft-derived cell lines, we showed, for the first time, the strong association of DP103 with the differential stages of cancer from normal epithelial to the high grade lesions. It is also the first time that DP103 is reported to be correlative to cancer progression, with its highest expression to be present in the metastatic cells.

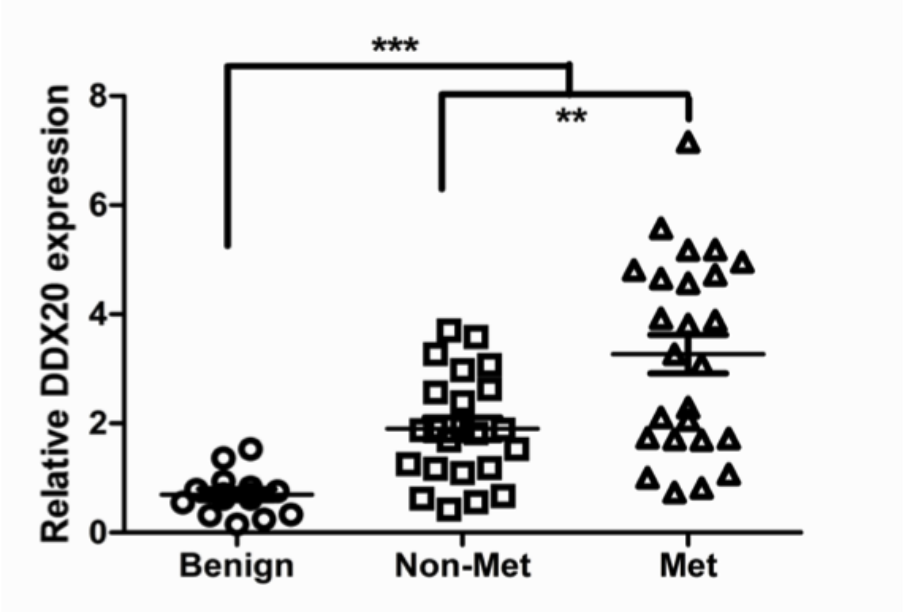

Figure 12. DP103 expression in human breast benign, non-metastatic (Non-Met) and metastatic (Met) tissues. Human patient samples were collected, RNA extracted and tested for DP103 expression (n=63, *** denotes $p<0.001$, ** denotes $p<0.01$)

3.2 Effects of down-regulation of DP103

Since DP103 has been shown to possess a correlation in its expression to the state of malignancy in breast cancer as well as its high expression in highly metastatic cell lines, it was hypothesized that down-regulation of DP103 in invasive breast cancer would decrease the invasive ability of the cells. Hence, two highly invasive breast cancer cell lines, MDA-MB-231 and BT549 were used in subsequent experiments.

Before performing any functional assay, validation of the efficiency of the knockdown of DP103 using RNAi technology was done. Two unique siRNAs against DP103 (Figure 13) were first tested individually or pooled together for their efficiency. The advantage of using pooled siRNAs is increasing on-target effect while reducing the off-target effects. Within a complex mixture, each siRNA is at a lower concentration used for individual setup. However, the on-target effect of multiple siRNAs is additive. Although each siRNA may also have an off-target effect, it is noted that it will be different for each siRNA in the mix and therefore, the off-target effects will be diluted out (Nathan, 2008).

In Figure 14, it was shown that the use of siDP103 #1 and #2 pooled together produced a better knockdown of DP103 as compared to them being used individually. Hence, this pooled mixture of siRNAs was used for all subsequent knockdown experiments and was labeled as ‘siDP103’ in this project. Furthermore, this knockdown of DP103 is effective transcriptionally and translationally in both MDA-MB-231 and BT549 cell lines (Figure 15).

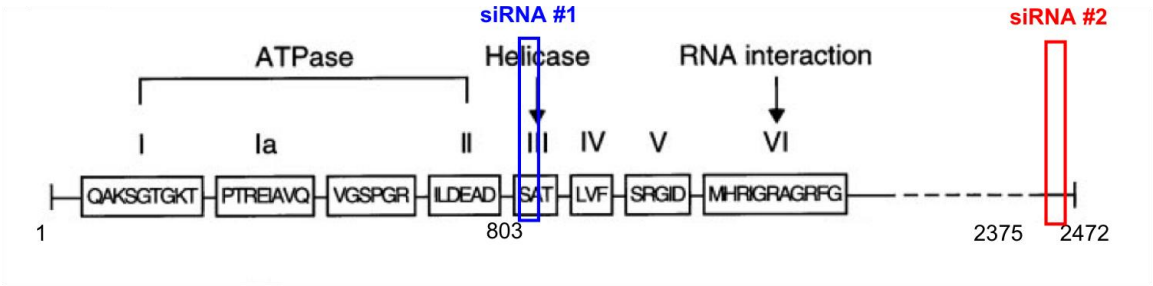

Figure 13. A pictorial representation of siRNA specific sites targeted at DP103 (modified from Ou et al., 2001).

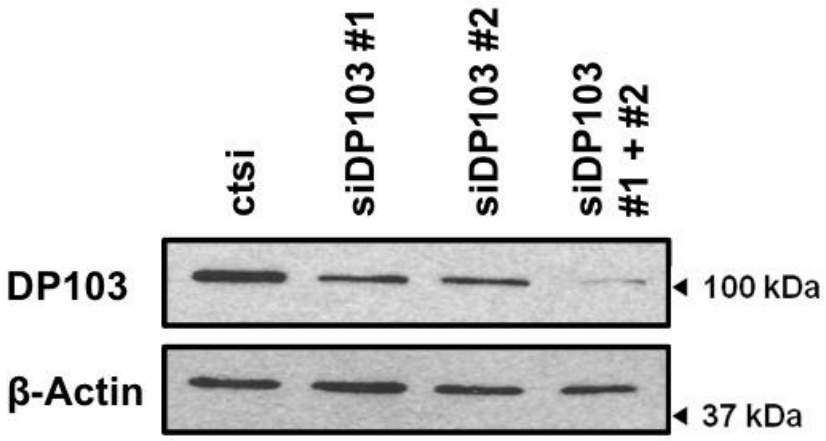

Figure 14. Pooled siRNA against DP103 showed better knockdown. MDA-MB-231 cells were transfected with various siRNAs either individually or pooled and then harvested for protein 48h after transfection. Western blotting was performed using DP103 antibody.

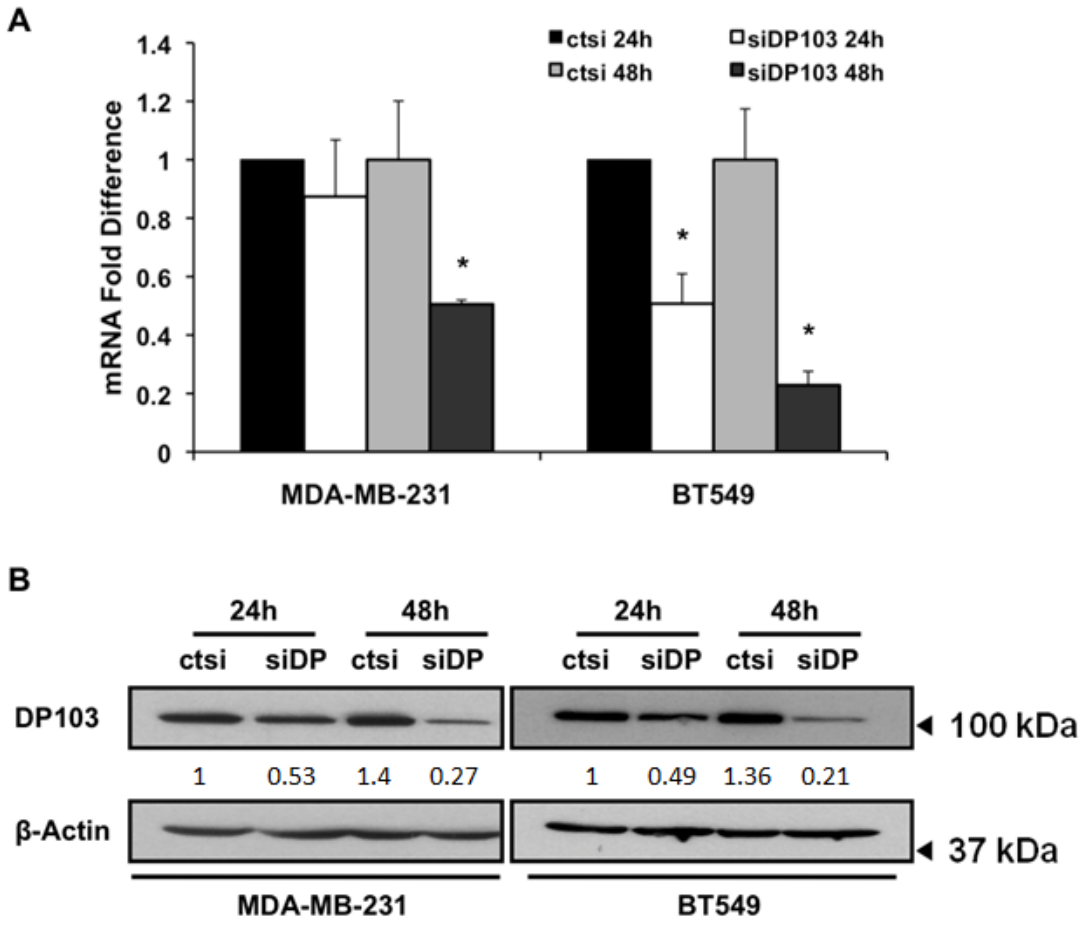

Figure 15. Validation of knockdown of DP103 in MDA-MB-231 and BT549. Cells were transfected with 2 unique siRNA against DP103 pooled together and then harvested for RNA and protein respectively at the times indicated. Realtime-PCR was performed with DP103 primer, normalized with 18S and represented as fold difference (A). Western blotting was performed using DP103 antibody. The densitometry values (indicated below the respective blots) were normalized with respect to the β-actin control (B). * denotes $p<0.05$.

3.2.1 Knockdown of DP103 on cell viability

Tumor formation stems from the inability to regulate cell cycle, causing erratic and uncontrollable cell growth. Cancer cells have to overcome several checkpoints in order to proliferate. Limitless replicative potential and evasion of apoptosis are two hallmarks of cancers (Hanahan and Weinberg, 2011) and since DP103 expression increases with the extent of tumor progression, we would like to ask if DP103 plays a role in the aberrant growth of breast cancer cells.

To check for cell viability, MTT assay was performed and the suppression of DP103 did not affect the viability in both MDA-MB-231 and BT549 cells at 24h and 48h (Figure 16). Importantly, this means that any changes seen in subsequent assays can be attributed to the decrease in DP103 expression after knockdown, and not due to the differences in the viability of the breast cancer cells. At the same time, our data also suggest that DP103 does not have any effect on short term cell viability of the cells, though more experiments will be needed to determine if it has any role in cell cycle, apoptosis or long term cell viability.

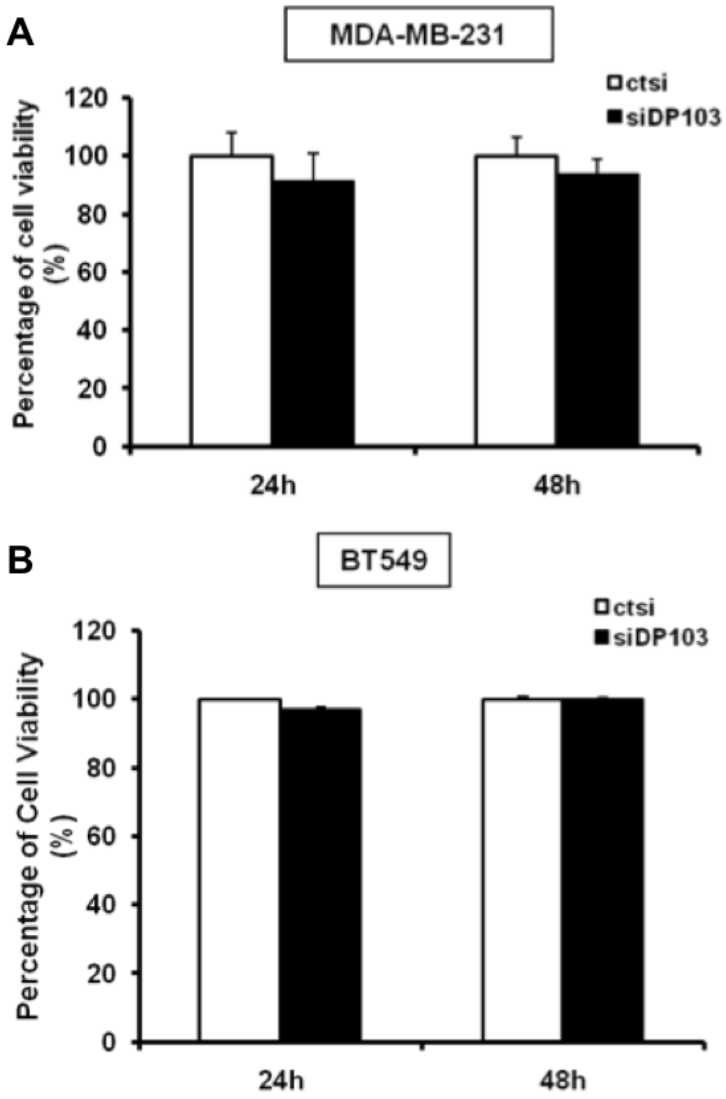

Figure 16. Cell viability is not affected when DP103 is knocked down. MDA-MB-231 (A) and BT549 cells (B) were seeded into 12-well plates and transfected with either control siRNA or siRNA against DP103. MTT solution was added and absorbance read at 550nm to measure cell viability. The percentage of cell viability was then calculated using ctsi as 100%. Data represents the average reading of three independent experiments.

3.2.2 Knockdown of DP103 on cell migration using wound healing assay

We next investigated the effect of DP103 down-regulation on cell migration using the wound healing assay. This method is one of the earliest developed to study directional cell migration in an *in vitro* model. It mimics cell migration during wound healing *in vivo*. By physically creating an artificial 'wound' in a cell monolayer, capturing and comparing images at the beginning and at the end of the assay, the migration rate of the cells can be quantified (Amin et al., 2003; Fahmy et al., 2003).

As shown in Figure 17A, there was a marked decrease in the number of cells migrating into the wound in both MDA-MB-231 and BT549 cells after 48h. The difference in the gap distance of the wound at the start and the end of the assay would indicate the perpendicular distance that the cells move. The distances measured after 48h were subtracted from the original length of the wound at the start of the assay. Subsequently, these measurements were converted to percentages showing migration distance as compared to the control cells at 0h. In MDA-MB-231, there was a decrease in migration distance of about 52% upon suppression of DP103, whereas that in BT549, the decrease was about 43.5% (Figure 17B).

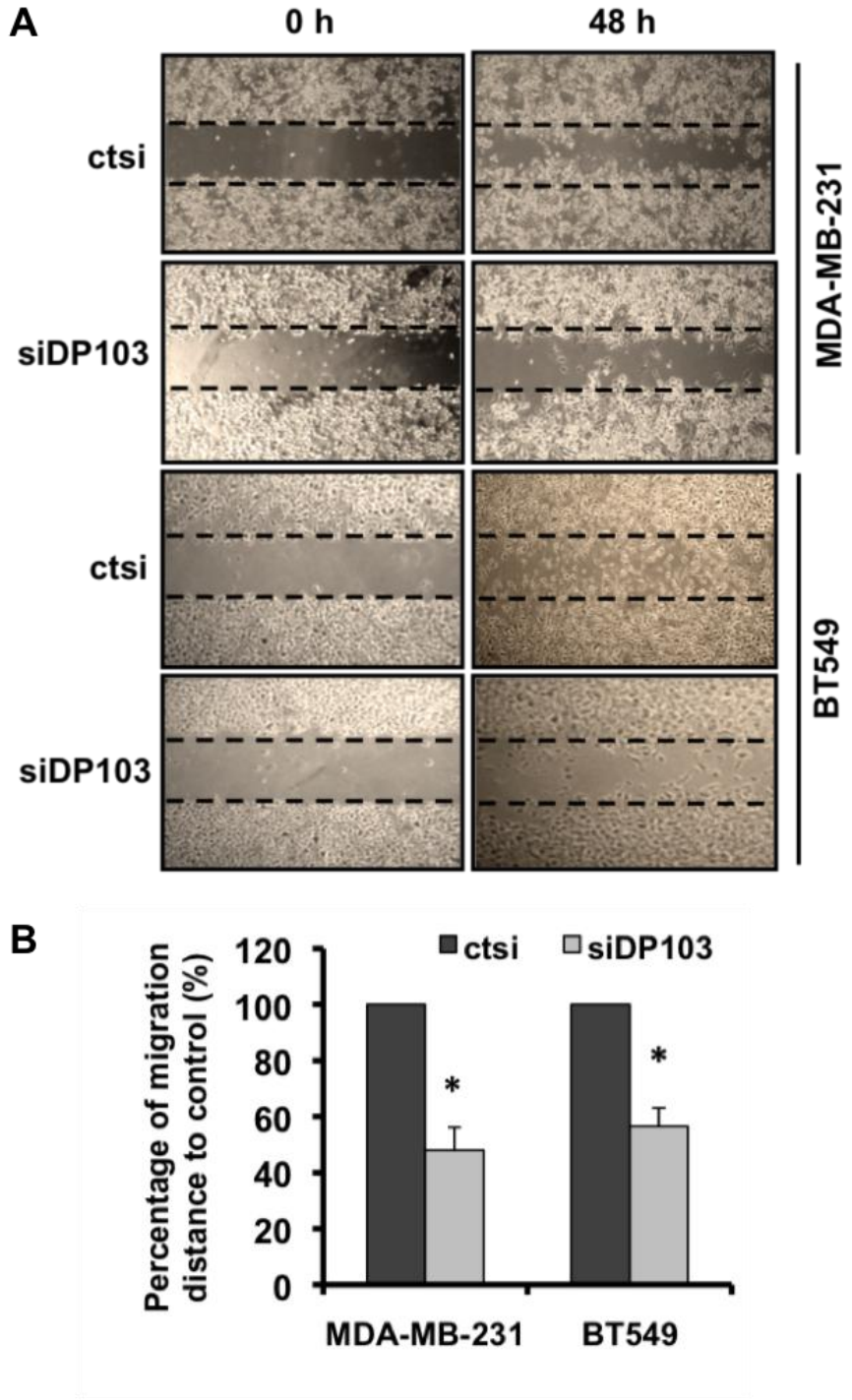

Figure 17. Cells migration was reduced when DP103 was down-regulated. siRNA against DP103 was transfected in MDA-MB-231 and BT549 cells. They were then seeded to confluency. A wound was made and pictures taken at 0h and 48h to depict wound healing ability (A). The migration distances of cells were measured at 3 separate regions after wound healing assay (B). * denotes $p<0.05$.

3.2.3 Knockdown of DP103 on cell migration using non-wound healing assay

The disadvantage of the wound healing assay is the lack of a defined wound surface area, or gap between cells. These wounds can be varying in sizes and widths, which inhibit consistent results and create variation from well to well. In addition, mechanical wounding induces other processes like anoikis (Grossmann, 2002) when some cells are detached from the tissue culture plates. Cells are also damaged physically, stimulating repair proceeses or inducing cell death (Miyake and McNeil, 2003; Woolley and Martin, 2000). All these contribute to experimental noise and additional assays should be performed to support findings from the wound healing assay.

A two-dimensional non-wound migration assay was done in collaboration with Prof Lim Chwee Teck (Division of Bioengineering and Department of Mechanical Engineering, NUS) and his team to study the migratory behavior of MDA-MB-231 with and without DP103 expression as described in materials and methods. Briefly, control and transfected cells were allowed to grow to confluency in a cylinder on a tissue-culture plate. Fifty cells in each condition were tracked for the distance they moved over a period of 24h and the average monolayer edge distance was tabulated and plotted on a graph in Figure 18A.

The two-dimensional track plots of the cells were depicted in Figure 18B. The left panels, top and bottom, showed cells transfected with control siRNA and the right panels, top and bottom showed cells transfected with siRNA against DP103. The top panels showed the entire tracks made by the 50 cells while the bottom panels showed the ending points of each cell tracks. The starting points of each cell track were

moved to the origin of the graph, without changing the directionality of the tracks, thus allowing us to observe the effective dispersal of the cells with respect to their individual starting points. The centre of mass is defined as the average distance from the origin that a single cell would be displaced if it were to represent the displacements of all the tracked cells taken together. A circle of this diameter would allow an estimate of the number of cells that have actually displaced to larger distances than the average displacement for that experiment (as shown in Figure 18B). The control condition shows a higher percentage (72%) of cells outside a circle with a radius equal to the center of mass compared to 44% when DP103 was suppressed. These results further confirm that cell migration and displacement with respect to the starting points of the cells were significantly reduced when DP103 was knocked down in the MDA-MB-231 cells as compared to the control cells. This higher number of cells outside the center of mass showed that they have an increased outward dispersion than that in cells with knockdown of DP103.

The data of individual cell tracks from our two-dimensional non-wound migration assay was then analyzed for various cell migration parameters in Figure 19. Accumulated distance (AD) is an indicator of motility of individual cells whereas Euclidean distance (ED) gives an idea about the actual dispersion of the cells with respect to their starting positions. On the other hand, confinement ratio is an indicator of straightness of the cell paths and reflects the stability of directions of the lamellipod polarization over time. Lamellipod polarizations are primarily responsible for laying down the foundations for directionality of the cells by affecting focal adhesion distribution and hence the contractility of the cells leading to cell motility (Dulyaninova et al., 2007; Smith et al., 2007). The control cells (ctsi) showed an

increase in the migration distances (AD and ED) of individual cells that significantly decreased in the DP103 knock down cells (siDP103) ($p=0.05$) (Figure 19, top 2 panels). These results agree with the measurements performed by the wound healing and the monolayer edge distances (Figures 17 and 18). Furthermore, there was a decrease in the mean cell speed after suppression of DP103 (Figure 19, bottom left panel). The confinement ratios however did not show a significant difference indicating that knockdown of DP103 decreased the motility of the cells but not their directionality (Figure 19, bottom right panel). These observations suggest that depletion of DP103 affected the intracellular motility mechanisms in MDA-MB-231 cells but not the lamellipod polarization.

These results from Figures 17 to 19 indicated that the downregulation of DP103 expression reduced the overall migration of the cells including the motility of individual cells but did not affect the directionality in the cells.

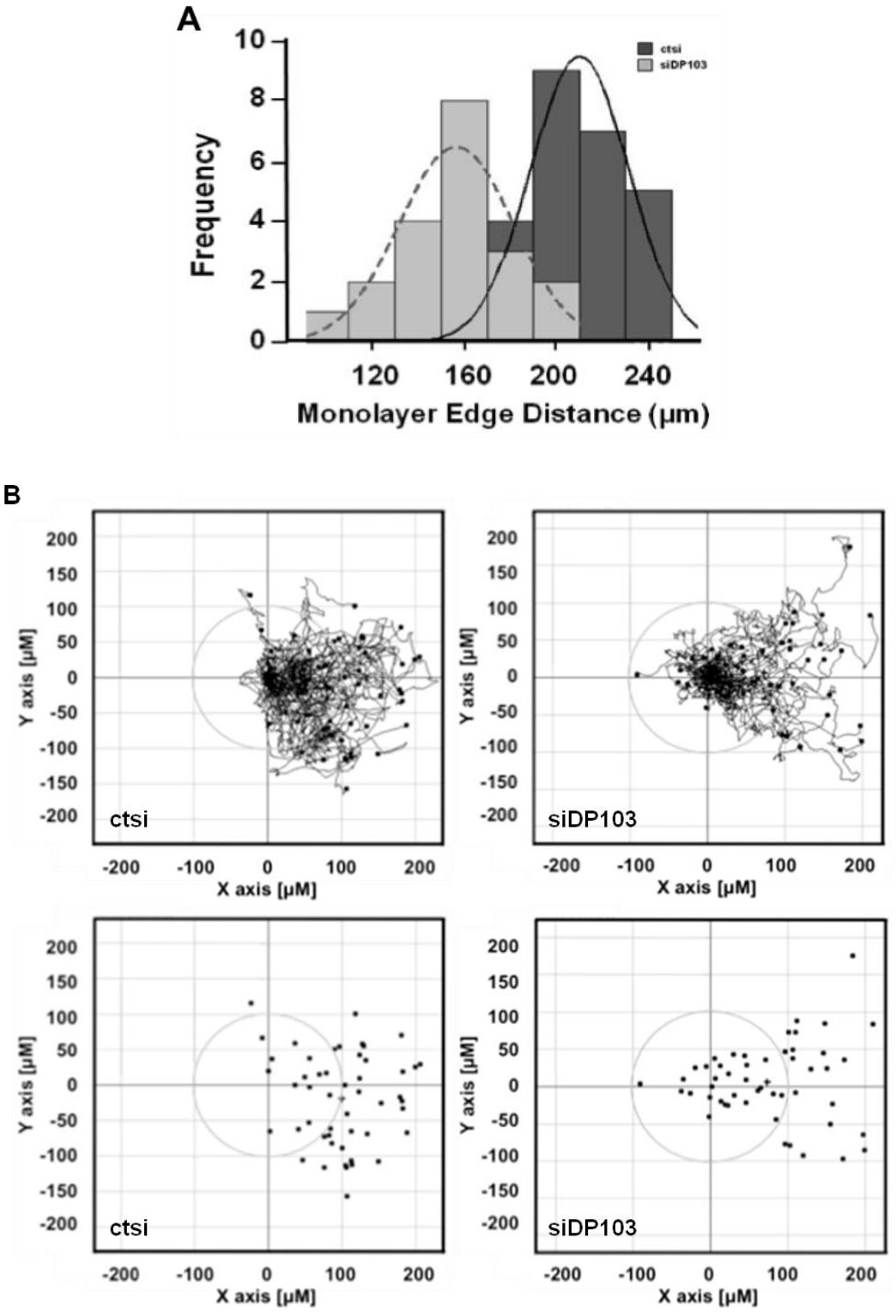

Figure 18. Cells after knockdown of DP103 showed decreased cell motility. MDA-MB-231 cells were subjected to siRNA knockdown of DP103. Monolayer edge distance of the cells (A) and dispersion patterns (B) were tracked using live microscopy.

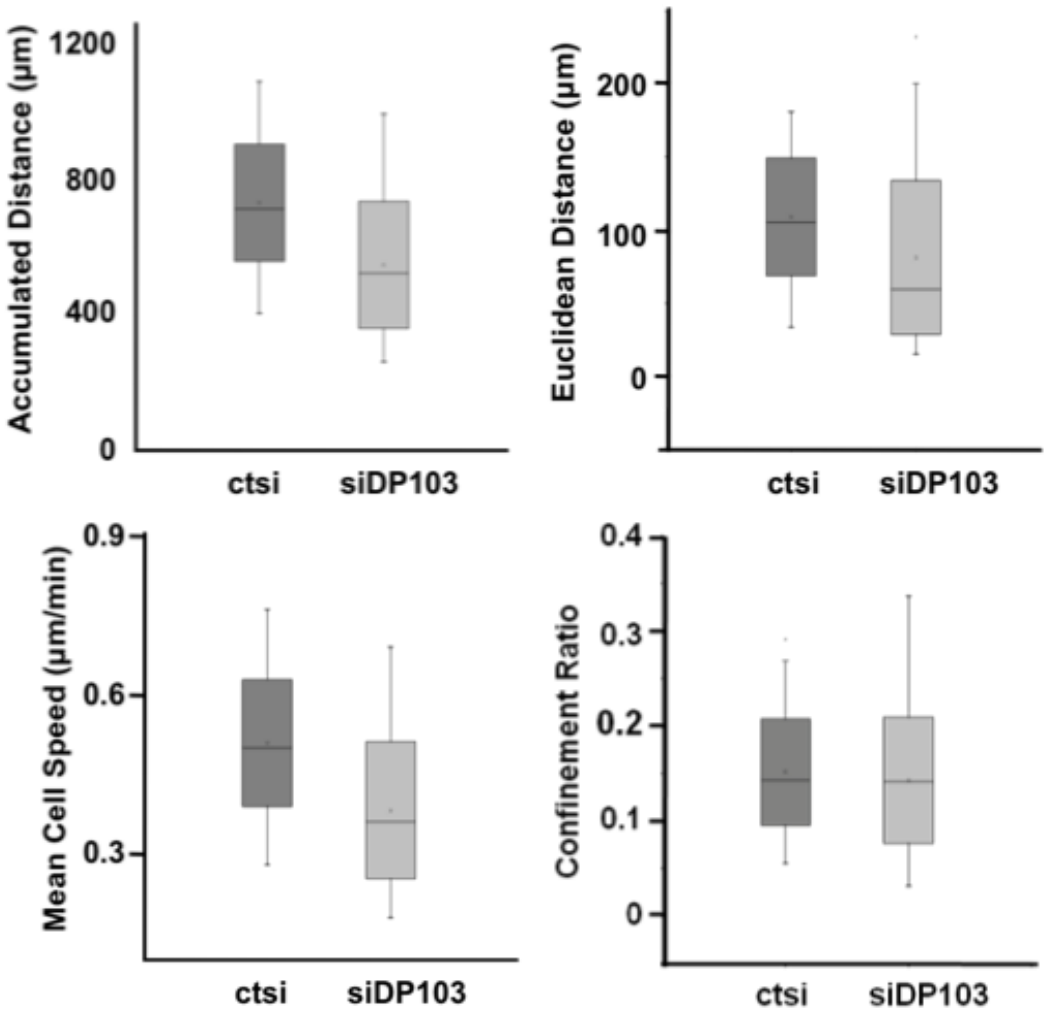

Figure 19. Cells after knockdown of DP103 affected the intracellular motility mechanisms in MDA-MB-231 but not the directionality. Graphs of different parameters were plotted using data from Figure 18.

3.2.4 Knockdown of DP103 on cell invasion

Since we had previously shown that DP103 is upregulated in highly invasive breast cancer cells, we next explored effects of decreased DP103 expression on tumor cell invasion. The matrigel transwell chambers were used, which consist of an 8μm pore size PET membrane with a thin layer of matrigel basement membrane matrix. The matrigel matrix serves as a reconstituted basement membrane *in vitro*. The layer occludes the pores of the membrane, blocking non-invasive cells from invading through the membrane. In contrast, invasive cells are able to detach themselves and invade through the matrigel matrix and the membrane pores.

MDA-MB-231 and BT549 cells were seeded into the chamber after siRNA transfection had been done the previous day. We removed the matrigel matrix membrane from the casing after 24h upon seeding, stained the cells on the underside of the membranes and showed that transient knockdown of DP103 resulted in a decrease of invading cells through the membrane (Figure 20A), with percentages drop in 53.2% and 67.8% in MDA-MB-231 and BT549 respectively (Figure 20B).

In another attempt to reconstitute a micro-environment as closely to *in vivo* conditions, we performed a three-dimensional collagen gel assay in collaboration with Prof Lim Chwee Teck and his graduate student, Ms Sun Wei (Division of Bioengineering and Department of Mechanical Engineering, NUS). We constructed a collagen hydrogel block and seeded MDA-MB-231 cells in the centre of the block. Using live microscopy, we tracked each cells over 10h. The tracks taken by the control and DP103 knockdown cells were then overlaid and compared. As shown in Figure 21A, with the suppression of DP103, there was a slight reduction in the spread

of red tracks as compared to that of the control cells, represented by the green tracks. Notably, some of the control cells are more dispersed outwards into the collagen gel. Cell speed of the cells was also averaged over each track and plotted into a histogram (Figure 21B). The medians of cell speed are 14.4μm/h and 10.8μm/h for ctsi and siDP103 cells respectively. This meant that the cells treated with siDP103 traveled slower than the control cells. Since this was done on a 3D collagen gel, it was an indication that with the suppression of DP103 expression, the cells were less invasive, further confirming our previous observation using the transwell matrigel chambers.

Pseudopodial protrusion and the dynamic actin cytoskeleton remodeling have long been associated with tumor cell migration and invasion (Guirguis et al., 1987; Lauffenburger and Horwitz, 1996). MDA-MB-231 cells characteristically show a branching morphogenesis. Interestingly, we observed a loss of the pseudopodia protrusions in the cell after the suppression of DP103 by siRNA (Figure 22), indicating that DP103 indeed has a role in cell metastasis and its depletion halts the progression of their invasion.

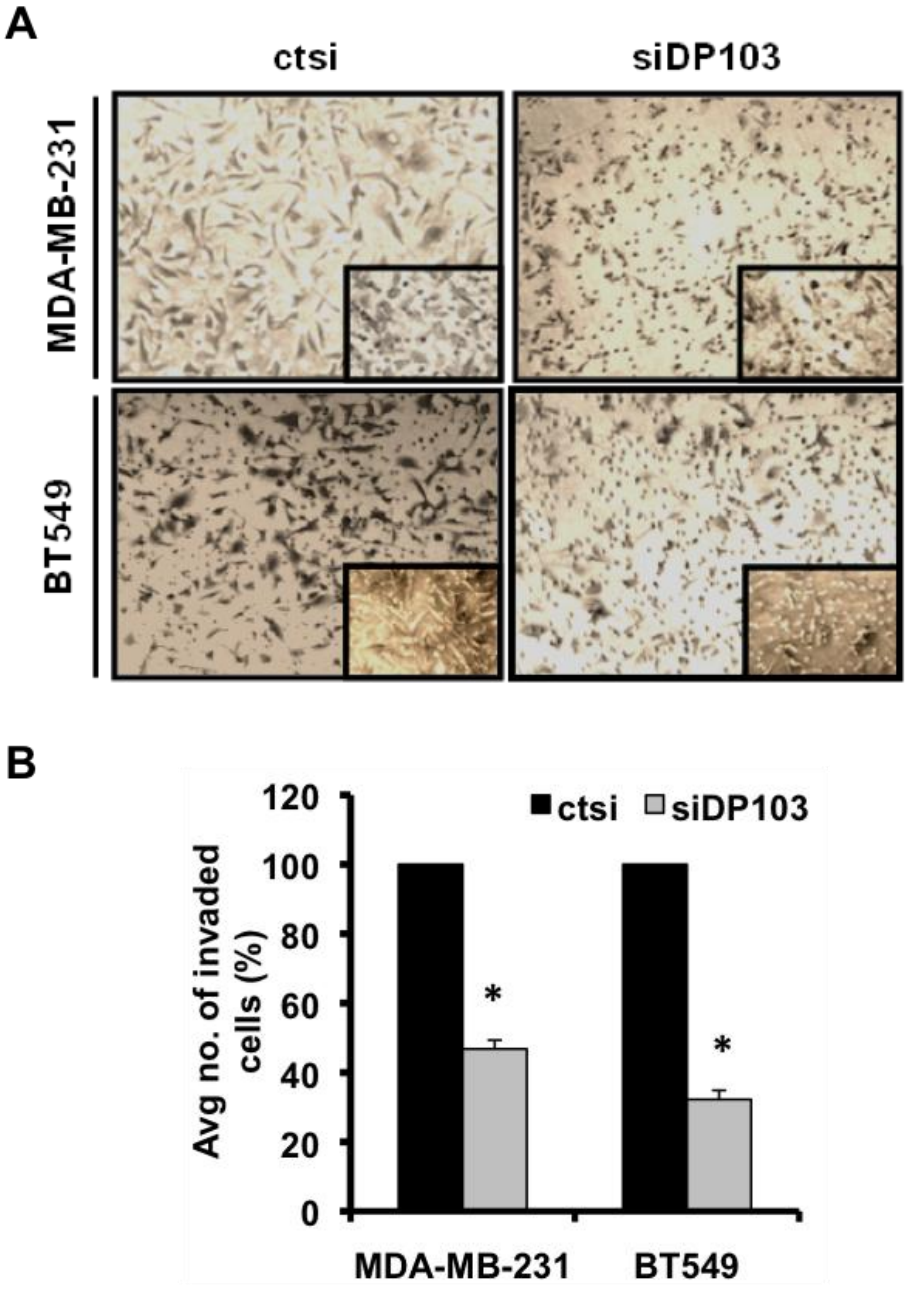

Figure 20. Cells after knockdown of DP103 showed decreased cell invasion. 2 x 10^5 MDA-MB-231 and BT549 cells were seeded into the upper chamber of the transwell invasion chamber with serum free media after siDP103 transfection for 48h. The membranes of the chambers were stained with crystal violet solution and mounted on microscope and pictures taken. Insert shows representative picture in higher magnification (A). The number of cells that invaded through the transwell invasion chambers were counted in five randomly selected microscope field and plotted on a graph (B). * denotes $p<0.05$.

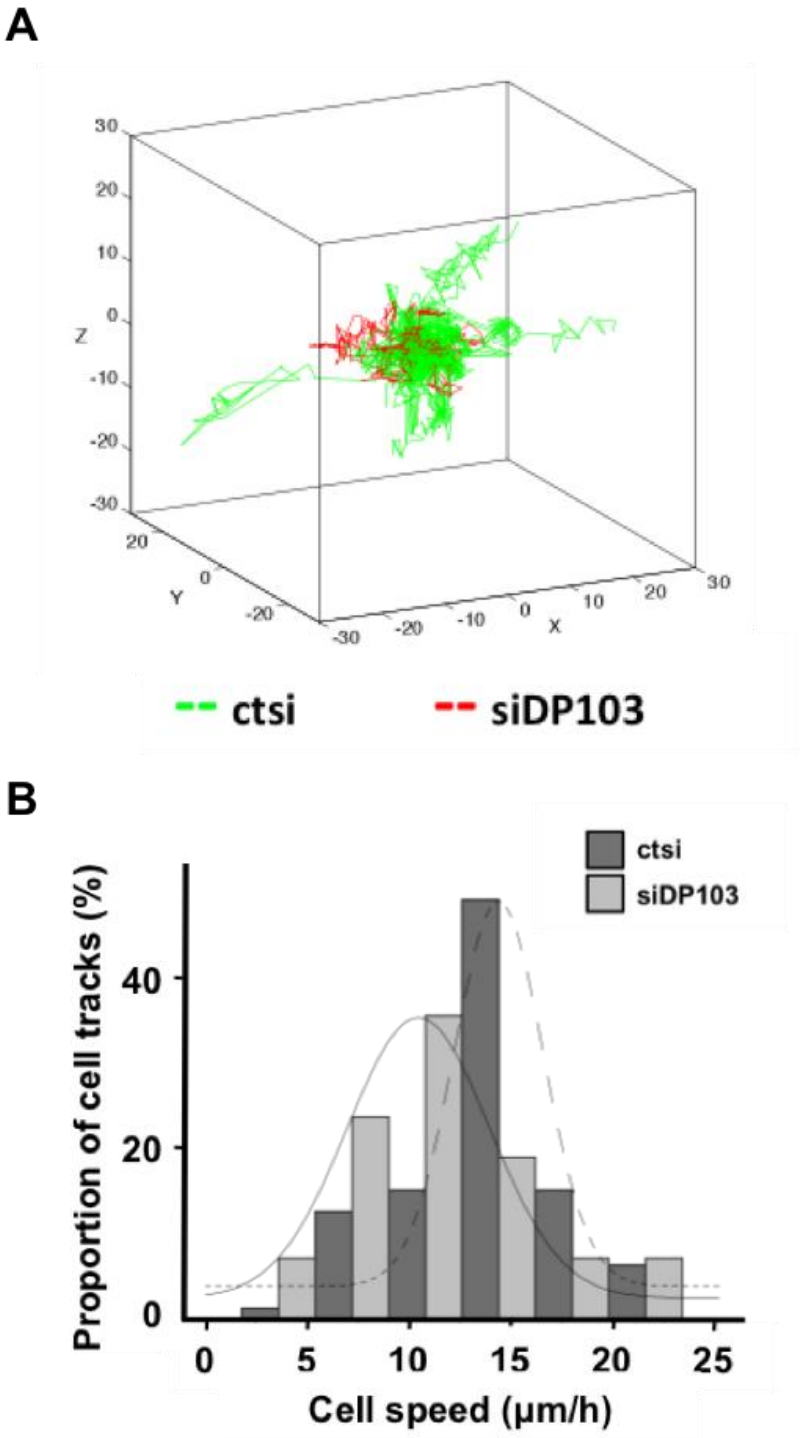

Figure 21. MDA-MB-231 cells showed less dispersion and reduced cell speed in a 3D collagen gel upon knockdown of DP103. Cell displacement (µm) tracks over 10 hours in 3D collagen gel. The tracks of a population of cells (n>50) were adjusted to start from the same origin (0,0,0). Control cells are depicted with green tracks while siDP103 treated cells are in red (A). The histogram of cells speed averaged over each track, track number >50. The height of each column corresponds to the percentage of tracks of a certain speed (B).

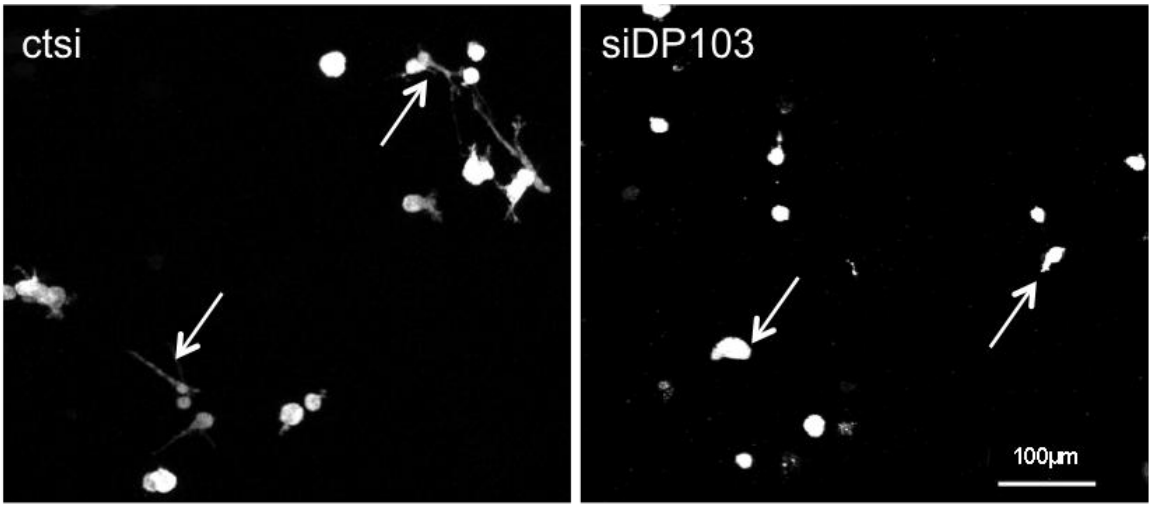

Figure 21. Morphology of MDA-MB-231 cells in the 3D collagen hydrogel after knockdown of DP103. Pictures taken from capturing images during live tracking of the cells over a period of 10h. Scale bar represents 100µm.

3.3 Effect of Over-expression of DP103

To further substantiate our loss-of-function findings above, we then questioned if a gain-of-function of DP103 would reverse our previous observations and alter the cells' behavior.

3.3.1 Over-expression of DP103 on cell invasion

We transfected MDA-MB-231 cells with DP103 plasmid for 24h before seeding some of the cells into the matrigel chamber while harvesting the reminding cells for western blotting to quantify the amount of overexpression.

Figure 23A showed successful overexpression of DP103 protein in MDA-MB-231 cells, indicating that the cells in the invasion assay were also overexpressed with DP103. This forced expression of DP103 significantly promoted invasion by about 1.5 folds as observed in the transwell invasion assay (Figure 23B and C).

Importantly, when we repeated the same setup using MCF10A, a normal human breast epithelial cell line, with low invasive potential and a low level of DP103 expression (as seen previously in Figure 9), it also showed increased invasion by at least 4 folds upon forced expression of DP103 (Figure 24). These strongly suggest that increasing levels of DP103 alone would result in transforming cells transforming into an invasive phenotype. Henceforth, again, for the first time, we demonstrate the oncogenicity potential of DP103, and that DP103 is a metastasis-associated gene.

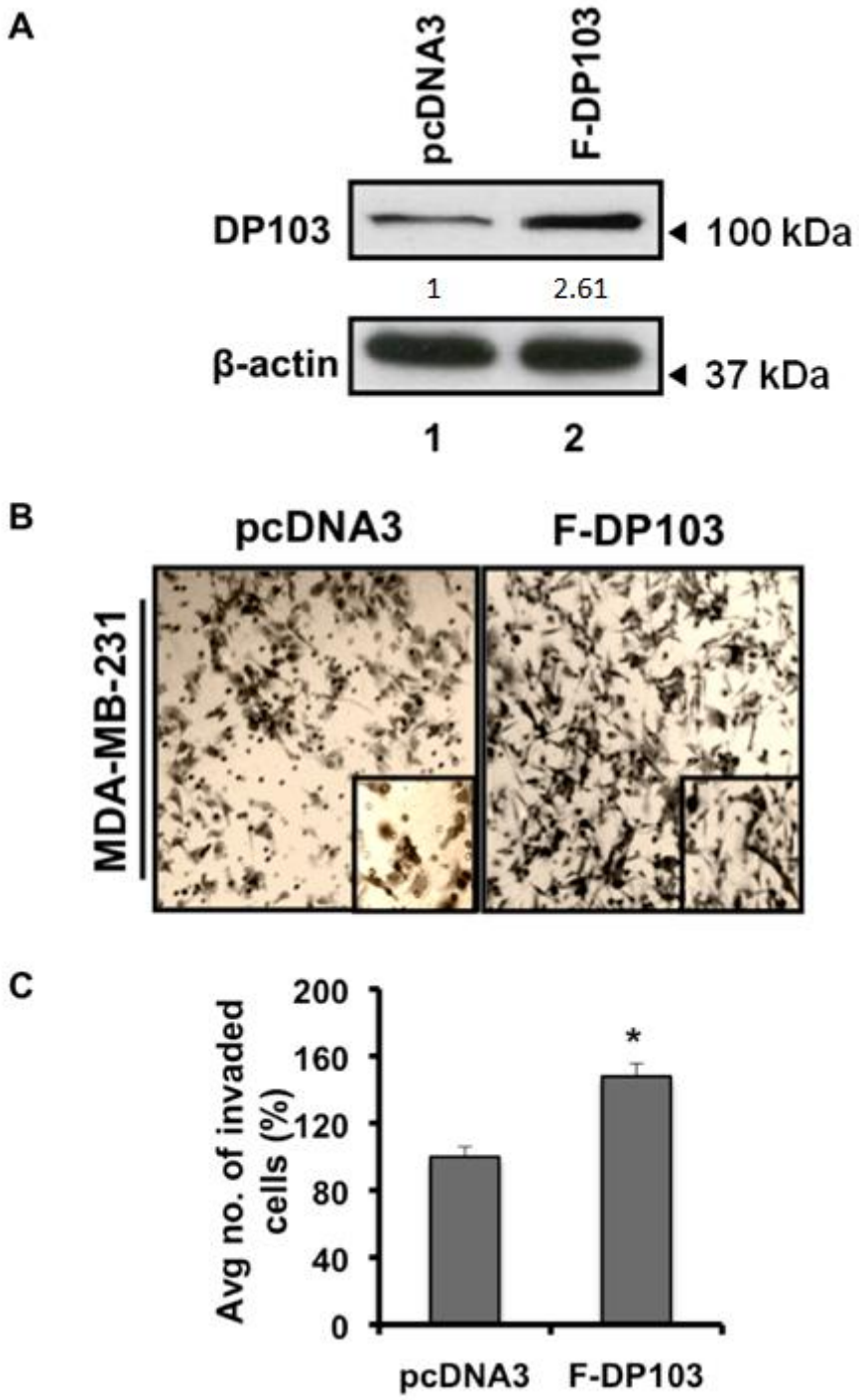

Figure 23. Over-expression of DP103 in MDA-MB-231 increased cell invasion. MDA-MB-231 cells were transfected with pcDNA3 and pcDNA3-FLAG-DP103 (F-DP103). Cells were harvested and lysed, and cell extracts were immunoblotted with anti-DP103 antibodies. The densitometry values (indicated below the blot) were normalized with respect to the β-actin control (A). MDA-MB-231 cells were prepared for invasion assay (B). MDA-MB-231 cells that invaded through the chambers were counted and plotted (C). * denotes $p<0.05$.

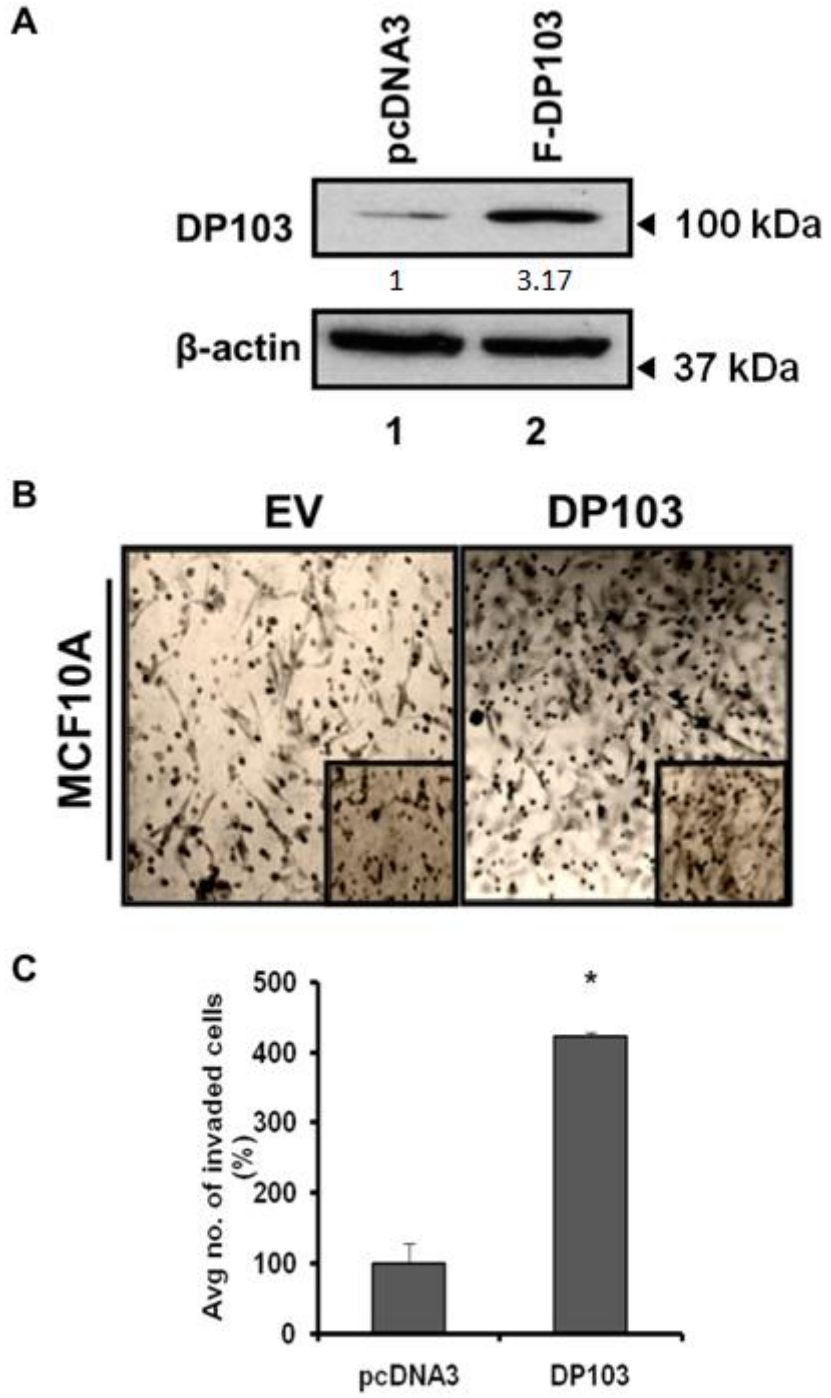

Figure 24. Over-expression of DP103 in MCF10A increased cell invasion. MCF10A cells were transfected with pcDNA3 and pcDNA3-FLAG-DP103 (F-DP103). Cells were harvested and lysed, and cell extracts were immunoblotted with anti-DP103 antibodies. The densitometry values (indicated below the blot) were normalized with respect to the β-actin control (A). MCF10A cells were prepared for invasion assay (B). MCF10A cells that invaded through the chambers were counted in five randomly selected microscope field and plotted (C). * denotes $p<0.05$.

3.3.2 Over-expression of DP103 in a metastasis qPCR array

Cell invasion requires the complex coregulation of cytoskeletal reorganization and cell motility as well as proteolyis and interaction with the extracellular matrix. Since DP103 is a metastasis-associated gene and over-expression of DP103 increases metastasis, we seek to identify the metastatic genes modulated by it.

We established a 'metastatic qPCR array' in which 13 genes known to be involved in metastasis were selected to be used for the array (Table 4). β-actin, HPRT and GAPDH were used as 'housekeeping' genes. Using BT549 cells with or without DP103 overexpression by lentivirus infection, we measured the mRNA levels of these 13 genes.

The over-expression of DP103 did not alter the mRNA expression of genes like NME1, PLAU, SERPINB5 or MTA1, but several other genes like MMP1, TIMP1 and TIMP3 were upregulated slightly. Significantly, MMP9 or matrix metalloproteinase 9 was increased by 2.66 folds, indicating that MMP9 might be a major modulator of invasion mediated by DP103 (Table 5).

Gene	Gene Name	References
MTA2	Metastasis associated gene 2	(Fu et al., 2011; Li et al., 2010)
NME1	Nucleoside diphosphate kinase A	(Boissan et al., 2010; Polanski et al., 2011)
PLAU	Urokinase-type plasminogen activator	(Yoshizawa et al., 2011)
MET	Hepatocyte growth factor receptor	(Lee et al., 2006)
PLAUR	Urokinase-type plasminogen activator receptor	(Huang et al., 2011; Margheri et al., 2005)
MMP1	Matrix Metalloproteinase 1	(Egeblad and Werb, 2002; Milde-Langosch et al., 2004)
SERPINB5	Serpin peptidase inhibitor, clade B member 5	(Findeisen et al., 2008)
MMP2	Matrix Metalloproteinase 2	(Bourboulia and Stetler-Stevenson, 2010; Li et al., 2004)
SERPINE1	Serpin peptidase inhibitor, clade E member 1	(Nagahara et al., 2010)
MMP9	Matrix Metalloproteinase 9	(Adamson et al., 2000; Liu et al., 2010; Wu et al., 2008)
TIMP1	Metallopeptidase inhibitor 1	(Baramova et al., 1994; Jinga et al., 2006)
MTA1	Metastasis associated gene 1	(Mahoney et al., 2002; Marzook et al., 2011)
TIMP3	Metallopeptidase inhibitor 3	(Bourboulia and Stetler-

		Stevenson, 2010; Brew and Nagase, 2010)

Table 4. List of metastatic related genes and references that are used in the 'metastatic qPCR array'.

Gene	Gene Name	Fold Change (±SD)	P-value
MTA2	Metastasis associated gene 2	1.173883 (±0.023156)	0.1418
NME1	Nucleoside diphosphate kinase A	0.935731 (±0.022723)	0.8644
PLAU	Urokinase-type plasminogen activator	1.089051 (±0.231132)	0.2914
MET	Hepatocyte growth factor receptor	1.458452 (±0.040862)	0.0036
PLAUR	Urokinase-type plasminogen activator receptor	1.154275 (±0.026637)	0.0499
MMP1	Matrix Metalloproteinase 1	1.88218 (±0.165944)	0.0445
SERPINB5	Serpin peptidase inhibitor, clade B member 5	1.040501 (±0.335911)	0.5561
MMP2	Matrix Metalloproteinase 2	0.80275 (±0.110911)	0.6882
SERPINE1	Serpin peptidase inhibitor, clade E member 1	0.845209 (±0.218096)	0.5754
MMP9	Matrix Metalloproteinase 9	2.668643 (±0.000182)	0.0026
TIMP1	Metallopeptidase inhibitor 1	1.535293 (±0.062558)	0.0043
MTA1	Metastasis associated gene 1	1.225943 (±0.067582)	0.0387
TIMP3	Metallopeptidase inhibitor 3	1.659162 (±0.224292)	0.0372

Table 5. Effects of forced expression of DP103 in BT549 cells on expression of genes functionally involved in metastatic progression. Results are represented as fold change in mRNA levels in BT549-DP103 cells relative to the control cells. Fold change values are representative of three independent mRNA replicates. Values less than 1 indicate decreased expression and more than 1 indicates increased expression of the specific mRNA. Results are derived from three independent sets.

3.4 Is MMP9 expression and activity modulated by DP103?

MMP9 belongs to the family of zinc-dependent endopeptidases capable of degrading all kinds of extracellular matrix in normal physiological processes, such as embryonic development, reproduction and tissue remodeling, as well as in disease processes like arthritis and metastasis. MMP9, in particular, is capable of degrading type IV collagen found richly in basement membrane and had been observed to be strongly correlated in malignant breast tumors (Hanemaaijer et al., 2000).

Till this point, we showed MMP9 to be significantly upregulated when DP103 was overexpressed in BT549 invasive breast cancer cells. In order to validate this observation, as well as to confirm if MMP9 is functionally active in increasing invasion as observed previously, we returned to our previous human patients and cell lines models and sought to elucidate a possible relationship between MMP9 and DP103.

3.4.1 Expression of MMP9 in breast cell lines and tissues

Using the same panel of breast cell lines from Figure 9 to maintain consistency in our results, we screened for MMP9 mRNA and protein expression levels.

In concordant to expression levels of DP103, we showed that the highly invasive cell lines, MDA-MB-231 and BT549 display the highest levels of basal *MMP9* gene expressions while the low metastatic and normal breast cell lines, BT474, MCF10A and 184A1 display the lowest levels of *MMP9* (Figure 25A). Not surprisingly, we saw the same trend in their protein expressions (Figure 25B).

We then used the same cohort of human patient breast tissues from Figure 12 and performed real-time PCR to analyze MMP9 mRNA expression. Similarly, the highest expression of MMP9 was seen in the primary breast tumor tissues that metastasized compared to the primary breast tumor tissues that did not. The breast benign tissues which served as a control displayed the lowest mRNA levels of MMP9 (Figure 26).

Collectively, we demonstrated similar findings as shown in known literatures that high MMP9 expression is associated with invasiveness in cancer cells (Gong et al., 2000; Kim et al., 2006a; van Kempen and Coussens, 2002).

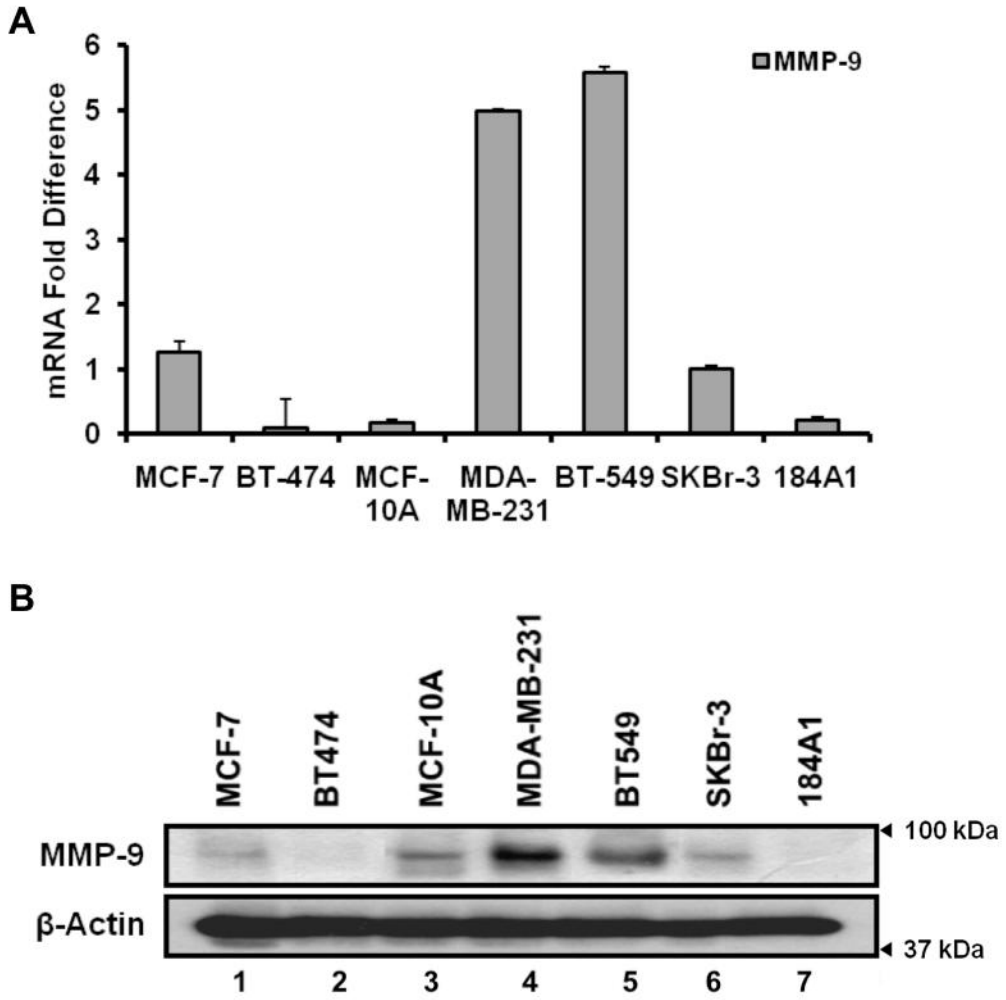

Figure 25. MMP9 expression in a panel of breast cell lines. RNA of different breast cell lines were extracted and qPCR were performed with MMP9 primer, normalized with 18S and represented as fold difference (A). Cells of different breast cell lines were harvested, lysed for protein and western blotting was performed using MMP9 antibody (B).

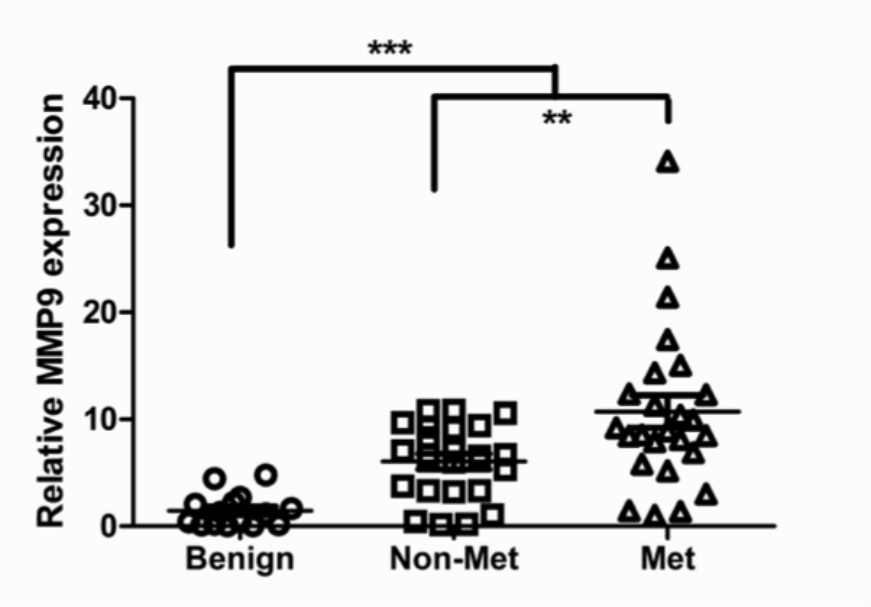

Figure 26. MMP9 expression in human breast benign, non-metastatic (Non-Met) and metastatic (Met) tissues. Samples were collected and tested for MMP9 mRNA expression (n=63, *** denotes $p<0.001$, ** denotes $p<0.01$).

3.4.2 Correlation of MMP9 with DP103 expression

We have shown that both DP103 and MMP9 levels are high in aggressively invasive cells lines and tissues. Hence, a Pearson correlation coefficient analysis was done to measure the association between these two genes.

The Pearson correlation coefficient or Pearson product-moment correlation coefficient is widely used as a measure of the strength of linear dependence between two variables. The correlation coefficient ranges from -1 to 1. A value of 0 indicates that there is no association between the two variables. A value greater than 0 indicates a positive association and a value less than 0 indicates a negative association. Generally, a value ranging from ±0.1 to ±0.3 has a small strength of association. A value ranging from ±0.3 to ±0.5 has a medium strength of association and value ranging from ±0.5 to ±1.0 has a strong strength of association.

From the panel of breast cell lines, the Pearson correlation coefficient was calculated to be $r = 0.913$, suggesting a strong correlation of DP103 to MMP9 expressions (Figure 27A). Furthermore, from the cohort of 63 human breast tissues, the Pearson correlation coefficient was $r = 0.513$, indicating that there is indeed a positive association of levels of DP103 and MMP9 in both *in vitro* and *in vivo* models (Figure 27B).

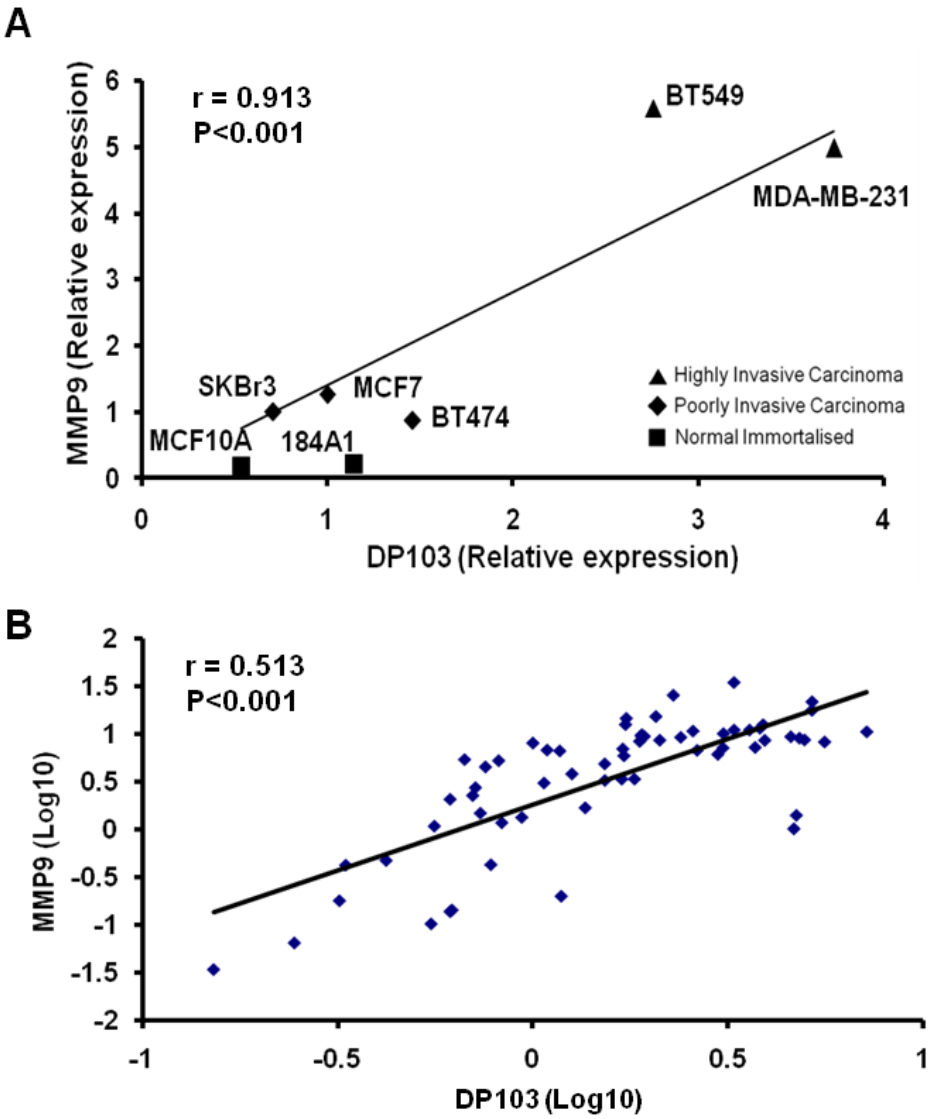

Figure 27. DP103 and MMP9 levels are correlated. Pearson's Correlation Coefficient was determined between the mRNA expression of DP103 and MMP9 in various breast cell lines. DP103 expression was positively correlated with MMP9 expression (A). DP103 and MMP9 expression levels in 63 human breast patients were determined and showed positive correlation (B).

3.4.3 High expressions of DP103 and MMP9 lead to poor prognosis

Since high MMP9 expression is closely associated with poor prognosis in other cancer types like nasopharyngeal, squamous cell carcinoma and lymphoma (Liu et al., 2010; Mitra et al., 2008; Sakata et al., 2004), we performed immunohistochemical (IHC) staining of tissues from the same patients cohort used in Figures 7 and 8 for MMP9 expression.

For comparison of survival outcomes in relation to DP103 and MMP9 expressions, the group with intermediate (2+) and high (3+) pathological scoring was classified as "high" while those with low (1+) or undetectable (0) were classified as "low". Using this grouping, a Kaplan-Meier analysis was performed to investigate the association of MMP9 and DP103 expressions with survival in AJCC (American Joint Committee on Cancer) stages 3 and 4 breast cancer patients with the differences assessed by log-rank.

The Kaplan-Meier analysis is an estimator for estimating the survival function from life-time data. It is often used to measure the fraction of patients living for a certain amount of time after treatment. From the cohort of breast cancer patients, we screened for their DP103 levels and selected those showing elevated levels of DP103. In this subcohort, we measured their MMP9 levels. The survival curves in Figure 28A show that in these patients with abundant DP103 expression, they had poor overall survival when their MMP9 expression was also high (n=55, p=0.029). Figure 28B showed representative pictures of MMP9 staining on the breast tissues.

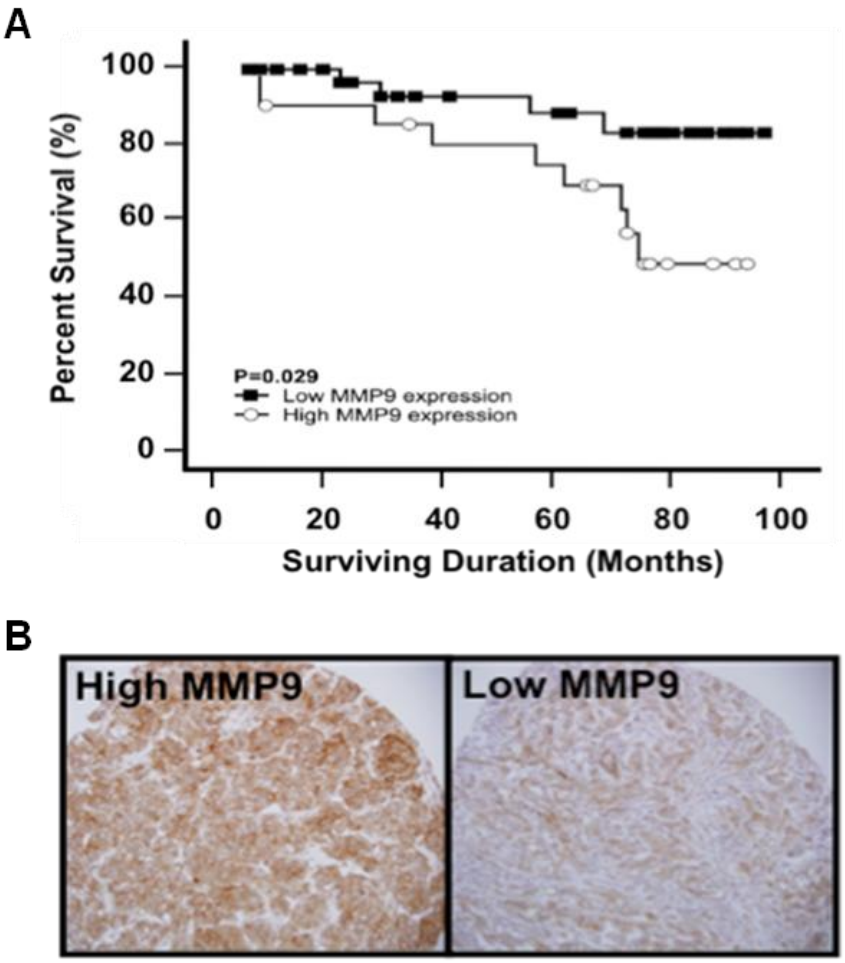

Figure 28. Patients with high DP103 and MMP9 expressions had lower survival rates. Kaplan-Meier curves showing differences of MMP9 expression in relation to surviving duration in high DP103 expressing cases (n=55). Cases with high MMP9 and high DP103 expression (mean, 69; months, n=21) have significantly shorter survival duration (p=0.029) compared to those with low MMP9 and high DP103 expression (mean, 86 months; n=34). Cases that are still surviving are censored at the date of last follow-up (denotes by squares and circles on the line plots) (A). Representative pictures of immunohistochemical staining of breast cancer biopsies with high DP103 expression for MMP9 are shown (B).

3.4.4 Suppression of DP103 reduced MMP9 transcript and protein levels

In an attempt to establish a direct link between DP103 and MMP9, DP103 was suppressed via siRNA technology. This resulted in a significant decrease in MMP9 mRNA levels at both 24h and 48h compared to the control cells in all the three invasive breast cancer cell lines, MDA-MB-231, BT549 and HS578t (Figure 29A). Additionally, the decrease in MMP9 mRNA transcripts related well with a drop in its protein levels too (Figure 29B), an indication that DP103 might be regulating the transcription activity of MMP9.

MMPs are known to be pro-enzyme and a cleavage of the pro-domain is necessary for the activation of this enzyme to perform its activity. Henceforth, to confirm the decrease in MMP9 protein levels corroborated with the decreased activity of the enzyme, we performed a gelatin gel zymography in MDA-MB-231.

MMP9 enzyme is capable of degrading gelatin. Since active MMP9 is a secreted enzyme, we collected the supernatant after transfection and ran an electrophoresis gel that was mixed with gelatin. If the enzyme is active, gelatin will be degraded in the gel and a clear band will be seen after staining the gel with Coomassie Blue. The gelatin gel zymography can also detect the activity of MMP2, which belongs to the same subfamily as MMP9.

As a positive control, we treated MCF10A cells with increasing concentrations of Tumor Necrosis Factor α (TNFα) and collected the cells for gelatin gel zymography. Upon such stimulation, MMP9 activity increases (Stuelten et al., 2005) and this is shown in Figure 30 with increasing clearing of the bands (Lanes 1-4). When DP103

was depleted in MDA-MB-231 cells, the clear band disappeared, indicating a loss of MMP9 activity (Figure 30, lanes 5-6). MMP2 activity, on the other hand, showed no effect to depletion of DP103 (Figure 30, bottom bands).

Thus, we can conclude that DP103 protein is modulating the transcriptional expression of MMP9 and thereby affecting the activity of this endopeptidase and thus metastasis.

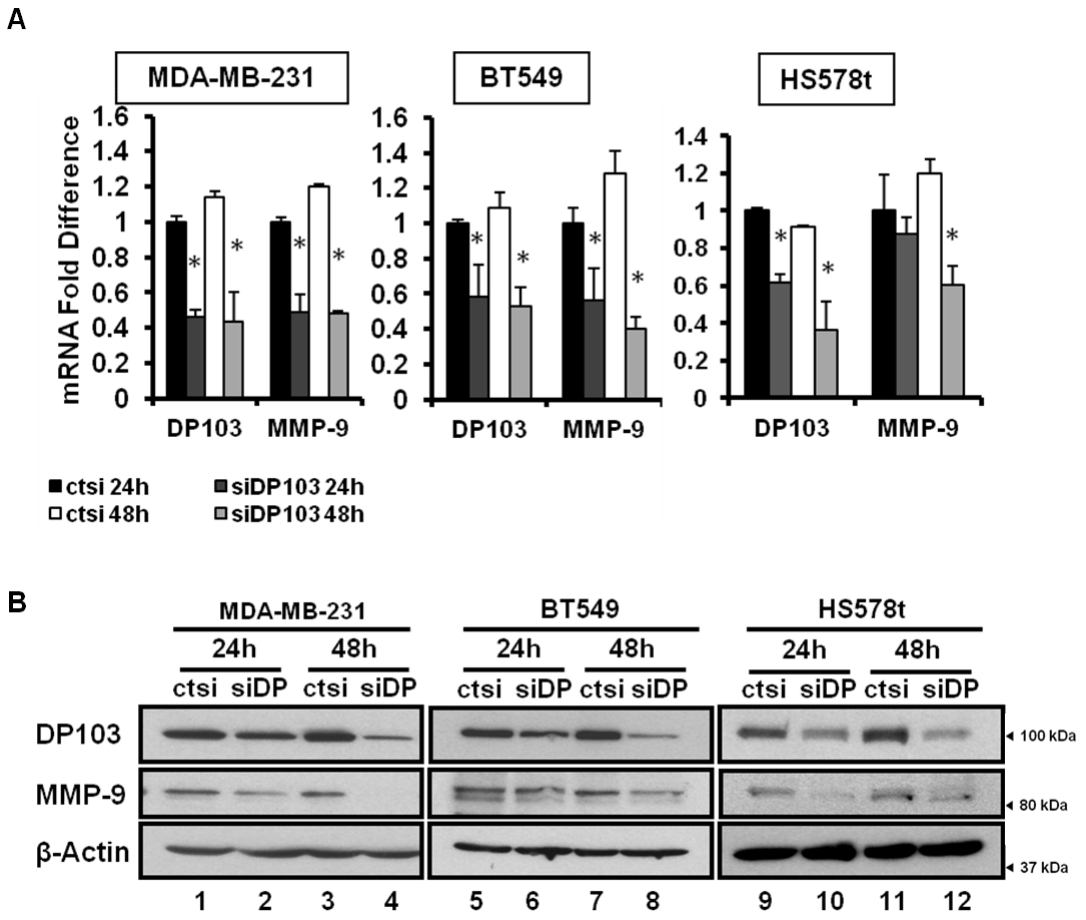

Figure 29. Knockdown of DP103 reduced MMP9 levels. MDA-MB-231, BT549 and HS578t cells were transfected with control siRNA (ctsi) and siRNA against DP103 (siDP103). Cells were harvested and lysed for RNA and protein. qPCR and western blotting were performed with DP103 and MMP9 primers and antibodies, showing that MMP9 mRNA (A) and protein levels (B) decreased after DP103 knockdown. mRNA levels were normalized with 18S and represented as fold difference.

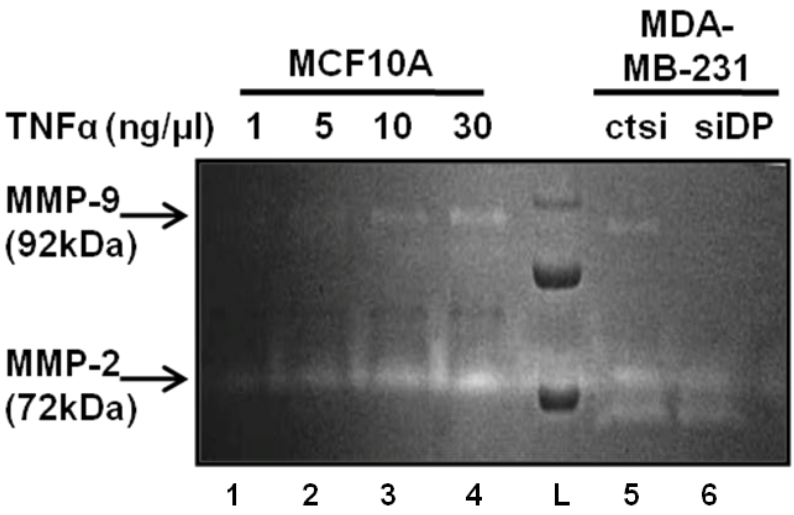

Figure 30. MMP9 activity was decreased with suppression of DP103. MDA-MB-231 cells were transfected with control or siRNA against DP103. For a MMP9 control, MCF-10A cells were treated with 1, 5, 10 or 30ng/ml for 24 h. Growth media were collected and MMP9 activity was measured in gelatin zymography gel. L represents protein ladder.

3.4.5 Invasion was inhibited with use of specific MMP9 inhibitor

We had shown that MMP9 activity was decreased by downregulating DP103 and the latter brought about the inhibition of metastasis in invasive breast cancer cell lines. However, in our 'metastatic qPCR array', we saw several other MMPs also upregulated in the process even though the fold changes are not as elevated as MMP9. In order to confirm that MMP9 is the main molecular effector of this observation, we performed matrigel transwell assay with or without several MMPs inhibitors.

We used a specific MMP2/9 inhibitor (SB-3CT) and a broad spectrum MMPs inhibitor (GM6001) and showed that invasion of MDA-MB-231 cells through the matrigel matrix was inhibited by about 38% by both inhibitors (Figure 31). We then treated the cells with specific MMP9 inhibitor and observed that it prevented the cells from migrating through the matrix by about 50%. Importantly, forced overexpression of DP103 alone increased the invasion of MDA-MB-231. However, in the presence of the specific MMP9 inhibitor, this effect was abrogated when DP103 was forced overexpressed (Figure 32). These suggest that MMP9 is the major endopeptidase modulated by DP103 for cell invasion in this project.

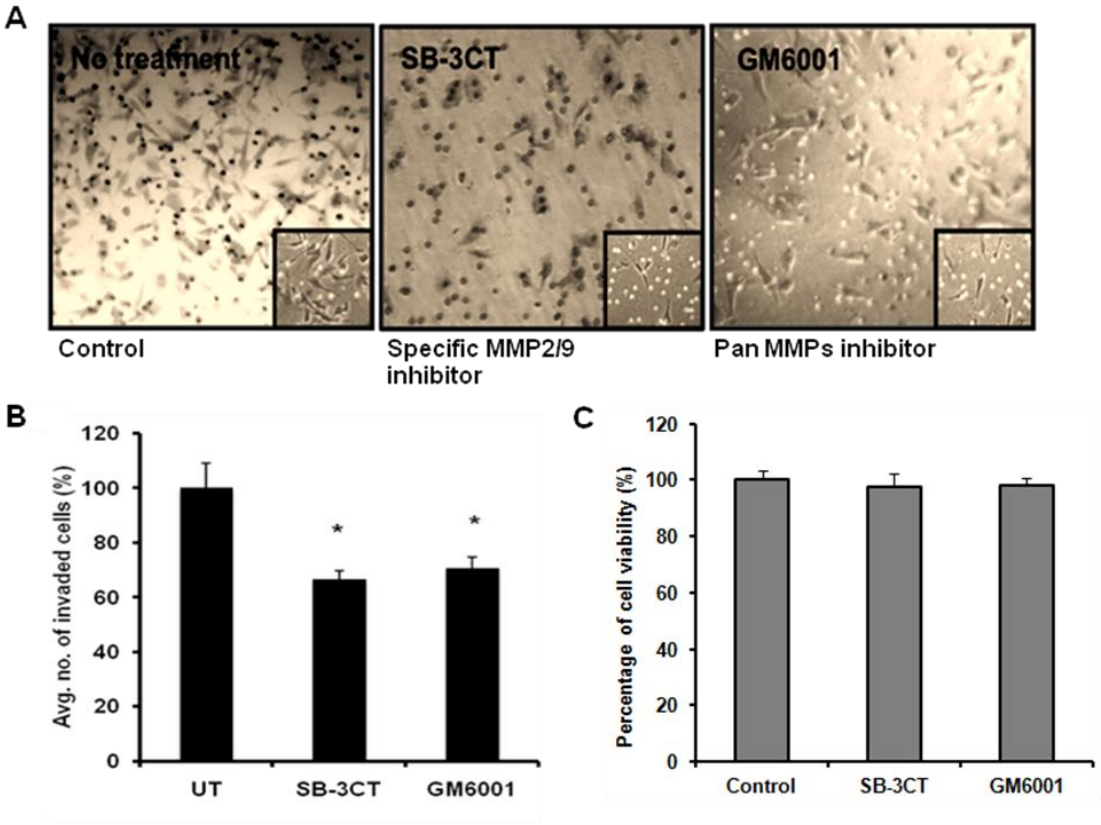

Figure 31. Cell invasion is also inhibited by pan-MMPs and specific MMP2/9 inhibitors. 2 x 10^5 MDA-MB-231 cells were seeded into the upper chamber of the tranwell invasion chamber with serum free media with either MMP2/9 inhibitor (SB-3CT, 10μM) or pan-MMPs inhibitor (GM6001, 50μM). After 24h, the membranes of the chambers were stained with crystal violet solution and mounted on microscope slides and pictures taken. Insert shows representative picture in higher magnification (A). The number of cells that invaded through the transwell invasion chambers were counted in five randomly selected microscope fields and plotted on a graph (B). MMPs inhibitors did not show any cytotoxicity from crystal violet assay (C). * denotes $p<0.05$.

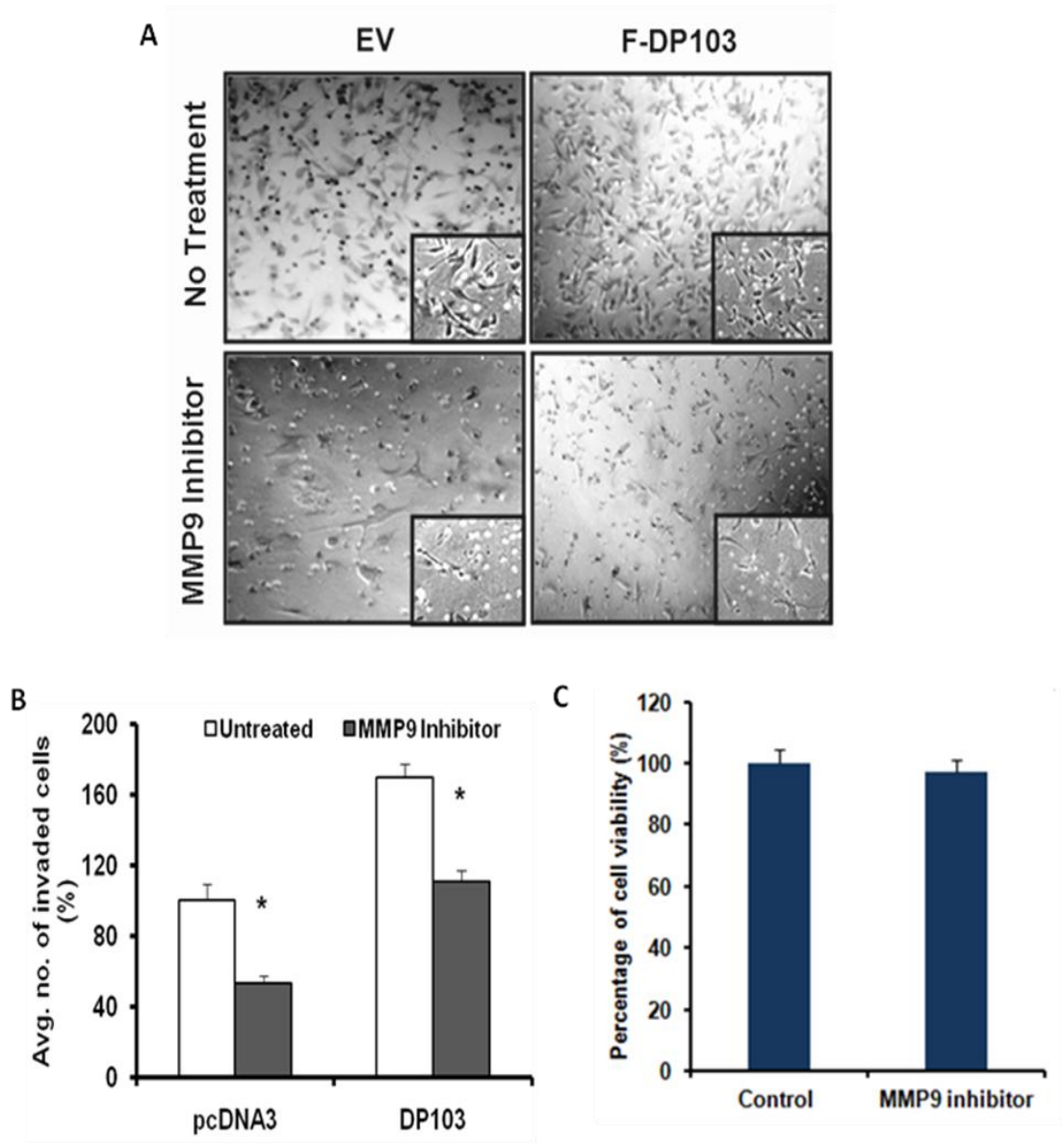

Figure 32. Invasion was reduced with specific MMP9 inhibitor. 2 x 10^5 MDA-MB-231 cells transfected with either empty vector (EV) or over-expressed with F-DP103 were seeded into the upper chamber of the tranwell invasion chamber with serum free media with or without MMP9 Inhibitor I (1μM). After 24h, the membranes of the chambers were stained with crystal violet solution and mounted on microscope slides and pictures taken. Insert shows representative picture in higher magnification (A). The number of cells that invaded through the transwell invasion chambers were counted in five randomly selected microscope fields and plotted on a graph (B). MMP9 specific inhibitor did not show any cytotoxicity from crystal violet assay (C). * denotes $p<0.05$.

3.5 How does DP103 regulate MMP9 expression?

Transcriptional regulation of MMP9 involves a relatively large repertoire of transcriptional factors that includes AP-1, AP-2, Ets, NF-κB, and SP-1 out of which AP-1 (Adamson et al., 2000; Milde-Langosch et al., 2004; Nair et al., 2008), and NF-κB (Chou et al., 2010; Ricca et al., 2000) are postulated to be the major regulators in cancers. Given that depletion of DP103 expression in three invasive cell lines decreased MMP9 mRNA, we sought to elucidate the transcription factor DP103 is acting on.

3.5.1 Suppression of DP103 inhibits NF-κB activity

The dual-luciferase reporter assay serves to measure the activity of the reporter gene in question. The firefly luciferase reporter is measured first with the first 'glow-type' luminescent signal. After quantifying this, the reaction is quenched and the *Renilla* luciferase reaction is initiated. The first reading was then normalised with *Renilla* reading and the total protein concentration.

To determine whether NF-κB or AP-1 activity is affected when subjected to the downregulation of DP103, MDA-MB-231 cells were first transfected with siDP103 for 24h. They were then transiently transfected with either a NF-κB responsive firefly luciferase reporter or an AP-1 responsive firefly luciferase reporter. As a control for cell numbers and transfection efficiency, cells were also co-transfected with *Renilla* vector. 24h later, measurements of the respective reporter activity were made. From Figure 33, we observed that the activity of NF-κB was reduced with suppression of DP103, but not that of AP-1. This indicates that DP103 is regulating NF-κB activity specifically.

In order to confirm our luciferase assay results, we did an electrophoretic mobility shift assay or EMSA. EMSA is an affinity electrophoresis technique used to study protein-DNA interactions and it can determine if a protein is capable of binding to a given DNA sequence. We incubated the nuclear extracts with a radioactive labeled oligonucleotide probe which contains the specific recognition sequence for NF-κB. If NF-κB subunit are present in the nuclear extracts, their interaction with the probe shifts the band of the labeled probe up since the complex of probe and NF-κB subunit has a lower electrophoretic mobility than the probe alone. The intensity of the shifted band is a measure for the amount of NF-κB in the nuclear fraction.

In the first 2 lanes of Figure 34A (left), we showed that while the basal NF-κB activity is high in untransfected cells, it decreased drastically upon suppression of DP103. Oct-1 probe served as a control for even loading across samples (Figure 34A, right).

The microenvironment of cancers are known to be under constant pressures, for example hypoxia or genotoxic stress. This, in turn, causes the activation of signal transduction pathways to deal with such stress. The NF-κB pathway is one of the main pathway to transcribe to overcome such ordeal (Lisanti et al., 2010). As such, we wanted to mimic the physiological conditions of the tumor to be under genotoxic stress. Given that NF-κB transcriptional activity is also known to be affected by genotoxic stress inducers like doxorubicin, etoposide (VP16) and camptothecin (Huang et al., 2003; Lee et al., 2011; Mabb et al., 2006), we sought to investigate if depletion of DP103 would have any effects in the presence of such inducers. The NF-κB binding ability increased under the treatment of doxorubicin, etoposide or

camptothecin on MDA-MB-231 as compared to the untreated cells. However, after downregulation of DP103, the binding ability of NF-κB decreased in all three drug treatments (Figure 34A, left). Figure 34B showed successful knockdown of DP103 protein by siRNA in the EMSA setup.

Additionally, it is of interest to note that there is a concomitant increase of DP103 upon stimulation by NF-κB genotoxic stress inducers (Figure 34B), leading to a possibility that DP103 protein expression may be induced by activation of NF-κB itself. This warrants a need for further in-depth analysis.

Following this observation, we further validated the EMSA results by returning to perform luciferase assay again, but with the addition of NF-κB genotoxic stress inducers. Figure 35 showed that while the basal NF-κB activity increased with the respective genotoxic drugs, when depleted of DP103, the increment in NF-κB activity was less prominent. On the other hand, the AP-1 activity was not altered regardless of genotoxic stimuli or suppression of DP103 (Figure 36), paralleling the findings from our EMSA assay previously.

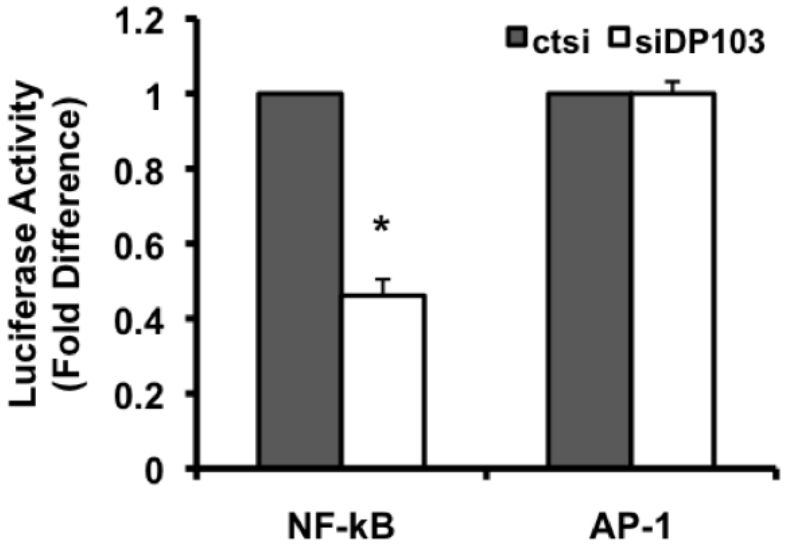

Figure 33. Downregulation of DP103 caused a decrease in NF-κB luciferase activity but not AP-1. Control siRNA and siDP103 treated MDA-MB-231 cells were transfected with Renilla and luciferase reporter plasmid containing NF-κB or AP-1. The cells were then harvested with passive lysis buffer to carry out luciferase assay. Results are expressed in fold difference, and are the average of 3 separate experiments. * denotes $p<0.05$.

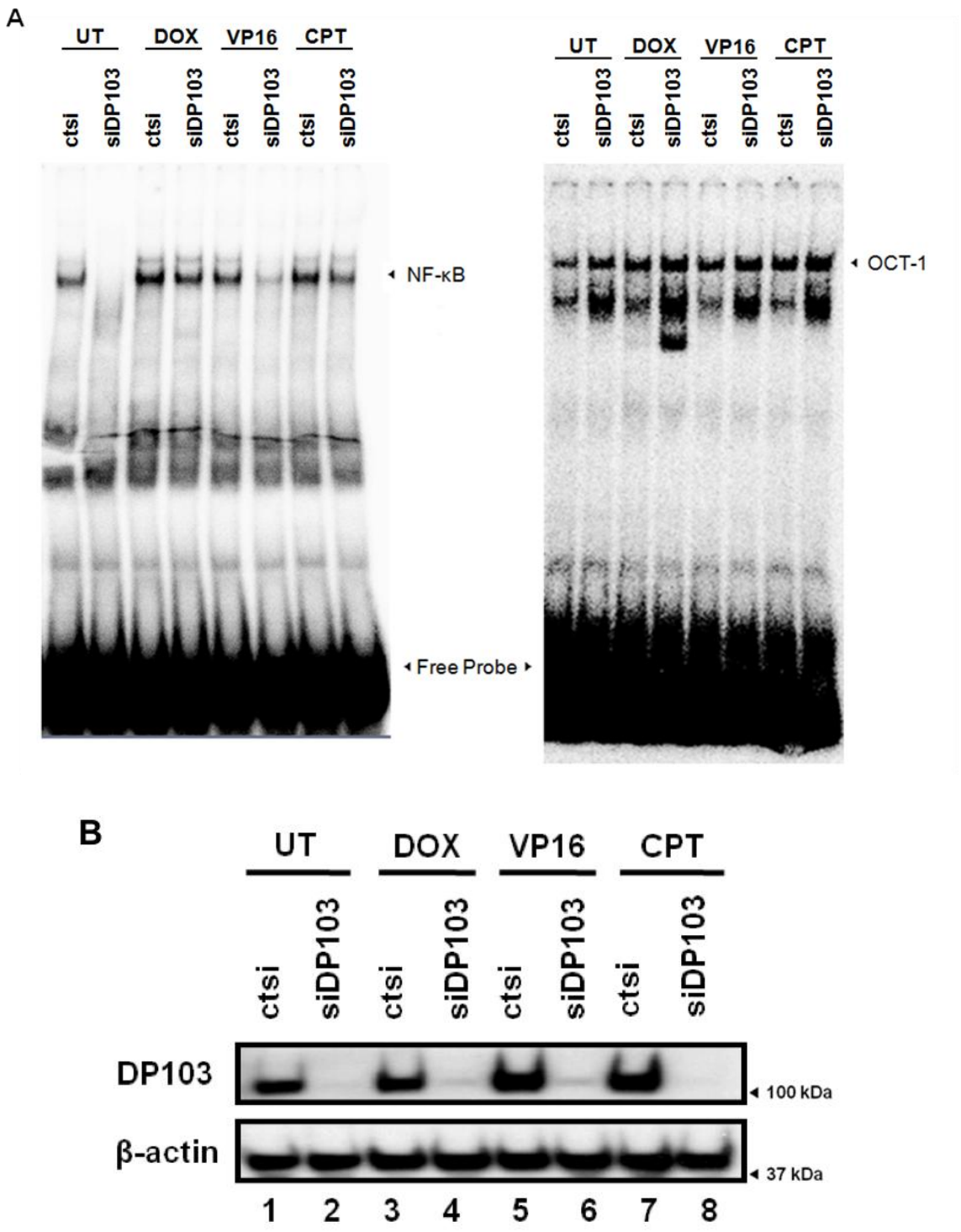

Figure 34. Downregulation of DP103 decreases NF-κB DNA binding ability in EMSA. MDA-MB-231 cells were transfected with control or siRNA against DP103. Cells were treated with 25μM doxorubicin (DOX) for 60 min, 10μM VP16 for 90 min and 10μM CPT for 120 min. Total cell extracts were prepared, NF-κB activities were measured by EMSA. An Oct-1 probe was served as an EMSA control (A). Western blot showing efficient knockdown of DP103 for EMSA assays (B). UT represents untreated.

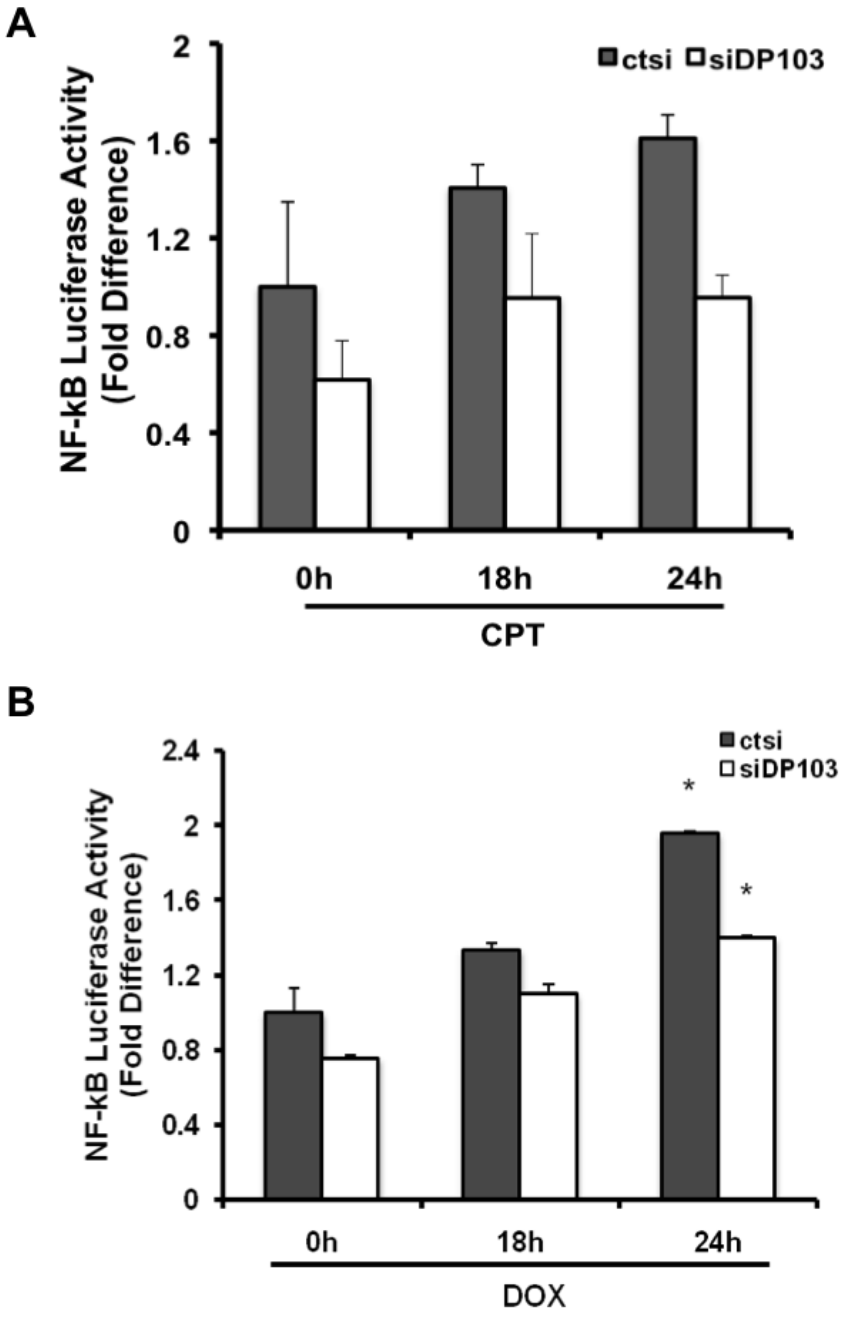

Figure 35. Downregulation of DP103 decreases NF-κB luciferase activity under genotoxic stimuli. Control siRNA and siDP103 treated MDA-MB-231 cells were transfected with Renilla and luciferase reporter plasmid containing NF-κB. The cells were subsequently stimulated with 10μM CPT (A) or DOX (B) for 18h and 24h and then harvested with passive lysis buffer to carry out luciferase assay. Results are expressed in fold difference, and are the average of 3 separate experiments. * denotes $p<0.05$.

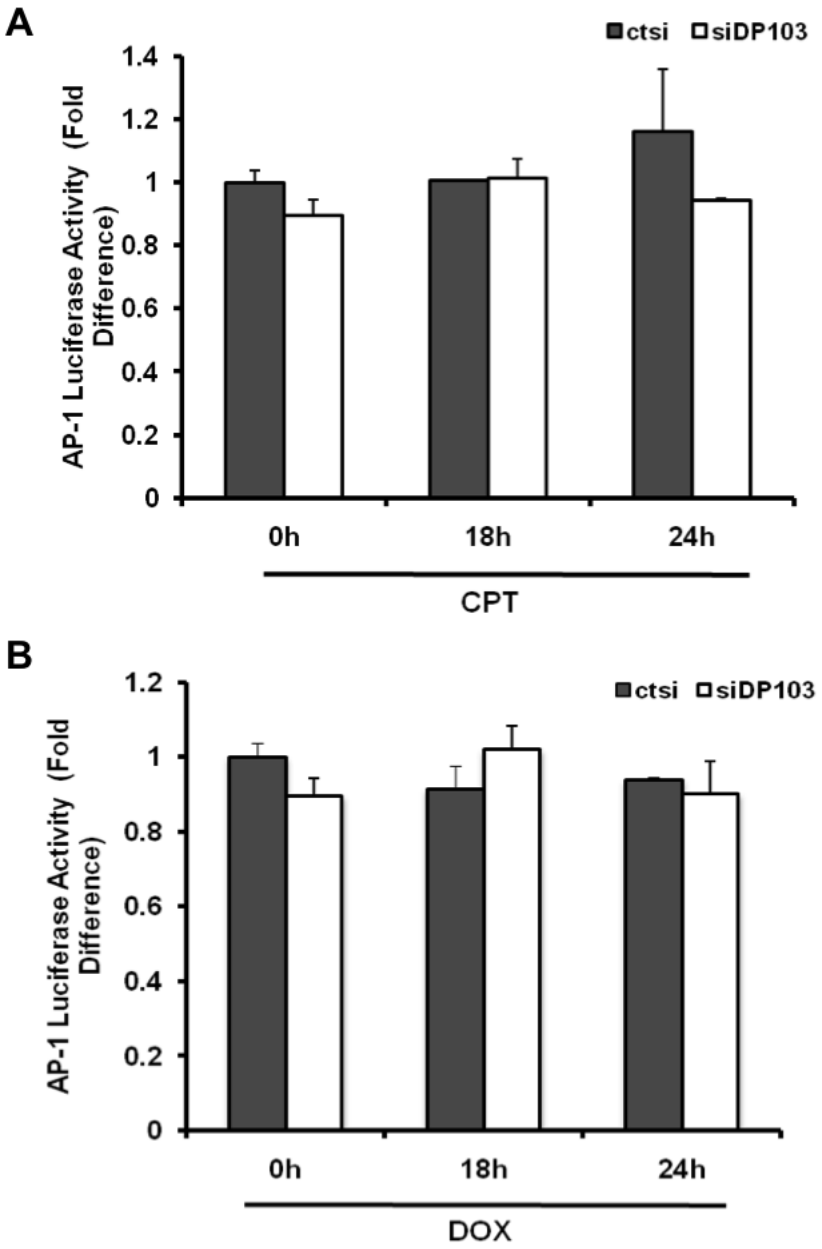

Figure 36. Downregulation of DP103 does not decrease AP-1 luciferase activity under genotoxic stimuli. Control siRNA and siDP103 treated MDA-MB-231 cells were transfected with Renilla and luciferase reporter plasmid containing AP-1. The cells were subsequently stimulated with 10μM CPT (A) or DOX (B) for 18h and 24h and then harvested with passive lysis buffer to carry out luciferase assay. Results are expressed in fold difference, and are the average of 3 separate experiments. * denotes $p<0.05$.

3.5.2 Suppression of DP103 increased cells' sensitivity to genotoxic drugs

Since NF-κB but not AP-1 transcriptional activity was affected by DP103, we postulated that the downstream targets of NF-κB would also be downregulated if the activity decreased, but not so in AP-1. Hence, we checked some of NF-κB and AP-1 regulated genes.

In addition to MMP9, ICAM-1 and CXCR4 are also regulated by NF-κB (Helbig et al., 2003; Xue et al., 2009). While the levels of these proteins decreased upon downregulation of DP103, the protein level of c-Jun, regulated by AP-1 (Kaminska et al., 2000) remained unchanged (Figure 37).

Since NF-κB activation by genotoxic stimuli is linked to cell viability and apoptosis (Karin, 2006), we determined the viability of MDA-MB-231 cells under genotoxic stress when they are depleted of DP103 in another attempt to confirm the link between DP103 to NF-κB. Using camptothecin and doxorubicin, both displayed cell death of about 20 to 30% in untransfected cells. However, when DP103 levels were suppressed, the viability of the cells were compromised to 50.32% and 53.44% in the presence of camptothecin or doxorubicin respectively (Figure 38). Representative pictures of the staining of the cells were shown at the bottom of the graphs in Figure 38.

Collectively, we had confirmed that DP103 interferes with the transcriptional activity of NF-κB, and in turn regulates the expression levels of its downstream target genes and functions.

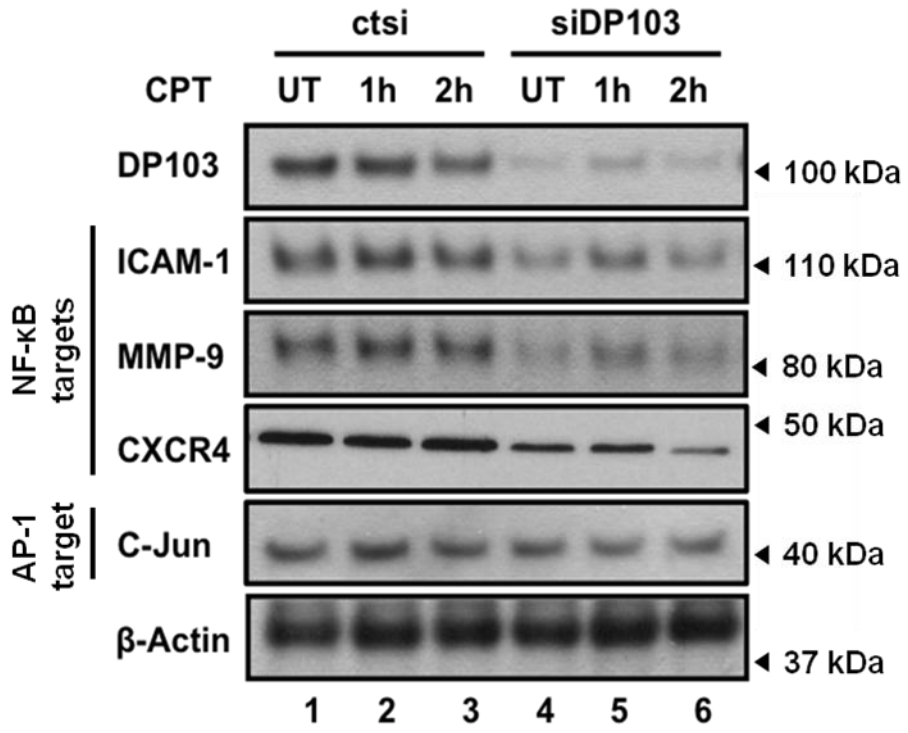

Figure 37. Downregulation of DP103 reduces NF-κB targeted proteins, but not that of AP-1. MDA-MB-231 cells were transfected with siDP103 for 48h and subjected to CPT (10μM) stimulation at the indicated time. Cells were harvested and then evaluated by Western blotting with NF-κB- and AP-1-targeted proteins. UT represents untreated.

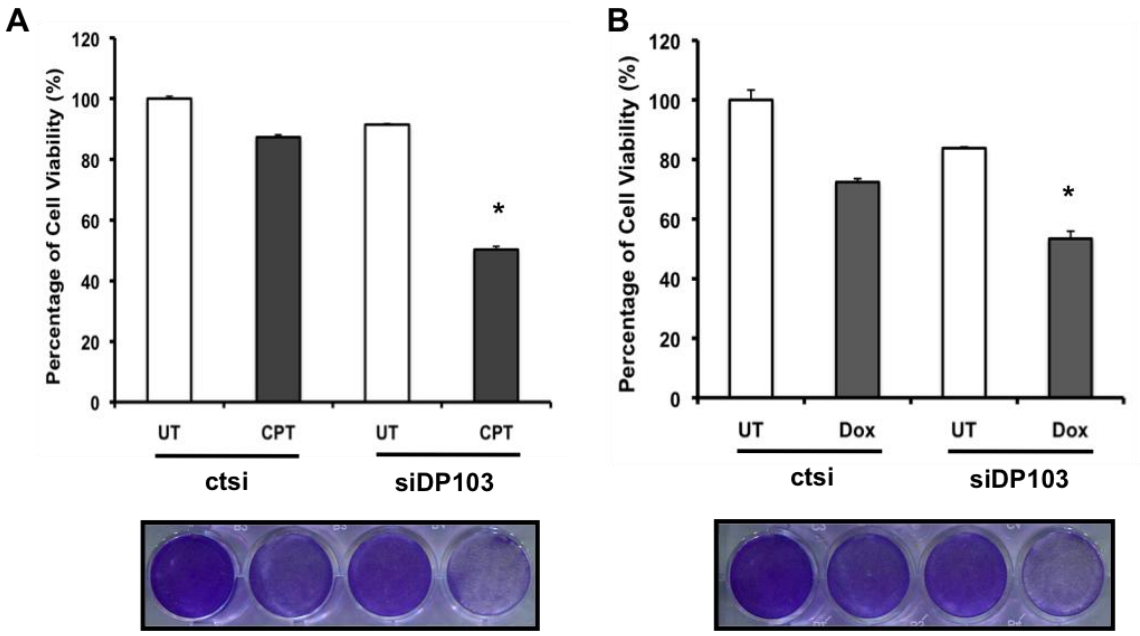

Figure 38. Downregulation of DP103 caused cells to be more sensitive to genotoxic drugs. MDA-MB-231 cells were transfected with ctsi or siDP103 and treated with or without 25μM CPT (A) or 10 μM Dox (B) for 48h, before staining by crystal violet solution to determine cell viability. Scanned pictorial representation of the treatment (bottom) before dissolving the crystals and graphs showing percentage of cell viability from 3 separate experiments. UT represents untreated. * denotes $p<0.05$.

3.6 How does DP103 fit into the NF-κB pathway?

The NF-κB family consists of several important proteins and under different stimuli, they act under different pathways to elicit different cellular responses. We had established an association between DP103 and the NF-κB pathway. There are numerous possibilities as to which DP103 may interfere with the transcriptional activity of NF-κB. DP103 may act to regulate the levels of important NF-κB proteins like p65, NEMO or IKK2. On the other hand, it might be possible that DP103 is involved in some post-translational modifications like phosphorylation or SUMOylation of NF-κB members. Our group previously showed DP103 to be modulating SF-1 via SUMO modifications (Lee et al., 2005b), thereby causing its repression. Henceforth, we speculated a possible role of DP103 in SUMOylation in the NF-κB pathway.

3.6.1 DP103 does not change endogenous levels of NF-κB related proteins

We first tested the levels of some of the NF-κB members after downregulation of DP103 and showed that there was no effect in the protein levels of p65, NEMO and IKK2 (Figure 39). Hence, we ruled out the possibility that DP103 is directly regulating these proteins at the transcript levels.

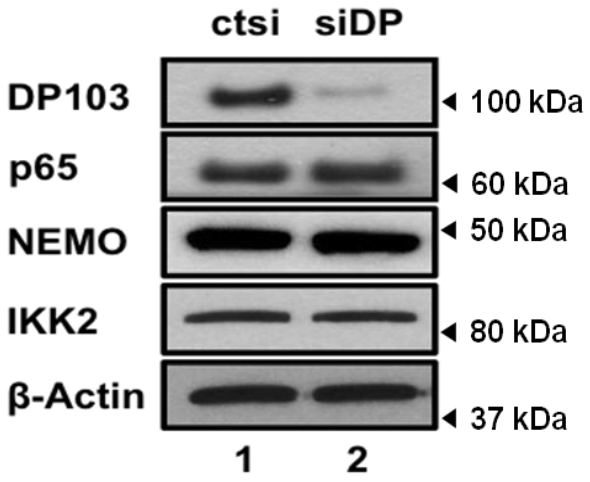

Figure 39. DP103 does not regulate NF-κB members. MDA-MB-231 cells were transfected with control siRNA (ctsi) and siRNA against DP103 (siDP103). Cells were harvested, lysed and cell extracts were immunoblotted with various antibodies.

3.6.2 DP103 interacts with NEMO and mediates its SUMOylation under genotoxic stress

Since we have previously showed that the DP103 is required for activation of NF-κB activity under genotoxic stress, we turned our focus to post-translational modification that occurred under genotoxic stimuli.

Huang et al., 2003 first published that IκB kinase gamma (IKKγ) regulatory subunit NEMO (NF-κB essential modulator) undergoes SUMOylation by SUMO-1 under genotoxic stress inducers like camptothecin and doxorubicin. Hence, we explored a possible physical interaction between DP103 and NEMO. Genotoxic agents were used in our setup to enhance the SUMOylation effects on NEMO.

We treated MDA-MB-231 cells with camptothecin and collected the lysates for immunoprecipitation assays. We show for the first time that DP103 interacts with NEMO in unstimulated conditions as well as with camptothecin (Figure 40, lanes 1-3). We went on to test if SUMOylation of NEMO is affected and observed a time dependent increase in SUMOylation upon camptothecin treatment (Figure 40, lanes 1-3). Furthermore, this SUMOylation is diminished with knockdown of DP103 (Figure 40, lanes 4-6).

Taken together, we concluded that DP103 is necessary for the SUMOylation of NEMO under genotoxic stimuli.

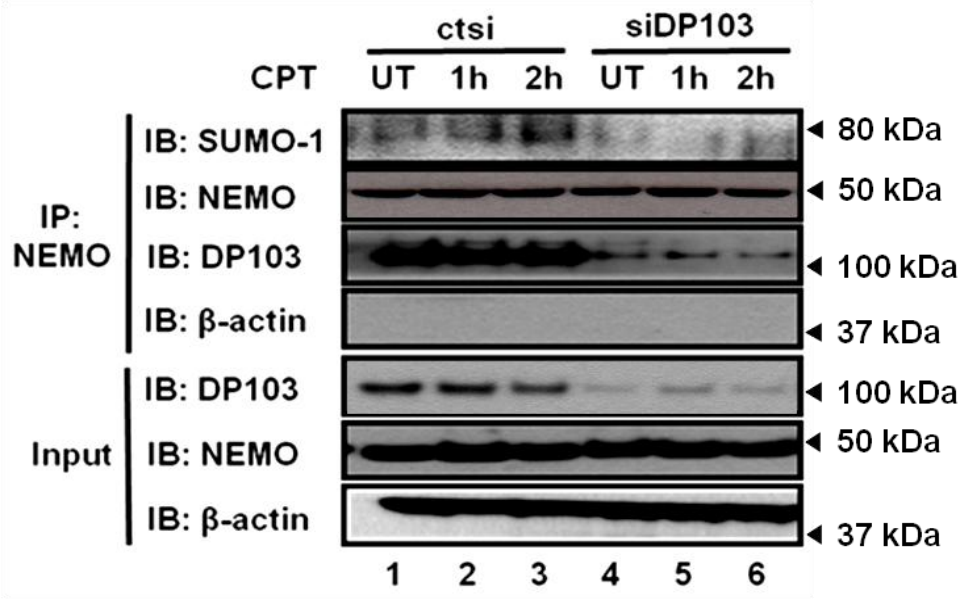

Figure 40. DP103 is required for the SUMOylation of NEMO. Control and siRNA against DP103 treated MDA-MB-231 cells were stimulated with 10μM CPT for 1h or 2h and then harvested and lysed. The cell lysates were immunoprecipitated with NEMO antibody and then evaluated by Western blotting with indicated antibodies. UT represents untreated. UT represents untreated.

3.6.3 RNA helicase activity of DP103 is not required for SUMOylation of NEMO and increased metastasis

DP103 belongs to the DEAD box family of helicases, which shares several conserved and unique motifs, including the Walker A and B motifs. These motifs are involved in the binding of nucleoside triphosphates required for its helicase activity (Linder, 2006). Some members in this family like DDX3 and DDX1 have been found to require its ATP-dependent helicase for their functions (Garbelli et al., 2011; Ishaq et al., 2009), while several others like p68 do not (Clark et al., 2008; Zhao and Jain, 2011).

To investigate if the helicase activity of DP103 is required for SUMOylation of NEMO, we generated a full length DP103 GNT mutant where the critical lysine residue (GKT) that is needed to bind ATP was mutated to an asparagine residue, GNT (Caruthers and McKay, 2002; Fry et al., 1986; Kim et al., 1998) (Figure 41A). Changing the conserved GKT to GNT has been shown to reduce ATP binding in RNA helicases by 98% (Richter et al., 1996).

We subsequently show forced overexpression of the helicase-dead mutant (GNT) retained its ability to SUMOylate NEMO just as efficient as forced overexpression of the wild type DP103 (WT) (Figure 41B). Additionally, the helicase-dead mutant (GNT) also retained its ability to induce invasion in MDA-MB-231 cells (Figure 42), demonstrating helicase activity of DP103 is not required for our observed metastasis effects.

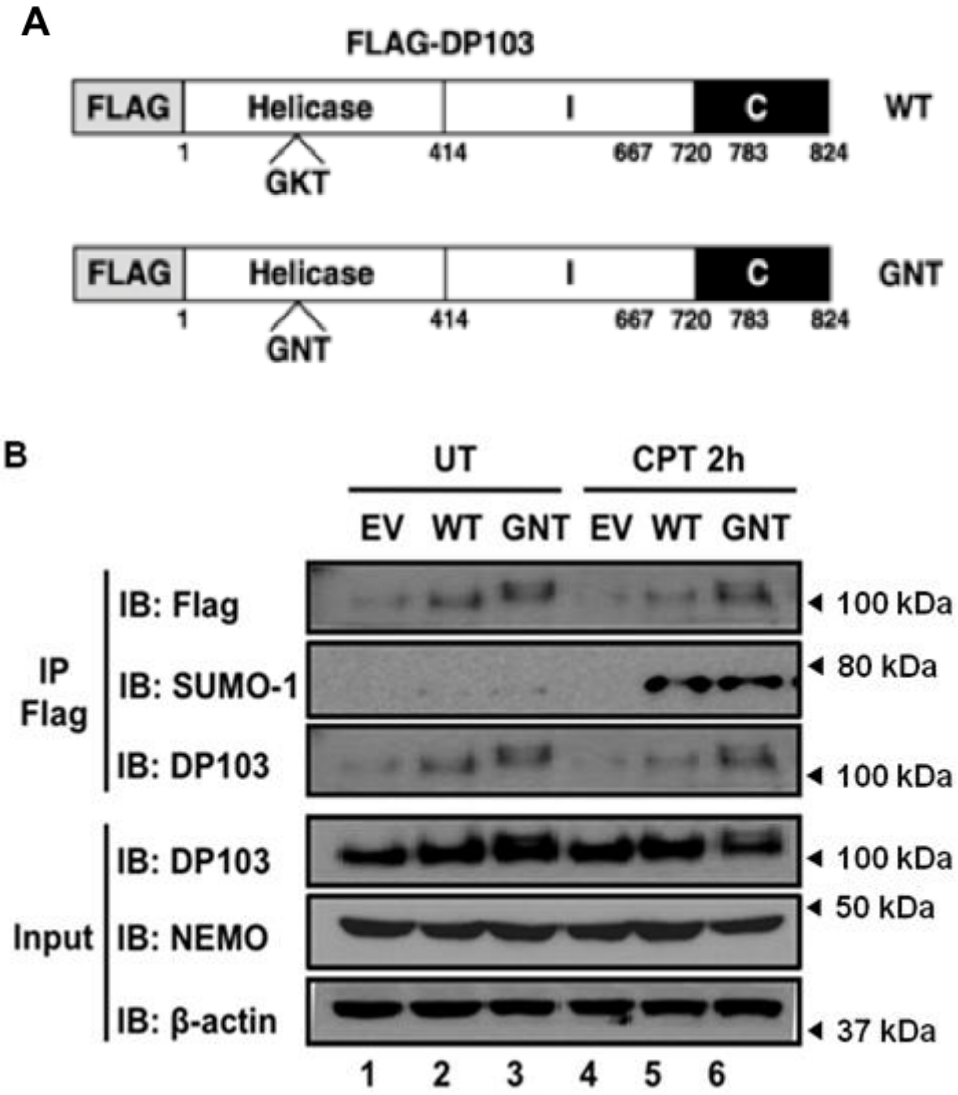

Figure 41. Helicase activity of DP103 is not required for SUMOylation of NEMO. Pictorial map showing the FLAG-tagged wild-type (WT) and single amino acid mutated at helicase domain (GNT) of DP103 (A). MDA-MB-231 cells were stimulated with 10μM CPT for 2h and then harvested and lysed. The cell lysates were immunoprecipitated with NEMO antibody and then evaluated by Western blotting with indicated antibodies. UT represents untreated.

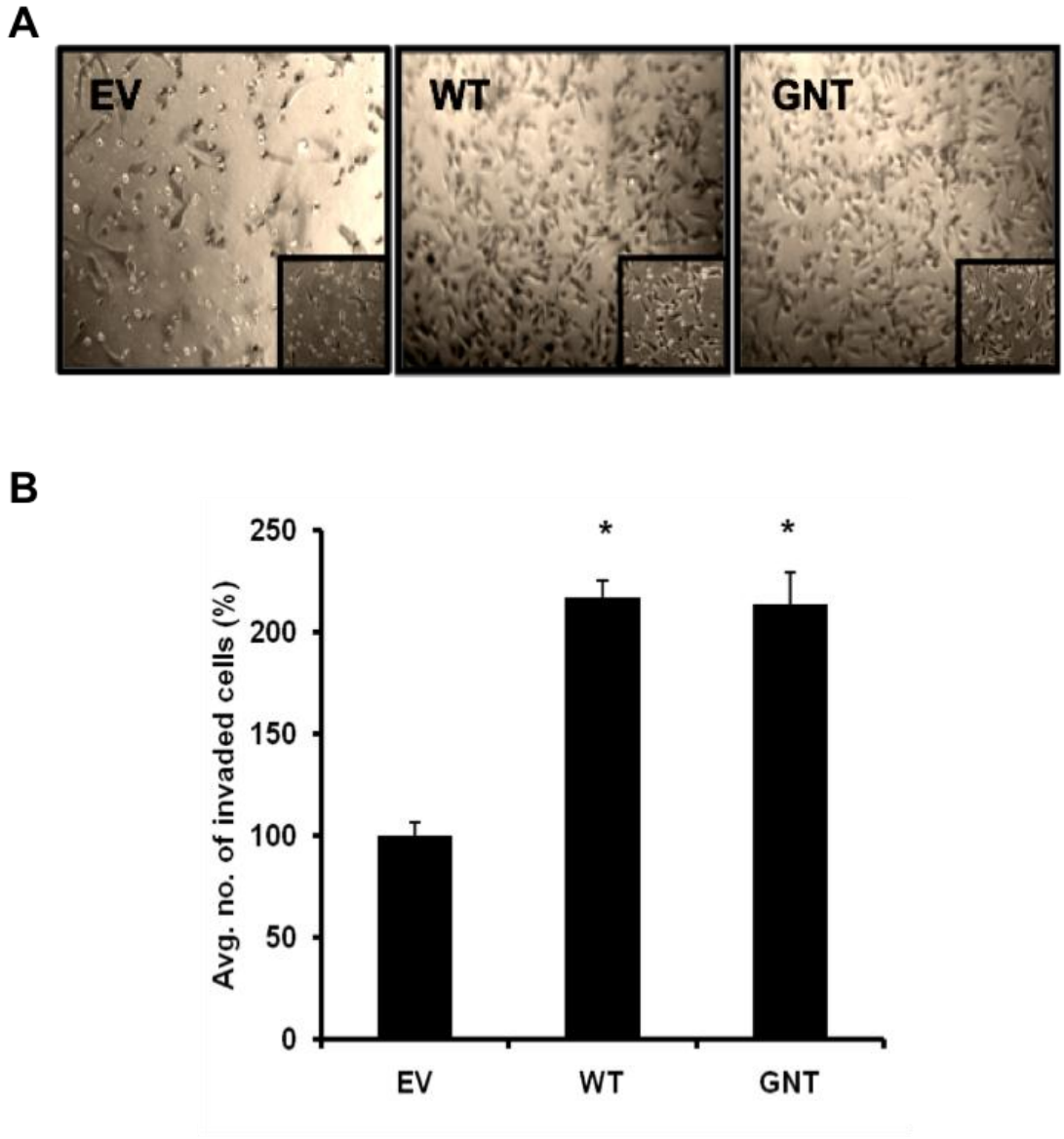

Figure 42. Helicase activity of DP103 is not required for increased invasion of MDA-MB-231 cells. 2 x 10^5 MDA-MB-231 cells transfected with either empty vector (EV), wild-type DP103 (WT) or GNT mutant (GNT) were seeded into the upper chamber of the tranwell invasion chamber with serum free media after siRNA transfection for 48h. The membranes of the chambers were then stained with crystal violet solution and mounted on microscope slides and picture taken. Insert shows representative picture in higher magnification (A). The number of cells that invaded through the transwell invasion chambers were counted in five randomly selected fields and plotted on a graph (B). * denotes $p<0.05$.

3.6.4 Genotoxic agent increases interaction of DP103 with PIASy and SENP2

Mabb *et al.*, 2006 showed that PIASy (protein inhibitor of activated STATy) interacts with NEMO, enhances NEMO SUMOylation and activates NF-κB in response to genotoxic agents. Furthermore, PIASy preferentially stimulates SUMO modification of NEMO by SUMO-1, but not SUMO-2 and SUMO-3. SENP1, one of the six Sentrin/SUMO-specific proteases, had also been shown to be able to deSUMOylate NEMO *in vitro*.

In another paper, Lee et al., 2011 observed that SENP2, a Sentrin/SUMO-specific protease, is the major SUMO protease that interacts most efficiently with NEMO (instead of SENP1) and inhibits NF-κB activation induced by genotoxic agents. SENP2 was also found to be more proficient than SENP1 in deSUMOylating NEMO.

We thus seek to test in our system if DP103 associates with PIASy, SENP1 and/or SENP2. We first attempted to establish PIASy-mediated SUMOylation of NEMO under camptothecin treatment in our system using MDA-MB-231 cells. We showed that PIASy indeed enhances the SUMOylation of NEMO (Figure 43A). Subsequently, we explored the possibilities of their associations by performing a co-IP assay. Without VP16 treatment, there was no interaction between DP103 and PIASy, SENP1 or SENP2 (Figure 43B, Lanes 1-6). Upon VP16 treatment, DP103 interacted with PIASy and SENP2. SENP1 interaction is, however, not inducible (Figure 43B, Lanes 7-11). Hence, DP103 interacts with NEMO, PIASy and SENP2 in the same complex.

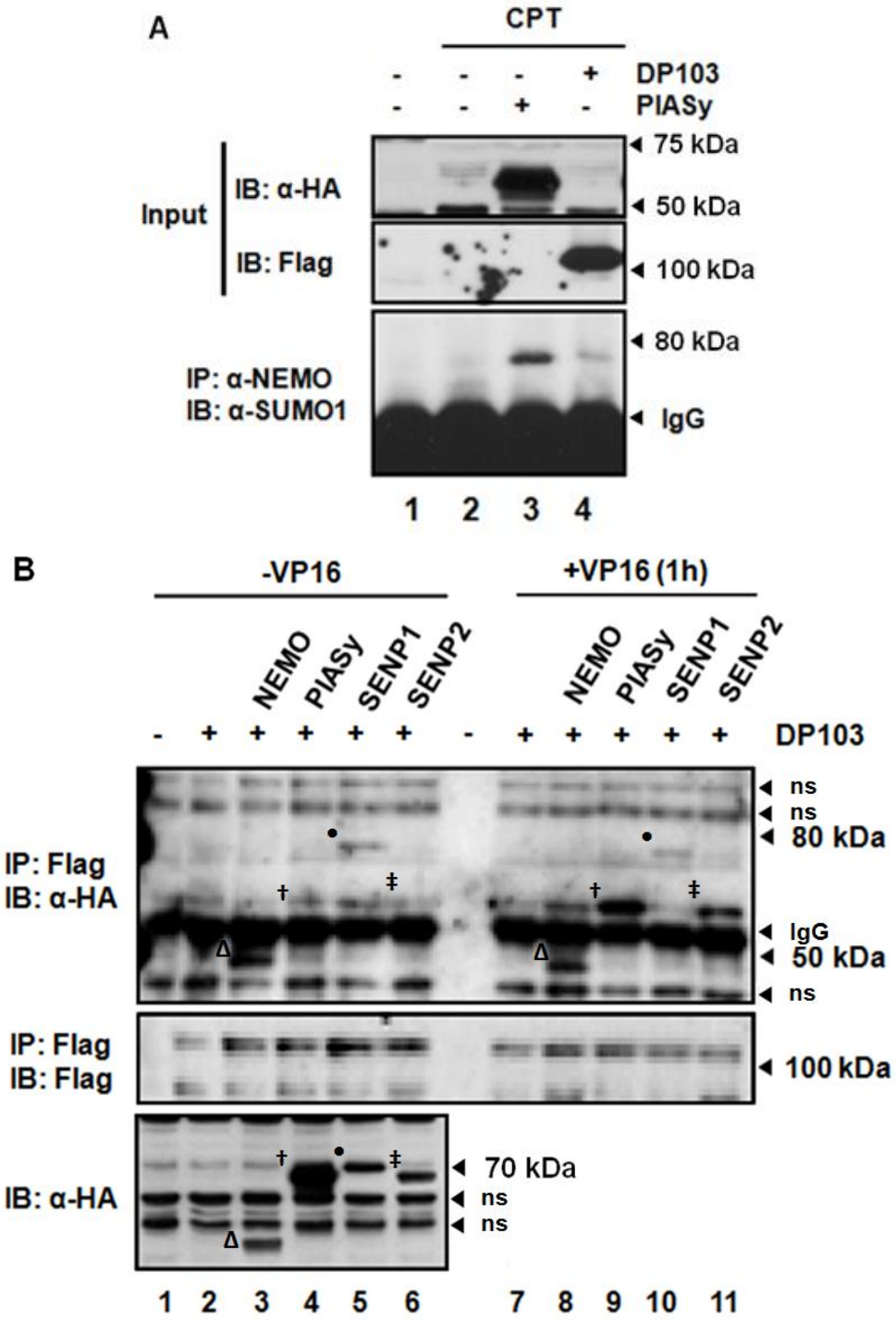

Figure 43. Genotoxic agent increased interaction of DP103 with PIASy and SENP2. MDA-MB-231 cells were transfected with Flag-DP103 or HA-PIASy. Cells were treated with CPT (10μM) for 1h before harvested, lysed and performed IP with anti-NEMO antibody. They were analysed by immunoblotting using anti-SUMO1 antibody (A). HEK293 cells were transfected with Flag-DP103 along with the indicated constructs tagged with HA. Cells were either left untreated or treated with VP16 (10μM) for 1h and processed for co-IP analysis. Δ: NEMO band, †: PIAS band, •: SENP1 band, Δ: SENP2 band, ns: non-specific band (B).

3.6.5 DP103 enhances NEMO-PIASy interaction while decreasing NEMO-SENP2 interaction

We have previously showed that increased DP103 enhances SUMOylation of NEMO (Figure 40). It is however unclear if DP103 helps in enhancing SUMOylation directly or inhibits the deSUMOylation machinery.

Since PIASy is the E3 ligase for SUMOylation of NEMO, we seek to determine if the addition of both DP103 and PIASy could cause any alterations to this effect. At the same time, we would like to determine if DP103 serves to inhibit deSUMOylation of NEMO with SENP2.

We performed an *in vitro* SUMOylation assay with recombinant SUMO-1, SUMO E1 and Ubc9 (SUMO E2) protein, together with PIASy, DP103 and/or SENP2. The *in vitro* SUMOylation assay helps to confirm if a particular protein is involved in the SUMOylation process. From Figure 44A, we observed that while PIASy alone is able to SUMOylate NEMO, the addition of DP103 enhanced *in vitro* SUMOylation of NEMO mediated by PIASy (Lanes 3 and 4). It is however, not clear whether DP103 prevented deSUMOylation by SENP2 *in vitro* (Lane 5) and further analysis need to be carried out to confirm this. It is necessary to note that these samples were ran on a 8% acrylamide gel for a prolonged period of time (2h at 130V) in an attempt to separate the PIASy and SENP2 bands, as seen in Figure 44A, right. Samples from Figure 43B were ran on a 4-12% gradient acrylamide gel at 130V for 1h, thus the appearances of the bands of PIASy and SENP2 appeared to be similar in molecular weight.

When different amounts of DP103 were analysed in their abilities to interact with NEMO, SENP2 and PIASy, we observed that increasing DP103 increases NEMO-DP103 interaction while at the same time increases NEMO-PIASy interaction. We also noticed that NEMO-SENP2 interaction decreases with increasing DP103 levels (Figure 44B).

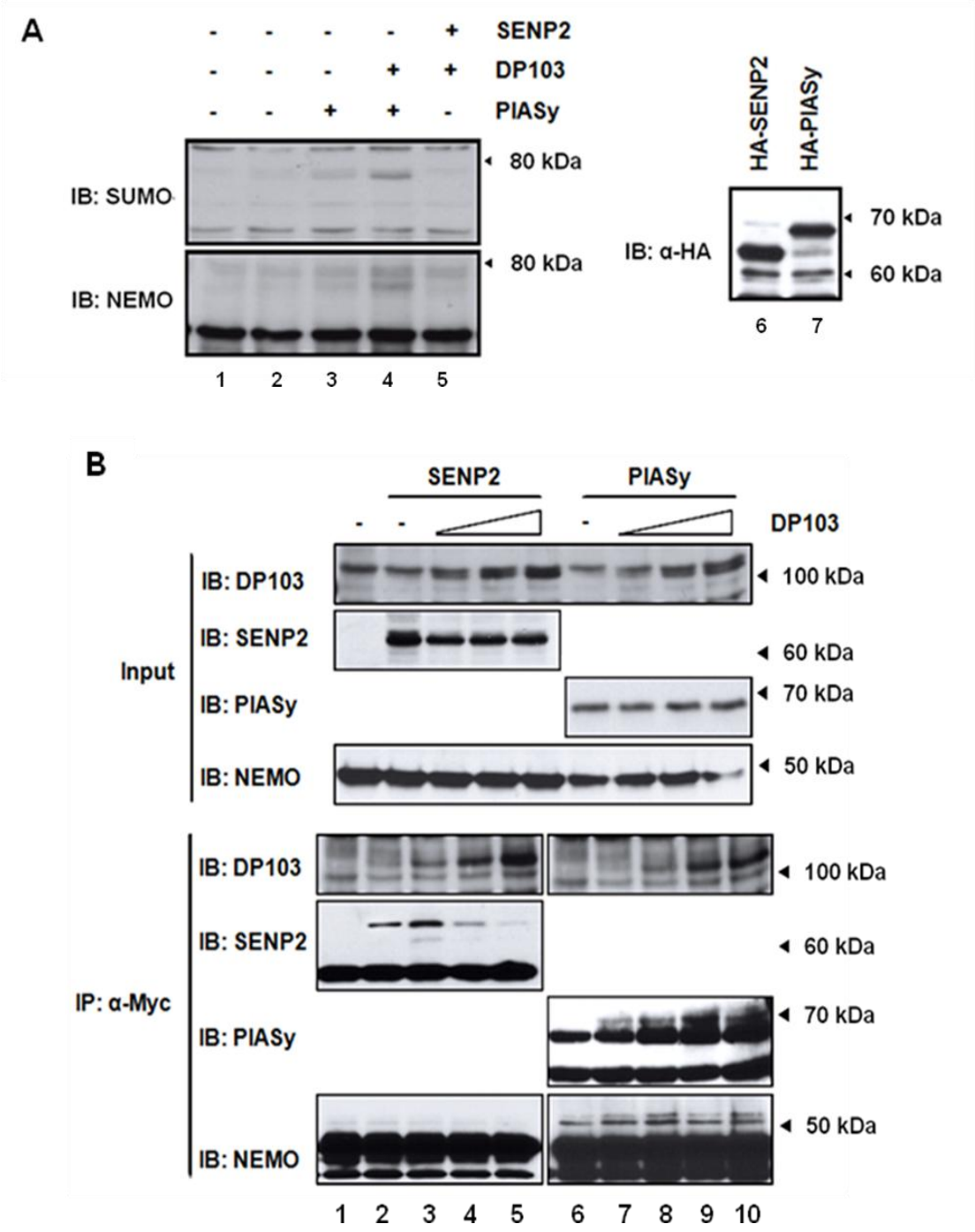

Figure 44. DP103 enhanced NEMO-PIASy interaction while decreased NEMO-SENP2 interaction. *In vitro* SUMOylation was performed with recombinant SUMO-1, SUMO E1 and Ubc9 proteins. The samples were then subjected to SDS-PAGE and immunoblotted with indicated antibodies (A). HEK293 cells were transfected with Myc-NEMO, Flag-SENP2, HA-PIASy and/or increasing dose of Flag-DP103. After 24h, cells were incubated with CPT (10μM) for 1h, performed IP using anti-Myc antibody and immunoblotted with indicated antibodies (B).

3.6.6 DP103 expression in the nucleus is increased in high grade tumors

Given that SUMOylation of NEMO is a nuclear event such that free NEMO need to be translocated into the nucleus before the series of post-translational modifications can occur (Huang et al., 2003), the subcellular localization of DP103 expression will be of immersed interest should the interaction between DP103 and NEMO we elucidated proved to be true.

We took several breast patient tissues from normal breast epithelium to differential grades of infiltrating ductal carcinomas and stained for DP103 protein. Indeed, increased expression of DP103 in the nucleus could be observed in high grade tumors during breast cancer progression. The normal breast epithelial cells showed mild to moderate cytosolic expression, further signifying its very low constitutive levels in normal breast cells also confirmed earlier in Chapter 3.1 (Figure 45).

Clearly, DP103 has once again showed its increase of expression in breast tumorigenesis and its augmentation into a nuclear expression in the Grade 3 tumors may be an indication of increased interaction with NEMO and thereby lead to invasion and metastasis.

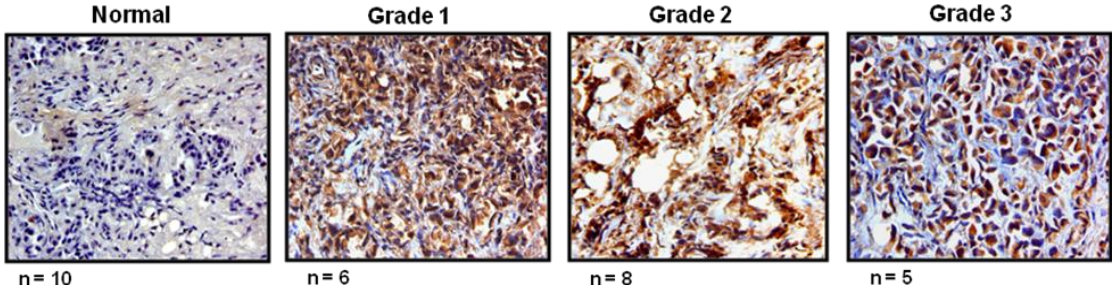

Figure 45. Increased DP103 expression in nucleus of high grade tumors. DP103 was stained in different breast patient tissues of normal breast epithelium and varying tumor grades.

3.7 Targeting DP103 clinically

We have shown DP103 to be a prognostic marker for metastatic breast cancer, and it is essential for SUMOylation of NEMO, thereby activating of NF-κB. An efficient method of targeting DP103 specifically will therefore be a good therapeutic option for the treatment of metastatic breast cancers in human.

Therapeutic use of siRNA over the years has been plagued with several limitatations, such as low enzymatic tolerability, poor cellular uptake, cellular internalization as well as non-specific targeting of tissues (Guo et al., 2010; Pirollo and Chang, 2008; Tamura and Nagasaki, 2010). As such, many groups have tried to design nanoparticles (Hasan et al., 2011), cation polymer (Nimesh et al., 2011) or liposomes (Kundu et al., 2011) to encapsulate the siRNA before delivering them *in vivo*. Despite that, the efficacy and safety issues of each method need to be intensively addressed before bringing them into clinical applications (Shim and Kwon, 2010). Hence, we decided to adopt the use of a clinically available drug, belonging to the family of statins in bid to inhibit DP103 (See Introduction, Chapter 1.6.3). Given the known link of statins to NK-κB as well as to cancer metastasis, and the elucidation of DP103 to have a pivotal role in the progression of metastasis, we speculate that actions of statins to inhibit metastasis is via the downregulation of DP103 expression in the cell.

3.7.1 Statins downregulate DP103 expression

We selected two statins, Simvastatin (Trade name: Zocor) and Lovastatin (Trade name: Mevacor) for use in this project. Simvastatin is a synthetic derivate from a fermentatio product of *Aspergillus terreus*, while Lovastatin is derived from fermentation of oyster mushrooms and red yeast rice (Kang et al., 2009; Sassano and Platanias, 2008).

Following Simvastatin and Lovastatin treatments in MDA-MB-231 cells, we observed a dose-dependent decrease in the levels of CXCR4 and MMP9 which are downstream targets of NF-κB as reported by others (Biswas et al., 2001; Helbig et al., 2003; Rehman and Wang, 2008). More importantly, we also noticed similar trend of decrease in both mRNA and protein expressions of DP103 (Figure 46).

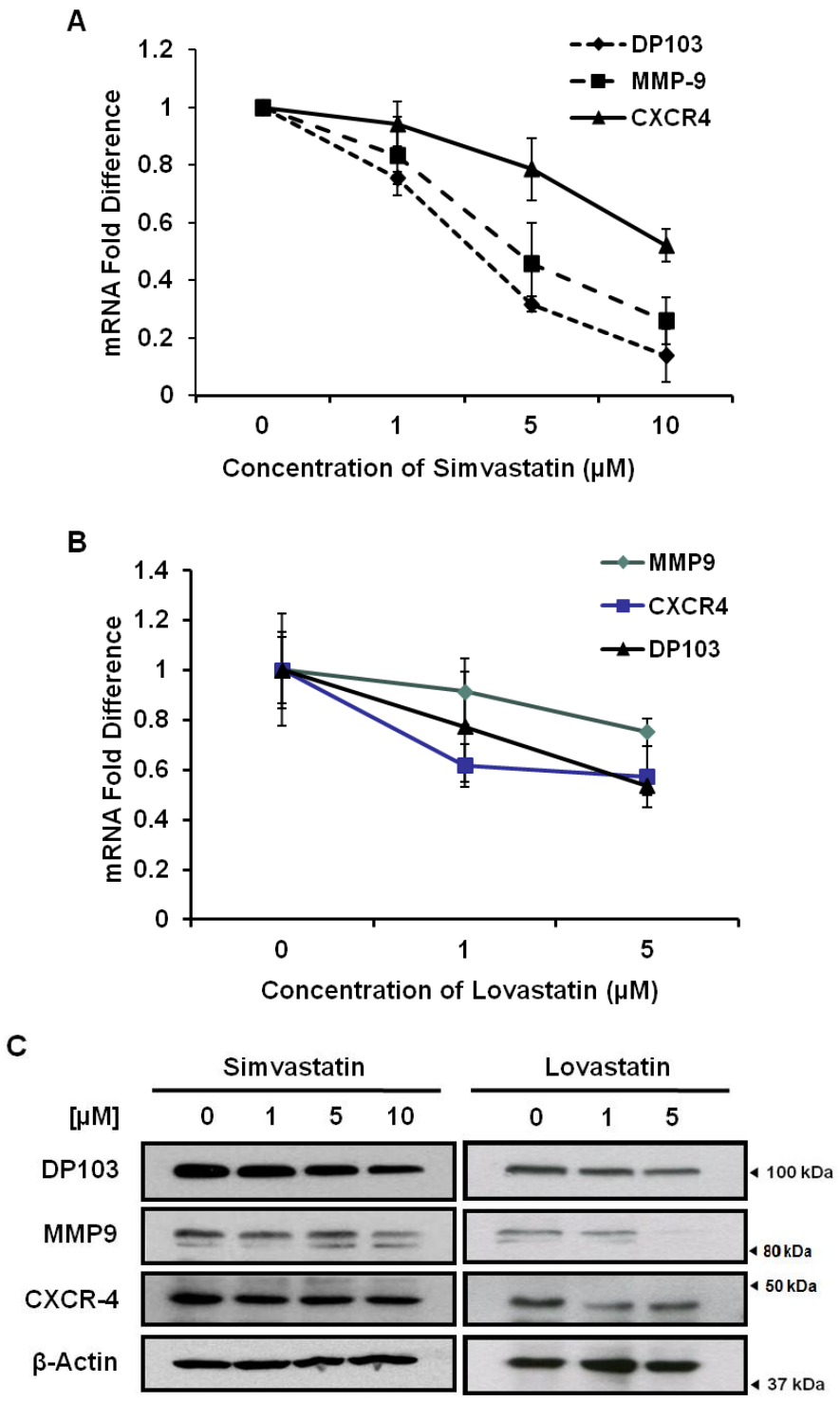

Figure 46. Statins are able to downregulate DP103 expressions. MDA-MB-231 cells were subjected to Simvastatin and Lovastatin treatments. RNA and protein were extracted and analysed using Real-time PCR (A and B) and Western blotting (C) respectively.

3.7.2 Overexpression of DP103 rescues the inhibitory effect of simvastatin on invasion

Since Simvastatin is able to downregulate DP103 and MMP9, and that we have previously shown that DP103 controls the expressions of NF-κB related protein via positive modulation of its activity, it is hypothesized that the drug brings down the expression of DP103, which inhibits NF-κB activity, thereby causing a decrease in MMP9 levels and reduced invasion.

To test this hypothesis, we designed a rescue experiment where we treated MDA-MB-231 cells transfected with either empty vector or Flag-DP103 with Simvastatin. From Figure 47C, we showed the effective overexpression of DP103, and that this upregulation alone is able to increase invasion by two folds from the transwell invasion assay (Figure 47A top panel). Additionally, as with reported observations (Kang et al., 2009), Simvastatin alone is able to inhibit invasion by about 50% (Figure 47A left panels and Figure 47B). However, when the overexpressed cells were treated with Simvastatin, the anti-invasive effect of the drug is rescued with the percentage of invaded cells reduced by almost 100% (Figure 47).

Collectively, we show the effective use of statins to downregulate DP103 expression in cancer cells. This suppression of DP103 can be positioned to be under the axis of statins-DP103-NF-κB-metastasis. To further validate our findings and extrapolate to clinical relevance, we performed an *in vivo* study.

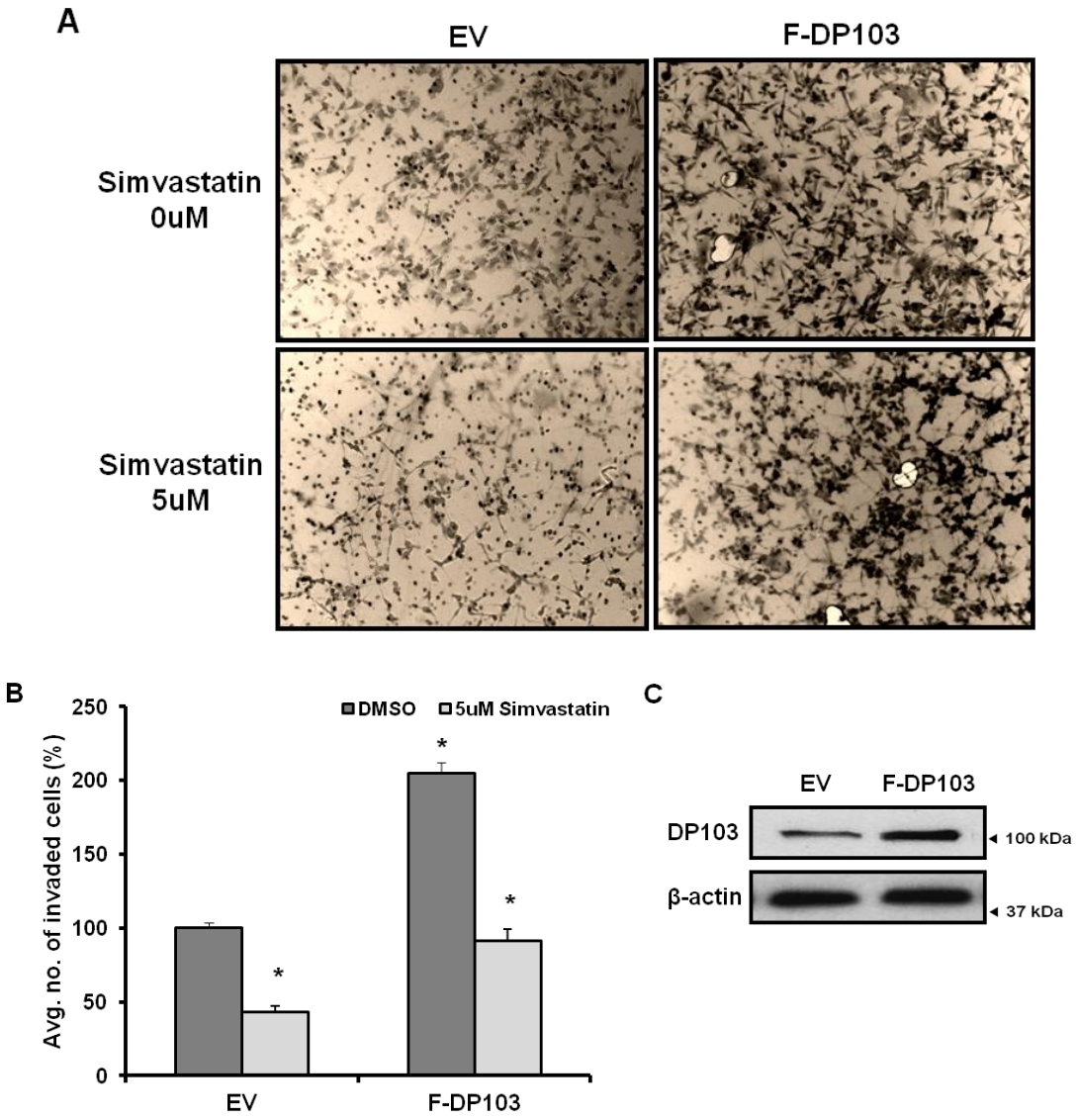

Figure 47. Overexpression of DP103 rescues the inhibitory effect of simvastatin on invasion. 2 x 10^5 MDA-MB-231 cells transfected with either empty vector (EV) or Flag-DP103 (F-DP103), treated with or without Simvastatin were seeded into the upper chamber of the tranwell invasion chamber. After 24h, the membranes of the chambers were stained with crystal violet solution and mounted on microscope slides (A). Graph showing the percentage of cells that invaded through the membrane (B). Western blot showing effective overexpression of DP103 (C). * denotes $p<0.05$.

3.7.3 Simvastatin fed mice showed reduced metastasis and decreased DP103 expression

The *in vivo* model was done in collaboration with Dr Zhu Tao (Hefei National Laboratory for Physical Sciences at Microscale and School of Life Sciences, University of Science and Technology of China, Hefei, Anhui, P.R. China) to confirm the reduction of metastasis upon downregulation of DP103 in mice.

Two groups of 8 female nude mice each were injected into the tail veins with MDA-MB-231 cells (1 x 10^6 cells suspended in 200μl PBS) for two weeks. The mice were then fed them with either vehicle (DMSO) or 25 mg/kg Simvastatin for a period of six weeks before they were sacrificed as described in the materials and methods.

Lung tissues were removed from the mice and stained with H&E to show micrometastases. Figure 48A showed pictures of lungs with grossly cystic lung micrometastases in the control group. On the other hand, the pictures of lungs from the Simvastatin treated group showed significantly fewer visible lung metastases. These results were further confirmed by quantifying the number of micrometastasis colonies (Figure 48B). Also, the level of human housekeeping gene hypoxanthine-guanine-phosphoribosyltransferase (hHPRT) was analyzed using real-time PCR as it does not cross-react with its mouse counterpart, providing an accurate measure of the amount of injected human cells in the mice. A decrease in hHPRT level was observed in the Simvastatin treated group mice, indicating a reduction of metastasis of MDA-MB-231 cells in the lungs (Figure 48C).

We performed immunohistochemistry staining on these lung tissues of the mice and showed decreased DP103 and MMP9 expressions (Figure 49), confirming our previous observations that Simvastatin decreases DP103 expression in MDA-MB-231 and thereby reduces cell invasion.

Put together, our hypothesis to use simvastatin to reduce DP103 expression in mice is sound and effective. Furthermore, these findings corroborate with our previous *in vitro* data that the suppression of DP103 reduces metastasis.

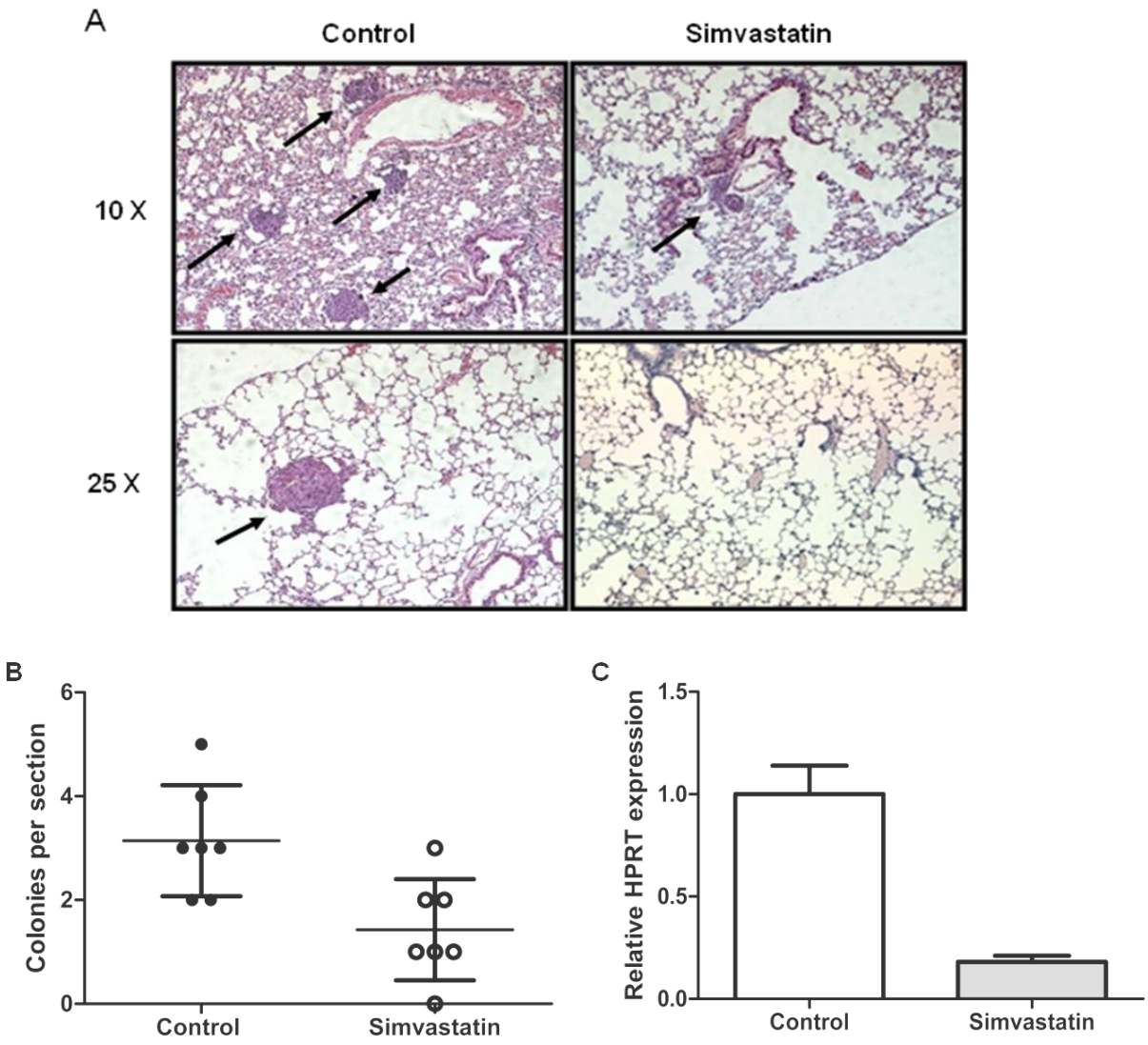

Figure 48. Simvastatin fed mice showed reduced metastasis. 1 x 10^6 MDA-MB-231 cells suspended in 200µl PBS were injected into tail vein of female nude mice. Groups of 8 mice each were injected intra-peritoneal (i.p.) with either vehicle alone or with 25 mg/kg Simvastatin 3 times a week for 6 weeks. Representative hematoxylin and eosin staining were shown in (A). The number of metastatic colonies formed were quantified and represented in graph (B). To quantify cancer metastasis in mouse lungs, qRT-PCR for human hypoxanthine-guanine-phosphoribosyltransferase (hHPRT) was performed on Trizol-isolated total RNA using described primers for hHPRT and mouse 18S rRNA (C).

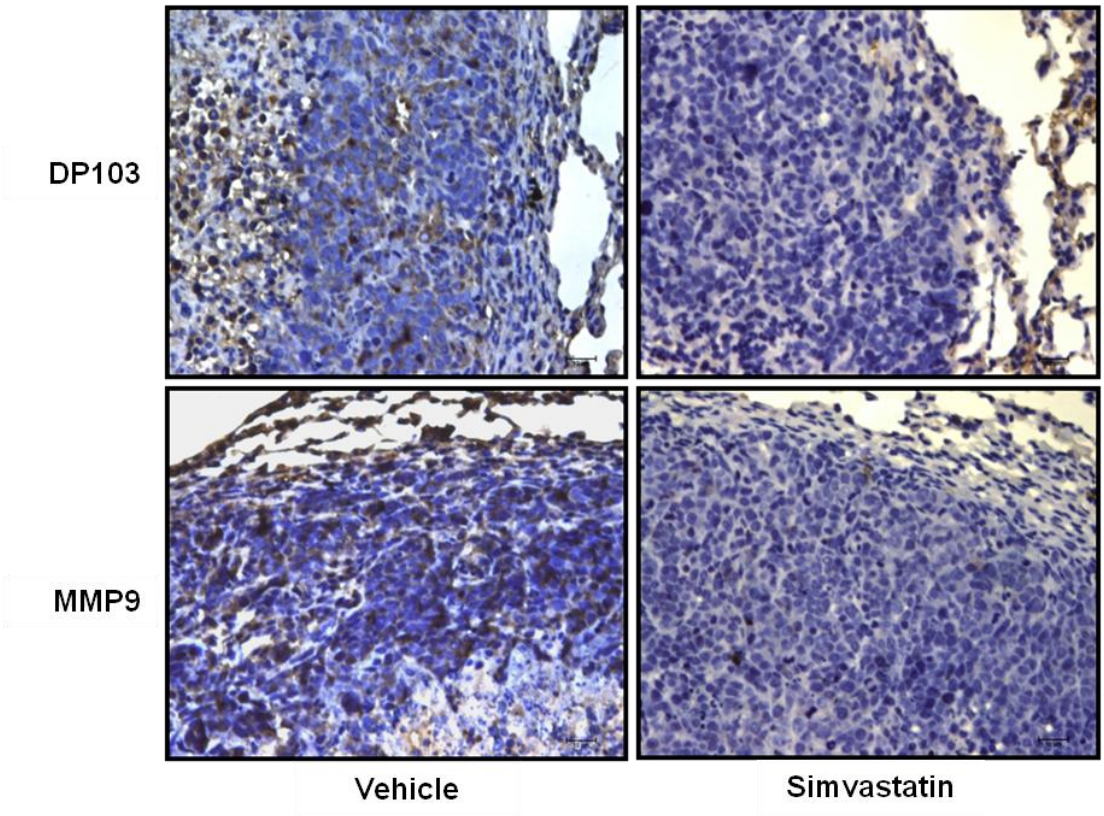

Figure 49. Lung tissues from Simvastatin treated mice showed reduced DP103 and MMP9 expression. Formalin-fixed, paraffin-embedded lung tissue was cut into 5 μm section, de-paraffinized in xylene, rehydrated through graded ethanol, quenched for endogenous peroxidase activity in 3% (v/v) hydrogen peroxide, and processed for antigen retrieval by heating in 10 mM citrate buffer (pH 6.0) at 90-100°C. Sections were incubated at 4°C overnight with DP103 and MMP9 antibody.

CHAPTER 4 DISCUSSIONS

Breast carcinoma is the most common malignancy among women and its treatment is possible if diagnosed at an early stage. The 5-year survival rates for stages 0 to 2 breast cancer are as high as 99% and 80%, and rapidly decline to 44% and 15% for stages 3 and 4. Despite the high survival rates for early stage breast cancer, most of such tumors are left unnoticed without regular mammogram tests. Established biomarkers such as estrogen receptor (ER), progesterone receptor (PR) and HER2 have been playing significant roles in the selection and management of patients for endocrine therapy. Whilst effective targeted therapeutic modalities exist for women with hormone receptor positive and HER2 positive disease, chemotherapy is the only systemic therapy available for women with triple-negative cancer.

Triple-negative breast cancer is clearly a distinct clinical subtype, from the perspective of hormone receptors and HER2 expression. Additionally, these tumors have unique characteristics including increased mitotic activity, high Ki67 index and high nuclear-cytoplasmic ratio which are identified in high grade invasive carcinomas (Fulford et al., 2006; Livasy et al., 2006; Rakha et al., 2006). The relatively aggressive clinical course, poor prognosis (Dent et al., 2007; Haffty et al., 2006) and lack of therapeutic options (Thike et al., 2010) for this type of tumors have intensified current interest in this patient group and represent an important clinical challenge.

The identification of triple-negative breast cancer currently relies on immunohistochemistry and flueorescence *in-situ* hybridisation (FISH), a process that requires strict quality control (Gown, 2008). At the same time, there is no stringent

assay or a standard criteria established globally to define accurately this subtype of breast cancer. Elucidating more validated prognostic markers for triple-negative breast cancer will therefore help in the characterization of patients into the correct subgroups.

Prognostic markers are indicators of aggressiveness, invasiveness, extent of spread of tumors and thus correlate with survival independent of systemic therapy and can be used to select patients at risk. On the other hand, predictive markers predict the response of a patient to a specific therapeutic intervention. Patients with early-stage breast cancer usually have microscopic metastasis at the time of diagnosis, and coupled with the fact that triple-negative breast tumors are associated with more aggressiveness (Dent et al., 2007), many molecular markers can therefore be studied to elucidate if they possess prognostic or predictive values.

Current treatment strategies for such tumors involve chemotherapy agents such as the platinum salts, anthracyclines and taxanes (2005; Andre et al., 2010; Liedtke et al., 2008; Sirohi et al., 2008). As discussed in the introduction, anthracycline-based regimens showed optimistic results of the pathological response rate of the patients in studies. Similarly, platinum therapy for triple-negative breast tumor patients displayed impressive preclinical results, particularly in tumors also having BRCA mutations. However, these therapies require closer scrutiny as focused and large-scale trials have not been performed. The increased heterogeneity of tumors in a larger group of patients will pose a huge challenge in determining if these drugs will show good efficacy in the overall survival and disease-free survival as well as the extent of the severity of side effects that these drugs will deliver.

A potential prognostic target for triple-negative breast cancer is PARP. Increased awareness of PARP can be seen from the rapidity of translation from preclinical experiments into clinical advances (Farmer et al., 2005; O'Shaughnessy et al., 2011). From preclinical studies, researchers showed that BRCA deficient tumors displayed increased sensitivity to PARP inhibitors (Byrski et al., 2008; Farmer et al., 2005), sparking off the start of several clinical trials on PARP inhibitors as a single agent or in combination regimens in patients with BRCA mutations (Kortmann et al., 2011; von Minckwitz et al., 2011). Olaparib (AstraZeneca), a PARP inhibitor, showed an overall response rate of 41% among 27 patients assigned to the drug without significant toxicity. The use of iniparib (Sanofi), another PARP inhibitor, also displayed impressive clinical benefits by prolonging the progression-free survival from 3.6 months to 5.9 months when combined with carboplatin and gemcitabine in a Phase II trial. As such, PARP inhibitors hold significant potential for the treatment of triple-negative breast cancers with minimal toxicity and is likely to be highly tumor specific towards the absence of BRCA (Farmer et al., 2005; Tutt et al., 2010). owever, it is notable that despite its important role in the cellular response to genotoxic stress, PARP1 is not required for survival in the absence of such an insult. $PARP1^{-/-}$ mice are viable and fertile (D'Amours et al., 1999; de Murcia et al., 1997).

In view of all these, there remains a fuzzy area for physicians to accurately determine the type of therapies to render to the patients. Thus, it sparks off an active interest and a pressing need to find novel biomarkers that are unique to triple-negative breast cancers as well as novel prognostic markers to determine responsiveness to therapeutic interventions.

DEAD-box family members belong to the family of RNA helicases and are involved in numerous RNA processes (Rocak and Linder, 2004). Several researches have been done on different DEAD-box family members on their importance in numerous cancers. p68 has been extensively studied to be involved in aberrant post-translational modifications in colorectal cancers (Causevic et al., 2001) and is also a transcriptional coactivator of the p53 tumor suppressor gene (Bates et al., 2005). On the other hand, Ddx3 is involved in the transformation of epithelial to mesenchymal transition via downregulation of E-cadherin (Botlagunta et al., 2008), and other members like Ddx1 and Ddx48 are predominantly overexpressed in retinobastomas and pancreatic cancers respectively (Godbout et al., 1998; Xia et al., 2005).

The knowledge of DP103, despite being characterized a decade ago (Grundhoff et al., 1999), remains few and limited. DP103 was found to be an interacting partner with several proteins, including EBNA2 and EBNA3C which regulate transcription of both latent viral and cellular genes (Grundhoff et al., 1999); SMN to modulate gene expression via pre-mRNA splicing (Zieve and Sauterer, 1990); METS to repress the transcription of cell cycle control genes in macrophages (Klappacher et al., 2002); Egr/Krox-20 to repress itself in vertebrate hindbrain (Gillian and Svaren, 2004) and FOXL2 to induce apoptosis in Chinese hamster ovary cells (Lee et al., 2005a).

More information on the mechanism of how DP103 represses transcription arose during the discovery of the role of DP103 in the development of steroid-producing glands and the ventromedial hypothalamus (Ou et al., 2001). DP103 was shown to be essential for the co-repression of SF-1, thereby modulating its transcriptional activity via SUMOylation modification (Lee et al., 2005b). On top of that, the importance of

DP103 physiologically was greatly reflected when it was shown that homozygous knockout DP103 mice are embryonic lethal, having failed to develop beyond the two-cell stage (Mouillet et al., 2008), strongly indicating an essential role in growth and development.

Preliminary observations showed that DP103 expression were found to be overexpressed in highly proliferating cells, for instance in primary malignant melanoma patient tissues (Grundhoff et al., 1999) and lymphoma patients (Ghobrial et al., 2005). Microarray analyses also reflected DP103 to be upregulated in lymphoma patients (Ghobrial et al., 2005), in CRC patients that developed distal metastases (http://www.ebi.ac.uk/arrayexpress [Array express ID: E-GEOD-18105]). Additionally, DP103 was found to be a potential target for the inhibition of metastasis from a US patent (Publication Number: US 2010/0004190 A1) in 2010. All these resulted to the establishment of our hypothesis that DP103 is associated with cancer.

From our tissue microarray results, we found a significant number of patients with DP103 being highly expressed in their invasive breast tissues compared to the very low expression in their matched normal tissues. This is also seen in the panel of breast cell lines representing different status of tumors. While normal breast cells and poorly invasive breast carcinomas showed low levels of DP103, it is overexpressed in highly invasive breast cancers. It is also necessary to note that the expressions of DP103 are higher in the ERα negative cell lines (MDA-MB-231, BT549) as opposed to the ERα positive cell lines (MCF7, BT474).

To demonstrate the relevance of DP103 with tumor progression, we observed the DP103 expressions in xenograft-derived cell lines from the MCF10AT series. This panel of cell lines are derived from cells from the same parental source at different stages of cancer, therefore representing the breast cancer progression model. The levels of DP103 are seen to have a positive correlation with increasing degree of malignancies, signifying a tight association of DP103 expression with tumorigenesis. We verified the same observation in *in vivo* studies when we tested primary human patients samples and immunohistochemical stained them for DP103 expression. Tissues that were derived from primary tumors which distal showed metastases were revealed to have the highest level of DP103 expression as compared to tumors which did not metastasize.

The importance of DP103 in ERα negative breast cancer was elucidated next. While the downregulation of DP103 did not affect the viability of the cells, it resulted in reduced cell migration, cell invasion and a loss of pseudopodial protusions, all demonstrated repeatedly by our various 2D and 3D setups. These symbolize the involvement of DP103 in the process of cancer metastasis. Conversely, overexpression of DP103 in MDA-MB-231 increased the invasive ability of the cells by about 2 folds. More importantly, overexpression of DP103 alone in the normal epithelial breast cell line, MCF10A, which displayed very low ability to invade, was able to cause the cells to invade by about 4 folds, demonstrating an oncogenic function of DP103.

In an attempt to elucidate the genes involved in this downregulation of DP103-dependent inhibition of metastasis, we performed a metastatic qPCR array and saw

MMP9 to be overexpressed by more than 2-fold when DP103 was stably overexpressed in BT549. Having found a target gene, we returned to our initial panel of different breast cell lines and observed that MMP9 expression was upregulated in the same highly invasive cell lines, MDA-MB-231 and BT549 which also showed higher DP103 expression. Similarly from our primary human patient breast tissue samples, MMP9 expression was revealed to be higher in tumor tissues that had metastasized. However, these observations are not unknown since the association of MMP9 to cancer invasiveness has long been established (Gong et al., 2000; Kim et al., 2006a; van Kempen and Coussens, 2002). Despite that, a novel finding from our project is from the correlation studies done using results from the panel of different cell lines and the primary human patient breast tissues. We showed strong positive association of the levels of DP103 and MMP9 ($r = 0.913$ and $r = 0.513$ respectively).

To determine if there is any clinical significance of this newfound association between DP103 and MMP9, we retrieved data from 55 breast cancer patients in Singapore and selected those showing elevated levels of DP103 expression. In this subcohort, patients who were detected with elevated MMP9 levels had poorer overall survival ($p = 0.029$), suggesting strongly that the co-occurrence of high levels of DP103 and MMP9 predicted poorer prognosis in patients. This data, however, was unable to verify the correlation of these two genes. At the same time, a 'reverse' Kaplan Meier analysis in which patients with high MMP9 expressions are selected for the determination of survival rate in relation to the levels of DP103 would further strengthen our findings.

Since the inhibition of metastasis by DP103 also involved MMP9, we speculated that the suppression of DP103 could possibly cause a reduction in MMP9 protein and thereby inhibit invasion. This was proven to be true when the protein and mRNA levels of this protein was decreased following the inhibition of DP103 by siRNA techonology. Additionally, this decrement reflected the loss of MMP9 enzymatic activity in our gelatin gel zymography experiment. MMP9 was also revealed to be the major endopeptidase to be modulating the inhibition of invasiveness when the synthetic inhibitor specific to MMP9 alone was able to suppress the migratory ability of MDA-MB-231 across the transwell invasion chamber, a phenotype that could be rescued by the overexpression of DP103. After establishing the DP103-MMP9-metastasis axis, we next explored the signaling pathway in which DP103 is involved in to regulate MMP9.

The initiation of activation of signal transduction pathways has been widely documented by the interaction of specific ligands with their cell surface receptors. This resulted in a cascade of events transmitting signals from the cytoplasm into the nucleus, activating transcription factors, ultimately altering gene expressions. Several mechanisms had been elucidated to perform these functions. They include GPCR (Liggett, 2011), transmembrane signaling by phosphorylation, MAP kinase pathways (Zhu et al., 2011), JAK/STAT pathway (Slattery et al., 2011), Wnt/Frizzled pathway (Katanaev, 2010), Notch pathway (Bridges et al., 2011), NF-κB pathway (Hayden and Ghosh, 2004) and more. Many of these pathways modulate the metastasis cascade.

There is a myriad of transcription factors involved in the regulation of MMP9, some of which include AP-1 and NF-κB, both of which act under different physiological

conditions depending on the type of stimuli (Adamson et al., 2000; Milde-Langosch et al., 2004). A novel and important discovery in our studies is the involvement of DP103 in the NF-κB pathway. From our dual-luciferase and EMSA assays, we discovered that the down-regulation of DP103 led to a significant decrease in NF-κB activity. This decrease in NF-κB activity is specific as the activity of AP-1, another transcription regulator of MMP9, is not affected by the suppression of DP103. This is further verified when we saw decreased levels of other NF-κB regulated metastatic genes like CXCR4 and ICAM1 when DP103 was suppressed. From our immunoprecipitation experiments, we observed that DP103 interacts with NEMO, but not other NF-κB members like p65, p50 or IκB, and the suppression of DP103 did not affect the protein levels of these members. This indicates that DP103 is not regulating NEMO and other members at transcriptional level of the NF-κB members. We speculated that post-translational modifications may be a possible way that DP103 is involved in. Additionally, we observed an increase in DP103 protein levels during the induction of NF-κB activity, signifying a possibility that DP103 may itself be an NF-κB target. It is indeed worth to look further in bid to elucidate the transcriptional machinery of DP103 by examining its promoter region for putative NF-κB binding sites.

Several post-translational modifications are present in the NF-κB atypical pathway. Unlike the canonical pathway, the initiation of this pathway occurs during times when cells are exposed to stress from both exogenous and endogenous genotoxic or DNA-damaging agents. NEMO, as its name suggests, is essential for modulating the regulation of the IKK complex. Under the effect of genotoxic agents, DNA double strand breaks occur and initiate a series of nuclear post-translational modifications of

NEMO before being extruded into the cytoplasm where it complexes with IKKα/β subunits to carry out its function to phosphorylate IκBα, releasing the inhibitory effect on the NF-κB dimers, p65 and p50, and therefore activating NF-κB in the nucleus (Huang et al., 2003). These NEMO post-translational modifications are critically required for NF-κB activation as individual mutations in the acceptor sites for these post-transcriptional modifications completely block NF-κB activation by multiple genotoxic agents (Wu and Miyamoto, 2008). The uniqueness of the atypical NF-κB pathway is that the initiation of activation occurs in the nucleus and is transferred to the cytoplasm, or namely, the 'nuclear-to-cytoplasmic' signaling pathway.

As discussed previously, triple-negative breast cancers with BRCA mutations are more susceptible to DNA damaging agents (Farmer et al., 2005). A connection between this susceptibility and aberrant NF-κB activation via the DNA-damage-dependent atypical pathway in breast cancers may be plausible. Understanding the mechanism may provide a deeper insight of the physiological roles of various molecules in this signaling event, especially that in breast cancers and at the same time shed light into the search for a probable therapeutic target for breast cancers as well as other cancers.

Besides establishing that NF-κB activity was reduced in the absence of DP103, we also demonstrated similar decrease in NF-κB activity upon different genotoxic stimuli, doxorubicin, camptothecin and etoposide which are known activators of NF-κB. Since we previously showed DP103 does not modulate NF-κB members at the transcriptional level and that it interacts with NEMO, we hypothesized that DP103 regulates the activity or function of NEMO via post-translational modifications.

NEMO undergoes several post-translational modifications in the atypical pathway, including the translocation of free cytoplasmic NEMO into the nucleus, SUMOylated, phosphorylated and subsequently ubiquitinated. The addition of Ub groups onto NEMO causes it to be extruded into the cytoplasm and enters the canonical pathway to activate NF-κB. A plausible connection can be drawn here from the fact that DP103 acts as a co-repressor for SF-1 via SUMO modification (Lee et al., 2005b; Ou et al., 2001).

As SUMOylation is a rapid and reversible process, it is difficult to detect the levels of SUMOylated NEMO under basal conditions. Additionally, the SUMOylation process cannot be separated from the deSUMOylation process. To overcome the limitation of a relatively low percentage of SUMOylation that has significant effects on many biological processes, we employed the use of genotoxic drugs, doxorubicin, camptothecin and epotoside to enhance the SUMOylation of NEMO (Huang et al., 2003). We showed DP103 to be essential for the SUMOylation of NEMO under camptothecin stimulus due to an increase seen in SUMOylated NEMO. In addition, downregulation of DP103 halts this post-translational modification, both basal and with genotoxic stimuli, thereby inhibiting NF-κB activation. The paramount significance of this finding is that for the first time, we elucidated DP103 to be a critical regulator for the SUMO modification of NEMO.

As DP103 belongs to the family of RNA helicases, the involvement of the helicase activity in the SUMOylation of NEMO is of interest. In this family of RNA helicases, ATP is required for the unwinding of RNA and several members are known to display both ATP-dependent as well as ATP-independent functions (Bates et al., 2005;

Botlagunta et al., 2008; Chao et al., 2006; Rocak et al., 2005). In our study, we demonstrated that the helicase activity of DP103 is dispensable for this SUMO modification. Cells transfected with the helicase dead GNT mutant showed no difference in the SUMOylation strength of DP103 to NEMO and did not affect the cells' invasion ability. This is in concordance to previous findings that DP103 helicase activity is not required for SUMOylation of SF-1 to occur (Lee et al., 2005b; Ou et al., 2001).

SUMOylation is a highly dynamic and coordinated process, and is involved in a variety of cellular processes for growth, development, apoptosis as well as cancer metastasis (Bettermann et al., 2011; Hirata et al.; Kessler et al., 2011; Pot and Bonni, 2008). However, many basic questions regarding components, mechanisms and consequences remain unanswered. For instance, the list of characterised enzymes appear to be short considering the large number of target proteins that are modified in a regulated manner. Additionally, there may be many SUMO enzymes that are not discovered yet, as well as regulatory elements like co-factors involved in SUMOylation and deSUMOylation. Knowledge of how SUMOylation is involved in metastasis is also limited, despite the increasing focus in this area in recent years. It is particularly important to note that in prostate cancer, the levels of endogenously SUMOylated reptin protein in metastatic prostate cell line LNCaP was found to be higher compared with that in the normal prostate epithelial cells RWPE1. Furthermore, the expression levels of Ubc9, SUMO E2 enzyme were increased in metastatic cancer cells while the levels of deSUMOylating enzyme SENP1 was reduced (Kim et al., 2006b; Kim et al., 2005). It is thus speculated that proteins

regulating the expression levels of these SUMO enzymes are also associated to the progression of cancer metastasis.

To validate our hypothesis, we performed a pull-down assay and observed the interaction of DP103 with PIASy and SENP2, but not SENP1. Together with our previous results, DP103 fits all the descriptions to be the regulatory protein in SUMOylation. We went on to perform an *in vitro* SUMOylation assay and showed that the addition of both DP103 and PIASy further enhanced NEMO SUMOylation compared to PIASy alone. This observation is similar with the study done by Lee et al., 2005b in that DP103 increased PIAS-dependent SF-1 SUMOylation. Moreover, our immunoprecipitation experiments highlighted that the interactions between DP103 and NEMO, and NEMO and PIASy were progressively enhanced upon expression of increasing amounts of DP103, indicating an increase in the levels of NEMO SUMOylation.

On the other hand, the possible role of DP103 in inhibiting deSUMOylation of NEMO cannot be overlooked. We demonstrated the substrate specificity to SENP2 when DP103 was observed to interact with it but not SENP1 in the pull-down assay. However, the addition of both SENP2 and DP103 in the *in vitro* SUMOylation assay did not abolish the deSUMOylation effect of SENP2. Despite this, we found the interaction between NEMO and SENP2 to be decreasing with increasing levels of DP103. Put together, DP103 prevents the interaction of NEMO and SENP2 to occur, thereby reducing SUMOylation of NEMO.

Although Lee et al., 2005 first described the role of DP103 in SUMOylation, there are several novel facets that our study has uncovered. First, unlike our study which shows that genotoxic stress mediated SUMOylation reaction is aided by DP103, no physiological stimuli was identified which aided this reaction towards SF-1. Second, while SUMOylation of SF-1 can repress transcription, SUMOylation of NEMO promotes activation of NF-κB dependent transcription. Finally, in contrast to SUMOylation of SF-1 by DP103 that can directly regulate gene expression, SUMOylation of NEMO affects activity of a kinase complex, namely the IKK complex, which may have other substrates besides IκB and hence DP103-mediated SUMOylation of NEMO has the potential to affect other signaling mechanisms in cancer.

p68, another member of the DEAD-box family, has been found to be able to function as both a transcriptional activator and repressor. SUMOylation of itself proved to hold the delicate call to which function p68 should perfrom. A K53R mutant of p68 that renders it unSUMOylated is unable to interact with HDAC1 and hence a more effective co-activator (Moore et al., 2010). The SUMOylated form of p68, on the other hand, is an efficient transcriptional repressor (Bates et al., 2005). Though DP103 had not been shown to be SUMOylated for the modulation of its own activity, the presence of a SUMOylation interacting motif (SIM) at its C-terminal may be an indication for such a possibility. This will be important for future works as a tool for drug targeting to 'turn off' or 'on' its function.

Our findings thus far revealed DP103 to be a prognostic marker for breast cancer metastasis and that its suppression will lead to reduced cell invasion. At the same time, we showed a mechanism by which this inhibition occurred via SUMO modification of NEMO in the atypical NF-κB pathway. Importantly, this downregulation of DP103 increased the susceptibility of the cells to genotoxic stress from our viability studies where cell death was increased by about 30% compared to the cells treated with camptothecin or doxorubicin alone, or with suppression of DP103 alone. These provide a foundation for mouse models or possibly preclinical trials to be set up to validate the efficacy of this combinatorial therapy for the treatment of triple-negative breast cancer.

A limitation in our suggested combinatorial therapy is the method to suppress DP103 in invasive cells. In our project, we had been using the small interfering RNA technology to reduce the DP103 expression. However, systemic use of siRNA for therapies is still controversial due to the limitations of siRNA such as low enzymatic tolerability, cellular internalization and body distribution after systemic administration (Guo et al., 2010; Pirollo and Chang, 2008; Tamura and Nagasaki, 2010). Moreover, because intact, functional siRNA must be delivered into the target cell to reach an effective intracellular concentration, the problem of potential side effects due to general transfection of normal, nontarget tissues must be addressed critically. In order to overcome this, we attempted to use a commercially available therapeutic drug to produce the same effect as that of the siRNAs.

Statins have been used clinically for the treatment of hypercholesterolemia. They act by inhibiting the rate-limiting enzyme of the mevalonate pathway, 3-hydroxy-3-

methylglutaryl-CoA reductase. Despite that, statins have been shown to demonstrate anti-cancer properties over the years (Denoyelle et al., 2001; Kang et al., 2009; Li and Brown, 2009). Importantly, simvastatin and lovastatin are able to inhibit breast cell invasion with a reduction in MMP9 and MMP2 protein expressions (Kang et al., 2009; Mandal et al., 2011). Furthermore, Aberg and group described induction of apoptosis by simvastatin to happen via inhibition on the NF-κB pathway (Aberg et al., 2008). Other studies have also attributed effects of simvastatin like attenuation of growth and malignant potential in esophageal adenocarcinoma (Sadaria et al., 2011), reduction in pulmonary artery hypertension (Liu et al., 2011) and cardioprotection from ischemic-reperfusion injury (Malik et al., 2011) to be through the suppression of NF-κB activity.

With these knowledge, we hypothesized that statins inhibit invasion in breast cancers through inhibition of DP103-dependent NF-κB activation. Our results showed that simvastatin decreased DP103 levels at the transcriptional level and inhibit invasion. NF-κB-regulated metastatic genes, CXCR4 and MMP9 were also reduced in a dose-dependent manner under statins treatment. Furthermore, forced expression of DP103 upon simvastatin treatment abrogated this effect. Added evidence came from our *in vivo* studies, where similar observations were seen from nude mice that were injected with MDA-MB-231 cells. Mice that were fed with simvastatin showed lesser lung metastases as compared to the vehicle. Immunohistochemical staining of tissues extracted from these metastases revealed a decrease in DP103 as well as MMP9 expressions, confirming our hypotheses and mechanism of action. Hence, we demonstrated, for the first time, a direct link of statins-DP103-NF-κB-metastasis on the same axis in breast cancer cells.

Putting all our findings together, a signaling cascade with or without genotoxic stimuli that involves DP103, NEMO and NF-κB is proposed (Figure 50). In resting cells there is likely a competition between PIASy and SENP2 to bind the substrate, NEMO. Under conditions when DP103 levels are limiting, such as in normal cells, we speculate that it is the interplay between these factors that keeps SUMOylated NEMO levels under equilibrium and prevents constitutive activation of NF-κB and metastatic switch. In contrast, in cancer cells when DP103 levels become high (due to genetic or epigenetic changes), DP103 prevents the binding/recruitment of SENP2 to the substrate (NEMO). This then allows PIASy to bind and SUMOylate NEMO, a reaction that is also aided by DP103. In effect, these dual activities of DP103 could make NEMO more prone to constitutive SUMOylation and hence contribute to NF-κB constitutive activation in cancer cells.

Given that constitutive activation of NF-κB can also lead to the acquisition of resistance to chemotherapy, a hallmark of highly aggressive cancers, DP103-mediated NF-κB activation could not just be providing a metastatic switch to cells but also making tumor cells acquire other factors that govern carcinogenesis, namely ability to resist death and also reprogram metabolism (Mauro et al., 2011), both of which are also now known to be regulated by NF-κB activity. Indeed reduction of NF-κB signaling by downregulating DP103 sensitizes them to chemotherapy induced cell death.

Although constitutive activation of NF-κB is a well-documented phenomenon in cancer, increased levels of enzymes such as PIASy that can keep NEMO in a constitutively active state are not seen in cancer cells. Indeed it is highly tempting to

speculate that the levels of PIASy are not limiting in cancer cells but since the levels of DP103 are, it is the increase in levels of DP103 that marks the switch from a non-metastatic to metastatic state in a number of cancer cells. How this switch in DP103 expression occurs is a fundamental unanswered question that must be addressed in the future. Furthermore, understanding what turns on and keeps levels of DP103 high in cancer cells will provide us with a new set of therapeutic targets. Also what reprogramming a cancer cell undergoes to live with elevated levels of a RNA helicase is an important aspect of cancer biology that could make us understand the metastatic switch.

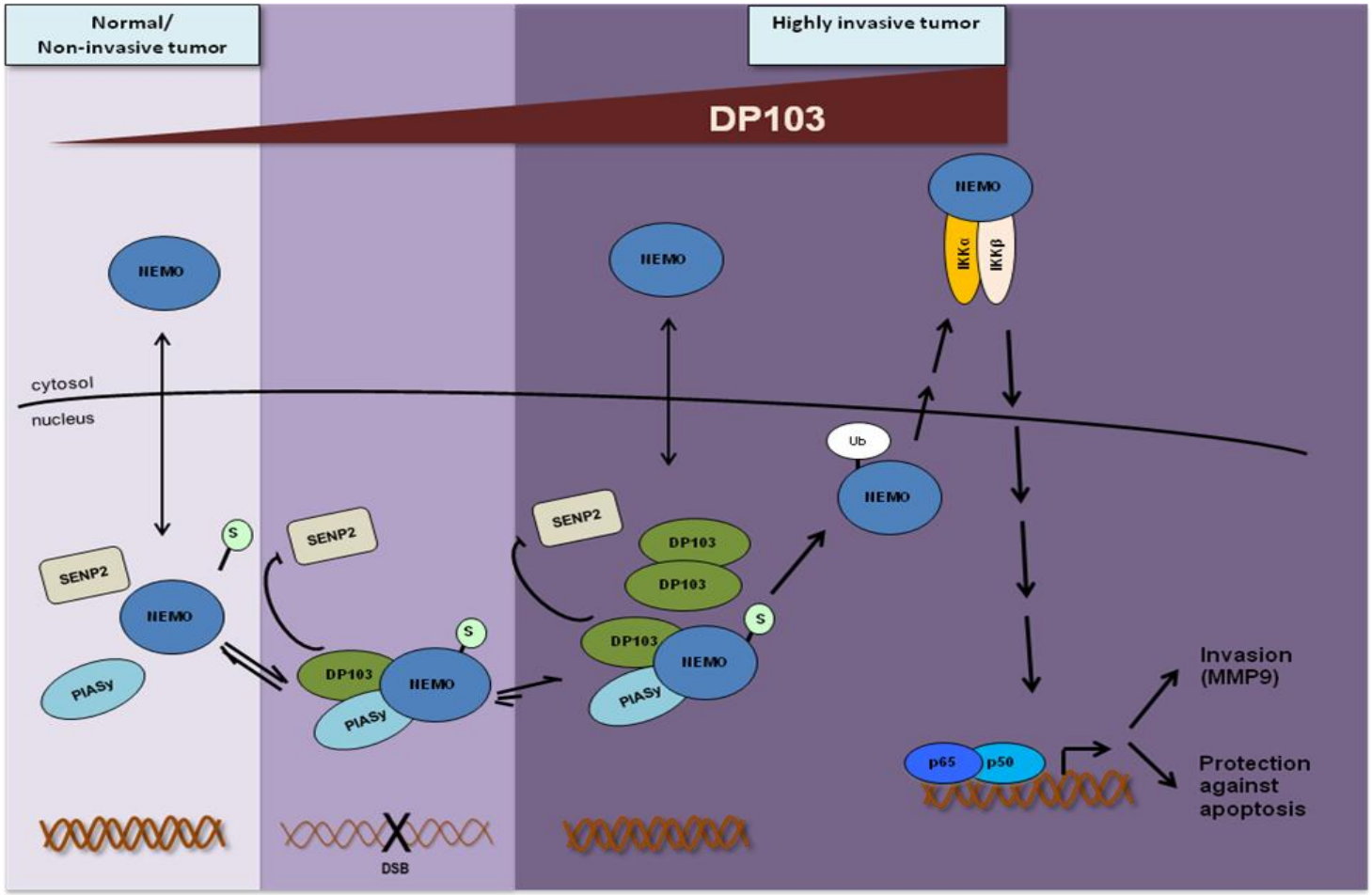

Figure 50. Proposed model of DP103 regulation in NF-κB atypical signaling pathway. DP103 associates with NEMO and mediates the SUMOylation of NEMO in a PIASy-dependent manner under genotoxic stress, progressing down the cascade to turn on NF-κB activation. SENP2 interaction with NEMO, at the same time, was decreased in the presence of DP103. DSB denotes DNA double strand break.

CHAPTER 5 FUTURE DIRECTIONS AND CONCLUSIONS

Our work starts with the interesting observation that DP103 is upregulated in highly proliferating cells, and particularly in metastatic breast cancer cells. Further *in vitro*, *in vivo* and functional works allowed us to support, for the first time, an unsuspected role of DP103 in cancer metastasis through modulation of the NF-κB pathway. Hereby, we present evidence to the role of DP103 in the NF-κB atypical signaling pathway. It is also the first detailed report describing the regulation of NEMO SUMOylation.

The possible clinical applications of our findings cannot be overemphasized. As DP103 expression correlates with the state of malignancies, it can be used as a prognostic marker to define breast cancer patients at the risk of developing metastases. Due to the heterogeneity of tumors, the response from breast cancer patients may not be complete. Predictive markers are of importance to accurately determine if certain treatment will be effective, as well as receiving the correct treatment early to eradicate the tumor. The potential of DP103 as a predictive marker for therapeutic intervention will thus be of immense interest.

NF-κB signaling pathway is an important pathway regulating cancer progression at many levels. At the same time, the persistent activation of NF-κB is observed in the highly aggressive breast cancers as well as in tumors acquiring resistance to drug treatments. Despite these knowledge, members in the NF-κB family are not 'druggable' as basal NF-κB activity is required for normal physiological responses like transcription of related

genes during stress, immune responses during microbial attacks or for survival especially in tumors. Therefore, targeting molecules involved in the regulation of NF-κB activation will be more probable.

As an essential regulator of NEMO SUMOylation in the NF-κB pathway, DP103 plays a critical role in modulating the transcriptional activity of NF-κB. In order to ensure thorough consistency on our findings using different techniques, further experiments can be done for validation. For example, the SUMOylation levels of NEMO in different breast cell lines can be done to confirm that increased SUMO modification occurs in malignant cells, as well as to draw stronger correlation to the levels of DP103.

Further experiments can be done to map the site(s) of interaction between DP103 and NEMO. It is likely to involve the C-terminal region of DP103, given that previous studies had shown numerous interactions between the C-terminus and its target substrates (Charroux et al., 1999; Grundhoff et al., 1999). At the same time, this will shed light into whether DP103 and SENP2 bind to NEMO on the same residue. Put together, knowledge of this interaction provides a potential clinical application to design small molecule inhibitors to competitively block the interactions and hence, inhibit NF-κB transcription.

A long term implication of our findings is the possibility of an effective combinatorial therapeutic intervention using simvastatin (or other drugs to suppress DP103) and a genotoxic agent for the treatment of aggressive triple-negative breast cancers. Simvastatin reduces DP103 expression, which increases the susceptibility of the cancer

cells to genotoxic agents, thus killing the cancer cells. However, more studies will need to be carried out to confirm, validate and test for efficacy and toxicity of such combinatorial therapy. It is worthy to remind that DP103 expressions are low in normal breast tissues and therefore, this can be used as a targeted therapy towards metastatic cancers without possibly causing severe side effects.

We extended our study to other types of cancer and found that downregulation of DP103 also inhibit the invasiveness of cells in prostate cancer cell line PC3 and in colorectal cancer cell line HCT116 (data not shown, included in patent). As such, extrapolation of the role of DP103 into these cancers is worthy be explored further.

In conclusion, we uncover a novel role of DP103 in cancer metastasis and show it to be a co-activator in transcription. At the same time, we reveal DP103 to be critically important in the SUMO modification of NEMO and for the first time, a co-regulator in this pathway. Our findings in this project brings about a plethora of possibilities to further unravel different functions of DP103 in tumorigenesis. On the other hand, the study of its role in hormone-positive breast cancer is also of our interest and is currently underway in our laboratory.

REFERENCES

(2005). Effects of chemotherapy and hormonal therapy for early breast cancer on recurrence and 15-year survival: an overview of the randomised trials. In Lancet, (England), pp. 1687-1717.

Aberg, M., Wickstrom, M., and Siegbahn, A. (2008). Simvastatin induces apoptosis in human breast cancer cells in a NFkappaB-dependent manner and abolishes the anti-apoptotic signaling of TF/FVIIa and TF/FVIIa/FXa. In Thromb Res, (United States), pp. 191-202.

Adamson, R., Logan, M., Kinnaird, J., Langsley, G., and Hall, R. (2000). Loss of matrix metalloproteinase 9 activity in Theileria annulata-attenuated cells is at the transcriptional level and is associated with differentially expressed AP-1 species. In Mol Biochem Parasitol, (Netherlands), pp. 51-61.

Alkuraya, F. S., Saadi, I., Lund, J. J., Turbe-Doan, A., Morton, C. C., and Maas, R. L. (2006). SUMO1 haploinsufficiency leads to cleft lip and palate. In Science, (United States), p. 1751.

Amin, K., Li, J., Chao, W. R., Dewhirst, M. W., and Haroon, Z. A. (2003). Dietary glycine inhibits angiogenesis during wound healing and tumor growth. Cancer Biol Ther *2*, 173-178.

Anderson, W. F., Chen, B. E., Jatoi, I., and Rosenberg, P. S. (2006). Effects of estrogen receptor expression and histopathology on annual hazard rates of death from breast cancer. Breast Cancer Res Treat *100*, 121-126.

Andre, F., Campone, M., O'Regan, R., Manlius, C., Massacesi, C., Sahmoud, T., Mukhopadhyay, P., Soria, J. C., Naughton, M., and Hurvitz, S. A. (2010). Phase I study of everolimus plus weekly paclitaxel and trastuzumab in patients with metastatic breast cancer pretreated with trastuzumab. J Clin Oncol *28*, 5110-5115.

Angst, B. D., Marcozzi, C., and Magee, A. I. (2001). The cadherin superfamily: diversity in form and function. J Cell Sci *114*, 629-641.

Arora, T., Liu, B., He, H., Kim, J., Murphy, T. L., Murphy, K. M., Modlin, R. L., and Shuai, K. (2003). PIASx is a transcriptional co-repressor of signal transducer and activator of transcription 4. J Biol Chem *278*, 21327-21330.

Bailey, D., and O'Hare, P. (2004). Characterization of the localization and proteolytic activity of the SUMO-specific protease, SENP1. In J Biol Chem, (United States), pp. 692-703.

Balk, S. P., and Knudsen, K. E. (2008). AR, the cell cycle, and prostate cancer. Nucl Recept Signal *6*, e001.

Balko, J. M., and Arteaga, C. L. (2011). Dead-box or black-box: is DDX1 a potential biomarker in breast cancer? Breast Cancer Res Treat *127*, 65-67.

Baramova, E. N., Coucke, P., Leprince, P., De Pauw-Gillet, M. C., Bassleer, R., and Foidart, J. M. (1994). Evaluation of matrix metalloproteinases and serine proteases activities in three B16 melanoma cell lines with distinct tumorigenic potential. Anticancer Res *14*, 841-846.

Bates, G. J., Nicol, S. M., Wilson, B. J., Jacobs, A. M., Bourdon, J. C., Wardrop, J., Gregory, D. J., Lane, D. P., Perkins, N. D., and Fuller-Pace, F. V. (2005). The DEAD box protein p68: a novel transcriptional coactivator of the p53 tumour suppressor. In EMBO J, (England), pp. 543-553.

Bauer, K. R., Brown, M., Cress, R. D., Parise, C. A., and Caggiano, V. (2007). Descriptive analysis of estrogen receptor (ER)-negative, progesterone receptor (PR)-negative, and HER2-negative invasive breast cancer, the so-called triple-negative phenotype: a population-based study from the California cancer Registry. Cancer *109*, 1721-1728.

Bayer, P., Arndt, A., Metzger, S., Mahajan, R., Melchior, F., Jaenicke, R., and Becker, J. (1998). Structure determination of the small ubiquitin-related modifier SUMO-1. In J Mol Biol, (England: 1998 Academic Press), pp. 275-286.

Bettermann, K., Benesch, M., Weis, S., and Haybaeck, J. (2011). SUMOylation in carcinogenesis. Cancer Lett *2*, 113-125.

Bischof, O., and Dejean, A. (2007). SUMO is growing senescent. Cell Cycle *6*, 677-681.

Bischof, O., Schwamborn, K., Martin, N., Werner, A., Sustmann, C., Grosschedl, R., and Dejean, A. (2006). The E3 SUMO ligase PIASy is a regulator of cellular senescence and apoptosis. Mol Cell *22*, 783-794.

Biswas, D. K., Cruz, A. P., Gansberger, E., and Pardee, A. B. (2000). Epidermal growth factor-induced nuclear factor kappa B activation: A major pathway of cell-cycle progression in estrogen-receptor negative breast cancer cells. In Proc Natl Acad Sci U S A, (United States), pp. 8542-8547.

Biswas, P., Mantelli, B., Delfanti, F., Cota, M., Vallanti, G., de Filippi, C., Mengozzi, M., Vicenzi, E., Lazzarin, A., and Poli, G. (2001). Tumor necrosis factor-alpha drives HIV-1 replication in U937 cell clones and upregulates CXCR4. Cytokine *13*, 55-59.

Bloom, H. J., and Richardson, W. W. (1957). Histological grading and prognosis in breast cancer; a study of 1409 cases of which 359 have been followed for 15 years. Br J Cancer *11*, 359-377.

Boissan, M., De Wever, O., Lizarraga, F., Wendum, D., Poincloux, R., Chignard, N., Desbois-Mouthon, C., Dufour, S., Nawrocki-Raby, B., Birembaut, P., *et al.* (2010). Implication of metastasis suppressor NM23-H1 in maintaining adherens junctions and limiting the invasive potential of human cancer cells. Cancer Res *70*, 7710-7722.

Bookstein, R., Lee, E. Y., To, H., Young, L. J., Sery, T. W., Hayes, R. C., Friedmann, T., and Lee, W. H. (1988). Human retinoblastoma susceptibility gene: genomic organization and analysis of heterozygous intragenic deletion mutants. Proc Natl Acad Sci U S A *85*, 2210-2214.

Botlagunta, M., Vesuna, F., Mironchik, Y., Raman, A., Lisok, A., Winnard, P., Jr., Mukadam, S., Van Diest, P., Chen, J. H., Farabaugh, P., *et al.* (2008). Oncogenic role of DDX3 in breast cancer biogenesis. In Oncogene, (England), pp. 3912-3922.

Bourboulia, D., and Stetler-Stevenson, W. G. (2010). Matrix metalloproteinases (MMPs) and tissue inhibitors of metalloproteinases (TIMPs): Positive and negative regulators in tumor cell adhesion. Semin Cancer Biol *20*, 161-168.

Bramhall, S. R., Rosemurgy, A., Brown, P. D., Bowry, C., and Buckels, J. A. (2001). Marimastat as first-line therapy for patients with unresectable pancreatic cancer: a randomized trial. J Clin Oncol *19*, 3447-3455.

Brew, K., and Nagase, H. (2010). The tissue inhibitors of metalloproteinases (TIMPs): an ancient family with structural and functional diversity. Biochim Biophys Acta *1803*, 55-71.

Bridges, E., Oon, C. E., and Harris, A. (2011). Notch regulation of tumor angiogenesis. Future Oncol *7*, 569-588.

Bridges, E. M., and Harris, A. L. (2011). The angiogenic process as a therapeutic target in cancer. Biochem Pharmacol *81*, 1183-1191.

Brown, P. D. (2000). Ongoing trials with matrix metalloproteinase inhibitors. Expert Opin Investig Drugs *9*, 2167-2177.

Buitrago, D., Keutgen, X. M., Crowley, M., Filicori, F., Aldailami, H., Hoda, R., Liu, Y. F., Hoda, R. S., Scognamiglio, T., Jin, M., *et al.* (2011). Intercellular Adhesion Molecule-1 (ICAM-1) is Upregulated in Aggressive Papillary Thyroid Carcinoma. Ann Surg Oncol *3*, 973-980.

Byrski, T., Gronwald, J., Huzarski, T., Grzybowska, E., Budryk, M., Stawicka, M., Mierzwa, T., Szwiec, M., Wisniowski, R., Siolek, M., *et al.* (2008). Response to neo-adjuvant chemotherapy in women with BRCA1-positive breast cancers. Breast Cancer Res Treat *108*, 289-296.

Campbell, L., Hunter, K. M., Mohaghegh, P., Tinsley, J. M., Brasch, M. A., and Davies, K. E. (2000). Direct interaction of Smn with dp103, a putative RNA helicase: a role for Smn in transcription regulation? Hum Mol Genet *9*, 1093-1100.

Caretti, G., Schiltz, R. L., Dilworth, F. J., Di Padova, M., Zhao, P., Ogryzko, V., Fuller-Pace, F. V., Hoffman, E. P., Tapscott, S. J., and Sartorelli, V. (2006). The RNA helicases p68/p72 and the noncoding RNA SRA are coregulators of MyoD and skeletal muscle differentiation. Dev Cell *11*, 547-560.

Caruthers, J. M., and McKay, D. B. (2002). Helicase structure and mechanism. In Curr Opin Struct Biol, (England), pp. 123-133.

Causevic, M., Hislop, R. G., Kernohan, N. M., Carey, F. A., Kay, R. A., Steele, R. J., and Fuller-Pace, F. V. (2001). Overexpression and poly-ubiquitylation of the DEAD-box RNA helicase p68 in colorectal tumours. Oncogene *20*, 7734-7743.

Cavallaro, U., and Christofori, G. (2004). Cell adhesion and signalling by cadherins and Ig-CAMs in cancer. Nat Rev Cancer *4*, 118-132.

Chabalier, C., Lamare, C., Racca, C., Privat, M., Valette, A., and Larminat, F. (2006). BRCA1 downregulation leads to premature inactivation of spindle checkpoint and confers paclitaxel resistance. In Cell Cycle, (United States), pp. 1001-1007.

Chao, C. H., Chen, C. M., Cheng, P. L., Shih, J. W., Tsou, A. P., and Lee, Y. H. (2006). DDX3, a DEAD box RNA helicase with tumor growth-suppressive property and transcriptional regulation activity of the p21waf1/cip1 promoter, is a candidate tumor suppressor. In Cancer Res, (United States), pp. 6579-6588.

Charroux, B., Pellizzoni, L., Perkinson, R. A., Shevchenko, A., Mann, M., and Dreyfuss, G. (1999). Gemin3: A novel DEAD box protein that interacts with SMN, the spinal muscular atrophy gene product, and is a component of gems. J Cell Biol *147*, 1181-1194.

Cheng, J., Bawa, T., Lee, P., Gong, L., and Yeh, E. T. (2006). Role of desumoylation in the development of prostate cancer. Neoplasia *8*, 667-676.

Cheng, J., Wang, D., Wang, Z., and Yeh, E. T. (2004). SENP1 enhances androgen receptor-dependent transcription through desumoylation of histone deacetylase 1. Mol Cell Biol *24*, 6021-6028.

Choong, L. Y., Lim, S., Chong, P. K., Wong, C. Y., Shah, N., and Lim, Y. P. (2010). Proteome-wide profiling of the MCF10AT breast cancer progression model. PLoS One *5*, e11030.

Choong, L. Y., Lim, S. K., Chen, Y., Loh, M. C., Toy, W., Wong, C. Y., Salto-Tellez, M., Shah, N., and Lim, Y. P. (2011). Elevated NRD1 metalloprotease expression plays a role in breast cancer growth and proliferation. Genes Chromosomes Cancer *50*, 837-847.

Chou, Y. C., Sheu, J. R., Chung, C. L., Chen, C. Y., Lin, F. L., Hsu, M. J., Kuo, Y. H., and Hsiao, G. (2010). Nuclear-targeted inhibition of NF-kappaB on MMP-9 production by N-2-(4-bromophenyl) ethyl caffeamide in human monocytic cells. In Chem Biol Interact, (Ireland), pp. 403-412.

Christofori, G., and Semb, H. (1999). The role of the cell-adhesion molecule E-cadherin as a tumour-suppressor gene. Trends Biochem Sci *24*, 73-76.

Chung, C. D., Liao, J., Liu, B., Rao, X., Jay, P., Berta, P., and Shuai, K. (1997). Specific inhibition of Stat3 signal transduction by PIAS3. Science *278*, 1803-1805.

Clark, E. L., Coulson, A., Dalgliesh, C., Rajan, P., Nicol, S. M., Fleming, S., Heer, R., Gaughan, L., Leung, H. Y., Elliott, D. J., *et al.* (2008). The RNA helicase p68 is a novel androgen receptor coactivator involved in splicing and is overexpressed in prostate cancer. In Cancer Res, (United States), pp. 7938-7946.

Clendening, J. W., Pandyra, A., Boutros, P. C., El Ghamrasni, S., Khosravi, F., Trentin, G. A., Martirosyan, A., Hakem, A., Hakem, R., Jurisica, I., and Penn, L. Z. (2010). Dysregulation of the mevalonate pathway promotes transformation. In Proc Natl Acad Sci U S A, (United States), pp. 15051-15056.

Cogswell, P. C., Guttridge, D. C., Funkhouser, W. K., and Baldwin, A. S., Jr. (2000). Selective activation of NF-kappa B subunits in human breast cancer: potential roles for NF-kappa B2/p52 and for Bcl-3. Oncogene *19*, 1123-1131.

Collins, L. C., Martyniak, A., Kandel, M. J., Stadler, Z. K., Masciari, S., Miron, A., Richardson, A. L., Schnitt, S. J., and Garber, J. E. (2009). Basal cytokeratin and epidermal growth factor receptor expression are not predictive of BRCA1 mutation status in women with triple-negative breast cancers. Am J Surg Pathol *33*, 1093-1097.

Crawford, P. A., Polish, J. A., Ganpule, G., and Sadovsky, Y. (1997). The activation function-2 hexamer of steroidogenic factor-1 is required, but not sufficient for potentiation by SRC-1. Mol Endocrinol *11*, 1626-1635.

Curran, S., and Murray, G. I. (2000). Matrix metalloproteinases: molecular aspects of their roles in tumour invasion and metastasis. Eur J Cancer *36*, 1621-1630.

D'Amours, D., Desnoyers, S., D'Silva, I., and Poirier, G. G. (1999). Poly(ADP-ribosyl)ation reactions in the regulation of nuclear functions. Biochem J *342 (Pt 2)*, 249-268.

Dalbadie-McFarland, G., and Abelson, J. (1990). PRP5: a helicase-like protein required for mRNA splicing in yeast. Proc Natl Acad Sci U S A *87*, 4236-4240.

Daniel, A. R., Faivre, E. J., and Lange, C. A. (2007). Phosphorylation-dependent antagonism of sumoylation derepresses progesterone receptor action in breast cancer cells. Mol Endocrinol *21*, 2890-2906.

Dawson, P. J., Wolman, S. R., Tait, L., Heppner, G. H., and Miller, F. R. (1996). MCF10AT: a model for the evolution of cancer from proliferative breast disease. Am J Pathol *148*, 313-319.

de la Cruz, J., Kressler, D., and Linder, P. (1999). Unwinding RNA in Saccharomyces cerevisiae: DEAD-box proteins and related families. In Trends Biochem Sci, (England), pp. 192-198.

De Laurentiis, M., Arpino, G., Massarelli, E., Ruggiero, A., Carlomagno, C., Ciardiello, F., Tortora, G., D'Agostino, D., Caputo, F., Cancello, G., *et al.* (2005). A meta-analysis on the interaction between HER-2 expression and response to endocrine treatment in advanced breast cancer. Clin Cancer Res *11*, 4741-4748.

de Murcia, J. M., Niedergang, C., Trucco, C., Ricoul, M., Dutrillaux, B., Mark, M., Oliver, F. J., Masson, M., Dierich, A., LeMeur, M., *et al.* (1997). Requirement of poly(ADP-ribose) polymerase in recovery from DNA damage in mice and in cells. Proc Natl Acad Sci U S A *94*, 7303-7307.

Denoyelle, C., Vasse, M., Korner, M., Mishal, Z., Ganne, F., Vannier, J. P., Soria, J., and Soria, C. (2001). Cerivastatin, an inhibitor of HMG-CoA reductase, inhibits the signaling pathways involved in the invasiveness and metastatic properties of highly invasive breast cancer cell lines: an in vitro study. Carcinogenesis *22*, 1139-1148.

Dent, R., Trudeau, M., Pritchard, K. I., Hanna, W. M., Kahn, H. K., Sawka, C. A., Lickley, L. A., Rawlinson, E., Sun, P., and Narod, S. A. (2007). Triple-negative breast cancer: clinical features and patterns of recurrence. In Clin Cancer Res, (United States), pp. 4429-4434.

Deryugina, E. I., and Quigley, J. P. (2006). Matrix metalloproteinases and tumor metastasis. Cancer Metastasis Rev *25*, 9-34.

Desantis, C., Siegel, R., Bandi, P., and Jemal, A. (2011). Breast cancer statistics, 2011. CA Cancer J Clin *6*, 409-418.

Desterro, J. M., Rodriguez, M. S., Kemp, G. D., and Hay, R. T. (1999). Identification of the enzyme required for activation of the small ubiquitin-like protein SUMO-1. J Biol Chem *274*, 10618-10624.

Di Bacco, A., Ouyang, J., Lee, H. Y., Catic, A., Ploegh, H., and Gill, G. (2006). The SUMO-specific protease SENP5 is required for cell division. In Mol Cell Biol, (United States), pp. 4489-4498.

Dong, J. T., Lamb, P. W., Rinker-Schaeffer, C. W., Vukanovic, J., Ichikawa, T., Isaacs, J. T., and Barrett, J. C. (1995). KAI1, a metastasis suppressor gene for prostate cancer on human chromosome 11p11.2. Science *268*, 884-886.

Dong, J. T., Suzuki, H., Pin, S. S., Bova, G. S., Schalken, J. A., Isaacs, W. B., Barrett, J. C., and Isaacs, J. T. (1996). Down-regulation of the KAI1 metastasis suppressor gene during the progression of human prostatic cancer infrequently involves gene mutation or allelic loss. Cancer Res *56*, 4387-4390.

Dulyaninova, N. G., House, R. P., Betapudi, V., and Bresnick, A. R. (2007). Myosin-IIA heavy-chain phosphorylation regulates the motility of MDA-MB-231 carcinoma cells. Mol Biol Cell *18*, 3144-3155.

Egeblad, M., and Werb, Z. (2002). New functions for the matrix metalloproteinases in cancer progression. Nat Rev Cancer *2*, 161-174.

Endoh, H., Maruyama, K., Masuhiro, Y., Kobayashi, Y., Goto, M., Tai, H., Yanagisawa, J., Metzger, D., Hashimoto, S., and Kato, S. (1999). Purification and identification of p68 RNA helicase acting as a transcriptional coactivator specific for the activation function 1 of human estrogen receptor alpha. Mol Cell Biol *19*, 5363-5372.

Eroles, P., Bosch, A., Alejandro Perez-Fidalgo, J., and Lluch, A. (2012). Molecular biology in breast cancer: Intrinsic subtypes and signaling pathways. Cancer Treat Rev *38*, 698-707.

Fahmy, R. G., Dass, C. R., Sun, L. Q., Chesterman, C. N., and Khachigian, L. M. (2003). Transcription factor Egr-1 supports FGF-dependent angiogenesis during neovascularization and tumor growth. Nat Med *9*, 1026-1032.

Falcone, D. J., McCaffrey, T. A., Haimovitz-Friedman, A., and Garcia, M. (1993). Transforming growth factor-beta 1 stimulates macrophage urokinase expression and release of matrix-bound basic fibroblast growth factor. J Cell Physiol *155*, 595-605.

Farmer, H., McCabe, N., Lord, C. J., Tutt, A. N., Johnson, D. A., Richardson, T. B., Santarosa, M., Dillon, K. J., Hickson, I., Knights, C., *et al.* (2005). Targeting the DNA repair defect in BRCA mutant cells as a therapeutic strategy. In Nature, (England), pp. 917-921.

Feng, W., and Williams, T. (2003). Cloning and characterization of the mouse AP-2 epsilon gene: a novel family member expressed in the developing olfactory bulb. Mol Cell Neurosci *24*, 460-475.

Fett, J. W., Strydom, D. J., Lobb, R. R., Alderman, E. M., Bethune, J. L., Riordan, J. F., and Vallee, B. L. (1985). Isolation and characterization of angiogenin, an angiogenic protein from human carcinoma cells. Biochemistry *24*, 5480-5486.

Findeisen, P., Rockel, M., Nees, M., Roder, C., Kienle, P., Von Knebel Doeberitz, M., Kalthoff, H., and Neumaier, M. (2008). Systematic identification and validation of candidate genes for detection of circulating tumor cells in peripheral blood specimens of colorectal cancer patients. Int J Oncol *33*, 1001-1010.

Folkman, J. (1995). Angiogenesis in cancer, vascular, rheumatoid and other disease. Nat Med *1*, 27-31.

Fry, D. C., Kuby, S. A., and Mildvan, A. S. (1986). ATP-binding site of adenylate kinase: mechanistic implications of its homology with ras-encoded p21, F1-ATPase, and other nucleotide-binding proteins. Proc Natl Acad Sci U S A *83*, 907-911.

Fu, J., Qin, L., He, T., Qin, J., Hong, J., Wong, J., Liao, L., and Xu, J. (2011). The TWIST/Mi2/NuRD protein complex and its essential role in cancer metastasis. Cell Res *21*, 275-289.

Fujita, T., Kobayashi, Y., Wada, O., Tateishi, Y., Kitada, L., Yamamoto, Y., Takashima, H., Murayama, A., Yano, T., Baba, T., *et al.* (2003). Full activation of estrogen receptor alpha activation function-1 induces proliferation of breast cancer cells. In J Biol Chem, (United States), pp. 26704-26714.

Fulford, L. G., Easton, D. F., Reis-Filho, J. S., Sofronis, A., Gillett, C. E., Lakhani, S. R., and Hanby, A. (2006). Specific morphological features predictive for the basal phenotype in grade 3 invasive ductal carcinoma of breast. In Histopathology, (England), pp. 22-34.

Fulford, L. G., Reis-Filho, J. S., Ryder, K., Jones, C., Gillett, C. E., Hanby, A., Easton, D., and Lakhani, S. R. (2007). Basal-like grade III invasive ductal carcinoma of the breast: patterns of metastasis and long-term survival. In Breast Cancer Res, (England), p. R4.

Garbelli, A., Beermann, S., Di Cicco, G., Dietrich, U., and Maga, G. (2011). A motif unique to the human DEAD-box protein DDX3 is important for nucleic acid binding, ATP hydrolysis, RNA/DNA unwinding and HIV-1 replication. In PLoS One, (United States), p. e19810.

Gazzerro, P., Proto, M. C., Gangemi, G., Malfitano, A. M., Ciaglia, E., Pisanti, S., Santoro, A., Laezza, C., and Bifulco, M. (2012). Pharmacological actions of statins: a critical appraisal in the management of cancer. In Pharmacol Rev, (United States), pp. 102-146.

Genestie, C., Zafrani, B., Asselain, B., Fourquet, A., Rozan, S., Validire, P., Vincent-Salomon, A., and Sastre-Garau, X. (1998). Comparison of the prognostic value of Scarff-Bloom-Richardson and Nottingham histological grades in a series of 825 cases of breast cancer: major importance of the mitotic count as a component of both grading systems. Anticancer Res *18*, 571-576.

Germain, D. R., Graham, K., Glubrecht, D. D., Hugh, J. C., Mackey, J. R., and Godbout, R. (2011). DEAD box 1: a novel and independent prognostic marker for early recurrence in breast cancer. Breast Cancer Res Treat *127*, 53-63.

Ghobrial, I. M., McCormick, D. J., Kaufmann, S. H., Leontovich, A. A., Loegering, D. A., Dai, N. T., Krajnik, K. L., Stenson, M. J., Melhem, M. F., Novak, A. J., *et al.* (2005). Proteomic analysis of mantle-cell lymphoma by protein microarray. In Blood, (United States), pp. 3722-3730.

Ghosh, S., and Karin, M. (2002). Missing pieces in the NF-kappaB puzzle. In Cell, (United States), pp. S81-96.

Ghosh-Choudhury, N., Mandal, C. C., and Ghosh Choudhury, G. (2010). Simvastatin induces derepression of PTEN expression via NFkappaB to inhibit breast cancer cell growth. In Cell Signal, (England: Published by Elsevier Inc.), pp. 749-758.

Gibson, L., Lawrence, D., Dawson, C., and Bliss, J. (2009). Aromatase inhibitors for treatment of advanced breast cancer in postmenopausal women. Cochrane Database Syst Rev, CD003370.

Gillian, A. L., and Svaren, J. (2004). The Ddx20/DP103 dead box protein represses transcriptional activation by Egr2/Krox-20. J Biol Chem *279*, 9056-9063.

Girdwood, D., Bumpass, D., Vaughan, O. A., Thain, A., Anderson, L. A., Snowden, A. W., Garcia-Wilson, E., Perkins, N. D., and Hay, R. T. (2003). P300 transcriptional repression is mediated by SUMO modification. In Mol Cell, (United States), pp. 1043-1054.

Godbout, R., Packer, M., and Bie, W. (1998). Overexpression of a DEAD box protein (DDX1) in neuroblastoma and retinoblastoma cell lines. J Biol Chem *273*, 21161-21168.

Gong, Y. L., Xu, G. M., Huang, W. D., and Chen, L. B. (2000). Expression of matrix metalloproteinases and the tissue inhibitors of metalloproteinases and their local invasiveness and metastasis in Chinese human pancreatic cancer. J Surg Oncol *73*, 95-99.

Gospodarowicz, D. (1976). Humoral control of cell proliferation: the role of fibroblast growth factor in regeneration, angiogenesis, wound healing, and neoplastic growth. Prog Clin Biol Res *9*, 1-19.

Gostissa, M., Hengstermann, A., Fogal, V., Sandy, P., Schwarz, S. E., Scheffner, M., and Del Sal, G. (1999). Activation of p53 by conjugation to the ubiquitin-like protein SUMO-1. EMBO J *18*, 6462-6471.

Gown, A. M. (2008). Current issues in ER and HER2 testing by IHC in breast cancer. Mod Pathol *21 Suppl 2*, S8-S15.

Gradishar, W. J. (2010). Adjuvant endocrine therapy for early breast cancer: the story so far. Cancer Invest *28*, 433-442.

Grossmann, J. (2002). Molecular mechanisms of "detachment-induced apoptosis--Anoikis". Apoptosis *7*, 247-260.

Grundhoff, A. T., Kremmer, E., Tureci, O., Glieden, A., Gindorf, C., Atz, J., Mueller-Lantzsch, N., Schubach, W. H., and Grasser, F. A. (1999). Characterization of DP103, a novel DEAD box protein that binds to the Epstein-Barr virus nuclear proteins EBNA2 and EBNA3C. J Biol Chem *274*, 19136-19144.

Guirguis, R., Margulies, I., Taraboletti, G., Schiffmann, E., and Liotta, L. (1987). Cytokine-induced pseudopodial protrusion is coupled to tumour cell migration. Nature *329*, 261-263.

Guo, D., Li, M., Zhang, Y., Yang, P., Eckenrode, S., Hopkins, D., Zheng, W., Purohit, S., Podolsky, R. H., Muir, A., *et al.* (2004). A functional variant of SUMO4, a new I kappa B alpha modifier, is associated with type 1 diabetes. In Nat Genet, (United States), pp. 837-841.

Guo, P., Coban, O., Snead, N. M., Trebley, J., Hoeprich, S., Guo, S., and Shu, Y. (2010). Engineering RNA for targeted siRNA delivery and medical application. Adv Drug Deliv Rev *62*, 650-666.

Haffty, B. G., Yang, Q., Reiss, M., Kearney, T., Higgins, S. A., Weidhaas, J., Harris, L., Hait, W., and Toppmeyer, D. (2006). Locoregional relapse and distant metastasis in conservatively managed triple negative early-stage breast cancer. In J Clin Oncol, (United States), pp. 5652-5657.

Halmosi, R., Berente, Z., Osz, E., Toth, K., Literati-Nagy, P., and Sumegi, B. (2001). Effect of poly(ADP-ribose) polymerase inhibitors on the ischemia-reperfusion-induced oxidative cell damage and mitochondrial metabolism in Langendorff heart perfusion system. Mol Pharmacol *59*, 1497-1505.

Hanahan, D., and Weinberg, R. A. (2011). Hallmarks of cancer: the next generation. In Cell, (United States: 2011 Elsevier Inc), pp. 646-674.

Hanemaaijer, R., Verheijen, J. H., Maguire, T. M., Visser, H., Toet, K., McDermott, E., O'Higgins, N., and Duffy, M. J. (2000). Increased gelatinase-A and gelatinase-B activities in malignant vs. benign breast tumors. In Int J Cancer, (United States: 2000 Wiley-Liss, Inc.), pp. 204-207.

Hardeland, U., Steinacher, R., Jiricny, J., and Schar, P. (2002). Modification of the human thymine-DNA glycosylase by ubiquitin-like proteins facilitates enzymatic turnover. EMBO J *21*, 1456-1464.

Hasan, W., Chu, K., Gullapalli, A., Dunn, S. S., Enlow, E. M., Luft, J. C., Tian, S., Napier, M. E., Pohlhaus, P. D., Rolland, J. P., and Desimone, J. M. (2011). Delivery of Multiple siRNAs Using Lipid-Coated PLGA Nanoparticles for Treatment of Prostate Cancer. Nano Lett *1*,287-292.

Hay, R. T. (2005). SUMO: a history of modification. In Mol Cell, (United States), pp. 1-12.

Hayden, M. S., and Ghosh, S. (2004). Signaling to NF-kappaB. In Genes Dev, (United States), pp. 2195-2224.

Helbig, G., Christopherson, K. W., 2nd, Bhat-Nakshatri, P., Kumar, S., Kishimoto, H., Miller, K. D., Broxmeyer, H. E., and Nakshatri, H. (2003). NF-kappaB promotes breast cancer cell migration and metastasis by inducing the expression of the chemokine receptor CXCR4. In J Biol Chem, (United States), pp. 21631-21638.

Hirata, F., Thibodeau, L. M., and Hirata, A. Ubiquitination and SUMOylation of annexin A1 and helicase activity. Biochim Biophys Acta 2010 Sep;1800(9):899-905 Epub 2010 Mar 30.

Hoffmann, A., and Baltimore, D. (2006). Circuitry of nuclear factor kappaB signaling. In Immunol Rev, (Denmark), pp. 171-186.

Huang, T. T., Wuerzberger-Davis, S. M., Wu, Z. H., and Miyamoto, S. (2003). Sequential modification of NEMO/IKKgamma by SUMO-1 and ubiquitin mediates NF-kappaB activation by genotoxic stress. In Cell, (United States), pp. 565-576.

Huang, W. S., Chin, C. C., Chen, C. N., Kuo, Y. H., Chen, T. C., Yu, H. R., Tung, S. Y., Shen, C. H., Hsieh, Y. Y., Guo, S. E., *et al.* (2011). Stromal cell-derived factor-1/CXC receptor 4 and b1 integrin interaction regulates urokinase-type plasminogen activator expression in human colorectal cancer cells. J Cell Physiol *3*,1114-1122.

Hurst, D. R., Xie, Y., Edmonds, M. D., and Welch, D. R. (2009). Multiple forms of BRMS1 are differentially expressed in the MCF10 isogenic breast cancer progression model. Clin Exp Metastasis *26*, 89-96.

Irizarry, R. A., Bolstad, B. M., Collin, F., Cope, L. M., Hobbs, B., and Speed, T. P. (2003). Summaries of Affymetrix GeneChip probe level data. Nucleic Acids Res *31*, e15.

Ishaq, M., Ma, L., Wu, X., Mu, Y., Pan, J., Hu, J., Hu, T., Fu, Q., and Guo, D. (2009). The DEAD-box RNA helicase DDX1 interacts with RelA and enhances nuclear factor kappaB-mediated transcription. J Cell Biochem *106*, 296-305.

Ishikawa, F., Miyazono, K., Hellman, U., Drexler, H., Wernstedt, C., Hagiwara, K., Usuki, K., Takaku, F., Risau, W., and Heldin, C. H. (1989). Identification of angiogenic

activity and the cloning and expression of platelet-derived endothelial cell growth factor. Nature *338*, 557-562.

Jamieson, D. J., Rahe, B., Pringle, J., and Beggs, J. D. (1991). A suppressor of a yeast splicing mutation (prp8-1) encodes a putative ATP-dependent RNA helicase. Nature *349*, 715-717.

Jang, H. D., Yoon, K., Shin, Y. J., Kim, J., and Lee, S. Y. (2004). PIAS3 suppresses NF-kappaB-mediated transcription by interacting with the p65/RelA subunit. J Biol Chem *279*, 24873-24880.

Jankowsky, E., and Jankowsky, A. (2000). The DExH/D protein family database. Nucleic Acids Res *28*, 333-334.

Jara-Lazaro, A. R., Thilagaratnam, S., and Tan, P. H. (2010). Breast cancer in Singapore: some perspectives. Breast Cancer *17*, 23-28.

Jinga, D. C., Blidaru, A., Condrea, I., Ardeleanu, C., Dragomir, C., Szegli, G., Stefanescu, M., and Matache, C. (2006). MMP-9 and MMP-2 gelatinases and TIMP-1 and TIMP-2 inhibitors in breast cancer: correlations with prognostic factors. In J Cell Mol Med, pp. 499-510.

Johnson, J. P. (1999). Cell adhesion molecules in the development and progression of malignant melanoma. Cancer Metastasis Rev *18*, 345-357.

Kaminska, B., Pyrzynska, B., Ciechomska, I., and Wisniewska, M. (2000). Modulation of the composition of AP-1 complex and its impact on transcriptional activity. Acta Neurobiol Exp (Wars) *60*, 395-402.

Kang, J. S., Saunier, E. F., Akhurst, R. J., and Derynck, R. (2008). The type I TGF-beta receptor is covalently modified and regulated by sumoylation. Nat Cell Biol *10*, 654-664.

Kang, S., Kim, E. S., and Moon, A. (2009). Simvastatin and lovastatin inhibit breast cell invasion induced by H-Ras. Oncol Rep *21*, 1317-1322.

Karin, M. (2006). Nuclear factor-kappaB in cancer development and progression. In Nature, (England), pp. 431-436.

Katanaev, V. L. (2010). The Wnt/Frizzled GPCR signaling pathway. Biochemistry (Mosc) *75*, 1428-1434.

Kaufman, B., Mackey, J. R., Clemens, M. R., Bapsy, P. P., Vaid, A., Wardley, A., Tjulandin, S., Jahn, M., Lehle, M., Feyereislova, A., *et al.* (2009). Trastuzumab plus anastrozole versus anastrozole alone for the treatment of postmenopausal women with human epidermal growth factor receptor 2-positive, hormone receptor-positive metastatic

breast cancer: results from the randomized phase III TAnDEM study. J Clin Oncol *27*, 5529-5537.

Kessler, J. D., Kahle, K. T., Sun, T., Meerbrey, K. L., Schlabach, M. R., Schmitt, E. M., Skinner, S. O., Xu, Q., Li, M. Z., Hartman, Z. C., *et al.* (2011). A SUMOylation-Dependent Transcriptional Subprogram Is Required for Myc-Driven Tumorigenesis. Science *335*,348-353.

Kim, D. W., Sovak, M. A., Zanieski, G., Nonet, G., Romieu-Mourez, R., Lau, A. W., Hafer, L. J., Yaswen, P., Stampfer, M., Rogers, A. E., *et al.* (2000). Activation of NF-kappaB/Rel occurs early during neoplastic transformation of mammary cells. Carcinogenesis *21*, 871-879.

Kim, H. J., Park, C. I., Park, B. W., Lee, H. D., and Jung, W. H. (2006a). Expression of MT-1 MMP, MMP2, MMP9 and TIMP2 mRNAs in ductal carcinoma in situ and invasive ductal carcinoma of the breast. Yonsei Med J *47*, 333-342.

Kim, H. P., Yoon, Y. K., Kim, J. W., Han, S. W., Hur, H. S., Park, J., Lee, J. H., Oh, D. Y., Im, S. A., Bang, Y. J., and Kim, T. Y. (2009). Lapatinib, a dual EGFR and HER2 tyrosine kinase inhibitor, downregulates thymidylate synthase by inhibiting the nuclear translocation of EGFR and HER2. PLoS One *4*, e5933.

Kim, J. H., Choi, H. J., Kim, B., Kim, M. H., Lee, J. M., Kim, I. S., Lee, M. H., Choi, S. J., Kim, K. I., Kim, S. I., *et al.* (2006b). Roles of sumoylation of a reptin chromatin-remodelling complex in cancer metastasis. Nat Cell Biol *8*, 631-639.

Kim, J. H., Kim, B., Cai, L., Choi, H. J., Ohgi, K. A., Tran, C., Chen, C., Chung, C. H., Huber, O., Rose, D. W., *et al.* (2005). Transcriptional regulation of a metastasis suppressor gene by Tip60 and beta-catenin complexes. Nature *434*, 921-926.

Kim, J. L., Morgenstern, K. A., Griffith, J. P., Dwyer, M. D., Thomson, J. A., Murcko, M. A., Lin, C., and Caron, P. R. (1998). Hepatitis C virus NS3 RNA helicase domain with a bound oligonucleotide: the crystal structure provides insights into the mode of unwinding. Structure *6*, 89-100.

Klappacher, G. W., Lunyak, V. V., Sykes, D. B., Sawka-Verhelle, D., Sage, J., Brard, G., Ngo, S. D., Gangadharan, D., Jacks, T., Kamps, M. P., *et al.* (2002). An induced Ets repressor complex regulates growth arrest during terminal macrophage differentiation. Cell *109*, 169-180.

Klein, T., and Bischoff, R. (2011). Physiology and pathophysiology of matrix metalloproteases. Amino Acids *41*, 271-290.

Korolev, S., Yao, N., Lohman, T. M., Weber, P. C., and Waksman, G. (1998). Comparisons between the structures of HCV and Rep helicases reveal structural similarities between SF1 and SF2 super-families of helicases. Protein Sci *7*, 605-610.

Kortmann, U., McAlpine, J. N., Xue, H., Guan, J., Ha, G., Tully, S., Shafait, S., Lau, A., Cranston, A. N., O'Connor, M. J., *et al.* (2011). Tumor growth inhibition by olaparib in BRCA2 germline-mutated patient-derived ovarian cancer tissue xenografts. Clin Cancer Res *17*, 783-791.

Kundu, A. K., Chandra, P. K., Hazari, S., Ledet, G., Pramar, Y. V., Dash, S., and Mandal, T. K. (2011). Stability of lyophilized siRNA nanosome formulations. Int J Pharm *2*,525-534.

Kuo, H. Y., Chang, C. C., Jeng, J. C., Hu, H. M., Lin, D. Y., Maul, G. G., Kwok, R. P., and Shih, H. M. (2005). SUMO modification negatively modulates the transcriptional activity of CREB-binding protein via the recruitment of Daxx. In Proc Natl Acad Sci U S A, (United States), pp. 16973-16978.

Kwong, A., Mang, O. W., Wong, C. H., Chau, W. W., Law, S. C., and Hong Kong Breast Cancer Research, G. (2011). Breast cancer in Hong Kong, Southern China: the first population-based analysis of epidemiological characteristics, stage-specific, cancer-specific, and disease-free survival in breast cancer patients: 1997-2001. Ann Surg Oncol *18*, 3072-3078.

Lauffenburger, D. A., and Horwitz, A. F. (1996). Cell migration: a physically integrated molecular process. In Cell, (United States), pp. 359-369.

Lee, K., Pisarska, M. D., Ko, J. J., Kang, Y., Yoon, S., Ryou, S. M., Cha, K. Y., and Bae, J. (2005a). Transcriptional factor FOXL2 interacts with DP103 and induces apoptosis. Biochem Biophys Res Commun *336*, 876-881.

Lee, K. H., Choi, E. Y., Kim, M. K., Hyun, M. S., Jang, B. I., Kim, T. N., Kim, S. W., Song, S. K., Kim, J. H., and Kim, J. R. (2006). Regulation of hepatocyte growth factor-mediated urokinase plasminogen activator secretion by MEK/ERK activation in human stomach cancer cell lines. Exp Mol Med *38*, 27-35.

Lee, M. B., Lebedeva, L. A., Suzawa, M., Wadekar, S. A., Desclozeaux, M., and Ingraham, H. A. (2005b). The DEAD-box protein DP103 (Ddx20 or Gemin-3) represses orphan nuclear receptor activity via SUMO modification. In Mol Cell Biol, (United States), pp. 1879-1890.

Lee, M. H., Mabb, A. M., Gill, G. B., Yeh, E. T., and Miyamoto, S. (2011). NF-kappaB Induction of the SUMO Protease SENP2: A Negative Feedback Loop to Attenuate Cell Survival Response to Genotoxic Stress. Mol Cell *43*, 180-191.

Leivonen, S. K., and Kahari, V. M. (2007). Transforming growth factor-beta signaling in cancer invasion and metastasis. Int J Cancer *121*, 2119-2124.

Levi, E., Fridman, R., Miao, H. Q., Ma, Y. S., Yayon, A., and Vlodavsky, I. (1996). Matrix metalloproteinase 2 releases active soluble ectodomain of fibroblast growth factor receptor 1. Proc Natl Acad Sci U S A *93*, 7069-7074.

Levy, A. T., Cioce, V., Sobel, M. E., Garbisa, S., Grigioni, W. F., Liotta, L. A., and Stetler-Stevenson, W. G. (1991). Increased expression of the Mr 72,000 type IV collagenase in human colonic adenocarcinoma. Cancer Res *51*, 439-444.

Lewis Phillips, G. D., Li, G., Dugger, D. L., Crocker, L. M., Parsons, K. L., Mai, E., Blattler, W. A., Lambert, J. M., Chari, R. V., Lutz, R. J., *et al.* (2008). Targeting HER2-positive breast cancer with trastuzumab-DM1, an antibody-cytotoxic drug conjugate. Cancer Res *68*, 9280-9290.

Li, H. C., Cao, D. C., Liu, Y., Hou, Y. F., Wu, J., Lu, J. S., Di, G. H., Liu, G., Li, F. M., Ou, Z. L., *et al.* (2004). Prognostic value of matrix metalloproteinases (MMP-2 and MMP-9) in patients with lymph node-negative breast carcinoma. In Breast Cancer Res Treat, (Netherlands), pp. 75-85.

Li, N., Banin, S., Ouyang, H., Li, G. C., Courtois, G., Shiloh, Y., Karin, M., and Rotman, G. (2001). ATM is required for IkappaB kinase (IKKk) activation in response to DNA double strand breaks. In J Biol Chem, (United States), pp. 8898-8903.

Li, S. J., and Hochstrasser, M. (1999). A new protease required for cell-cycle progression in yeast. Nature *398*, 246-251.

Li, S. J., and Hochstrasser, M. (2000). The yeast ULP2 (SMT4) gene encodes a novel protease specific for the ubiquitin-like Smt3 protein. Mol Cell Biol *20*, 2367-2377.

Li, Y., and Brown, P. H. (2009). Prevention of ER-negative breast cancer. Recent Results Cancer Res *181*, 121-134.

Li, Y., Vandenboom, T. G., 2nd, Wang, Z., Kong, D., Ali, S., Philip, P. A., and Sarkar, F. H. (2010). miR-146a suppresses invasion of pancreatic cancer cells. Cancer Res *70*, 1486-1495.

Liedtke, C., Mazouni, C., Hess, K. R., Andre, F., Tordai, A., Mejia, J. A., Symmans, W. F., Gonzalez-Angulo, A. M., Hennessy, B., Green, M., *et al.* (2008). Response to neoadjuvant therapy and long-term survival in patients with triple-negative breast cancer. In J Clin Oncol, (United States), pp. 1275-1281.

Liggett, S. B. (2011). Phosphorylation barcoding as a mechanism of directing GPCR signaling. Sci Signal *4*, pe36.

Linder, P. (2003). Yeast RNA helicases of the DEAD-box family involved in translation initiation. In Biol Cell, (France), pp. 157-167.

Linder, P. (2006). Dead-box proteins: a family affair--active and passive players in RNP-remodeling. Nucleic Acids Res *34*, 4168-4180.

Linder, P., and Slonimski, P. P. (1989). An essential yeast protein, encoded by duplicated genes TIF1 and TIF2 and homologous to the mammalian translation initiation factor eIF-4A, can suppress a mitochondrial missense mutation. Proc Natl Acad Sci U S A *86*, 2286-2290.

Lip, P. L., Blann, A. D., Hope-Ross, M., Gibson, J. M., and Lip, G. Y. (2001). Age-related macular degeneration is associated with increased vascular endothelial growth factor, hemorheology and endothelial dysfunction. In Ophthalmology, (United States), pp. 705-710.

Lipton, A., Ali, S. M., Leitzel, K., Demers, L., Chinchilli, V., Engle, L., Harvey, H. A., Brady, C., Nalin, C. M., Dugan, M., *et al.* (2002). Elevated serum Her-2/neu level predicts decreased response to hormone therapy in metastatic breast cancer. J Clin Oncol *20*, 1467-1472.

Lisanti, M. P., Martinez-Outschoorn, U. E., Chiavarina, B., Pavlides, S., Whitaker-Menezes, D., Tsirigos, A., Witkiewicz, A., Lin, Z., Balliet, R., Howell, A., and Sotgia, F. (2010). Understanding the "lethal" drivers of tumor-stroma co-evolution: emerging role(s) for hypoxia, oxidative stress and autophagy/mitophagy in the tumor micro-environment. Cancer Biol Ther *10*, 537-542.

Liu, B., Liao, J., Rao, X., Kushner, S. A., Chung, C. D., Chang, D. D., and Shuai, K. (1998). Inhibition of Stat1-mediated gene activation by PIAS1. Proc Natl Acad Sci U S A *95*, 10626-10631.

Liu, B., Yang, R., Wong, K. A., Getman, C., Stein, N., Teitell, M. A., Cheng, G., Wu, H., and Shuai, K. (2005). Negative regulation of NF-kappaB signaling by PIAS1. In Mol Cell Biol, (United States), pp. 1113-1123.

Liu, Q., Fischer, U., Wang, F., and Dreyfuss, G. (1997). The spinal muscular atrophy disease gene product, SMN, and its associated protein SIP1 are in a complex with spliceosomal snRNP proteins. In Cell, (United States), pp. 1013-1021.

Liu, W. M., and Zhang, X. A. (2006). KAI1/CD82, a tumor metastasis suppressor. Cancer Lett *240*, 183-194.

Liu, Z., Li, L., Yang, Z., Luo, W., Li, X., Yang, H., Yao, K., Wu, B., and Fang, W. (2010). Increased expression of MMP9 is correlated with poor prognosis of nasopharyngeal carcinoma. In BMC Cancer, (England), p. 270.

Liu, Z. Q., Liu, B., Yu, L., Wang, X. Q., Wang, J., and Liu, H. M. (2011). Simvastatin has beneficial effect on pulmonary artery hypertension by inhibiting NF-kappaB expression. Mol Cell Biochem *354*, 77-82.

Livasy, C. A., Karaca, G., Nanda, R., Tretiakova, M. S., Olopade, O. I., Moore, D. T., and Perou, C. M. (2006). Phenotypic evaluation of the basal-like subtype of invasive breast carcinoma. In Mod Pathol, (United States), pp. 264-271.

Lukiw, W. J., Pelaez, R. P., Martinez, J., and Bazan, N. G. (1998). Budesonide epimer R or dexamethasone selectively inhibit platelet-activating factor-induced or interleukin 1beta-induced DNA binding activity of cis-acting transcription factors and cyclooxygenase-2 gene expression in human epidermal keratinocytes. Proc Natl Acad Sci U S A *95*, 3914-3919.

Luo, X., Ikeda, Y., and Parker, K. L. (1994). A cell-specific nuclear receptor is essential for adrenal and gonadal development and sexual differentiation. In Cell, (United States), pp. 481-490.

Mabb, A. M., Wuerzberger-Davis, S. M., and Miyamoto, S. (2006). PIASy mediates NEMO sumoylation and NF-kappaB activation in response to genotoxic stress. In Nat Cell Biol, (England), pp. 986-993.

Mahoney, M. G., Simpson, A., Jost, M., Noe, M., Kari, C., Pepe, D., Choi, Y. W., Uitto, J., and Rodeck, U. (2002). Metastasis-associated protein (MTA)1 enhances migration, invasion, and anchorage-independent survival of immortalized human keratinocytes. Oncogene *21*, 2161-2170.

Malik, S., Sharma, A. K., Bharti, S., Nepal, S., Bhatia, J., Nag, T. C., Narang, R., and Arya, D. S. (2011). In vivo cardioprotection by pitavastatin from ischemic-reperfusion injury through suppression of IKK/NF-kappaB and upregulation of pAkt-e-NOS. J Cardiovasc Pharmacol *58*, 199-206.

Mandal, C. C., Ghosh-Choudhury, N., Yoneda, T., and Choudhury, G. G. (2011). Simvastatin prevents skeletal metastasis of breast cancer by an antagonistic interplay between p53 and CD44. In J Biol Chem, (United States), pp. 11314-11327.

Mannello, F., and Tonti, G. A. (2009). Statins and breast cancer: may matrix metalloproteinase be the missing link. In Cancer Invest, (United States), pp. 466-470.

Margheri, F., D'Alessio, S., Serrati, S., Pucci, M., Annunziato, F., Cosmi, L., Liotta, F., Angeli, R., Angelucci, A., Gravina, G. L., *et al.* (2005). Effects of blocking urokinase receptor signaling by antisense oligonucleotides in a mouse model of experimental prostate cancer bone metastases. Gene Ther *12*, 702-714.

Marzook, H., Li, D. Q., Nair, V. S., Mudvari, P., Reddy, S. D., Pakala, S. B., Santhoshkumar, T. R., Pillai, M. R., and Kumar, R. (2011). Metastasis-associated protein 1 drives tumor cell migration and invasion through transcriptional repression of RING finger protein 144A. J Biol Chem *8*,5615-5626.

Mathew, J., and Perez, E. A. (2011). Trastuzumab emtansine in human epidermal growth factor receptor 2-positive breast cancer: a review. Curr Opin Oncol *23*, 594-600.

Mauro, C., Leow, S. C., Anso, E., Rocha, S., Thotakura, A. K., Tornatore, L., Moretti, M., De Smaele, E., Beg, A. A., Tergaonkar, V., *et al.* (2011). NF-kappaB controls energy homeostasis and metabolic adaptation by upregulating mitochondrial respiration. Nature cell biology *13*, 1272-1279.

Menge, T., Hartung, H. P., and Stuve, O. (2005). Statins--a cure-all for the brain? Nat Rev Neurosci *6*, 325-331.

Meyer, T., and Hart, I. R. (1998). Mechanisms of tumour metastasis. Eur J Cancer *34*, 214-221.

Milde-Langosch, K., Roder, H., Andritzky, B., Aslan, B., Hemminger, G., Brinkmann, A., Bamberger, C. M., Loning, T., and Bamberger, A. M. (2004). The role of the AP-1 transcription factors c-Fos, FosB, Fra-1 and Fra-2 in the invasion process of mammary carcinomas. In Breast Cancer Res Treat, (Netherlands: 2004 Kluwer Academic Publishers), pp. 139-152.

Miller, L. D., Coffman, L. G., Chou, J. W., Black, M. A., Bergh, J., D'Agostino, R., Jr., Torti, S. V., and Torti, F. M. (2011). An iron regulatory gene signature predicts outcome in breast cancer. Cancer Res *71*, 6728-6737.

Mitra, R. S., Goto, M., Lee, J. S., Maldonado, D., Taylor, J. M., Pan, Q., Carey, T. E., Bradford, C. R., Prince, M. E., Cordell, K. G., *et al.* (2008). Rap1GAP promotes invasion via induction of matrix metalloproteinase 9 secretion, which is associated with poor survival in low N-stage squamous cell carcinoma. In Cancer Res, (United States), pp. 3959-3969.

Miyake, K., and McNeil, P. L. (2003). Mechanical injury and repair of cells. Crit Care Med *31*, S496-501.

Monteagudo, C., Merino, M. J., San-Juan, J., Liotta, L. A., and Stetler-Stevenson, W. G. (1990). Immunohistochemical distribution of type IV collagenase in normal, benign, and malignant breast tissue. Am J Pathol *136*, 585-592.

Moore, H. C., Jordan, L. B., Bray, S. E., Baker, L., Quinlan, P. R., Purdie, C. A., Thompson, A. M., Bourdon, J. C., and Fuller-Pace, F. V. (2010). The RNA helicase p68 modulates expression and function of the Delta133 isoform(s) of p53, and is inversely associated with Delta133p53 expression in breast cancer. In Oncogene, (England), pp. 6475-6484.

Moore, M. J., Hamm, J., Dancey, J., Eisenberg, P. D., Dagenais, M., Fields, A., Hagan, K., Greenberg, B., Colwell, B., Zee, B., *et al.* (2003). Comparison of gemcitabine versus the matrix metalloproteinase inhibitor BAY 12-9566 in patients with advanced or

metastatic adenocarcinoma of the pancreas: a phase III trial of the National Cancer Institute of Canada Clinical Trials Group. J Clin Oncol *21*, 3296-3302.

Mouillet, J. F., Yan, X., Ou, Q., Jin, L., Muglia, L. J., Crawford, P. A., and Sadovsky, Y. (2008). DEAD-box protein-103 (DP103, Ddx20) is essential for early embryonic development and modulates ovarian morphology and function. Endocrinology *149*, 2168-2175.

Muller, S., Berger, M., Lehembre, F., Seeler, J. S., Haupt, Y., and Dejean, A. (2000). c-Jun and p53 activity is modulated by SUMO-1 modification. J Biol Chem *275*, 13321-13329.

Murata, T., Ishibashi, T., Khalil, A., Hata, Y., Yoshikawa, H., and Inomata, H. (1995). Vascular endothelial growth factor plays a role in hyperpermeability of diabetic retinal vessels. Ophthalmic Res *27*, 48-52.

Nagahara, A., Nakayama, M., Oka, D., Tsuchiya, M., Kawashima, A., Mukai, M., Nakai, Y., Takayama, H., Nishimura, K., Jo, Y., *et al.* (2010). SERPINE2 is a possible candidate promotor for lymph node metastasis in testicular cancer. Biochem Biophys Res Commun *391*, 1641-1646.

Nair, R. R., Avila, H., Ma, X., Wang, Z., Lennartz, M., Darnay, B. G., Boyd, D. D., and Yan, C. (2008). A novel high-throughput screening system identifies a small molecule repressive for matrix metalloproteinase-9 expression. In Mol Pharmacol, (United States), pp. 919-929.

Nakshatri, H., Bhat-Nakshatri, P., Martin, D. A., Goulet, R. J., Jr., and Sledge, G. W., Jr. (1997). Constitutive activation of NF-kappaB during progression of breast cancer to hormone-independent growth. Mol Cell Biol *17*, 3629-3639.

Nathan, B. (2008). RNAi technologies: a screen whose time has arrived. Nature Methods *5*, 361-368.

Nicol, S. M., and Fuller-Pace, F. V. (1995). The "DEAD box" protein DbpA interacts specifically with the peptidyltransferase center in 23S rRNA. Proc Natl Acad Sci U S A *92*, 11681-11685.

Nikkola, J., Vihinen, P., Vuoristo, M. S., Kellokumpu-Lehtinen, P., Kahari, V. M., and Pyrhonen, S. (2005). High serum levels of matrix metalloproteinase-9 and matrix metalloproteinase-1 are associated with rapid progression in patients with metastatic melanoma. In Clin Cancer Res, (United States), pp. 5158-5166.

Nimesh, S., Gupta, N., and Chandra, R. (2011). Cationic polymer based nanocarriers for delivery of therapeutic nucleic acids. J Biomed Nanotechnol *7*, 504-520.

Nishi, K., Morel-Deville, F., Hershey, J. W., Leighton, T., and Schnier, J. (1988). An eIF-4A-like protein is a suppressor of an Escherichia coli mutant defective in 50S ribosomal subunit assembly. Nature *336*, 496-498.

O'Shaughnessy, J., Osborne, C., Pippen, J. E., Yoffe, M., Patt, D., Rocha, C., Koo, I. C., Sherman, B. M., and Bradley, C. (2011). Iniparib plus chemotherapy in metastatic triple-negative breast cancer. N Engl J Med *364*, 205-214.

Okuma, T., Honda, R., Ichikawa, G., Tsumagari, N., and Yasuda, H. (1999). In vitro SUMO-1 modification requires two enzymatic steps, E1 and E2. In Biochem Biophys Res Commun, (United States: 1999 Academic Press.), pp. 693-698.

Ou, Q., Mouillet, J. F., Yan, X., Dorn, C., Crawford, P. A., and Sadovsky, Y. (2001). The DEAD box protein DP103 is a regulator of steroidogenic factor-1. Mol Endocrinol *15*, 69-79.

Overall, C. M., and Lopez-Otin, C. (2002). Strategies for MMP inhibition in cancer: innovations for the post-trial era. In Nat Rev Cancer, (England), pp. 657-672.

Owerbach, D., McKay, E. M., Yeh, E. T., Gabbay, K. H., and Bohren, K. M. (2005). A proline-90 residue unique to SUMO-4 prevents maturation and sumoylation. In Biochem Biophys Res Commun, (United States), pp. 517-520.

Pahl, H. L. (1999). Activators and target genes of Rel/NF-kappaB transcription factors. Oncogene *18*, 6853-6866.

Pandey, V., Jung, Y., Kang, J., Steiner, M., Qian, P. X., Banerjee, A., Mitchell, M. D., Wu, Z. S., Zhu, T., Liu, D. X., and Lobie, P. E. (2010). Artemin Reduces Sensitivity to Doxorubicin and Paclitaxel in Endometrial Carcinoma Cells through Specific Regulation of CD24. Transl Oncol *3*, 218-229.

Patel, N. M., Nozaki, S., Shortle, N. H., Bhat-Nakshatri, P., Newton, T. R., Rice, S., Gelfanov, V., Boswell, S. H., Goulet, R. J., Jr., Sledge, G. W., Jr., and Nakshatri, H. (2000). Paclitaxel sensitivity of breast cancer cells with constitutively active NF-kappaB is enhanced by IkappaBalpha super-repressor and parthenolide. Oncogene *19*, 4159-4169.

Perl, A. K., Wilgenbus, P., Dahl, U., Semb, H., and Christofori, G. (1998). A causal role for E-cadherin in the transition from adenoma to carcinoma. Nature *392*, 190-193.

Pirollo, K. F., and Chang, E. H. (2008). Targeted delivery of small interfering RNA: approaching effective cancer therapies. Cancer Res *68*, 1247-1250.

Polanski, R., Maguire, M., Nield, P. C., Jenkins, R. E., Park, B. K., Krawczynska, K., Devling, T., Ray-Sinha, A., Rubbi, C. P., Vlatkovic, N., and Boyd, M. T. (2011). MDM2 interacts with NME2 (non-metastatic cells 2, protein) and suppresses the ability of NME2 to negatively regulate cell motility. Carcinogenesis *32*, 1133-1142.

Pot, I., and Bonni, S. (2008). SnoN in TGF-beta signaling and cancer biology. Curr Mol Med *8*, 319-328.

Potts, P. R., and Yu, H. (2007). The SMC5/6 complex maintains telomere length in ALT cancer cells through SUMOylation of telomere-binding proteins. In Nat Struct Mol Biol, (United States), pp. 581-590.

Poukka, H., Karvonen, U., Janne, O. A., and Palvimo, J. J. (2000). Covalent modification of the androgen receptor by small ubiquitin-like modifier 1 (SUMO-1). Proc Natl Acad Sci U S A *97*, 14145-14150.

Prat, A., and Baselga, J. (2008). The role of hormonal therapy in the management of hormonal-receptor-positive breast cancer with co-expression of HER2. Nat Clin Pract Oncol *5*, 531-542.

Prat, A., Parker, J. S., Karginova, O., Fan, C., Livasy, C., Herschkowitz, J. I., He, X., and Perou, C. M. (2010). Phenotypic and molecular characterization of the claudin-low intrinsic subtype of breast cancer. Breast Cancer Res *12*, R68.

Price, A., Shi, Q., Morris, D., Wilcox, M. E., Brasher, P. M., Rewcastle, N. B., Shalinsky, D., Zou, H., Appelt, K., Johnston, R. N., *et al.* (1999). Marked inhibition of tumor growth in a malignant glioma tumor model by a novel synthetic matrix metalloproteinase inhibitor AG3340. Clin Cancer Res *5*, 845-854.

Qian, P. X., Zuo, Z., Wu, Z. S., Meng, X., Li, G., Wu, Z., Zhang, W., Tan, S., Pandey, V., Yao, Y., *et al.* (2011). Pivotal role of reduced let-7g expression in breast cancer invasion and metastasis. In Cancer Res *20*,6463-6474.

Rakha, E. A., El-Sayed, M. E., Green, A. R., Lee, A. H., Robertson, J. F., and Ellis, I. O. (2007). Prognostic markers in triple-negative breast cancer. Cancer *109*, 25-32.

Rakha, E. A., Putti, T. C., Abd El-Rehim, D. M., Paish, C., Green, A. R., Powe, D. G., Lee, A. H., Robertson, J. F., and Ellis, I. O. (2006). Morphological and immunophenotypic analysis of breast carcinomas with basal and myoepithelial differentiation. J Pathol *208*, 495-506.

Rehman, A. O., and Wang, C. Y. (2008). SDF-1alpha promotes invasion of head and neck squamous cell carcinoma by activating NF-kappaB. J Biol Chem *283*, 19888-19894.

Ricca, A., Biroccio, A., Del Bufalo, D., Mackay, A. R., Santoni, A., and Cippitelli, M. (2000). bcl-2 over-expression enhances NF-kappaB activity and induces mmp-9 transcription in human MCF7(ADR) breast-cancer cells. In Int J Cancer, (United States: 2000 Wiley-Liss, Inc.), pp. 188-196.

Richter, L., Bone, J. R., and Kuroda, M. I. (1996). RNA-dependent association of the Drosophila maleless protein with the male X chromosome. Genes Cells *1*, 325-336.

Ring, A., and Dowsett, M. (2004). Mechanisms of tamoxifen resistance. Endocr Relat Cancer *11*, 643-658.

Robertson, J. F., Llombart-Cussac, A., Rolski, J., Feltl, D., Dewar, J., Macpherson, E., Lindemann, J., and Ellis, M. J. (2009). Activity of fulvestrant 500 mg versus anastrozole 1 mg as first-line treatment for advanced breast cancer: results from the FIRST study. In J Clin Oncol, (United States), pp. 4530-4535.

Rocak, S., Emery, B., Tanner, N. K., and Linder, P. (2005). Characterization of the ATPase and unwinding activities of the yeast DEAD-box protein Has1p and the analysis of the roles of the conserved motifs. In Nucleic Acids Res, (England), pp. 999-1009.

Rocak, S., and Linder, P. (2004). DEAD-box proteins: the driving forces behind RNA metabolism. In Nat Rev Mol Cell Biol, (England), pp. 232-241.

Rodriguez, M. S., Dargemont, C., and Hay, R. T. (2001). SUMO-1 conjugation in vivo requires both a consensus modification motif and nuclear targeting. J Biol Chem *276*, 12654-12659.

Rogers, R. S., Horvath, C. M., and Matunis, M. J. (2003). SUMO modification of STAT1 and its role in PIAS-mediated inhibition of gene activation. J Biol Chem *278*, 30091-30097.

Rosas-Acosta, G., Russell, W. K., Deyrieux, A., Russell, D. H., and Wilson, V. G. (2005). A universal strategy for proteomic studies of SUMO and other ubiquitin-like modifiers. In Mol Cell Proteomics, (United States), pp. 56-72.

Rottenberg, S., Nygren, A. O., Pajic, M., van Leeuwen, F. W., van der Heijden, I., van de Wetering, K., Liu, X., de Visser, K. E., Gilhuijs, K. G., van Tellingen, O., *et al.* (2007). Selective induction of chemotherapy resistance of mammary tumors in a conditional mouse model for hereditary breast cancer. In Proc Natl Acad Sci U S A, (United States), pp. 12117-12122.

Rozen, F., Edery, I., Meerovitch, K., Dever, T. E., Merrick, W. C., and Sonenberg, N. (1990). Bidirectional RNA helicase activity of eucaryotic translation initiation factors 4A and 4F. Mol Cell Biol *10*, 1134-1144.

Sacks, F. M., Pfeffer, M. A., Moye, L. A., Rouleau, J. L., Rutherford, J. D., Cole, T. G., Brown, L., Warnica, J. W., Arnold, J. M., Wun, C. C., *et al.* (1996). The effect of pravastatin on coronary events after myocardial infarction in patients with average cholesterol levels. Cholesterol and Recurrent Events Trial investigators. N Engl J Med *335*, 1001-1009.

Sadaria, M. R., Reppert, A. E., Yu, J. A., Meng, X., Fullerton, D. A., Reece, T. B., and Weyant, M. J. (2011). Statin therapy attenuates growth and malignant potential of human esophageal adenocarcinoma cells. J Thorac Cardiovasc Surg *142*, 1152-1160.

Saitoh, H., and Hinchey, J. (2000). Functional heterogeneity of small ubiquitin-related protein modifiers SUMO-1 versus SUMO-2/3. J Biol Chem *275*, 6252-6258.

Sakata, K., Satoh, M., Someya, M., Asanuma, H., Nagakura, H., Oouchi, A., Nakata, K., Kogawa, K., Koito, K., Hareyama, M., and Himi, T. (2004). Expression of matrix metalloproteinase 9 is a prognostic factor in patients with non-Hodgkin lymphoma. Cancer *100*, 356-365.

Sampson, D. A., Wang, M., and Matunis, M. J. (2001). The small ubiquitin-like modifier-1 (SUMO-1) consensus sequence mediates Ubc9 binding and is essential for SUMO-1 modification. J Biol Chem *276*, 21664-21669.

Santner, S. J., Dawson, P. J., Tait, L., Soule, H. D., Eliason, J., Mohamed, A. N., Wolman, S. R., Heppner, G. H., and Miller, F. R. (2001). Malignant MCF10CA1 cell lines derived from premalignant human breast epithelial MCF10AT cells. Breast Cancer Res Treat *65*, 101-110.

Sapadin, A. N., and Fleischmajer, R. (2006). Tetracyclines: nonantibiotic properties and their clinical implications. In J Am Acad Dermatol, (United States), pp. 258-265.

Sassano, A., and Platanias, L. C. (2008). Statins in tumor suppression. Cancer Lett *260*, 11-19.

Schwab, M. (1991). Enhanced expression of the cellular oncogene MYCN and progression of human neuroblastoma. Adv Enzyme Regul *31*, 329-338.

Sentis, S., Le Romancer, M., Bianchin, C., Rostan, M. C., and Corbo, L. (2005). Sumoylation of the estrogen receptor alpha hinge region regulates its transcriptional activity. Mol Endocrinol *19*, 2671-2684.

Sharma, P. S., Sharma, R., and Tyagi, T. (2011). VEGF/VEGFR pathway inhibitors as anti-angiogenic agents: present and future. Curr Cancer Drug Targets *11*, 624-653.

Shibata, M. A., Ito, Y., Morimoto, J., and Otsuki, Y. (2004). Lovastatin inhibits tumor growth and lung metastasis in mouse mammary carcinoma model: a p53-independent mitochondrial-mediated apoptotic mechanism. In Carcinogenesis, (England), pp. 1887-1898.

Shim, M. S., and Kwon, Y. J. (2010). Efficient and targeted delivery of siRNA in vivo. FEBS J *277*, 4814-4827.

Shin, H. R., Boniol, M., Joubert, C., Hery, C., Haukka, J., Autier, P., Nishino, Y., Sobue, T., Chen, C. J., You, S. L., *et al.* (2010). Secular trends in breast cancer mortality in five East Asian populations: Hong Kong, Japan, Korea, Singapore and Taiwan. Cancer Sci *101*, 1241-1246.

Shin, S., Rossow, K. L., Grande, J. P., and Janknecht, R. (2007). Involvement of RNA helicases p68 and p72 in colon cancer. In Cancer Res, (United States), pp. 7572-7578.

Shinoda, K., Lei, H., Yoshii, H., Nomura, M., Nagano, M., Shiba, H., Sasaki, H., Osawa, Y., Ninomiya, Y., Niwa, O., and et al. (1995). Developmental defects of the ventromedial hypothalamic nucleus and pituitary gonadotroph in the Ftz-F1 disrupted mice. Dev Dyn *204*, 22-29.

Shuai, K. (2006). Regulation of cytokine signaling pathways by PIAS proteins. Cell Res *16*, 196-202.

Sirohi, B., Arnedos, M., Popat, S., Ashley, S., Nerurkar, A., Walsh, G., Johnston, S., and Smith, I. E. (2008). Platinum-based chemotherapy in triple-negative breast cancer. In Ann Oncol, (England), pp. 1847-1852.

Slattery, M. L., Lundgreen, A., Kadlubar, S. A., Bondurant, K. L., and Wolff, R. K. (2011). JAK/STAT/SOCS-signaling pathway and colon and rectal cancer. Mol Carcinog doi: 10.1002/mc.21841.

Sliva, D., Rizzo, M. T., and English, D. (2002). Phosphatidylinositol 3-kinase and NF-kappaB regulate motility of invasive MDA-MB-231 human breast cancer cells by the secretion of urokinase-type plasminogen activator. In J Biol Chem, (United States), pp. 3150-3157.

Smid, M., Wang, Y., Zhang, Y., Sieuwerts, A. M., Yu, J., Klijn, J. G., Foekens, J. A., and Martens, J. W. (2008). Subtypes of breast cancer show preferential site of relapse. In Cancer Res, (United States), pp. 3108-3114.

Smith, D. R., Polverini, P. J., Kunkel, S. L., Orringer, M. B., Whyte, R. I., Burdick, M. D., Wilke, C. A., and Strieter, R. M. (1994). Inhibition of interleukin 8 attenuates angiogenesis in bronchogenic carcinoma. J Exp Med *179*, 1409-1415.

Smith, L. A., Aranda-Espinoza, H., Haun, J. B., Dembo, M., and Hammer, D. A. (2007). Neutrophil traction stresses are concentrated in the uropod during migration. In Biophys J, (United States), pp. L58-60.

Sorlie, T. (2004). Molecular portraits of breast cancer: tumour subtypes as distinct disease entities. Eur J Cancer *40*, 2667-2675.

Sovak, M. A., Bellas, R. E., Kim, D. W., Zanieski, G. J., Rogers, A. E., Traish, A. M., and Sonenshein, G. E. (1997). Aberrant nuclear factor-kappaB/Rel expression and the pathogenesis of breast cancer. J Clin Invest *100*, 2952-2960.

Steeg, P. S. (2003). Metastasis suppressors alter the signal transduction of cancer cells. In Nat Rev Cancer, (England), pp. 55-63.

Stetler-Stevenson, W. G. (2008). The tumor microenvironment: regulation by MMP-independent effects of tissue inhibitor of metalloproteinases-2. Cancer Metastasis Rev *27*, 57-66.

Strauss, E. J., and Guthrie, C. (1994). PRP28, a 'DEAD-box' protein, is required for the first step of mRNA splicing in vitro. Nucleic Acids Res *22*, 3187-3193.

Stuelten, C. H., DaCosta Byfield, S., Arany, P. R., Karpova, T. S., Stetler-Stevenson, W. G., and Roberts, A. B. (2005). Breast cancer cells induce stromal fibroblasts to express MMP-9 via secretion of TNF-alpha and TGF-beta. In J Cell Sci, (England), pp. 2143-2153.

Sullu, Y., Demirag, G. G., Yildirim, A., Karagoz, F., and Kandemir, B. (2011). Matrix metalloproteinase-2 (MMP-2) and MMP-9 expression in invasive ductal carcinoma of the breast. In Pathol Res Pract *12*,747-753.

Takahashi, A., Sasaki, H., Kim, S. J., Tobisu, K., Kakizoe, T., Tsukamoto, T., Kumamoto, Y., Sugimura, T., and Terada, M. (1994). Markedly increased amounts of messenger RNAs for vascular endothelial growth factor and placenta growth factor in renal cell carcinoma associated with angiogenesis. Cancer Res *54*, 4233-4237.

Tamura, A., and Nagasaki, Y. (2010). Smart siRNA delivery systems based on polymeric nanoassemblies and nanoparticles. Nanomedicine (Lond) *5*, 1089-1102.

Tanner, N. K., and Linder, P. (2001). DExD/H box RNA helicases: from generic motors to specific dissociation functions. In Mol Cell, (United States), pp. 251-262.

Tatham, M. H., Jaffray, E., Vaughan, O. A., Desterro, J. M., Botting, C. H., Naismith, J. H., and Hay, R. T. (2001). Polymeric chains of SUMO-2 and SUMO-3 are conjugated to protein substrates by SAE1/SAE2 and Ubc9. In J Biol Chem, (United States), pp. 35368-35374.

Thike, A. A., Cheok, P. Y., Jara-Lazaro, A. R., Tan, B., Tan, P., and Tan, P. H. (2010). Triple-negative breast cancer: clinicopathological characteristics and relationship with basal-like breast cancer. In Mod Pathol, (United States), pp. 123-133.

Tischkowitz, M., Brunet, J. S., Begin, L. R., Huntsman, D. G., Cheang, M. C., Akslen, L. A., Nielsen, T. O., and Foulkes, W. D. (2007). Use of immunohistochemical markers can refine prognosis in triple negative breast cancer. In BMC Cancer, (England), p. 134.

Tonn, J. C., Kerkau, S., Hanke, A., Bouterfa, H., Mueller, J. G., Wagner, S., Vince, G. H., and Roosen, K. (1999). Effect of synthetic matrix-metalloproteinase inhibitors on invasive capacity and proliferation of human malignant gliomas in vitro. Int J Cancer *80*, 764-772.

Tsuda, H., Takarabe, T., Hasegawa, F., Fukutomi, T., and Hirohashi, S. (2000). Large, central acellular zones indicating myoepithelial tumor differentiation in high-grade invasive ductal carcinomas as markers of predisposition to lung and brain metastases. Am J Surg Pathol *24*, 197-202.

Turner, N. C., Reis-Filho, J. S., Russell, A. M., Springall, R. J., Ryder, K., Steele, D., Savage, K., Gillett, C. E., Schmitt, F. C., Ashworth, A., and Tutt, A. N. (2007). BRCA1 dysfunction in sporadic basal-like breast cancer. In Oncogene, (England), pp. 2126-2132.

Tutt, A., Robson, M., Garber, J. E., Domchek, S. M., Audeh, M. W., Weitzel, J. N., Friedlander, M., Arun, B., Loman, N., Schmutzler, R. K., *et al.* (2010). Oral poly(ADP-ribose) polymerase inhibitor olaparib in patients with BRCA1 or BRCA2 mutations and advanced breast cancer: a proof-of-concept trial. Lancet *376*, 235-244.

Uchida, S., Shimada, Y., Watanabe, G., Li, Z. G., Hong, T., Miyake, M., and Imamura, M. (1999). Motility-related protein (MRP-1/CD9) and KAI1/CD82 expression inversely correlate with lymph node metastasis in oesophageal squamous cell carcinoma. Br J Cancer *79*, 1168-1173.

Valabrega, G., Montemurro, F., and Aglietta, M. (2007). Trastuzumab: mechanism of action, resistance and future perspectives in HER2-overexpressing breast cancer. Ann Oncol *18*, 977-984.

van Kempen, L. C., and Coussens, L. M. (2002). MMP9 potentiates pulmonary metastasis formation. Cancer Cell *2*, 251-252.

von Minckwitz, G., Muller, B. M., Loibl, S., Budczies, J., Hanusch, C., Darb-Esfahani, S., Hilfrich, J., Weiss, E., Huober, J., Blohmer, J. U., *et al.* (2011). Cytoplasmic poly(adenosine diphosphate-ribose) polymerase expression is predictive and prognostic in patients with breast cancer treated with neoadjuvant chemotherapy. J Clin Oncol *29*, 2150-2157.

Watabe, M., Nagafuchi, A., Tsukita, S., and Takeichi, M. (1994). Induction of polarized cell-cell association and retardation of growth by activation of the E-cadherin-catenin adhesion system in a dispersed carcinoma line. J Cell Biol *127*, 247-256.

Watanabe, M., Yanagisawa, J., Kitagawa, H., Takeyama, K., Ogawa, S., Arao, Y., Suzawa, M., Kobayashi, Y., Yano, T., Yoshikawa, H., *et al.* (2001). A subfamily of RNA-binding DEAD-box proteins acts as an estrogen receptor alpha coactivator through the N-terminal activation domain (AF-1) with an RNA coactivator, SRA. EMBO J *20*, 1341-1352.

Weih, F., and Caamano, J. (2003). Regulation of secondary lymphoid organ development by the nuclear factor-kappaB signal transduction pathway. In Immunol Rev, (Denmark), pp. 91-105.

Weirich, C. S., Erzberger, J. P., Berger, J. M., and Weis, K. (2004). The N-terminal domain of Nup159 forms a beta-propeller that functions in mRNA export by tethering the helicase Dbp5 to the nuclear pore. In Mol Cell, (United States), pp. 749-760.

Weldon, C. B., Burow, M. E., Rolfe, K. W., Clayton, J. L., Jaffe, B. M., and Beckman, B. S. (2001). NF-kappa B-mediated chemoresistance in breast cancer cells. In Surgery, (United States), pp. 143-150.

Wilson, B. J., Bates, G. J., Nicol, S. M., Gregory, D. J., Perkins, N. D., and Fuller-Pace, F. V. (2004). The p68 and p72 DEAD box RNA helicases interact with HDAC1 and repress transcription in a promoter-specific manner. In BMC Mol Biol, (England), p. 11.

Wittinghofer, A., and Pai, E. F. (1991). The structure of Ras protein: a model for a universal molecular switch. Trends Biochem Sci *16*, 382-387.

Wong, W. W., Dimitroulakos, J., Minden, M. D., and Penn, L. Z. (2002). HMG-CoA reductase inhibitors and the malignant cell: the statin family of drugs as triggers of tumor-specific apoptosis. Leukemia *16*, 508-519.

Woolley, K., and Martin, P. (2000). Conserved mechanisms of repair: from damaged single cells to wounds in multicellular tissues. In Bioessays, (England), pp. 911-919.

Worsham, M. J., Pals, G., Schouten, J. P., Miller, F., Tiwari, N., van Spaendonk, R., and Wolman, S. R. (2006). High-resolution mapping of molecular events associated with immortalization, transformation, and progression to breast cancer in the MCF10 model. Breast Cancer Res Treat *96*, 177-186.

Wu, J. T., and Kral, J. G. (2005). The NF-kappaB/IkappaB signaling system: a molecular target in breast cancer therapy. J Surg Res *123*, 158-169.

Wu, Z. H., and Miyamoto, S. (2008). Induction of a pro-apoptotic ATM-NF-kappaB pathway and its repression by ATR in response to replication stress. In EMBO J, (England), pp. 1963-1973.
Wu, Z. H., Shi, Y., Tibbetts, R. S., and Miyamoto, S. (2006). Molecular linkage between the kinase ATM and NF-kappaB signaling in response to genotoxic stimuli. In Science, (United States), pp. 1141-1146.

Wu, Z. S., Wu, Q., Yang, J. H., Wang, H. Q., Ding, X. D., Yang, F., and Xu, X. C. (2008). Prognostic significance of MMP-9 and TIMP-1 serum and tissue expression in breast cancer. Int J Cancer *122*, 2050-2056.

Xia, Q., Kong, X. T., Zhang, G. A., Hou, X. J., Qiang, H., and Zhong, R. Q. (2005). Proteomics-based identification of DEAD-box protein 48 as a novel autoantigen, a prospective serum marker for pancreatic cancer. Biochem Biophys Res Commun *330*, 526-532.

Xu, Y. Z., Newnham, C. M., Kameoka, S., Huang, T., Konarska, M. M., and Query, C. C. (2004). Prp5 bridges U1 and U2 snRNPs and enables stable U2 snRNP association with intron RNA. In EMBO J, (England), pp. 376-385.

Xue, J., Thippegowda, P. B., Hu, G., Bachmaier, K., Christman, J. W., Malik, A. B., and Tiruppathi, C. (2009). NF-kappaB regulates thrombin-induced ICAM-1 gene expression in cooperation with NFAT by binding to the intronic NF-kappaB site in the ICAM-1 gene. In Physiol Genomics, (United States), pp. 42-53.

Yamaoka, T., Fujimoto, M., Ogawa, F., Yoshizaki, A., Bae, S. J., Muroi, E., Komura, K., Iwata, Y., Akiyama, Y., Yanaba, K., *et al.* (2011). The roles of P- and E-selectins and P-selectin glycoprotein ligand-1 in primary and metastatic mouse melanomas. In J Dermatol Sci, pp. 99-107.

Yang, L., Lin, C., Zhao, S., Wang, H., and Liu, Z. R. (2007). Phosphorylation of p68 RNA helicase plays a role in platelet-derived growth factor-induced cell proliferation by up-regulating cyclin D1 and c-Myc expression. In J Biol Chem, (United States), pp. 16811-16819.

Yang, X., Wei, L., Tang, C., Slack, R., Montgomery, E., and Lippman, M. (2000). KAI1 protein is down-regulated during the progression of human breast cancer. Clin Cancer Res *6*, 3424-3429.

Yoshizawa, K., Nozaki, S., Kitahara, H., Kato, K., Noguchi, N., Kawashiri, S., and Yamamoto, E. (2011). Expression of urokinase-type plasminogen activator/urokinase-type plasminogen activator receptor and maspin in oral squamous cell carcinoma: Association with mode of invasion and clinicopathological factors. Oncol Rep *26*, 1555-1560.

Young, S. R., Pilarski, R. T., Donenberg, T., Shapiro, C., Hammond, L. S., Miller, J., Brooks, K. A., Cohen, S., Tenenholz, B., Desai, D., *et al.* (2009). The prevalence of BRCA1 mutations among young women with triple-negative breast cancer. BMC Cancer *9*, 86.

Yu, Y., Yang, J. L., Markovic, B., Jackson, P., Yardley, G., Barrett, J., and Russell, P. J. (1997). Loss of KAI1 messenger RNA expression in both high-grade and invasive human bladder cancers. Clin Cancer Res *3*, 1045-1049.

Zhang, H., Saitoh, H., and Matunis, M. J. (2002). Enzymes of the SUMO modification pathway localize to filaments of the nuclear pore complex. Mol Cell Biol *22*, 6498-6508.

Zhao, J., Jin, S. B., Bjorkroth, B., Wieslander, L., and Daneholt, B. (2002). The mRNA export factor Dbp5 is associated with Balbiani ring mRNP from gene to cytoplasm. EMBO J *21*, 1177-1187.

Zhao, X., and Jain, C. (2011). DEAD-box proteins from Escherichia coli exhibit multiple ATP-independent activities. In J Bacteriol, (United States), pp. 2236-2241.

Zhu, C., Qi, X., Chen, Y., Sun, B., Dai, Y., and Gu, Y. (2011). PI3K/Akt and MAPK/ERK1/2 signaling pathways are involved in IGF-1-induced VEGF-C upregulation in breast cancer. J Cancer Res Clin Oncol *137*, 1587-1594.

Zieve, G. W., and Sauterer, R. A. (1990). Cell biology of the snRNP particles. Crit Rev Biochem Mol Biol *25*, 1-46.

Zogakis, T. G., and Libutti, S. K. (2001). General aspects of anti-angiogenesis and cancer therapy. Expert Opin Biol Ther *1*, 253-275.

APPENDICES

Appendix 1

Sequences of primers used in metastatic qPCR array

Gene	Abbreviation	Primer	Primer Sequence (5' → 3')
Beta-actin	β-actin	Forward	TTCCTGGGCATGGAGTC
		Reverse	CAGGTCTTTGCGGATGTC
Glyceraldehyde-3-phosphate dehydrogenase	GAPDH	Forward	TGCACCACCAACTGCTTAGC
		Reverse	GGCATGGACTGTGGTCATGAG
Metastasis associated 2	MTA2	Forward	CCGACGGCCTTATGCTCCT
		Reverse	CTGGGCCACCAGATCTTTGAC
Non-metastatic cells 1, protein	NME1	Forward	CTGCAGCCGGAGTTCAAAC
		Reverse	GCAATGAAGGTACGCTCACAGT
Plasminogen activator receptor	PLAUR	Forward	AATGGCCGCCAGTGTTACAG
		Reverse	CAGGAGACATCAATGTGTTC
Plasminogen activator, urokinase	PLAU	Forward	CACGCAAGGGGAGATGAA
		Reverse	ACAGCATTTTGGTGGTGACTT

Hepatocyte growth factor receptor	MET	Forward	TGGTGCAGAGGAGCAATGG
		Reverse	CATTCTGGATGGGTGTTTCCG
Matrix metallopeptidase 1	MMP1	Forward	AGCTAGCTCAGGATGACATTGATG
		Reverse	GCCGATGGGCTGGACAG
Serpin peptidase inhibitor, clade B	SERPINB5	Forward	CTACTTTGTTGGCAAGTGGATGAA
		Reverse	ACTGGTTTGGTGTCTGTCTTGTTG
Matrix metallopeptidase 2	MMP2	Forward	CAAAAACAAGAAGACATACATCTT
		Reverse	GCTTCCAAACTTCACGCTC
Serpin peptidase inhibitor, clade E	SERPINE1	Forward	CACAAATCAGACGGCAGCACT
		Reverse	CATCGGGCGTGGTGAACTC
Matrix metallopeptidase 9	MMP9	Forward	TGGGGGGCAACTCGGC
		Reverse	GGAATGATCTAAGCCCAG
Metallopeptidase inhibitor 1	TIMP1	Forward	CTTCTGGCATCCTGTTGTTG
		Reverse	AGAAGGCCGTCTGTGGGT
Metastasis assoicated gene 1	MTA1	Forward	GCTGTTACACCACACAGTCTT
		Reverse	GGACTCATGTTACTGCGGTT

			T
Metallopeptidase inhibitor 3	TIMP3	Forward	CCAGGACGCCTTCTGCAAC
		Reverse	CCTCCTTTACCAGCTTCTTC CC